Function of Nck adaptor proteins in the Unfolded Protein Response and Glucose Homeostasis in mice

By Mathieu Latreille

Department of Medicine
Division of Experimental Medicine
McGill University
Montreal, Quebec, Canada

A thesis submitted to McGill University in partial fulfillment
of the requirements for the degree of Doctor in Philosophy

Your file Votre référence
ISBN: 978-0-494-50946-3
Our file Notre référence
ISBN: 978-0-494-50946-3

ABSTRACT

The accumulation of unfolded proteins in the endoplasmic reticulum (ER) triggers the Unfolded Protein Response (UPR), an intracellular signaling network aimed at alleviating stress through the coordinated inhibition of mRNA translation and the transcriptional induction of ER chaperone genes. A few years ago, we identified an interaction between Nck signaling adaptors and the β-subunit of the eukaryotic initiation factor 2 (eIF2β). We ascertained that overexpression of Nck1 antagonizes ER stress-mediated inhibition of translation by decreasing phosphorylation of eIF2α on Ser51 by the PERK ser/thr protein kinase. In this thesis, I determined that Nck overexpression prevents the induction of ATF4 and CHOP genes associated with eIF2α phosphorylation in ER stress conditions. Conversely, mouse embryonic fibroblasts (MEFs) genetically deficient of Nck1 and Nck2 genes ($Nck1^{-/-}Nck2^{-/-}$) show increased levels of ATF4, GADD34 and CHOP in response to ER stress, further supporting a role for Nck in regulating the translational arm of the UPR. Concurrently, I found that Nck adaptors localize at the ER and are part of an eIF2α holophosphatase complex containing PP1c, a ser/thr phosphatase that dephosphorylates eIF2α on Ser51. Unexpectedly, however, I observed that RNA interference (RNAi)-mediated Nck1 depletion results in decreased levels of eIF2α phosphorylation and GADD34 induction in ER-stressed cells. Moreover, I uncovered a direct and SH2-mediated interaction between Nck and PERK. I provided strong evidence that PERK is phosphorylated on tyrosine residues *in vitro* and demonstrated that Tyr561 located in PERK juxtamembrane domain is virtually essential for the association with Nck adaptors. Therefore, I proposed that during the process of PERK activation, Tyr561 is phosphorylated and creates a binding site for Nck adaptors. I hypothesized that Nck is required for proper targeting and phosphorylation of eIF2α by PERK. To demonstrate this *in vivo*, I took advantage that obesity in mice causes ER stress in specific tissues. My data validate my hypothesis as eIF2α phosphorylation levels in liver and adipose tissue of obese mice were decreased by 45% in mice genetically inactivated of the *nck1* gene. Characterization of glucose homeostasis in normal and obese $Nck1^{-/-}$ and $Nck2^{-/-}$ knockout mice revealed marked alteration in glucose tolerance

and insulin sensitivity compared to controls, thereby shedding light on a new physiological function for these signaling adaptors in controlling glycaemia *in vivo.*

RÉSUMÉ

L'accumulation de protéines inadéquatement repliées dans le réticulum endoplasmique (RE) initie une réponse cellulaire appelée « Unfolded Protein Response » (UPR) amenant l'inhibition transitoire de la traduction générale des ARNm et l'augmentation de l'expression de chaperones et d'enzymes de maturation résidant dans le RE. Cette réponse cellulaire augmente la fonction de repliement et de sécrétion du RE et rétablie ainsi l'équilibre normal au sein cet organite. Au cours des dernières années, nous avons découvert que l'adaptateur protéique Nck interagit avec la sous-unité beta du facteur eukaryotique d'initiation de la traduction (eIF2β). De plus, la surexpression de Nck1 coïncide avec une augmentation de la synthèse protéique et une diminution de la phosphorylation d'eIF2α sur la Ser51 par la sér/thr protéine kinase PERK. Dans cette thèse, j'ai démontré que la surexpression de Nck prévient aussi l'induction transcriptionelle des gènes ATF4 et CHOP qui accompagnent la phosphorylation d'eIF2α induite dans des conditions de stress du RE. À l'inverse, l'induction d'ATF4, GADD34 et CHOP est augmentée en. conditions de stress du RE dans les fibroblastes dérivés d'embryons de souris dans lesquels les gènes *nck1* et *nck2* ont été inactivés (MEFs $Nck1^{-/-}Nck2^{-/-}$). J'ai également découvert qu'une fraction importante de Nck se retrouve au RE et fait partie intégrante d'un complexe moléculaire contenant la sér/thr phosphatase PP1c et ayant la capacité de déphosphoryler eIF2α. Cependant, j'ai observé que la déplétion de Nck1 par interférence d'ARN (ARNi), réduit la phosphorylation d'eIF2α et l'induction de GADD34 en réponse au stress du RE. De plus, j'ai établi que Nck associe PERK directement via son domaine SH2. J'ai observé que PERK est phosphorylé sur certains résidus tyrosine *in vitro*. J'ai établi que la Tyr561 localisée dans le domaine juxtamembrane de PERK est absolument requise pour son intéraction avec Nck. Ces résultats me permettent de proposer qu'au cours de l'activation de PERK, la Tyr561 est phosphorylée créant ainsi un site de liaison pour Nck. J'ai émis l'hypothèse que Nck favorise ainsi le recrutement d'eIF2α et sa phosphorylation par PERK. Afin de démontrer ceci *in vivo*, nous avons pris avantage du fait que l'obésité chez la souris induit un stress au niveau du RE dans certains tissus. Mes résultats valident cette hypothèse car j'ai mesuré une diminution de plus de 45% de la phosphorylation d'eIF2α dans le foie et

le tissues adipeux des souris génétiquement inactivées dans le gène *nck1* ($Nck1^{-/-}$). Une caractérisation phénotypique plus approfondie des souris $Nck1^{-/-}$ et $Nck2^{-/-}$ a permis de révéler une différence significative dans la tolérance au glucose ainsi que dans la sensibilité à l'insuline en comparaison aux souris normales. En conclusion, ces études nous ont permis de montrer que l'adaptateur protéique Nck joue un important rôle physiologique dans la régulation de la glycémie chez la souris.

PREFACE

This thesis has been written according to the guidelines for a manuscript-based thesis issued by the Faculty of Graduate and Post-doctoral studies of McGill University.

This thesis consists of a general introduction, one published paper, two manuscripts that will be sent for publication, a general discussion and a section describing contributions to original research.

Appendix 1 contains the reprint derived from Chapter II as well as two reprints of collaboration studies in which I participated during my Ph.D. Appendix 2 and 3 contains supplementary data not related to Chapter 2, 3 and 4, but which represent an important intellectual and technical contribution of myself. Appendix 4 contains biohazard and animal subjects certificates.

CONTRIBUTIONS OF AUTHORS

Chapters and manuscripts presented as the core of this thesis were entirely written by me with editorial comments and corrections by my supervisor, Dr. Louise Larose. The work presented in Chapter 2, 3 and 4 has respectively generated one published paper (Chapt. 2) and two manuscript that will sent for publication within the next months (Chapt. 3 and 4):

Chapter II

Latreille M. and Larose L. (2006) *J. Biol. Chem.* **281**:26633-26644

Chapter III

Latreille M. and Larose L. (2007) To be submitted for publication

Chapter IV

Latreille M., Bourret G., Laberge M.K. and Larose L. (2007) To be submitted for publication

The lab work described in Chapter 2 is entirely my own. In chapter 3, Genevieve Bourret contributed to the production of the antigen used in the generation of the PERK antibody. In chapter 4, Genevieve Bourret contributed to general mice handling, insulin measurements, and experiments involving isolated pancreatic islets (Fig. 4I), while Marie-Kristine Laberge performed immunoblotting experiments for the *in vivo* insulin signaling analysis (Fig. 7C-7D)

Other publications

1. Lettau M., Qian J., Linkermann A., **Latreille M.**, Larose L. Kabelitz D., Janssen O. (2006). The adaptor protein Nck interacts with Fas ligand: Guiding the death factor to the cytotoxic immunological synapse. *Proc. Natl. Acad. Sci. U.S.A.* **103** (15): 5917-5922

   Contribution: plasmid constructs and technical help with Nck1 RNAi (Fig. 8)

2. Li H., Zhu J., Aoudjit L., **Latreille M.**, Kawachi H., Larose L., Takano T. (2006). Rat nephrin modulates cell morphology via the adaptor protein Nck. *Biochem. Biophys. Res. Commun.* **349** (1): 310-316

   Contribution: reagent, protocol and technical help with Nck1 RNAi

3. Cardin E., **Latreille M.**, Khoury C., Greenwood M.T. and Larose L. (2007) Nck-1 selectively modulates eIF2α Ser51 phosphorylation by a subset of eIF2α-kinases. *FEBS*, submitted

   Contribution: lab work (Figure 2A-2B)

TABLE OF CONTENTS

LIST OF FIGURES

CHAPTER III

CHAPTER IV

LIST OF ABBREVIATIONS

Ack	activated Cdc42-associated kinase
Ala	alanine
APC	antigen presenting cell
APR	acute phase response
Arp2/3	actin related protein 2/3
ASK	apoptosis signal-regulated kinase
ATF	activating transcription factor
ATP	adenosine triphosphate
Azc	azetidine-2-carboxylic acid
Bak	Bcl-2 homologous antagonist/killer
Bax	Bcl-2-associated X protein
Bcl-2	B-cell lymphoma/leukemia-2
BiP	immunoglobulin heavy chain-binding protein
bpV(Phen)	bis-peroxovanadium 1,10-phenathroline
bZIP	basic leucine zipper
Ca^{2+}	calcium
CaMK	Ca^{2+}/calmodulin-dependent kinase
CAP	c-Cbl-associated protein
c-Cbl	Casitas B-lineage lymphoma
CD	chow diet
cDNA	complementary deoxyribonucleic acid
CEBP	CAAT enhancer binding protein
CHO	Chinese hamster ovary
CHOP	CEBP homologous protein
CNS	central nervous system
Cnx	calnexin
CRE	cAMP response element
CREB	cAMP response element binding
CReP	constitutive repressor of eIF2α phosphorylation

CRIB	Cdc42-Rac-interactive binding
CRP	C-reactive protein
Crt	Calreticulin
Cys	cysteine
DCC	deleted in colorectal cancer
DinR	Drosophila insulin receptor
Dock	Dreadlock
DNA	deoxyribonucleic acid
dsRNA	double stranded ribonucleic acid
DTT	dithiothreitol
EDEM	ER degradation-enhancing α-mannosidase-like protein
eIF	eukaryotic initiation factor
EGF	epidermal growth factor
EGFP	enhanced green fluorescent protein
EGFR	epidermal growth factor receptor
EHEC	enterohemorrhagic *Escherichia coli*
EPEC	enteropathogenic *Escherichia coli*
EphR	ephrin receptor
ER	endoplasmic reticulum
ERAD	endoplasmic reticulum-associated degradation
ERK	extracellular signal-regulated kinase
ERSE	endoplasmic reticulum stress response element
FAK	focal adhesion kinase
FFA	free fatty acid
FGFR	fibroblast growth factor receptor
Flt3	FMS-like tyrosine kinase 3
FSV	Fujinami sarcoma virus
GADD34	Growth Arrest and DNA Damage-Inducible Protein 34
GAP	GTPase-activating protein
GDP	guanosine 5'diphosphate
GEF	GTPase exchange factor

GFP	green fluorescent protein
GPI	glycosylphosphatidylinositol
Grb	growth factor receptor-bound
Grp	glucose regulated protein
GST	glutathione-S-transferase
GCN2	general control non-derepressible-2
GLP-1	glucagon-like peptide-1
GLP-1R	glucagon-like peptide-1 receptor
GLUT	glucose transporter
GTP	guanosine 5'triphosphate
HFD	high fat diet
HRI	heme regulated inhibitor
HSV	herpes simplex virus
IDDM	insulin-dependent diabetes mellitus
IGF1R	insulin-like growth factor 1 receptor
Ig	immunoglobulin
IKKβ	inhibitor of NF-κB kinase
IL	interleukin
ILK	integrin-linked kinase
IPK	inhibitor of PKR
IR	insulin receptor
IRE1	inositol-requiring protein-1
IRR	IR-related receptor
IRS	insulin receptor substrate
ISR	integrated stress response
ITAM	immunoreceptor tyrosine-based activation motif
JIP1	JNK-interacting protein 1
JM	juxtamembrane
JNK	c-Jun N-terminal kinase
K_{ATP}	ATP-sensitive transmembrane K^+-channel
Kb	kilobase

KDa	kilodalton
Km	Michaelis-Menten constant
LPS	lipopolysaccharide
Luc	luciferase
Lys	lysine
Met	methionine
MHC	histocompatibility complex
mRNA	messenger ribonucleic acid
mTOR	mammalian target of rapamycin
Nck	non-cytosolic kinase
NF-kB	Nuclear factor-kB
NIK	Nck-interacting kinase
NLD	N-terminal luminal domain
NSF	N-ethylmaleimide sensitive fusion protein
Pak	p21-activated serine/threonine kinase
PARP	poly(ADP-ribose) polymerase
PBS	phosphatase buffered saline
PC	prohormone convertase
PDGF	platelet growth factor
PDGFR	platelet growth factor receptor
PDI	protein disulfide isomerase
PERK	PKR-like endoplasmic reticulum kinase
PH	pleckstrin homology
PI3K	phosphoinositide-3 kinase
PINCH	Particularly interesting new cysteine-histidine rich protein
PIP_2	phosphatidylinositol 4,5-trisphosphate
PIP_3	phosphatidylinositol 3,4,5-trisphosphate
PKA	protein kinase A
PKR	dsRNA-activated protein kinase
PLCγ	phospholipase Cγ
PP1c	protein phosphatase 1

PP2A	protein phosphatase 2A
PTB	phosphotyrosine-binding
PtdCho	phosphatidylcholine
pY	phosphotyrosine
RER	rough reticulum endoplasmic
RIP	regulated intra-membrane proteolysis
RNA	ribonucleic acid
RNAi	RNA interference
RNAse	ribonuclease
ROS	reactive oxygen species
RTK	receptor tyrosine kinase
S1P	site-1 protease
S2P	site-2 protease
SAP	serum amyloid P-component
SDS-PAGE	sodium dodecylsulfate polyacrylamide gel electrophoresis
Ser	serine
SER	smooth ER
SERCA	smooth ER ca^{2+}-ATPase
SFK	Src-family kinase
SH	Src homology
siRNA	small interfering RNA
SNARE	soluble NSF attachment protein receptors
SREBP	sterol regulatory element binding protein
SRP	signal-recognition particle
T2D	type 2 diabetes
TAG	triacylglycerol
TβR	transforming growth factor β receptor
TCR	T cell receptor
Tg	thapsigargin
TGFβ	transforming growth factor β
Thr	threonine

Tir	translocated intimin receptor
Tm	tunicamycin
TM	transmembrane
TNFα	Tumor necrosis factor α
TRAF2	TNFα receptor-associated factor 2
tRNA	transfer ribonucleic acid
Trp	tryptophan
TUDCA	taurine-conjugated derivative
TUNEL	Terminal deoxynucleotidyl Transferase Biotin-dUTP Nick End Labeling
Tyr	tyrosine
uORF	upstream open reading frame
UPR	unfolded protein response
UPRE	unfolded protein response element
VGCC	voltage-gated ca^{2+} channel
WAS	Wiskott-Aldrich syndrome
WASp	Wiskott-Aldrich syndrome protein
WAVE	WASp-family verproline homologous protein
Wip	WASp-interacting protein
Wt	wild type
$XBP1^{u}$	X-box binding protein 1 uninduced
$XBP1^{s}$	X-box binding protein 1 spliced

ACKNOWLEDGMENTS

I would like to thank the Fond de la Recherche en Santé du Quebec and the McGill University Hospital Center (MUHC) Research Institute for their financial support over the course of my Ph.D. studies.

My thanks go to the members of my supervisory committee, Dr. Jean-Jacques Lebrun, Dr. Antonis Koromilas and Dr. Jin Liu for their scientific input and helpful discussions. I would like to express a special thank to Dr. Antonis Koromilas for his wisdom and scientific rigorousness, which contributed to surpass myself intellectually throughout my Ph.D. degree.

I would like to communicate my appreciation to the coordinating office of the Polypeptide laboratory (PPL). To Mary Lapenna, a professional and outstanding general lab manager, I am thankful for your help and appreciate the great efforts you made in trying to make our journey at PPL the nicest as possible. I also thank Dr. Barry Posner and Dr. Simon Wing for helpful scientific discussions throughout my years in the PPL. I would like to thank Gael Jean-Baptiste for her friendship and critical reading of sections of this thesis. I am thankful to Nathalie Bédard and Marie Plourde for their technical assistance and joyfulness. I implore that my future colleagues will be as nice as both of you and let me borrow their pipettes when mine is broken or provide me with TRIS-HCl buffer when I am out of solution... I would also thank everybody of the PPL and Larose laboratory for their friendship, help, and advices. Your presence made my stay at PPL a unique and pleasant experience. A special thank to Genevieve Bourret who pass me on numerous advices on mice handling and experimentation. Finally, I would like to express my distinctive gratefulness to my supervisor, Dr. Louise Larose, who welcomed me in her lab with a lot of sensitivity. Her encouragement throughout these years allowed me to explore different avenues of research throughout my Ph.D. degree, which forged the versatile researcher I feel I've turned into today. I am appreciative of your scientific and professional mentoring and I hope that this will accompany me throughout my career.

To finish, I would like to express my sincere and deepest gratitude to my parents and family. Your unconditional love played a major role in accomplishing this personal achievement and for that reason, I will be eternally beholden. Finally, I thank Christopher for his generous support, indulgence, and encouragement throughout the past years. You represented my inspiration in the most difficult moments of this bumpy road and hope this continues to be the case in our future projects. Ohhh…I almost forgot you Popi! Love you doggy and thank you for your great company while writing this thesis.

CHAPTER I

Introduction and literature review

1. SIGNAL TRANSDUCTION: OVERVIEW

Over the last 30 years, we have noticed the immergence of an important sphere of study that focuses on determining how cells appropriately respond to extracellular signals. Central to this process, is a family of plasma membrane receptors that detect various stimuli and relay signals to intracellular proteins by initiating a cascade of events regulating proliferation, differentiation, motility or programmed cell death (apoptosis). A common feature of these signaling events is the reversible assembly of large multi-protein complexes induced upon stimulation of receptor catalytic kinase activity. In the case of intracellular signaling pathways triggered by growth factors, ligand binding to receptor tyrosine kinases (RTKs) elicits receptor dimerization, autophosphorylation on tyrosine (Tyr) residues that stimulates the catalytic kinase activity of RTKs. This decorates receptors with high affinity binding sites in their cytoplasmic tails, which promote interaction with effector proteins. Alternatively, receptors devoid of such activity such as the transforming growth factor-β receptor (TβR), pair up with heterologous transmembrane protein kinases or non-receptor protein kinase allowing propagation of signals to downstream effector proteins.

Pioneer work by T. Pawson and colleagues in the early 90's led to the discovery and characterization of Src homology (SH) domains that provide the building blocks for RTK signaling pathways promoting the assembly and targeting of large molecular complexes required for signal propagation. So far, two prevalent SH domains mediate protein-protein interactions in growth factor signaling pathways: the SH2 and SH3 domains. The SH2 domain is a relatively small module of approximately 100 amino acids that is evolutionary conserved in many eukaryotes with ~116 different examples (representing ~106 distinct proteins) found in the human genome (321). This module was initially identified in the oncogenic Src family tyrosine kinase *v-fps*, the transforming activity of Fujinami sarcoma virus (FSV) (355). SH2 domains have subsequently been identified in a wide range of enzymatic signaling proteins such as PLC-γ and RasGAP, but also in a SH2/SH3 domain-containing family of adaptor proteins devoid of enzymatic activity containing Grb2, Crk and Nck (reviewed in (259, 319, 320). SH2 domains strictly mediate phosphotyrosine-based interactions. However, peptide library screenings revealed that the strong sequence-specific recognition results from a series of interactions

between residues C-terminal to the phosphotyrosine residue and SH2-domain residues (384, 435). Two invariant arginine residues found in all SH2 domains (Arg289 and Arg308 in human Nck1) coordinate the phosphate oxygen of the phosphotyrosine and are essential for high affinity phosphopeptide binding. (36, 319).

SH3 domains were first noted as sequence similarity between divergent signaling proteins such as the Src family of tyrosine kinases, the PLC-γ enzyme and the Crk adaptor (272, 387). Soon after the discovery of the SH3 domain, screening of expression libraries using isolated SH3 domains were initiated and lead to the identification of the binding specificity of this ~60 amino acid domain. Generally, the region bound by SH3 domains favors peptides bearing PxxP core motifs (where x is any amino acid) (338). Structural analysis of the Src SH3 domain complexed with a proline-rich peptide revealed that two highly conserved aromatic residues on the surface of the SH3 domain (corresponding to Trp38 and Trp39 in the most N-terminal SH3 domain of human Nck1) were involved in coordinating the diprolyl peptide found in ligands (105, 283, 465). In fact, mutation of these residues completely abolishes the function of SH3 domain toward proline-rich motifs. However, a rapidly growing list of SH3-based interactions reveals that this domain can also interact with peptide sequences that lack such motif, supporting the idea that SH3 domains are promiscuous and versatile modules that recognize diverse set of ligands (reviewed in (236)). Importantly, and in contrast to phosphotyrosine-based interactions induced by extracellular signals, peptide interactions with SH3 domains are thought to be constitutive.

The importance of phosphotyrosine- and proline-based interactions in cell signaling is highlighted by the identification of other structurally related domains that also recognize similar motifs in target proteins. For example, phosphotyrosine-binding (PTB) domain recognizes phosphotyrosine residues within the NPxY context (where x is any amino acid) (26, 194), while WW domains have the ability to bind proline-rich cores and phospho-Serine/Proline or phospho-Threonine/Proline sequences (260, 261, 393).

2. THE NCK FAMILY OF ADAPTOR PROTEINS

2.1. Identification and Anatomy of Nck adaptors

The Nck signaling adaptor is composed of three amino (N)-terminal SH3 domains followed by a carboxy (C)-terminal SH2 domain (Fig. 1). Nck is part of a family of adaptors composed exclusively of SH2 and SH3 domains that also contains Grb2 and Crk proteins (23). These adaptors are involved in transducing signals from RTKs, regulating essential cellular functions by either increasing the activity, local concentration or altering the subcellular localization of downstream effectors. The *nck* cDNA was initially isolated from a melanoma cDNA library using monoclonal antibodies produced against the melanoma-associated antigen MUC18 (231). Two years later, Margolis and colleagues identified a partial cDNA sequence with high homology to the Nck cDNA in a screen for SH2 domain-containing proteins that bind to the tyrosine phosphorylated form of the C-terminal segment of the epidermal growth factor receptor (EGFR) (265). This Nck related protein was called growth factor receptor-bound protein 4 (Grb4). It was only in the late 90's, when the full-length cDNA for Grb4 was isolated, did we noticed that Nck and Grb4 proteins represented in fact a small family of adaptor proteins encoded by two separate genes in mammals (*nck1/nckα/nck* and *nck2/nckβ/grb4*) (37, 59) and one gene in invertebrate such as *Drosophila melanogaster* (Dreadlock, Dock)(115) and *Caenorhabditis elegans* (59). The two murine *nck* genes are found on distinct chromosomes and encode protein products of 47 kilodalton (KDa). Mouse Nck1 and Nck2 amino acid sequence share 68% of identity with most of the variability being found within regions linking the SH domains (Fig. 1). Interestingly, Nck proteins have higher interspecies conservation (human vs. mouse) than the conservation of the two proteins within a given specie (59). This suggests that both Nck could play unique and conserved physiological roles. Analysis of the primary structure of both Nck isotypes revealed that a large number of conserved motifs are likely to become phosphorylated by various kinases and recognized to by several protein modules. In fact, post-translational modifications induced in response to growth factor stimulation such as phosphorylation were found to converge on Nck adaptors. EGF and PDGF stimulation of NIH 3T3 (mouse embryonic fibroblast cells) and A431 (human epithelial carcinoma cells) cells leads to the phosphorylation of Nck proteins on serine, threonine and tyrosine residues (238, 315). The

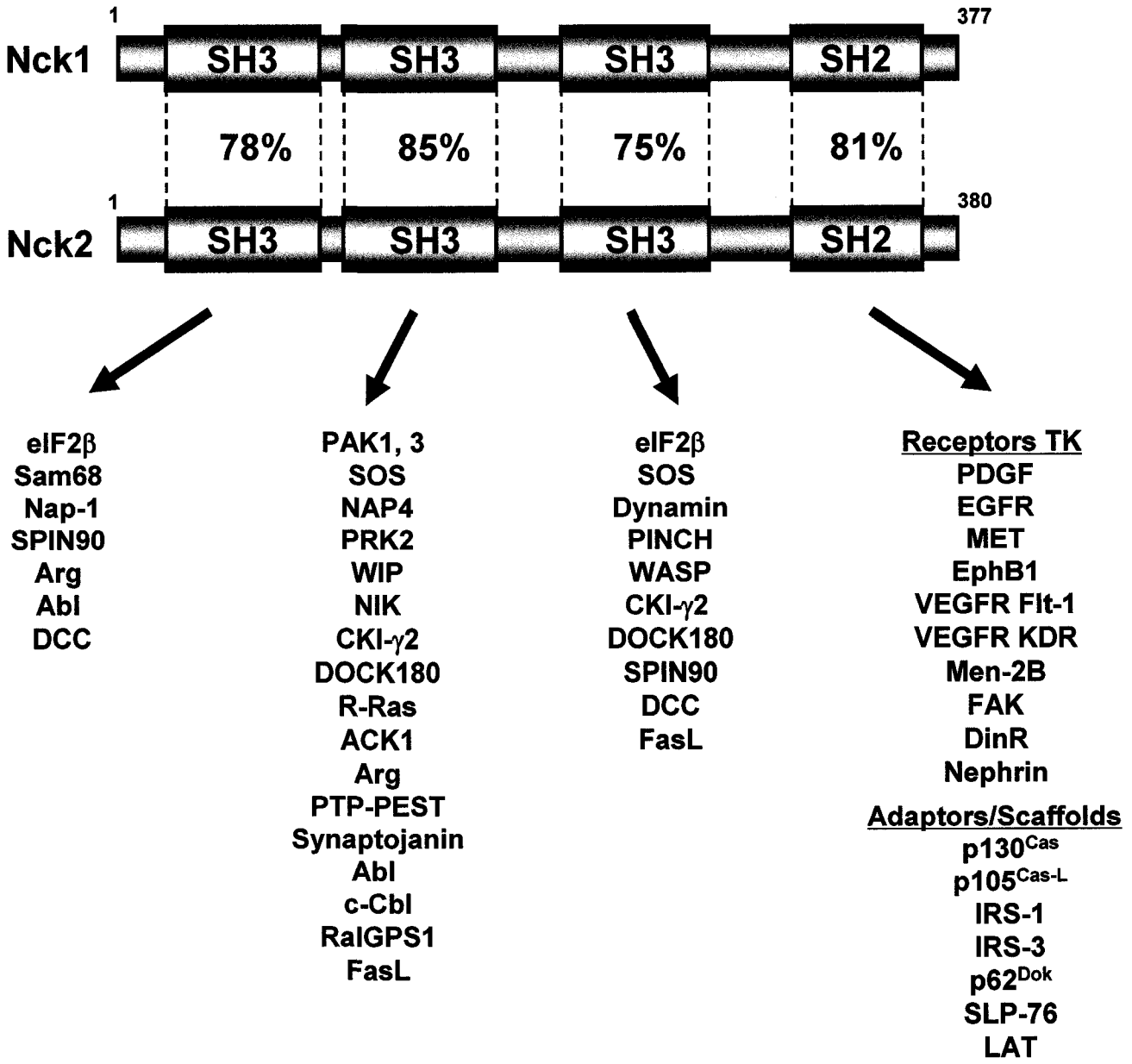

Figure 1. Anatomy of Nck adaptor proteins and current binding effectors.
Shown is the percentage of identity between Nck1 and Nck2 SH domains

exact residues in Nck that are targeted by phosphorylation are unknown neither the effect this phosphorylation has on the function of these signaling proteins.

2.2. Expression pattern of Nck adaptors

To gain insights into the biological processes regulated by Nck adaptors, Northern blot analysis of adaptor mRNA expression patterns in mouse tissues and various cell line was accomplished. For Nck1, a single RNA specie of 2.1 kilobases (Kb) was ubiquitously expressed in adult human and mouse tissues as well as in several cultured cell lines (37, 59, 238). Similarly, a 3.0 Kb corresponding to the Nck2 transcript is detected in most tissues in both human and mouse (37, 59, 414). Western blot analysis of adult mouse tissues reveal strong expression of Nck in all tissues extracts tested, while Nck2 appeared to be expressed at higher levels in thymus, spleen, and lungs and undetectable in liver and skeletal muscle (25). During embryogenesis, mice expressing a *lacZ* transgene under the control of Nck1 or Nck2 promoters show significant β-galactosidase activity in the head process, allantois and extraembryonic tissue at embryonic day 7.5 (E7.5). By midgastrulation (E8.5), Nck1 is expressed at low levels throughout the embryo, whereas Nck2 is highly expressed in mesoderm- and endoderm-derived structures such as the node, somites and the neural tube (25). Later on, both Nck1 and Nck2 are expressed in motor neurons, heart, gut, stomach, arteries, and somites of E10.5 embryos. Together, these expression analyses strongly suggest that the distinct, albeit overlapping, pattern of Nck1 and Nck2 expression could translate into mutually compensatory functional activities during embryogenesis and possibly in adult mice.

2.3. Targeted disruption of *nck* genes

Inactivation of either *nck1* or *nck2* gene in mice does not result in gross morphological or functional alterations, suggesting that Nck family members have redundant activities (25). In fact, numerous Nck1-interacting proteins also associate with Nck2 (see next section), demonstrating that these two adaptors do functionally compensate for one another. This was confirmed when the single $Nck1^{-/-}$ was crossed with the $Nck2^{-/-}$ mice (25). Such breeding experiment did not yield viable double homozygous offspring, demonstrating that the inactivation of both *nck1* and *nck2* genes results in embryonic lethality. The E9.5 embryonic lethality of the $Nck1^{-/-}Nck2^{-/-}$ embryos is caused by profound defects in mesoderm-derived

notochord (25). On the other hand, retention of a single allele of either *nck1* or *nck2* ($Nck1^{+/-}$ $Nck2^{-/-}$ or $Nck1^{-/-}Nck2^{+/-}$) is sufficient to generate viable, healthy and fertile mice.

2.4. Nck effectors and biological functions

Ever since the identification of Nck adaptors, intense efforts have been put together to determine the nature of proteins interacting with Nck proteins mainly through the implementation of yeast two-hybrid screenings. It was hypothesized that such achievement would give clues of the function of Nck adaptors and nature of signal transduction pathways involving these proteins. In fact, this approach was profitable and yielded enormous amount of information on the nature of proteins interacting with the SH2 and SH3 domains of Nck (Fig. 1). Today, more than 30 Nck SH3- and 15 SH2-binding proteins have been reported (47, 237). What became evident was the fact that of lot of proteins interacting via Nck SH3 domains were involved in cytoskeleton dynamics, such as Pak, WASp, Wip, FAK, Cap, Axin, Dynamin, Spin90, DOCK180, PINCH, Prk, Synaptojanin or Ack1, just to name a few. On the other hand, SH2-interacting proteins could be divided in two groups: RTKs and adaptors/scaffolds proteins. Therefore, it was suggested that different pools of Nck proteins associated with different effectors in distinct molecular complexes linking tyrosine phosphorylation via their SH2 domain to cytoskeleton regulators bound to their SH3 domains (47, 237). The only down side to this story is that the *in vivo* significance of the majority of these interactions, even more than 15 years after the discovery of Nck, remains to be determined. However, in the past 5 years, Dr. T. Pawson invested a lot of time and effort in order to fill this gap. Indeed, his group generated the Nck1 and Nck2 knockout mice, which were made available to the rest of the scientific community. Such pioneer work should contribute significantly at determining the function of Nck adaptors *in vivo*. Based on the large number of proteins interacting with Nck adaptors, an exhaustive and comprehensive description and analysis these interactions would represent a huge endeavor in the context of the current literature review. For these reasons, only a subset of Nck interactions will be discussed in the following paragraphs. Again, what will become evident when reading these lines is that most of the Nck binding proteins are closely linked to the regulation of actin dynamics, a central theme in Nck biology. Finally, information related to a novel interaction of Nck adaptors with an initiation translation factor will be described and serve to introduce the work presented in Chapters II, III and IV.

2.4.1 Nck and the WASp protein network

Mutation in the *wasp* gene causes the Wiscott-Aldrich syndrome (WAS), an X-linked recessive disease characterized by immunodeficiency associated with thrombocytopenia (reduced platelets number) manifested by eczema and recurrent infections (82). WAS patients have abnormal haematopoietic smooth cells surface, suggesting that WASp is associated with the regulation of the cytoskeleton. WASp is part of the verprolin-homology domain family of proteins, containing neural-WASp (N-WASp) and the distantly related WASp-family verproline homologous protein (WAVE) 1, 2, and 3 (258, 282, 398). WASp family proteins are important regulators of the actin cytoskeleton by promoting actin filament nucleation and branching through the activation of actin-related proteins 2 and 3 (Arp2/3) (398). Reorganization of actin filaments by WASp family proteins provides the force required for deformation of cell plasma membrane involved in multiple biological processes such as cell adhesion and motility (398). WASp contains an N-terminal Cdc42/Rac-interactive binding (CRIB) domain, a central proline-rich sequence that recruits signaling adaptors and a C-terminal VCA domain that binds actin monomer and the Arp2/3 complex. The interaction of Arp2/3 complex with the VCA domain of WASp proteins provides the burst of actin polymerization through activation of the actin-nucleating activity of the Arp2/3 (398). WASp activity is tightly regulated by an autoinhibited conformation mediated through an intramolecular interaction between its N-terminus and the VCA domain, and in this way, prevents spontaneous actin nucleation in the absence of input signals (345). The relief of WASp autoinhibition through the binding of Rho-family GTPases (Rac and Cdc42) or signaling adaptor proteins was found to be a central mechanism regulating signaling by WASp family proteins (93, 342, 345). Indeed, binding of GTP-bound Cdc42 to WASp CRIB domain allows recruitment of Arp2/3 and actin polymerization (156). Similarly, Nck and Grb2 SH2/SH3 domain-containing adaptors also bind WASp through its central proline-rich sequence promoting Arp2/3-mediated cytoskeleton remodeling (54, 343). Grb2, but not Nck, was found to cooperate with Cdc42 to stimulate the activation of N-WASp (54, 344), while WASp activation by Nck adaptors is stimulated by phosphatidylinositol 4,5 bisphosphate (PIP_2) (17, 346). Like Cdc42, Nck binding and PIP_2 reduce the affinity between the amino and carboxy termini of the WASp molecule (344). Although there is some disagreement about whether the second (346) or the third (343) SH3 domain of Nck is more crucial in binding WASp or N-WASp, cooperative SH3-mediated binding has been consistently observed (the three SH3

domains bind more strongly than individual SH3 domains). Given that SH3 domains bind proline-riche motifs with moderate affinity (dissociation constant Kd ~10 μM) (271), it was proposed that the affinity and selectivity of binding between Nck and WASp might be increased by multiple separate interactions between more than one SH3 domain of Nck and an extended proline-rich motif found in WASp (342). Interestingly, Riviera *et al.* demonstrated using an antibody-based system, that clustering of all three SH3 domains of Nck at the plasma membrane was sufficient in inducing local actin polymerization (including the formation of actin tails and spots) that required N-WASp, but not WAVE1 or Cdc42 (342). Given that tyrosine phosphorylation and PIP_2 cooperate to promote actin polymerization (351), it was proposed that binding of cytoskeletal proteins to phosphoinositides, particularly PIP_2, may promote their clustering into cholesterol- and sphingolipid-enriched membrane microdomains (i.e. lipid rafts) (342). It is tempting to speculate that clustering of Nck SH3 domains at the plasma membrane recruits N-WASp into close proximity to membrane domains with high local concentration of PIP_2, and that only the spatiotemporal coincidence of both activators causes full activation of N-WASp and triggers localized polymerization of actin.

Nck adaptors also participate in WAVE1-regulated Apr2/3 actin polymerization downstream of activated Rac1 (93). The inactive WAVE heterotetrameric complex is composed of WAVE, Abi, Nap1, SRA, and HSPC300 subunits. Importantly, Nap1 binds to Nck, while SRA1 binds to activated Rac (206, 207). WAVE1 complex regulation by Nck was demonstrated by testing the effect of recombinant full-length Nck to activate the actin nucleation activity of the WAVE1 complex purified from bovine brain extract (93). What became clear from these experiments is that Nck (and Rac) stimulates WAVE1-Arp2/3 nucleation activity independently of its SH2 domain and in a manner very similar to the action of Cdc42 on N-WASp (156). Given that Nck binds RTKs via its SH2 domain, it is believed that the function of Nck is to recruit the actin nucleating activity complex associated with WASp-Arp2/3 and WAVE1-Arp2/3 to membrane receptors such as the epidermal growth factor receptor (EGFR)(112, 238) or the platelet-derived growth factor receptor (PDGFR)(60, 315), and thereby link extracellular signals to actin dynamics.

2.4.2 Nck and T cell signaling

The molecules controlling actin polymerization have been studied in many cellular systems. T cell activation research unveils an important role for these molecules in proximal T cell antigen receptor (TCR) signaling events induced in response to TCR engagement with products bound to the major histocompatibility complex (MHC) on antigen presenting cells (APCs). For these signals to be interpreted correctly, TCR engagement brings the activation of protein kinases and phosphorylation of many substrates, including the TCR itself, and the formation of molecular complexes containing adaptors and enzymes (183, 359). The consequences of these proximal events include: 1) change in cellular shape and enhanced cell motility through reorganization of the cytoskeleton, and 2) upregulation of genes controlling T proliferation and differentiation (359). However, unlike RTKs, TCR cytoplasmic tails are very short and therefore are entailed to signal through CD3 dimeric units (CD3 γ, δ, ε, and ζ) that possess characteristic sequence motifs for tyrosine phosphorylation known as immunoreceptor tyrosine-based activation motifs (ITAMs). TCR engagement results in the activation of protein tyrosine kinases (Src family and ZAP70) that phosphorylate CD3 ITAMs, providing docking sites for numerous adaptors such as SLP-76 and Gads (418).

Using various biochemical experimental approaches and T cell imaging, it was demonstrated that Nck and WASP are recruited to the activated TCR in a Src kinase- and SLP76-dependent manner (13). Given that SLP76 interacts physically with the SH2 domain of Nck and Vav, a guanine nucleotide exchange for Rho GTPases, a simple model suggests that Nck targets the WASP-Arp2/3 to the TCR via its interaction with tyrosine phosphorylated SLP76 to stimulate actin polymerization and changes in cell shape (13, 468). However in 2002, Gil *et al.* added a new and unexpected element to that model by showing that after TCR engagement, Nck binds directly to the CD3ε chains of the TCR independently of protein tyrosine kinases activation (120). They provided evidence suggesting that this recruitment involves a conformational change of CD3ε that exposes a highly conserved proline-rich sequence recognized by the first SH3 domain of Nck (120). Recently, the Nck binding site within CD3ε was mapped to a PxxDY sequence that shares a tyrosine residue (Y166) with an ITAM targeted by the Lck and ZAP70 kinases (202). Importantly, phosphorylation of CD3ε Y166 abolishes Nck association, thus suggesting that phosphorylation of this residue serves as a

molecular switch during T cell activation that determines the capacity of CD3ε to interact with either SH3 or SH2 domain-containing proteins. However, knockin mice lacking this proline-rich sequence (where PPPVPNP is changed to AAAVANA) show impaired Nck recruitment to CD3ε, but normal proliferation and selection of T cell subsets in the thymus and spleen, suggesting that this interaction is not essential for T cell development and function (395). Moreover, if this model stands true, recruitment of Nck to the TCR would preclude the need for SLP76. However, SLP76-deficient T cells show defective Nck recruitment, suggesting that both models are not mutually exclusive.

2.4.3 Nck and axonal guidance

Nervous system function relies on the establishment of appropriate neuronal connections. Despite the enormous set of connections possible in both vertebrate and invertebrate nervous systems, patterns of neuronal connectivity are remarkably precise. Neurons extend an axon and dendrites from the cell body, which navigates toward its target region through the use of the growth cone. This structure, found at the leading edge of neuronal projections, is subjected to important cytoskeleton alterations as it responds to guidance molecules coming from the environment (186). Therefore, it is not surprising that Rho-family GTPases play a central role in this process (440). *Drosophila melanogaster* represents an excellent genetic model to study neurons projection targeting *in vivo* given that the development, connectivity and fate of photoreceptor (R cells) axons have been completely mapped. The fly eye is composed of 750 repeated units each containing eight R cells (R1-R8) (406). Moreover, each R cells has a clear and defined projection pattern, which is established during fly development. Dreadlock (Dock), the ortholog of Nck in *Drosophila melanogaster*, was identified in a genetic screen aimed at identifying mutants interfering with R cells targeting in the fly eye (115). Mutation in the *dock* gene disrupted signaling from the surface of the growth cone to the intracellular actin cytoskeleton, resulting in defects in R cell projection and targeting. Importantly, this phenotype can be rescued by driving expression of the human Nck1 cDNA under a neuronal promoter in Dock mutant flies (335). Given that tyrosine phosphorylation is playing an important role in guidance of the growth cone (24, 451), it was proposed that Nck could transduce phosphotyrosine-induced signals through its SH2 domain to the cytoskeleton through effectors bound to its SH3 domains. To test this hypothesis, Rao and colleagues studied the effect of point

mutations within Dock SH2 and SH3 domains on R cell connectivity (335). They found that the SH2 domain and the second SH3 domain are required to establish proper R cells projections (335). Interestingly, mutation in the yeast Ste20-related *Drosophila melanogaster* p21-activated ser/thr kinase (*Pak*) gene also results in defect in R cell pathfinding (157), suggesting that Pak could be involved in the Dock signaling pathway. Indeed, Dock and Pak colocalize in R-cells axons and growth cones, and both proteins physically interact through Dock second SH3 domain and a PxxP motif found in the amino-terminus of Pak (157). The interaction of Nck with Pak (Pak1 and Pak3) (11) has now been observed in many cell types besides neurons and validated by numerous independent laboratories (29, 112). Beside its kinase domain, Pak proteins contains a GTPase binding domain that associates both GTP-loaded Cdc42 and Rac1 resulting in stimulation of Pak catalytic kinase activity in response to its proper targeting at the plasma membrane (11). Recently, Pak has been shown to interact with the Rac exchange factor Pix (α and β), which contributes to activation of Cdc42, thereby making a link between Nck and Rho GTPase regulators of the cytoskeleton (12, 262). The current prevailing model of Pak activation proposes that in response to growth factor stimulation, Nck SH2 domain couples with phosphotyrosine residues on activated RTKs such as the EGFR (indirectly through the GTPase-activating protein GAP-associated $p62^{dok}$ protein) or PDGFR (directly via PDGFR Tyr751 for Nck1 or Tyr1009 for Nck2) causing targeting of Pak at the plasma membrane (60, 112, 238, 315). Subsequently, Pak encounters membrane-localized GTP-bound Cdc42 and Rac1 GTPases, which cause reciprocal activation of both proteins and leads to reorganization of actin cytoskeleton through activation of the WASP-Arp2/3 complex.

One important question raised from these studies is what are the upstream receptors involved in the control of photoreceptor axon guidance by Dock adaptors? In the past years, numerous guidance receptors were found transducing directional signals in axon. Dr L. Pick's group found that the *Drosophila melanogaster* insulin receptor (DInR) contributes to guidance of photoreceptor cell axons from the retina to the brain during the development of fly visual system (383). The first hint that DInR might be involved in axon pathfinding came when the authors identified Dock as a binding partner for the DInR cytoplasmic domain (383). Both Dock SH2 and SH3 domains were required to form a stable complex with DInR *in vitro* and *in vivo,* independently of Chico, the *Drosophila* insulin receptor substrate (IRS). This prompted

researchers to examine axon projections of DInR inactivated photoreceptor cells in the fly retina. Interestingly, DInR mutant fruit flies displayed pathfinding defects resembling those previously reported in *dock* mutant flies (115, 335). On the basis of these and other findings, they conclude that a Chico-independent DInR-Dock-Pak pathway controls retinal axon pathfinding through reorganization of actin cytoskeleton. However, what remains to be ascertained are the precise determinants in DInR underlying the interaction with Dock and whether mammalian insulin receptor (IR) actions involved in memory, learning and eating behavior utilizes this pathway or the well-described dInR-IRS-PI3K pathway.

The function of Nck in the control of axon and growth cone guidance in the central nervous system is also illustrated by the involvement of Nck adaptors in EphR-ephrin signal transduction. The 14 EphRs identified in vertebrates can be divided in two groups: those activated by cell membrane-bound ephrins-A (EphA1-A8) or ephrins-B (EphB1-B6)(2). Unlike glycosylphosphatidylinositol (GPI) anchored ephrin-A ligands (ephrin-A1 to A6), ephrin-B molecules (ephrin-B1 to B3) are transmembrane proteins with a short, but highly conserved cytoplasmic region. These EphR-ephrin interactions regulate cytoskeleton architecture and cell adhesion mainly through the activation of phosphoinositide-3-kinase (PI3K) (314) and Rho family GTPases (Rho, Rac1 and Cdc42) (434). The EphR-ephrin system has been shown to play important roles during embryogenesis in tissue patterning and organogenesis (somites and notochord) (2, 88). However, little information on the function of this system in adult mice was available until it was recently observed that both EphR/ephrins of the class A and B are highly expressed in pancreatic β-cells and required for glucose-stimulated insulin secretion in mice (211).

EphR binding to Ephrin triggers EphR RTK autophosphorylation on two highly conserved tyrosine residues within the juxtamembrane region (Tyr594 and Tyr600 in human EphB1). Concomitantly, the so-called 'forward' signaling is triggered through the recruitment of multiple SH2 domain-containing proteins such as RasGAP and Nck (97, 162, 388). Nck1 interacts directly with EphB1 (388), but indirectly to EphB2 via $p62^{dok}$ (162). Binding of Nck to EphB1 was found to occur through coupling of Nck SH2 domain to Tyr594 found in the juxtamembrane domain of EphB1 following ephrin-B1 treatment. Importantly, this interaction is

required for ephrin-B1-induced c-Jun terminal kinase (JNK) activation, which is mediated through the activation of the Nck-interacting kinase (NIK) (16, 388). On the other hand, the 'reverse signaling' occurring in response to the engagement of EphBs with ephrin-B ligands induces tyrosine phosphorylation of ephrin short cytoplasmic tail. Signaling from Src-family kinases (SFKs) and the fibroblast growth factor receptor (FGFR) were found to be involved in ephrin-B tyrosine phosphorylation (65, 313). Dr. M. Henkemeyer's group reproducibly identified a single SH2 domain-containing protein corresponding to Nck2 in a modified two-hybrid screen aimed at identifying molecules interacting in a phospho-dependent manner with ephrin B1 cytoplasmic tail. (68). It turned out to be that dominant negative mutant of Nck2 impaired ephrin-B1-induced stress-fiber dissolution by preventing focal adhesion kinase redistribution in cells (68). Few years later, Tyr298 was identified as the residue mediating the physical interaction between Nck2 and ephrin-B1 (30). Due to the high degree of conservation between EphR and ephrin ligands within species, Nck adaptors could represent critical signaling protein transducing signal from other EphR and ephrin ligands *in vivo*.

Lastly, Li *et al.* have shown that Nck1 interacts constitutively with deleted in colorectal cancer (DCC), a receptor for the guidance molecule Netrin-1 in commissural neurons (240). Although the Nck binding site still remains to be identified, it was suggested that a potential PxxP motif found in DCC cytoplasmic domain mediates a constitutive association of Nck to DCC via its first and/or third SH3 domains (240). However, a dominant negative form of Nck1 lacking the SH2 domain blocked netrin-1-induced Rac1-mediated membrane ruffling, suggesting that Nck SH2 domain is also required to induce cytoskeleton changes associated with DCC activation by netrin-1. Overall, these studies clearly demonstrate that Nck is an important regulator of cytoskeleton changes associated with neuronal circuits. Whether this will translate into defects in neuron connectivity in mice inactivated of either *nck1* or *nck2* gene still awaits to be demonstrated.

2.4.4 Nck, PINCH and integrin signaling

The vast majority of Nck SH3 domain-interacting proteins identified so far associate with both Nck isotypes via proline-rich motifs. However, one intriguing case is PINCH-1 (Particularly interesting new cysteine-histidine rich protein-1), a scaffolding protein interacting specifically

with the third SH3 domain of Nck2, but not Nck1, through a non-conventional mode of binding. PINCH proteins (PINCH-1 and -2) are involved in signaling from the integrin-linked kinase (ILK), a focal adhesion ser/thr protein kinase that emerged as a key protein acting at one of the early convergence points of integrin- and growth factor-signaling pathways (230, 450). PINCH-1 is an obligate partner of the integrin-linked kinase (ILK) functioning in the modulation of cell shape, motility, and survival (110). PINCH proteins are LIM domain-containing scaffolds (domains LIM1 to LIM5) that bind ILK and Nck2 through LIM1 and LIM4 domains, respectively (413, 414). However, the interaction between Nck2 and PINCH1 is not readily detectable by co-immunoprecipitation due to its extremely low affinity (Kd ~ 3 mM) (425) as compared to other SH3-mediated interactions displaying Kd within the μM range (271). In fact, Nck2 SH3 domain mode of binding to PINCH-1 depends on determinants distinct from those involved in classical SH3-mediated proteins interaction. Nuclear magnetic resonance (NMR) structure of the focal adhesion complex between PINCH-1 LIM4 domain and the third SH3 domain of Nck2 revealed that an extremely small binding interface as compared to other classical Nck SH3-mediated interactions. Intriguingly, Nck2 SH3 domain residues Asn250 and Asp257, and not the highly conserved Trp234 and Trp235, are directly involved in the binding to PINCH-1 (424). Importantly, expression of wild-type Nck2, but not a PINCH-1 binding-defective D257A point mutant, rescues the cell migration defect observed in $Nck1^{-/-}Nck2^{-/-}$ mouse embryonic fibroblasts (MEFs) (424). This suggests that the PINCH-1-Nck2 interaction could underlie rapid focal adhesion turnover during integrin signaling occurring in cell shape modulation and migration. Although these studies clearly demonstrate that weak protein-protein interactions are relevant in cell biology, the significance of the PINCH-1/Nck2 interaction is not clear since there is no evidence that this interaction exists in lower organisms such *Drosophila melanogaster.* Furthermore, the migratory phenotype of $Nck1^{-/-}Nck2^{-/-}$ MEFs can be rescued by the reexpression of Nck1, which does not interact with PINCH-1 (25). Further investigation of the PINCH-1/Nck2 interaction should help clarify these issues.

2.4.5 Nck and kidney podocyte biology

The glomerular filter of the kidneys has remained one of the most intriguing mysteries in the field of nephrology. How can this filtration unit be used continuously for 70 years or more without becoming clogged? Over the past years, new experimental tools were developed such as

different kidney cell lines, which contributed importantly at unraveling the basic mechanism regulating the filtration function of the kidneys. The glomerular filter is composed of three major components: the fenestrated endothelial cells, the glomerular basement membrane and the podocytes that form multiple interdigitating foot processes (219). Podocytes form an unusual intercellular junction, termed the slit diaphragm that spans the filtration slits through which the primary filtrate passes (114). Genetic analysis of patients affected by inherited glomerular diseases or genetically modified animal models has identified a number of proteins essential for an intact glomerular filtration barrier. Most of the identified proteins, such as Nephrin, turned out to be integral parts of the slit diaphragm within podocytes. Nephrin belongs to the immunoglobulin (Ig) superfamily comprising a large number of proteins that function as receptors as well as cell-adhesion molecules. Similar to other Ig-superfamily receptors, nephrin is 'activated' in response to a extracellular signal, which results in the phosphorylation of its cytoplasmic tail by Src-family kinases Fyn and Yes (223, 234, 427). Tremendous advances in understanding how the actin-based podocyte foot processes are maintained has been made in 2006 when the group of Dr. T. Pawson and Dr. L. Holzman independently found that the signaling adaptor Nck connects Nephrin to the actin cytoskeleton (182, 426). Both studies reported that Src family kinases (Src and Fyn) phosphorylate Nephrin cytoplasmic tail tyrosine residues 1176, 1193 and 1217 inducing Nephrin clustering and binding of the SH2 domain of Nck (Nck1 and Nck2). Interestingly, phosphorylation of Nephrin occurs transiently during glomerulogenesis and podocyte intercellular junction formation and in response to podocyte injury (426). This promotes localized actin polymerization through the mobilization of N-WASp at the plasma membrane and stimulation of Arp2/3-mediated actin nucleation. Moreover, podocyte-specific genetic ablation of both *nck1* and *nck2* genes using podocin promoter-driven expression of the Cre-recombinase results in viable, but growth-retarded mice characterized by glomerular defects by 3.5 weeks of age, leading to extensive proteinuria due to a lack of podocyte foot processes (podocyte effacement) in new born mutant mice. In fact, these pathological manisfestations are also found in Fyn knockout mice and in end-stage kidney diseases (182). As effacement of podocyte foot process typically arises owing to perturbations in the actin cytoskeleton (299), it was inferred that Nck is required for proper organization of the actin cytoskeleton in podocyte.

Although these studies strongly implicate Nck in Nephrin signaling *in vivo*, one should be cautious about the requirement of Nck in Nephrin signaling mainly for two reasons: First, Nck podocyte knockout mice developed by Dr. T. Pawson laboratory survive the neonatal period (at least up to 3.5 weeks of age), whereas the Nephrin knockout mice die within the first 24 hr after birth (410), suggesting that Nephrin has Nck-independent links with the cytoskeleton. Second, direct demonstration of defects in the cytoskeleton architecture in podocyte-specific Nck knockout mice still remains to be demonstrated. Unambiguous demonstration of the functional requirement of the Nephrin-Nck interaction in podocyte biology *in vivo* would be obtained by generating knockin mice in which all three Nephrin tyrosine residues involved in Nck binding are replaced by non-phosphorylatable phenylalanine residues.

2.4.6 Nck and *Escherichia coli* pathogenesis

Although most of the research has focused on the role of protein phosphorylation in mammalian cells, studies on the middle T-antigen of polyoma virus revealed an important role for tyrosine phosphorylation in infection agent biology (92). In a pioneering work by Deibel *et al.* (1998), enteropathogenic *Escherichia coli* (EPEC) was found to use a type III secretion system to translocate a protein called Tir (translocated intimin receptor) into epithelial cells where it becomes tyrosine phosphorylated (77). This human pathogen is part of a larger family of diarrheagenic infectious agents also containing the enterohemorrhagic *Escherichia coli* (EHEC) that forms unique structures called attaching and effacing (AE) lesions on the surface of intestinal epithelial cells. These lesions are characterized by the loss of microvilli and the generation of organized cytoskeleton structures containing filamentous actin beneath sites of bacterial attachment, called actin pedestals (51, 55).

Upon EPEC attachment to intestinal cells, Tir is delivered into cells where it adopts a hairpin loop conformation and serves as a bacterial receptor for the bacterial surface protein intimin that promotes initial adherence of EPEC on target cells (77, 201). The interaction between Tir and intimin is sufficient to induce pedestals formation and can be reproduced experimentally using intimin-coated beads and mammalian cells pre-infected with an EPEC strain that does not express intimin, but does translocate Tir and other effectors. Within the host cell, Tir is phosphorylated on tyrosine 474 (Tyr474) by the host Fyn kinase, resulting in binding

of the Nck SH2 domain, recruitment of N-WASp-Arp2/3, activation of actin polymerization and pedestal formation (126, 325). The importance of this interaction is highlighted by the observation that clustering of Nck by Tir is both necessary and sufficient to initiate localized actin assembly (49, 52). In contrast, Fyn, Nck and N-WASP deficient cells are impaired in their ability to form pedestals in response to EPEC infection (126, 247, 325). However, when *in vivo* intestinal colonization of an EPEC strain expressing a mutant Y474F Tir was addressed in mice, Tir tyrosine phosphorylation, N-WASp recruitment and actin focusing was still observed beneath adhering bacteria despite the absence of Nck recruitment (368). This contrast with the results obtained on the function of Y474 phosphorylation in cell culture, and suggests that other tyrosine residues likely contribute to actin assembly in an Nck-independent manner. Indeed, it was found that Tir Tyr454 is also phosphorylated, although at lower efficiency by Fyn, and promotes actin assembly (50). Surprisingly, these tyrosines differentially contribute to actin polymerization in a fashion reminiscent of actin 'tail' formation mediated by the vaccinia virus envelope protein A36R, which utilizes two similarly spaced phosphotyrosines to simultaneously recruit the Nck and Grb2 adaptors to activate the N-WASp-Arp2/3 complex (109, 363). However, neither phosphorylated Tyr454 nor Tyr474 directly bind Grb2 (50), suggesting that EPEC exploits additional phosphotyrosine-binding adaptors capable of initiating actin assembly via Tyr454. Unexpectedly, when the Y454F and Y474F substitutions are introduced in EPEC Tir, N-WASP recruitment (but not Nck) to pedestals *in vivo* is still observed (368). In contrast EHEC Tir protein neither contains residues corresponding to EHEP Tyr454 or Tyr474 nor any other detectable phosphotyrosines although EHEC is still able to bring reorganization of the actin cytoskeleton of infected cells (51). A systematic analysis of putative EHEC pathogenicity-island resulted in the identification of a proline-rich protein called TccP/EspF$_u$, which is translocated by the type III secretion system and triggers actin polymerization through N-WASp recruitment in a Nck-independent manner (53, 429). In the future, it will be interesting to determine whether these products encoded in bacterial genomes are required for EPEC- and EHEC colonization in mice.

2.4.7 Nck and mRNA translation

As highlighted above, numerous effectors of Nck regulate actin cytoskeleton dynamics in response to plasma membrane receptor activation. However, our group reported a novel function

for Nck adaptors in regulating initiation of mRNA translation through the modulation of eukaryotic initiation factor 2 (eIF2) activity (197, 198). eIF2 is a heterotrimeric complex (α, β, and γ-subunit) that drives the initiation of mRNA translation by carrying out the delivery of the methionyl-initiator tRNA to the 40S ribosomal subunit (153). We found that Nck, but not Grb2 or Crk, directly interacts with the β-subunit of eIF2 and that this interaction increases cap-dependent and cap-independent mRNA translation (198). Importantly, this effect is dependent on the functional integrity of the first and the third SH3 domains of Nck, those involved in the binding to eIF2β (197). Interestingly, we observed that a significant amount of Nck proteins localized at the endoplasmic reticulum (ER) using *in vitro*-based cell fractionation (289), suggesting that the binding of Nck to eIF2β might be linked to the ability of the ER to control secretory protein synthesis. Phosphorylation of eIF2α on Ser51 by the ER transmembrane protein PERK is a protective signaling event accompanying the activation of the Unfolded Protein Response (UPR) in response to accumulation of improperly synthesized secretory proteins in the ER lumen (see Chapter I section 3 for details). This prevents recycling of eIF2 into its active GTP-bound form by the nucleotide exchange factor eIF2B, transiently attenuating general mRNA translation and decreasing the synthesis burden on the ER (350). We observed that Nck overexpression decreases the phosphorylation of eIF2α on Ser51 and the attendant inhibition of translation in cultured cells exposed to chemical inducers of ER stress (197). Importantly, this correlated with reduced levels of PERK Thr980 phosphorylation, an event normally accompanying PERK kinase activation (197). On the other hand, MEFs derived from the $Nck1^{-/-}Nck2^{-/-}$ knockout mice show decreased translational activity, which correlates with increased levels of eIF2α phosphorylation (197). Furthermore, we found that the levels of Nck represent an important regulatory element controlling the ability of cells to overcome stress associated with the accumulation of misfolded proteins in the ER. Indeed, overexpression of Nck1 sensitizes cells to death in response to ER stress (197).

In collaboration with Dr. E. Chevet at McGill University, we also found that Nck adaptors regulate signaling from IRE1, an ER transmembrane protein that functions as a sensor of misfolded proteins in the ER (289). Nck binds both IRE1α and IREβ through its first and third SH3 domains, respectively. Interestingly, this regulates IRE-1-mediated ERK-1 activation and survival in response to the protein misfolding inducer azetidine-2-carboxylic acid (Azc) (289).

Together, these studies demonstrated that Nck, in addition to transducing signals from activated plasma membrane receptors, also transmits signals from intracellular organelles. Importantly, such spatio-temporal regulation could have clear repercussions on how we model signaling pathways utilizing such SH2/SH3 adaptors proteins. Intriguingly, up to now, no function has been associated to the SH2 domain of Nck in ER signaling. It will be interesting to address this issue and determine whether the function of Nck at the ER is still obeying to the rule governing signal transduction by activated RTKs, that is: coupling of phosphotyrosine residues to SH2 domains allowing recruitment of effectors through SH3 domains.

As reviewed here, numerous Nck-interacting proteins are intimately connected to reorganization of the cytoskeleton and converge on the activation of the Arp2/3 complex. What now seems a central theme in Nck physiology is their ability to regulate axon pathfinding by providing the driving force within the growth cone required for proper neuron connectivity. Whether all Nck binding partners function to modulate actin polymerization still remains to be determined. Studying Nck effectors involved in RNA metabolism such as the nuclear RNA binding protein Sam68 (225) or eIF2β (197, 198) might open new avenues of research and provide further information on the various processes regulated by Nck adaptors in cells. In fact, recent evidence supports that protein synthesis can occur in the growth cone themselves, remote from the cell body. Whether the function of Nck in growth cone also relates to their ability to modulate mRNA translation still needs to be addressed. Finally, the real challenge now is to address the significance of these interactions *in vivo*. The availability of Nck knockout mice should significantly contribute to decipher the physiological role of Nck adaptors.

3 SIGNALING FROM THE ENDOPLASMIC RETICULUM

3.1 Quality control in the endoplasmic reticulum

The ER represents the preponderant membranous system of eukaryotic cells. This network of closely interconnected membrane vesicles is linked with essentially all other cellular organelles including the nucleus. The ER is subjected to important rearrangements during the cell cycle. For instance, recent evidence demonstrate that the ER network is not disassembled into vesicles during mitosis, but rather is divided between daughter cells in cytokinesis (96). Two

different ER domains have been described: the smooth (SER) and rough ER (RER). Both can be distinguished visually in electron microscopy due primarily to the presence of bound ribosomes on the RER, but also at the structural levels where segregation of a certain amount proteins are responsible of specifying the identity and function of the SER and RER (430). As highlighted in various textbooks and reviews, the RER is the major site of protein synthesis designated for secretion and targeting at the plasma membrane or lysosomes. The transport of proteins across the ER membrane relies on the presence of a signal peptide in secretory proteins. Guiding and docking of the ribosome synthesizing the ER signal peptide is accomplished through a small RNA molecule called SRP or signal-recognition particle. The SRP attaches to the signal peptide as soon as it emerges from the ribosome and docks with the SRP receptor on the cytosolic side of the ER membrane where translocation of the polypeptide into the ER lumen is initiated. The RER provides an oxidative environment highly optimized for oxidation of cysteine residues required for intramolecular disulfide bond formation in nascent polypeptide chains (412). Consequently, the different redox and ionic milieus inside the cytoplasm and the ER have necessitated the existence of distinct chaperones networks controlling protein folding in both environments. In the ER, folding and modification of proteins are ensured by the presence of a large number of chaperone proteins and lectin sugar-binding proteins (352). In addition, the ER is the focal point for phospholipids and steroids synthesis (306), the storage of calcium ions and their regulated release into the cytosol (106). Therefore, it is not surprising that the ER homeostasis needs to be tightly regulated by means of different integrated systems assuring proper function of this organelle.

Proteins synthesized in the ER encounter quality control checkpoints that verify their aptness to proceed in the secretory pathway. For example, the calnexin (Cnx) / calreticulin (Crt) chaperones system assures proper folding of newly synthesized glycoproteins (279). If incompletely folded, the glycoprotein becomes a substrate for UDP-glucose:glycoprotein glucosyltransferase (UGGT), which re-attaches a single glucose only to non-native glycoprotein. This signals re-binding to Cnx/Crt and the cycle continues until a native conformation is achieved or until degradative processes are engaged. In this manner, molecules undergoing folding and assembly are kept out of the exocytic pathway until maturation is complete.

The flux of proteins into the ER is variable since it changes drastically depending on cellular demands. In such dynamic situations, the capacity of the ER lumen to synthesis and fold secretory polypeptides is adjusted through the activation of signaling pathways that maintain both the processivity and fidelity of the ER. Together, these signaling events represent another quality control system of the ER and are referred to as the Unfolded Protein Response (UPR) (Fig. 2) (136, 317). This cellular response is initiated in response to the accumulation of improperly folded proteins (i.e. ER stress). The UPR was first identified in monkey kidney cells (217), but it is now recognized that some elements of this cellular response are conserved in all eukaryotes studied to date. Two functional components of the UPR have been described. The first one, described in yeasts, relates to the coordinated transcriptional upregulation of ER luminal chaperones in response to ER stress (217). This long-term transcriptional program culminates in increasing the folding and oxidative capacity of the ER. The second component of the UPR relates to the transient inhibition of protein synthesis, which is believed to reduce the load of client proteins that enters the ER in stress conditions. (140, 142). Together, these two components of the UPR contribute at increasing the secretory function of the ER and alleviate stress. It now recognized that a broad spectrum of insults converge on the activation of the UPR. These include: nutrient deprivation (298), viral infection (149), alteration in oxidation-reduction balance (72, 412), and calcium stores depletion (316). Importantly, these stresses cause perturbation of the protein-folding environment in the ER owing to an imbalance between the load of client proteins facing the ER and the organelle capacity to cope with that load. In situation where the ER homeostasis cannot be re-established, cell death pathways are activated to protect the organism from the deleterious effects of protein misfolding in the ER. In the following lines, a detailed review of the UPR components and its effectors will be performed. Emphasis will be given to the physiological roles associated with the UPR, especially in relation to recent evidence pointing to a critical role for the UPR in pathological states such as diabetes.

3.2 Signal transducers of the Unfolded Protein Response

Over the past years, intensive efforts have been put together to delineate the components and effectors of signaling pathways activated in response to ER stress. What became evident was that accumulation of improperly folded polypeptides inside the ER lumen modulates the activity of different transmembrane proteins that signal to the cytosol and lead to important changes in

gene expression. As illustrated in Fig. 2, three ER stress transducers have been identified and define the UPR: 1) inositol-requiring protein-1 (IRE1); 2) activating-transcription factor-6 (ATF6); and 3) protein kinase RNA (PKR)-like ER kinase (PERK). Experimentally, ER stress can be induced by treating cells with pharmacological agents such dithiothreitol (DTT), which disrupts or prevents protein disulfide bonding; thapsigargin (Tg), an inhibitor of the ER Ca^{2+}-dependent ATPase; or tunicamycin (Tm), an inhibitor of protein glycosylation. However, ER stress sensors display distinct sensitivities toward different forms of ER stress. For instance, PERK is preferentially activated by Tg and DTT, while IRE1 is more sensitive to stress induced by DTT treatment (89).

3.2.1 Signaling by IRE1

The Ire1p protein was originally identified in a genetic screen aimed at identifying genes that regulated ER stress-mediated chaperones induction in the budding yeast *Saccharomyces cerevisiae* (70, 280). *hac1p* and *rlg1p* genes were also identified using similar screens. In fact, it turned out the Ire1p, Hac1p and Rlgp1 function in a common linear signaling pathway that governs a transcriptional program regulating the expression of Kar2 and Pdi1, the yeast counterparts of the luminal chaperones glucose-regulated protein 78/immunoglobulin binding protein (Grp78/BiP) and protein disulfide isomerase (PDI), respectively (95, 130). The importance of this pathway is demonstrated by the fact that in yeast, Ire1p is the sole ER stress sensor protein that signals the transcriptional reprogramming required to enhance the function of the ER in response to stress. A few years later, screening of a human fetal liver cDNA library with a probe corresponding to Ire1p led to the identification of the mammalian orthologs of Ire1p, called IRE1s (408). Two genes encoding IRE1 proteins are found in mammals: *ire1α* (408), and *ire1β* (437). Unlike IREβ whose expression is restricted to epithelial cells of the gastrointestinal tract (19), IRE1α is ubiquitous and shows high levels of expression in the pancreas and placenta (408, 420). IRE1 is a type I ER transmembrane protein composed of a N-terminal luminal domain (NLD) linked to a cytoplasmic segment containing ser/thr kinase and RNAse L-like endoribonuclease domains. For years, the regulatory mechanism controlling the activation of IRE1 in cells was thought to reside mostly in the binding of the BiP chaperone to the NLD of IRE1. BiP-bound IRE1 correlated with IRE1 hypophosphorylation and inactivation, while BiP-free IRE1 correlated with IRE1 hyperphosphorylation and activation (20, 303). Based

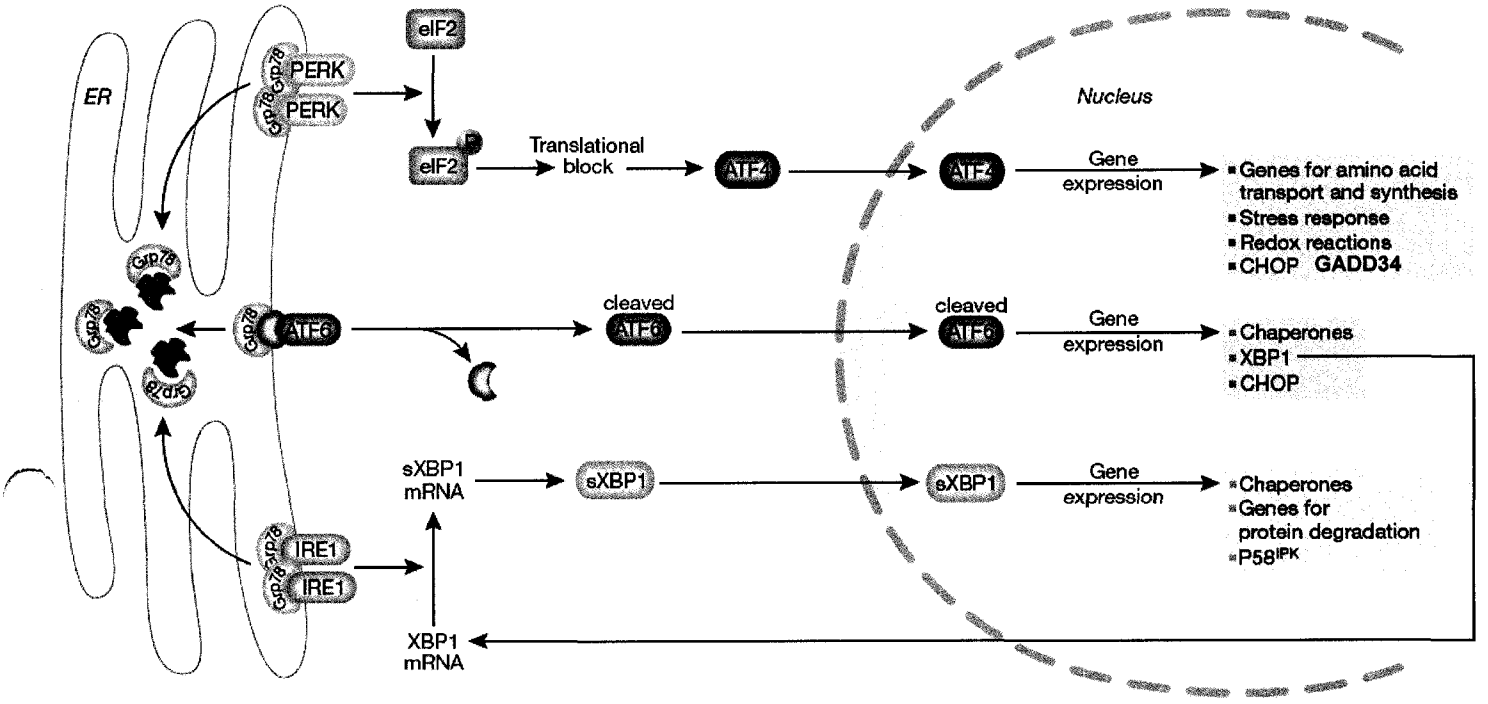

Figure 2. ER stress and the Unfolded Protein Response (UPR)
Adapted from Szegedzi *et al.* (2006) EMBO J. 7: 880-885

on these observations, it was concluded that BiP dissociates from IRE1 in response to ER stress to allow IRE1 dimerization and activation. However, mutants of Ire1p deleted of its BiP binding site were identified and still retained their ER stress-inducibility in yeast, suggesting that BiP is not the principal determinant regulating IRE1 activity (204, 301). Recently, the IRE1 NLD crystal was resolved and helped refine the current model of IRE1 activation. It was proposed that direct binding of misfolded proteins to IRE1 NLD, rather that dissociation of BiP, drives IRE1 dimerization through a MHC groove present at the interface of each dimer (71, 474). ER stress-induced dimerization of IRE1 results in *trans*-autophosphorylation of IRE1 via its cytosolic kinase domain, resulting in stimulation of its endoribonuclease activity and signaling (Fig. 2) (372, 445).

The IRE1 signaling pathway is highly conserved throughout organisms (286), but it is still unknown which effectors of IRE1 kinase catalytic activity are involved in propagating signals from stressed-ER. On the other hand, several groups characterized the endoribonuclease activity of IRE1 and found the Hac1p/XBP1^{u} mRNA as a proximal effector of IRE1 RNAse domain. IRE1 cleaves two sites within the XBP1^{u} (uninduced) mRNA leading to the removal of a 26 nucleotides intron sequence that initiates a unconventional splicing reaction producing a functional transcriptional regulator called XBP1^{s} (spliced) (48, 229, 460). This basic region-leucine zipper (bZIP) transcription factor XBP1^{s} is selectively expressed in ER stress conditions and recognizes *cis*-acting ER stress response elements (ERSE) in the promoter of ER resident chaperone genes including BiP, PDI and EDEM (227, 461). However, recent data show that the protein encoded by the XBP1^{u} mRNA is detected in the recovery phase of the UPR and plays an important role by acting as a dominant-negative regulator of XBP1^{s} transcriptional activity (463). In a genome-wide screen using DNA microarrays, Hollien *et al.* found that IRE1 regulates the degradation of a subset of mRNA encoding transmembrane protein such as the SPARC glycoprotein, or other secreted proteins that momentarily traffic in the ER before reaching their final destination (163). This repressive response is well suited to relieve acute ER stress, since it specifically prevents the synthesis of proteins that do not reside in the ER and increase ER function.

In yeast, many of the genes upregulated by the Ire1p-Hac1p signaling pathway encode rate-limiting enzymes involved in lipid biogenesis (409). Yeast strains deleted of Ire1p or Hac1p stop to grow within 5 hr of inositol depletion, suggesting that UPR-mediated phospholipid biosynthesis in essential for yeast survival (69). In fact, this is also true for metazoans. When engineered to express $XBP1^s$, NIH 3T3 fibroblasts show increased synthesis of phosphatidylcholine (PtdCho), the primary phospholipid of membranes, which augments volume and surface of the RER (386). Importantly, $XBP1^s$ expression stimulates the activity of enzymes (CK, CCT and CTP) involved in the cytidine diphosphocholine pathway of PtdCho biogenesis. $XBP1^s$ provide the first example of a transcription factor being sufficient to induce phospholipid biosynthesis and ER expansion in mammalian cells. This model is entirely consistent with the profound defects in ER development observed in XBP1-deficient- secretory cell (226).

Great strides have been made in the past few years in the understanding of complementary pathway activated in response to ER stress, called ER-associated degradation (ERAD). This evolutionary conserved cascade is involved in the retranslocation of misfolded proteins in the ER to the cytoplasm where they are ubiquitinated and degraded by the proteasome (327, 348, 432). Since the ERAD capacity is easily saturated in ER-stressed cells, some components of the ERAD machinery must be induced by the UPR in order to maintain the degradation activity (409). The IRE1-$XBP1^s$ signaling pathway was found to increases the expression of molecules such as EDEMs (ER degradation-enhancing α-mannosidase-like proteins - EDEM 1, 2, and 3) that promote recognition of substrates for degradation (166, 459). EDEM is a ER type II transmembrane lectin-like protein whose luminal domain shows significant homology to α1,2-mannosidase, but lacks such enzymatic activity. Results have demonstrated that overexpression of EDEM directs misfolded glycoproteins to the ERAD pathway (166, 177). The AAA-ATPase p97/VCP (also termed Cdc48p in yeast) is considered to be a key component for protein dislocation from the ER (179, 333, 456). One question that arised in the past years was what links EDEMs to p97/VCP? The answer to this question came with the identification of ER transmembrane Derlin proteins (Derlin 1, 2 and 3). These proteins are transcriptionally induced by $XBP1^s$ in stressed cells with a kinetic identical to the induction of EDEMs (242, 297). Downregulation of Derlin 2 and 3 by RNA interference (RNAi) impairs degradation of a misfolded mutant of the α1-proteinase inhibitor, a luminal protein that is

recognized by EDEMs and targeted for degradation by the ERAD pathway (166, 380). Therefore, the current model suggests that ERAD substrates are sequentially passed along by EDEMs, Derlins and the p97/VCP molecular complex allowing their dislocation and degradation by the proteasome. Given that only a subset of substrates are processed by ERAD, future investigations will be needed to understand how this selectivity is assured and whether it is regulated by specific determinants within substrates themselves.

Although the IRE1-XBP1^s axis seems to have pro-survival effects through the induction of ER chaperones, overexpression of IRE1 in cells results in apoptotic cell death, thus demonstrating that IRE1 has both anti- and pro-apoptotic properties. Mammalian IRE1 proteins are known to mediate the transient activation of the JNK kinase that occurs in response to overwhelming perturbations in ER function (Fig. 3) (420, 457). This proceeds through the recruitment of the adaptor protein TRAF2 to oligomerized IRE1 cytoplasmic domains leading to ASK1-dependent JNK activation (291). Moreover, IRE1-mediated clustering of TRAF2 has been linked to the activation of ER-localized caspase-12 in mice, a regulator of the executioner caspase-3 (284, 457). Since, no ortholog of caspase-12 is found in humans, it is believe that other caspases, such as caspases 7 and 9 might substitute for the loss of caspases-12 to initiate program cell death (394). In addition to their localization at the mitochondria, pro-apoptotic Bcl-2 family members Bax and Bak localize at the ER and modulate the UPR by directly interacting with IRE1α cytoplasmic segment (155). Bax$^{-/-}$Bak$^{-/-}$ double knockout mice respond abnormally to tunicamycin-induced ER stress in the liver and this correlates with reduced expression of XBP1^s and BiP, reduced JNK activation, and decreased number of apoptotic cells (155). Therefore, Bax and Bak represent important regulators of programmed apoptosis in cells undergoing unrecoverable ER stress. Furthermore, ER stress-induced Ca^{2+} mobilization results in secondary activation of mitochondrial Bax and Bak and execution of apoptosis (15). Importantly, these events are temporally coordinated with other death-inducing signals coming from other ER stress sensors (see Chapter I, section 3.2.5).

3.2.2 *In vivo* functions of IRE1 signaling

An important step in the characterization of cellular machineries transducing signals from stressed-ER is the generation of mice genetically inactivated in components of UPR. Targeted

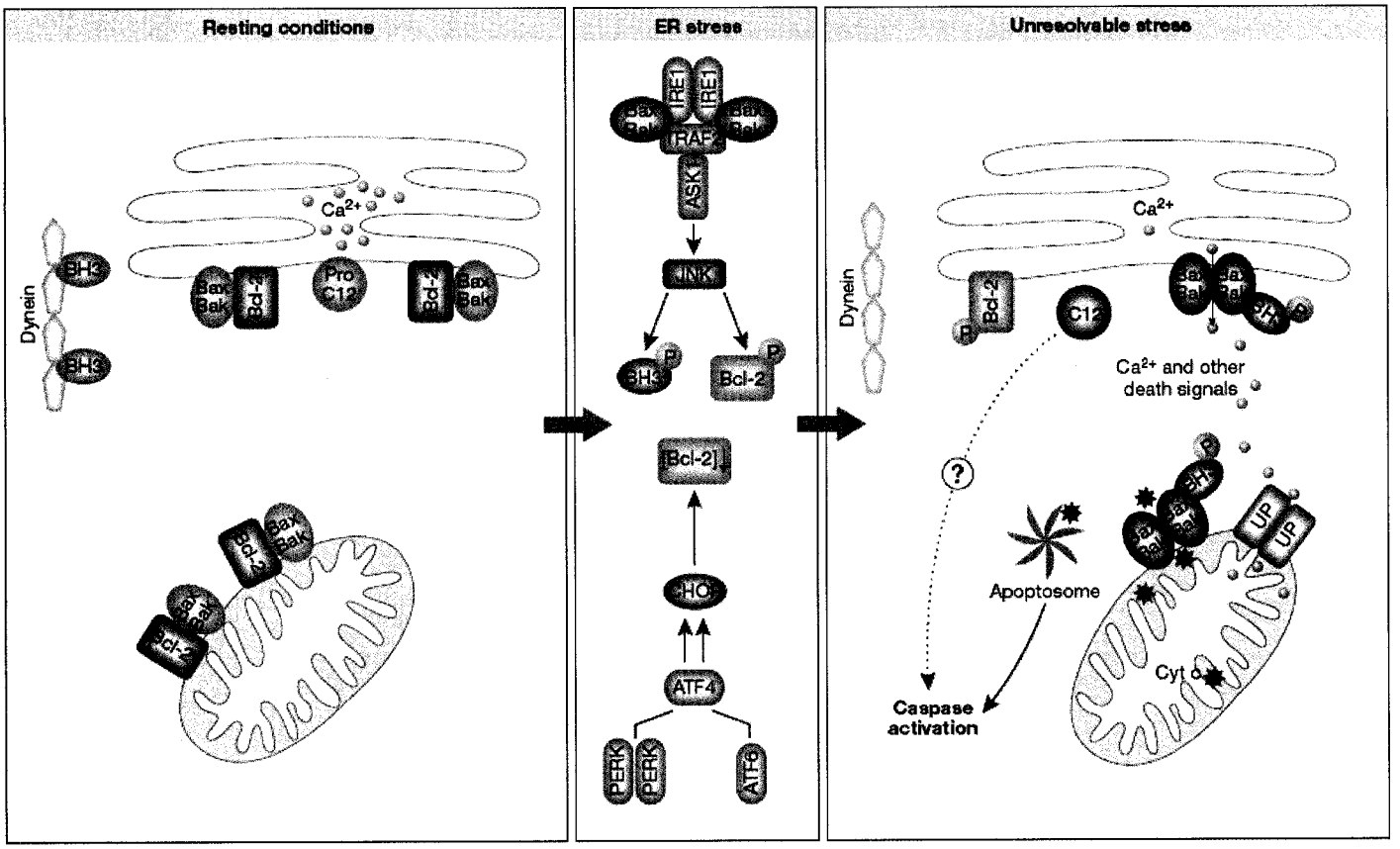

Figure 3. ER stress-induced apoptosis
Szegedzi E. *et al.* (2006) EMBO J. 7:880-885

deletion of *ire1* and *xbp1* genes in mice demonstrated that these proteins are particularly important during development as both IRE1α$^{-/-}$ and XBP1$^{-/-}$ embryos die at a similar gestation age (embryonic day 10)(268, 337, 420). However, genetic rescue experiments demonstrated that both IRE1α and XBP1^{s} play important physiological roles in secretory cells such as hepatocytes (336), salivary glands exocrine cells (226) and plasma B cells (173, 337, 471). Enormous amount of information on the role of XBP1^{s} in plasma B cells function have been obtained over the past years. Briefly, as B cell differentiation proceeds, IL-4 drives the expression of XBP1^{s}, which is required for lineage commitment in later stages of differentiation. At these stages, cells acquired an extensive ER that allows the production and secretion of extensive amount of immunoglobulin (Ig). This Ig production feeds-forward on the IRE1-XBP1^{s} signaling due to the inability of the ER to cope with such substantial Ig synthesis. Based on these observations, it was concluded that IRE1α-mediated XBP1 splicing controls a transcriptional network required for the differentiation and proliferation of secretory plasma B cells.

Other murine phenotypic analyses contributed considerably to the burst of information demonstrating a role for the IRE1 signaling pathway in regulating glucose metabolism. In response to elevation of glycaemia, pancreatic β-cells increases the rates of insulin biosynthesis and secretion to promote glucose uptake by peripheral tissues (357). Recently, Dr. F. Urano's group found that IRE1α is an important regulator of the glucose-stimulated insulin biosynthesis in C57BL/6 mice (245). Transient exposure of isolated pancreatic islets of Langerhans to high glucose concentration (16.7mM) results in a proportional increase in the phosphorylation of IRE1 and biosynthesis of insulin. Furthermore, depletion of IRE1α in the INS-1 pancreatic β-cell line decreased insulin biosynthesis, but not glucose-induced insulin secretion (245). Importantly, this effect is dependent on the kinase but not the endoribonuclease activity of IRE1α, since XBP1 mRNA splicing is not modulated by transient exposure to glucose. On the other hand, chronic exposure to glucose caused ER stress and activated both the kinase and endoribonuclease activity of IRE1α, leading to decreased insulin biosynthesis (245). These key findings describe a physiological regulatory mechanism by which the selective increase of IRE1α kinase activity contributes to insulin biosynthesis. However, under pathophysiological conditions such as insulin resistance where chronic hyperglycemia is instituted, both the kinase and endoribonuclease activities of IRE1α are stimulated due to the presence of ER stress, which could contribute to

pancreatic β-cell failure. Supportingly, the translational arm of the UPR was also found to be a critical regulator of insulin biosynthesis and pancreatic β-cell function (138)(see section 3.2.6). Crosstalks between IRE1 and IR signaling pathways have also been described and shown to play a critical role in determining the sensitivity of insulin in high fat diet (HFD)-induced obese mice (311)(see section 5.2 for details). Overall, the IRE1-XBP1 signaling pathway is determinant during embryogenesis and in adults mostly through its ability to transduce physiological ER stress signals that arise in situations of high demands in protein synthesis and secretion.

3.2.3 Signaling by ATF6 and ER bZIP factors

Unlike the yeast *Saccharomyces cerevisiae* in which Ire1p represents the sole ER stress sensor protein, metazoans acquired other ER stress sensing proteins, such as ATF6 (148). ATF6 is part of a growing family of ER-localized bZIP transcription factors containing CREB4 (391), Luman (252), OASIS (209), CREB-H (305) and BBH2F7 (210), that respond to the accumulation of misfolded protein in the ER (391). ATF6 is synthesized from two genes (*atf6α* and *atf6β*) that encode a precursor of 90 KDa and 110 KDa, respectively. The inactive precursor is ubiquitous. ATF6 is tethered to the ER membrane by a transmembrane domain and contains a stress-sensing portion in its C-terminus that projects into the ER lumen. In fact, this later portion shows a high degree of identity with IRE1 (and PERK; see Chapter I section 3.2.5) NLD. In unstressed cell, ATF6 is associated with BiP through its luminal domain and retained at the ER (374, 375). In response to ER stress, BiP is released from ATF6 thereby exposing a localization signal that triggers transport of the protein to the Golgi, and its processing by the site-1 and site-2 proteases (S1P and S2P) (374, 455). This results in the release of a N-terminal 50 KDa product that migrates to the nucleus and activates ERSE-regulated UPR genes (458, 461, 462). Such regulatory mechanism, known as regulated intra-membrane proteolysis (RIP), is also the basis of activation of sterol regulatory element binding proteins (SREBPs). These transcription factors are also found at the ER, but are exclusively involved in cholesterol (sterol) sensing and biosynthesis (132).

ATF6 was found to upregulate ER chaperone genes such as *bip*, *grp94*, and *pdi* (148), but also to feed-forward into the UPR by transactivating the *xbp1* gene (229, 460). Together, these observations indicate that during mammalian evolution, ATF6 signaling overlapped with that of

IRE1/XBP-1 to allow cells cope more efficiently with ER stress. On the other hand, why did evolution necessitate two *atf6* genes that redundantly control gene transcription? Comparison of the transactivation of a BiP promoter-driven Luciferase reporter gene (BiP-Luc) by ATF6α and ATF6β clearly demonstrated that both factors exhibit paralog-specific characteristics: ATF6α is a strong, but rapidly degraded ERSE gene inducer, while ATF6β, is a weak but slowly degraded ERSE gene inducer (403, 404). Supportingly, ATF6β inhibited ATF6α-mediated transactivation of an ERSE reporter gene in a dominant-negative manner (402, 403). Based on these results and the fact that ATF6α is induced prior to ATF6β during the UPR (147), it suggests that the relative levels of ATF6 proteins regulates the strength and duration of ATF6-dependent ERSE gene transcription.

3.2.4 *In vivo* function of ATF6 and ER bZIP factors

Unlike other stress sensor proteins, limited amount of information is available on the function of ATF6 and other RIP-regulated ER transcription factor in mice. Genetic inactivation of *atf6* genes in mice has not been reported yet, and would therefore represent an important step toward understanding the processes regulated by these transcription factors. On the other hand, Dr Kaufman's group found that CREB-H plays an important role in linking ER stress in the liver to the instigation of the systemic inflammatory component of innate immunity, called the acute phase response (APR)(111). To explore the physiological function of CREB-H, they silenced CREBH expression in mice using a lentivirus-based system driving expression of CREBH-specific hairpin small interfering RNAs (shRNAs) in single-cell mouse embryo. Gene chip analysis performed on liver derived from CREB-H knockout mice revealed that this factor regulates genes involved in the APR, such as CRP (C-reactive protein) or SAP (serum amyloid P-component) (470). Although liver development occurs normally in these mice, lower levels of SAP and CRP are detected in CREB-H RNAi mice challenged with potent inducers of the APR, such as LPS (lipopolysaccharide) or Tm (470). Interestingly, dominant-negative mutants of ATF6α and ATF6β abrogated CREB-H-mediated transactivation of SAP and CRP promoters, suggesting that the CREB-H and ATF6 signaling pathways converge in the APR. Importantly, this study reveals an unprecedented link between the development of ER stress in the liver and initiation of an acute inflammatory response. This may result in the development of novel therapeutics targeting the APR, which is now appreciated as a major contributor of numerous

inflammatory diseases such as atherosclerosis (135, 292, 318).

3.2.5 Signaling by PERK

Initial studies on the Ca^{2+} storage function of the ER revealed that Tg, an inhibitor of ER SERCA (Sarco/Endoplasmic Reticulum Ca^{2+}-ATPase)(449) and chelators of Ca^{2+} drastically reduced rates of proteins synthesis within minutes of treatment in cells (41, 42). Concomitantly, investigations aimed at determining which step(s) of mRNA translation is (are) inhibited by these agents were launched by many groups. What became evident was that Ca^{2+}-dependent regulation of translation affected polypeptide chain initiation, but not elongation or termination (62). Supportingly, Tg- and DTT-treated cells displayed increased phosphorylation of the α-subunit of eukaryotic initiation factor 2 (eIF2α) (44, 330), pointing to a cellular protein kinase mediating ER stress-induced inhibition of mRNA translation.

eIF2 is a GTP-binding multimeric complex consisting of three subunits termed α, β and γ. These show a high degree of conservation with the equivalent subunits of the yeast *Saccharomyces cerevisiae* eIF2 complex, underscoring their functional importance (99). As depicted in Fig. 4, the primary role of eIF2 is to deliver the Methionyl (Met) $tRNA_i$ to the 40S ribosomal subunit to form the eIF2·GTP·Met $tRNA_i$ 43S ternary complex (154). Joining of the mRNA to the 40S subunit is promoted by eIF3 and eIF4 factors. The factor eIF4E directly binds the m^7GpppX cap on eukaryotic mRNAs and through an interaction with the N terminus of eIF4G, recruits the cap-binding complex eIF4F, a heterotrimeric complex composed of eIF4E, eIF4G, and the DEAD-box RNA helicase eIF4A (121). The eIF4A is taught to unwind RNA secondary structures near the 5' end of the mRNA and allow the 40S subunit to scan down the mRNA searching for the AUG start codon (216). Upon AUG codon recognition, the GTP associated with eIF2γ is hydrolyzed to GDP in a reaction that requires the GTPase-activating protein eIF5. eIF5B catalyzes joining of the 60S ribosomal subunit, thereby resulting in the formation of the 80S complex and initiation of protein synthesis. The GDP-bound eIF2 complex that is released after GTP hydrolysis and 80S formation is recycled to eIF2-GTP by the action of eIF2B, a five-subunit guanine exchange factor (442). This allows retargeting of the Met $tRNA_i$ to

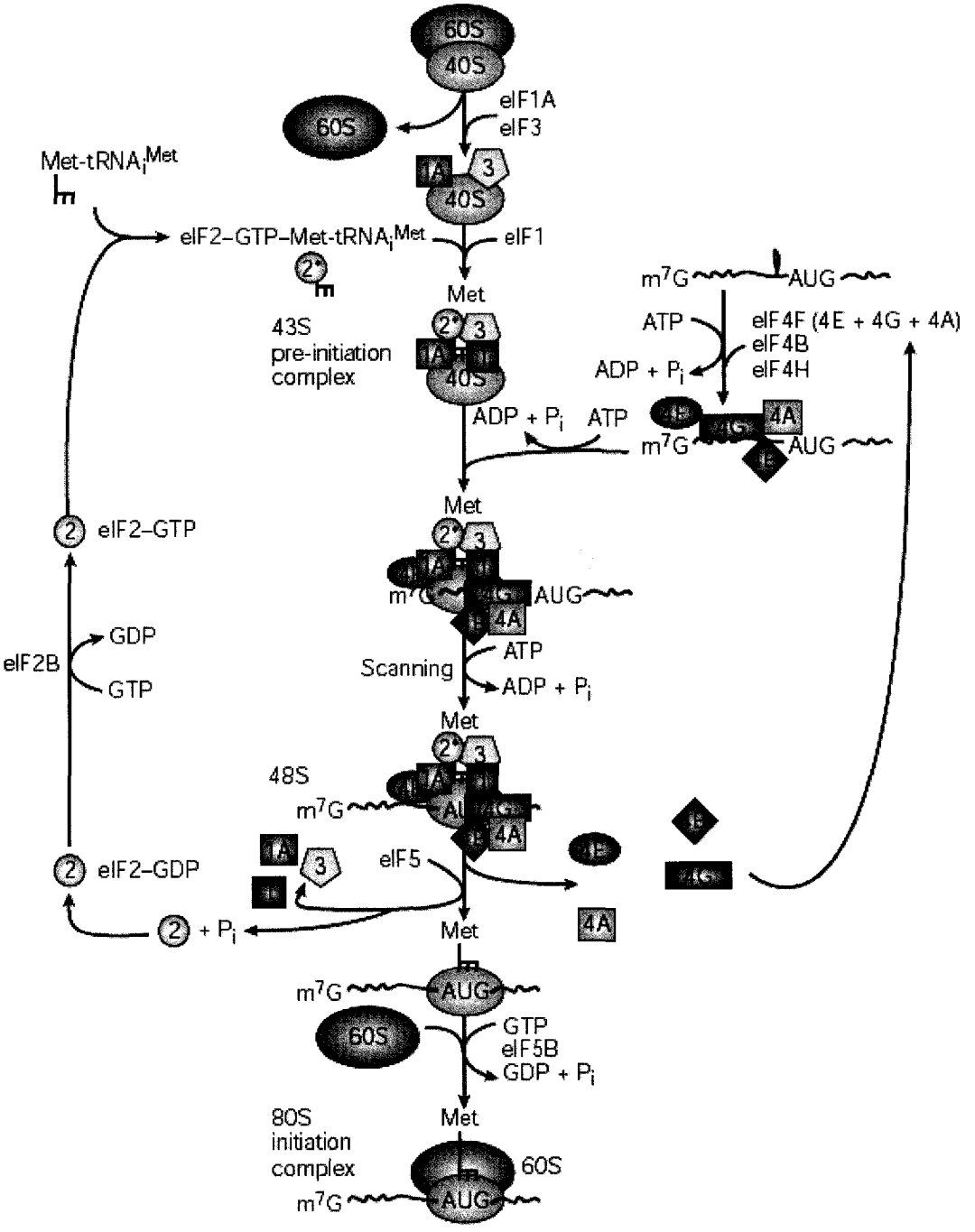

Figure 4. Translation initiation in eukaryotes
Holcik M. *et al.* (2005) Nature Rev.Mol.Cell.Bio. 6: 318-327

the 40S ribosomal subunit and a new round of translation initiation. Phosphorylation of eIF2α on Ser51 represents one of the best-characterized mechanisms of regulation of initiation of translation. This converts eIF2 from a substrate to a competitive inhibitor of eIF2B, thus preventing formnation of the 43S preinitiation complex and inhibiting global protein synthesis (154, 331).

eIF2α phosphorylation is induced in response to a growing list of stressful stimuli. To date, four eIF2α kinases have been identified in mammals: 1) PKR (dsRNA-activated protein kinase), a molecule activated by dsRNA during viral infection (43); 2) HRI (heme regulated inhibitor), a protein coupling mRNA translation with heme availability in erythroid cells (58); 3) GCN2 (general control non-derepressible-2), a kinase activated in response to amino acid deprivation (443); and 4) PERK (PKR-like endoplasmic reticulum kinase), a molecule activated upon accumulation of improperly folded secretory proteins in the ER (referred as to ER stress) (142, 378). In contrast to mammals, GCN2 represents the unique eIF2α kinase in yeasts. Past years revealed that inhibition of translation through the phosphorylation of eIF2α on Ser51 also occurs in cells exposed to reduced oxygen supply (hypoxia) (215), ultra-violet irradiations (80), proteasome inhibitors (180) or oxidants. In some cases, however, the identity of the kinase responsible is still debated. Stresses converging on the phosphorylation of eIF2α result in the sequestration of mRNA and eukaryotic translation initiation factors into cytoplasmic structures, termed stress granules (7, 8, 205). These contain many, if not all, of the components of the 48S preinitiation complex, but no 60S ribosomal subunits (199, 200). It now recognized that stress granules represent stalled translation initiation complexes that could be eventually redirected to P bodies for mRNA degradation by decay factors (377). Although some of these eIF2α kinases, in particular PKR, may have additional substrates and therefore exert additional effects, the phosphorylation of eIF2α that accompanies their activation leads to similar cellular effects, and was thus termed the integrated stress response (ISR) (349).

The identification of PERK by Harding *et al.* in 1999 represented a major advance in understanding how ER homeostasis is controlled as it uncovered a third ER stress sensor in metazoans that links perturbation of ER environment to translation rates (142). PERK is a type I transmembrane ER resident protein encoded by a single gene in mammals. It is composed of a

N-terminal luminal domain sensitive to upstream ER stress signals and a C-terminal ser/thr kinase domain facing the cytoplasm that phosphorylates eIF2α (142, 378). The primary structure of PERK kinase domain shows a high degree of identity with other eIF2α kinases, with PKR being the closest relative (40% of identity). Although the stress-sensing domain of PERK is distantly related to that of IRE1, both domains are interchangeable and can function as replacements for yeast Ire1p NLD (246). This demonstrates that secondary structures implicated in unfolded protein recognition and dimerization are conserved in PERK and IRE1 (71, 474). PERK is maintained inactive by the binding of the ER chaperone BiP to its luminal domain. When the folding capacity of the ER is exceeded, BiP is released from PERK and 'chaperonizes' misfolded proteins; loss of BiP binding correlates with PERK dimerization, *trans*-autophosphorylation, and phosphorylation of eIF2α on Ser51. This results in a transient attenuation of protein synthesis and decreased client protein translocation into the ER lumen (Fig. 2). Since PERK activation and eIF2α phosphorylation occurs within minutes following the development of ER stress (~3-5 min, personal observation), while activation of UPR target genes does not begin until 1–2 hours later, it suggests that the PERK signaling pathway is likely to be the first line of defense against ER stress. The importance of this regulatory mechanism is illustrated in MEFs inactivated of the *perk* gene or harboring a non-phosphorylatable Ala residue at position 51 (S51A) in eIF2α. These MEFs lines show hypersensitivity to ER stress agents due to their inability to phosphorylate eIF2α and inhibit general mRNA translation (140, 365). Therefore, active repression of protein synthesis protects cells against protein malfolding during ER stress, demonstrating that eIF2 phosphorylation is cytoprotective. Conversely, eIF2α phosphorylation was found to contribute to apoptosis in situation where perturbation and overload of ER-folding environment cannot be surmounted (394). However, what determines the apoptotic threshold of eIF2α-dependent signaling is poorly understood (see below).

Since its discovery, PERK-mediated phosphorylation of eIF2α was found to cause a rapid reprogramming of cellular gene expression at both the transcriptional and post-transcriptional levels in response to ER stress. One of the immediate effects of inhibition of translation in response to ER stress is the rapid clearance of short-live proteins such as cyclin D1 that causes cellular growth arrest (39, 40, 131). However, the most studied outcome of the translational arm of the UPR is the paradoxical and selective translational induction of the ubiquitously expressed

ATF4/CREB2 mRNA (Fig. 2). The murine 5' end of this mRNA possesses two upstream open reading frames (uORFs) that render translation sensitive to levels of the eIF2·GTP·Met $tRNA_i$ 43S ternary complex (281). The 5' proximal uORF1 is a positive-acting element that facilitates ribosome scanning and reinititation at the downstream uORF2 of the ATF4 mRNA. Unlike uORF1, uORF2 is an inhibitory element that causes dissociation of ribosomes from the ATF4 mRNA and prevents synthesis of ATF4. During stress conditions, reduction in the levels of the 43S ternary complex that accompanies phosphorylation of eIF2α increases the time required for scanning ribosomes to become competent to reinitiate translation at uORF2. This delayed reinitiation allows for ribosomes to scan through the inhibitory uORF2 and instead reinitiate at the ATF4 coding region resulting in the synthesis of the ATF4 transcription factor.

ATF4 belongs to the ATF/CREB (activating transcription factor/cyclic AMP response element binding protein) family of bZip transcription factors, which recognize the cAMP responsive element (CRE, consensus 5'-TGACGTCA-3') in target promoters through formation of homo-and heterodimers with other family members (428). ATF4 was found to regulate the translational recovery phase of the UPR that is required for synthesis of regulatory proteins late in the stress response through upregulation of the *gadd34* (Growth Arrest and DNA Damage-Inducible Protein 34) gene (46, 208, 256, 294, 295). Indeed, GADD34 overexpression decreased Tg-induced eIF2α phosphorylation without having any influence on PERK activation and phosphorylation (294). Conversely, $ATF4^{-/-}$ and $GADD34^{-/-}$ MEFs show prolonged eIF2α phosphorylation that prevents upregulation of BiP due to sustained translation repression (208, 256, 295). Importantly, this requires GADD34 interaction with protein phosphatase 1 (PP1c), through a highly conserved PP1c-binding motif (KVRF) in its C-terminus, which stimulates PP1c activity and promotes dephosphorylation of Ser51 in eIF2α (46, 67, 294). Interestingly, GADD34 shows a high degree of identity with other PP1c regulatory subunits found in eIF2α holophosphatase complexes. For example, CReP (Constitutive Repressor of eIF2α Phosphorylation) was identified as a regulator of eIF2α phosphorylation that allows ongoing protein synthesis in unstressed cells (184). On the other hand, herpes simplex virus (HSV) acquired ICP34.5, a GADD34-related virulence factor that allow virus to escape the translational block observed during infection through its ability to dephosphorylate eIF2α (150, 151). In all cases, PP1c is essential in directing eIF2α dephosphorylation.

Given that the phosphorylation of eIF2α is an intrinsic event promoting function and survival of cells in various stress conditions (251, 400), intense efforts are now being put together to identify small-molecules inhibitors of eIF2α holophosphatase complexes that confer cytoprotection against ISR-induced apoptosis. One of these, Salubrinal, identified by Boyce *et al.* was found to inhibit eIF2α dephosphorylation by modifying the composition of GADD34-related holophosphatase complexes (34). The promising action of this drug in treatment of several diseases involving eIF2α phosphorylation is underscored by data indicating that Salubrinal inhibits HSV replication and ER stress-induced neuronal cell death *in vivo* (34, 382).

One insightful approach used to identify potential ATF4-regulated genes was the development of comparative gene expression microarrays of WT and $ATF4^{-/-}$ MEFs (143). In such experimental setting, it was found that over 50% of the genes induced by Tm in control cells were reduced by more than 50% in $PERK^{-/-}$ cells, but only 25% in $ATF4^{-/-}$ cells, suggesting that signaling from PERK to UPR genes most likely involves other downstream effectors beside ATF4 (143). Anyhow, the main conclusion was that ATF4 is a master regulator of two important aspects of the ISR: 1) amino acid import/metabolism and resistance to oxidative stress, and 2) apoptosis. First, mRNAs encoding Asparagine synthase (Asns), Cystine/Glutamate exchanger (Slc3a2), Glycine transporter 1 (Glyt1) and the Arginine/Lysine transporter (Cat-1) were found to be downregulated in ER stressed $ATF4^{-/-}$ MEFs relative to controls, underscoring the significance of ATF4 in cellular amino acid synthesis and uptake (143). $ATF4^{-/-}$ cells required supplemental reducing compounds such glutathione or β-mercaptoethanol since these are defective in expression of genes involved in metabolism of sulfur-containing amino acids and glycine, a precursor of glutathione biosynthesis responsible of reducing endogenous peroxides (143). In fact, the UPR and glutathione biosynthesis are intimately linked to one each other as in situation of high demand in protein synthesis, the ER is subjected to accumulation of reactive oxygen species (ROS) sourcing from disulfide-bond formation (412). Therefore, UPR activation triggers an ATF4-dependent gene expression network meant to counteract oxidative stress within the ER through the upregulation of genes promoting reduction of ROS. These microarray analyses also revealed an ATF4-independent regulation of gene transcription in ER-stressed cells and found to reside in a transcriptional regulator called Nrf2 (NF-E2-related factor 2). Nrf2 is the other known substrate of the PERK protein kinase (73). In response to ER stress,

phosphorylation of Nrf2 by PERK triggers its translocation into the nucleus where it upregulates genes involved in redox metabolism such as glutathione-S-transferase (*gst*) or the rate-limiting enzyme in glutathione biosynthesis, γ-glutamylcysteine sythetase (*gcs*) (72, 73). Importantly, however, this occurs independently of eIF2α phosphorylation (73).

The other process regulated by the ATF4 transcriptional regulator is ER stress-induced apoptosis. One of the first genes identified as being directly regulated by ATF4 in response to ER stress encodes the transcription factor CHOP (C/EBP homologous protein) (102, 137). The importance of the ATF4 in CHOP regulation is highlighted by the almost complete loss of CHOP induction in $PERK^{-/-}$, S51A, and $ATF4^{-/-}$ MEFs (137, 143, 365). Initial transfection studies demonstrated that CHOP overexpression causes cell cycle arrest and apoptosis in various cell types, a process reversed by the overexpression of BiP (14, 270, 438). Conversely, $CHOP^{-/-}$ cells are resistant to apoptosis induced by ER stress-inducing agents (264, 476). Exactly how CHOP promotes cell death is poorly understood, but recent evidence helped resolve this issue. First, it was found that CHOP represses transcription from the Bcl-2 promoter and in this way promotes mitochondrial depolarization and apoptosis in ER stress conditions (270, 274). Likewise, Dr. A. Strasser and colleagues reported a role for Bim, a proapoptotic member of the Bcl-2 family, in CHOP-mediated apoptosis in ER stress cells (332). Given that CHOP was found to directly transactivate Bim promoter, it worth proposing that CHOP supplies pro-apoptotic signals by directly regulating the levels of Bcl-2 proteins in ER stress cells. In addition, gene expression analysis revealed that GADD34 promoter is also under the regulation of CHOP. It was proposed that GADD34 could promote death in the late phase of the UPR by causing deregulated protein synthesis and oxidative stress within the ER (264). Finally, TRB3 (*tribble*-related 3) a crucial inhibitor of AKT (87), was identified as a late ER-stress induced gene cooperatively regulated by both ATF4 and CHOP (300). Since the PERK signaling pathway brings PI3K-mediated activation of AKT in a strict eIF2α-dependent manner (196), it will be interesting to determine whether TRB3 represents a threshold protein that promotes apoptosis in the late phase of the UPR through its ability to inhibit the pro-survival functions associated with AKT activation (38). Moreover, this could complement the increase in mRNA stability of ATF4 and CHOP detected when cells experience insurmountable levels of ER stress, which is believed to push the Life/Death cellular balance over apoptosis (353). All together, activation of the

PERK signaling branch of the UPR leads to a large number of transcriptional and post-transcriptional changes that allow cells to increase ER function and survive momentarily until ER homeostasis is recovered. If stress persists, eIF2α-dependent signaling looses its cytoprotective role and promotes cells death through apoptosis. Therefore, ISR signaling needs to precisely be integrated in the spatio-temporal manner to allow appropriate response of cell to ER stress.

Accumulating evidence suggest that ER stress-induced eIF2α phosphorylation crosstalks with other signaling pathways triggered by diverse stressful conditions such as NF-kB activation (81), hypoxia signaling (21, 27, 103) and SREBP sterol-mediated signaling (141). These reports now provide the foundation for future investigations aimed at deciphering the molecular basis underlying pathological manifestations of diseases associated with dysfunction of the ER homeostasis.

3.2.6 *In vivo* functions of PERK signaling

Unfolded or misfolded ER client proteins can readily form highly toxic aggregates causing several pathological manifestations described as 'conformational diseases'. These diseases are directly linked with either defects in misfolding/aggregation/trafficking of mutant proteins or mutation in components of the UPR, such as in the Wolcott-Rallison syndrome (448). This rare autosomal recessive disease is characterized by inactivating mutations in the PERK coding gene (*perk/eif2ak3*) causing early infancy insulin-dependent diabetes mellitus (IDDM) (79). These patients present selective destruction of pancreatic insulin-secreting β-cells as well as epiphyseal dysplasia, osteoporosis, and growth retardation that develop at a later age. Importantly, this phenotype is completely recapitulated in the $PERK^{-/-}$ mice (139, 472). Initial characterization of PERK demonstrated high expression in the protein kinase in pancreas (139, 378). PERK knockout mice show progressive loss of insulin-secreting β-cells by apoptosis, resulting in hypoinsulinaemia, glucose intolerance and development of diabetes mellitus early after birth (139). However, the underlying cause of β-cell insufficiency found in PERK knockout mice was recently confronted by Zhang *et al.*, which claimed that this insufficiency is due to reduced differentiation and proliferation rather than increased β-cell death (473). The importance of PERK in maintaining normal islets function is further corroborated by the generation of β-cell

specific PERK knockout mice, which develop diabetes but display normal growth and skeletal development (473). Thus, PERK may serve as a checkpoint in pancreatic β-cells coupling the rate of insulin synthesis with the folding capacity of the ER.

Similarly, mouse neonates possessing a homozygous mutation at the eIF2α phosphorylation site (S51A) exhibit pancreatic β-cell deficiency (365). These mice died within 18 hours after birth due to hypoglycemia associated with defective gluconeogenesis (365). The severer phenotype of eIF2α S51A knockin mice is most likely explained by the fact this mutation abolishes signaling from all eIF2α kinases. Moreover, Scheuner *et al.* showed that mice heterozygous for the S51A substitution became obese and diabetic on high-fat diet (366). The profound glucose intolerance of these mice results from reduced insulin secretion accompanied by abnormal distention of the ER lumen, defective trafficking of proinsulin, and a reduced number of insulin granules in β-cells. It was thus proposed that the translational control couples insulin synthesis with folding capacity to maintain ER integrity. Together, these results clearly demonstrated that the regulation of mRNA translation through eIF2α phosphorylation is essential for the cellular response to ER stress and *in vivo* glucose homeostasis.

Recently, it was found that ATF4 is also a crucial factor regulating β-cell function and survival by being an effector of the glucagon-like peptide-1 (GLP-1) signaling pathway. Gut endocrine cell-secreted GLP-1 is now the center of attention of several groups due to its unique biological activities *in vivo*. These include: stimulation of glucose-dependent insulin biosynthesis/secretion and inhibition of glucagon secretion, while simultaneously enhancing the resistance of β-cells to apoptosis (86). Together, this makes GLP-1 agonists, such as Exendin-4, very efficient blood glucose lowering agents now used in the United States in the prevention and/or amelioration of diabetes in humans. These molecules act through the GLP-1 receptor (GLP-1R), a seven transmembrane receptor that couples to small G proteins and that signals via the activation of protein kinase A (PKA) (86). Interestingly, it appears that Exendin-4-mediated PKA activation potentiates ATF4 induction in ER stressed pancreatic β-cell lines resulting in massive induction of the *gadd34* gene, which promotes rapid recovery of global protein synthesis (467). In such context, rapid restoration of protein synthesis is expected to bring immediate increase in ER chaperones synthesis linked with UPR activation, and in this way, provide crucial

cellular survival signals. Although it is believed that such mechanism would underlie the protective function of GLP-1 agonist on pancreatic β-cells, further studies are required to determine whether GLP-1R signaling modulates other processes in β–cells that would also culminate in resistance of β-cells to ER stress-induced apoptosis.

The importance of eIF2α phosphorylation-dependent signaling in pancreatic β-cell survival is further illustrated by dosage of the *chop* gene in mice carrying a conformation-altering missense mutation (Cys96Tyr) in the *insulin 2* gene, also known as the Akita mice line ($Ins2^{C96Y/C96Y}$) (195, 464). This mutation disrupts a disulfide bond between the α and β chains of the insulin 2 molecule and induces a dramatic change in the conformation of the molecule. At 3 weeks of age, the Akita mouse model shows signs of ER stress based on increased BiP and CHOP expression in pancreatic β–cells (307, 436). These mice develop hyperglycemia and progressive β-cell apoptosis without becoming obese (195, 464). Targeted disruption of the *chop* gene in heterozygous Akita mice protects islet β–cells from apoptosis and delays the onset of diabetes by 8–10 weeks (307). Conversely, targeted inactivation of ATF3, a direct transcriptional regulator of CHOP in ER stress conditions, also conveys protection to pancreatic islet against nitric oxide-induced apoptosis (145, 309). Together, these results illustrate the critical role of CHOP in ER stress-mediated β–cells apoptosis *in vivo*.

Finally, a role for negative regulators of PERK, such as $p58^{IPK}$ (inhibitor of PKR), in pancreatic function was also demonstrated in mice. $p58^{IPK}$ is highly expressed in pancreatic β-cells and is induced by ATF6 through a conserved ERSE *cis*-acting element present in its promoter (421). $p58^{IPK}$ was initially found to associate with PERK and inhibit its ability to transduce signals in ER-stressed cells in the recovery phase of the UPR (421, 454). However, recent studies show that $p58^{IPK}$ also associates with the Sec61 translocon of the RER and is involved in extraction and degradation of unfolded proteins from the ER in situation of ER stress (310, 354). Targeted disruption of the $p58^{IPK}$ gene in mice causes profound glucose intolerance developing in males by 6 months of age that progress to fasting hyperglycemia at 1 year of age in some animals (222). In an heterozygous and asymptomatic Akita background ($Ins2^{WT/C96Y}$), homozygous inactivation of $p58^{IPK}$ causes elevated blood glucose which is not met by a corresponding increase in plasma insulin; instead, plasma insulin levels are very low, a finding

that correlates with a dramatic loss of islet mass (310). These findings indicate that $P58^{IPK}$ plays an important role in preserving the function of ER-stressed β-cells.

Recent advances in the study of endoplasmic reticulum overload by unfolded proteins uncovered mechanisms leading to pancreatic β-cell exhaustion. These studies demonstrate a trend toward a protective function of the mRNA translation block that accompanies phosphorylation of eIF2α in pancreatic β-cells *in vivo*. Conversely, elevated levels of CHOP promote apoptosis of β-cells, suggesting that a tight balance between pro-apoptotic and anti-apoptotic signals need to be established in these cells. The importance of the PERK signaling pathway in other pathological settings is now becoming evident. Indeed, activation of PERK and phosphorylation of eIF2α in multiple sclerosis prevents autoimmune-mediated demyelination, axonal damage, and oligodendrocyte loss (244). On the other hand, activation of this signaling pathway seems of bad prognostic for several other diseases such tumor development (103), brain and heart ischemia (9, 396), atherosclerosis (104, 133), or Alzheimer's disease (190, 191). Consequently, it reveals the need to identify small-molecule regulators that influence the rate/fidelity of the folding reaction in the ER (i.e. chemical chaperones) or target directly or indirectly components of the PERK signaling pathway (i.e. Salubrinal or Bortezomib) in order to treat conformational diseases (34, 141, 285, 444).

4 REGULATION OF GLUCOSE METABOLISM

4.1 Biological effects of insulin

The discovery of insulin in 1921 by the Canadian Frederick Banting in the laboratory of James Macleod at the University of Toronto was one of the great biological and medical advances of the twentieth century. In fact, many Nobel prizes recipients studied various aspects of insulin biology from its identification and determination of its primary structure to the development of assays to measure insulin levels. Together these studies contributed to establish insulin as a major determinant of metabolic regulation in mammals. The major function of insulin is to maintain plasma glucose levels within a range of approximately 4 to 7 mM in normal individuals (357). In the face of high circulating blood glucose concentrations, insulin is released from pancreatic β-cells, the endocrine portion of the pancreas, enters circulation and is

taken up by a number of tissues, including skeletal muscle, liver, and adipose tissue (also called peripheral tissues). This increase in circulating insulin levels stimulates glucose transport into muscle and adipose cells, and inhibits hepatic glucose production (gluconeogenesis). In addition to its primary effects on glucose homeostasis, insulin also stimulates fatty acid synthesis and storage of triglycerides in fat cells, and increases protein synthesis and inhibits protein breakdown in muscle (Fig. 5). In this manner, insulin plays key roles in the storage of ingested fuels. Other biological effects of insulin include regulation of gene transcription and mRNA turnover, protein synthesis, protein degradation and DNA synthesis, which proved to impinge on normal cellular growth and differentiation. In addition, studies over the last years revealed a central role of insulin signaling in lifespan and aging in diverse organisms, ranging from yeast to rodents (192). The broad array of physiological responses to insulin involves diverse processes such as the mobilization of glucose transporters, transcriptional regulation of specific genes and post-translational regulation of critical intracellular enzymes involved in metabolism. Due to the pleiotropic effects of insulin, defect in only one of these processes can result in failure of insulin to control glycaemia within normal range. In is now recognized that environmental and social factors, such as obesity, directly impact on the cellular actions of insulin by establishing insulin resistance in peripheral tissues. At the tissue level, resistance to insulin can result in an incapability of skeletal muscle and adipose tissue to uptake glucose or liver to inhibit glucose production in response to insulin. In the long term, resistance to insulin leads to pancreatic β-cells exhaustion and death. When insulin resistance is accompanied by dysfunction of pancreatic islet β-cells, it results in a failure to control blood glucose levels, a metabolic disorder known as Type 2 diabetes. Since this disease has emerged as one global health threats of the 21st century and that worldwide, characterization of the molecular events mediating insulin effects is mandatory and should help provide new ways of treating insulin resistance and T2D.

4.2 Insulin biosynthesis and secretion by pancreatic β-cells

Over the last 40 years, progress has been made in deciphering the cellular events involved in glucose-induced insulin biosynthesis and processing in pancreatic β-cells (122). Briefly, insulin is synthesized from the proinsulin precursor molecule in the ER where it is transported to the Golgi before being packed into secretory granules. As these secretory vesicles are transported to the plasma membrane, the calcium-rich and acidic environment of secretory

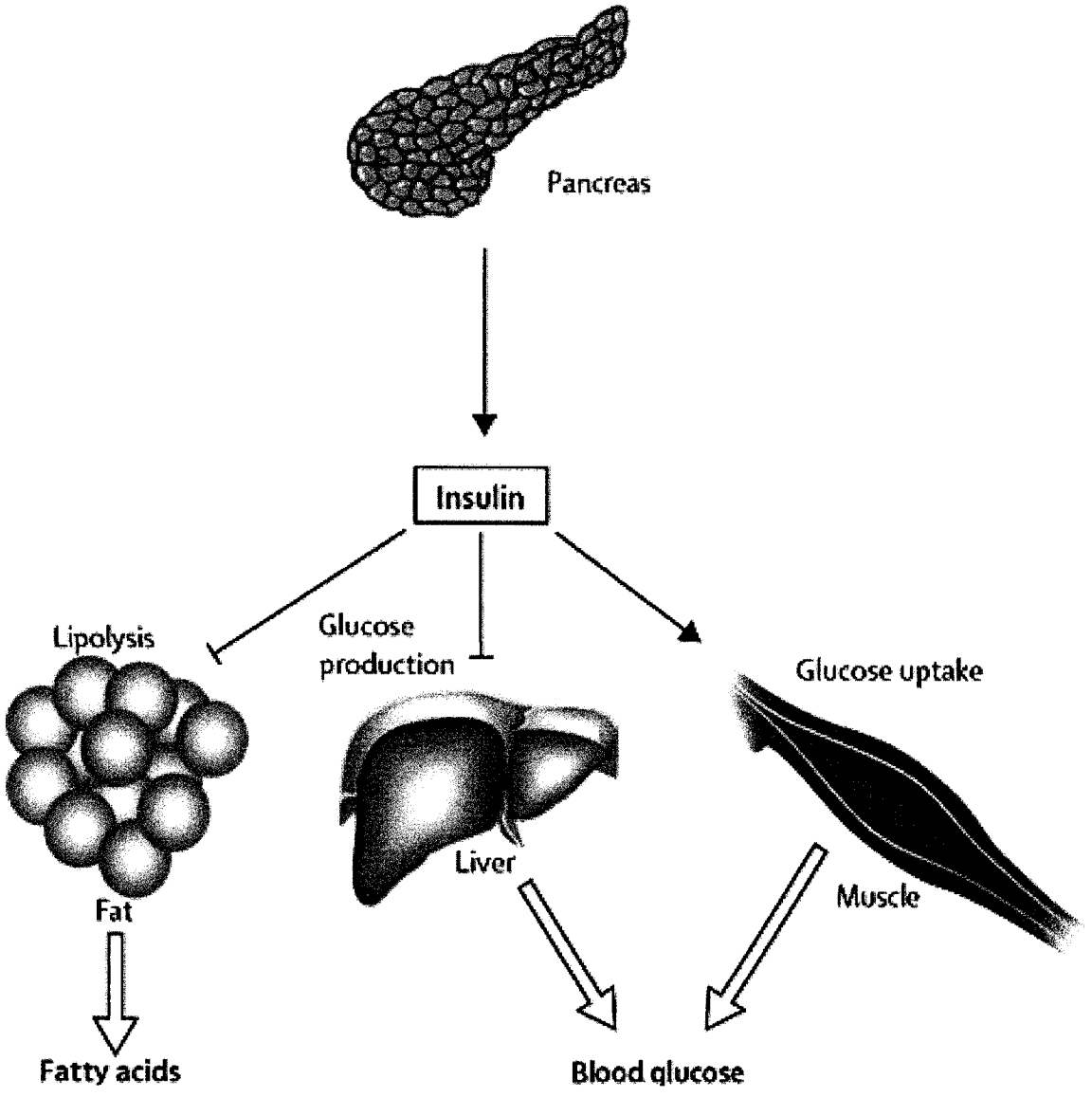

Figure 5. Biological effects of insulin
Adapted from Stumvoll M. *et al.* (2005) Lancet 365:1333-1346

granules promotes proinsulin processing by the concerted action of proteolytic enzymes, known as prohormone convertases (PC1 and PC2) and exoprotease carboxypeptidase E (389). Different regulatory mechanisms, such as glucose-induced *pc1* and *pc2* gene activation were found to increase insulin processing in response to elevation of glycaemia. PC1 and PC2 enzymes cooperatively remove the center portion of the proinsulin, or C-peptide, from the C- and N-terminal ends of the molecule (122). The remaining the α and β chains, are bound together by disulfide bonds and constitute the bioactive insulin molecule (51 amino acids in total), which mediates its effects by binding to its receptor, the insulin receptor (IR) found on target cells (5, 122, 266, 369).

Identification and delineation of general mechanisms and principles used to sense the presence of glucose and stimulate insulin secretion was, and is still today, a field of intense research efforts. Insulin secretion from pancreatic β–cells requires transport of glucose within β-cells and at least partial metabolism of the sugar (119). Glucose transport is not considered to have a regulatory role in β-cells because GLUT2 (Glucose Transporter-2), the main glucose carrier expressed in pancreatic β-cells, is in vast excess to what can be metabolized by β-cells (161). GLUT2-null mice are hyperglycaemic and relatively hypoinsulinaemic, supporting the fact that GLUT-2 is required for glucose sensing and insulin secretion by pancreatic β-cells (129). In humans, an inactivating mutation of GLUT2 is found in Fanconi-Bickel syndrome, a rare autosomal recessive disorder of glucose metabolism, characterized by glucose intolerance and fasting hypoglycaemia (360, 361). In pancreatic β-cell, glucose is rapidly targeted toward the glycolysis metabolic pathway where it is phosphorylated by glucokinase (Fig. 6A). Because phosphorylation of glucose by glucokinase is the rate-limiting step in glucose catabolism in pancreatic β-cells, glucokinase is generally considered as the primary β-cell glucose sensor (269). The increase in the cellular ATP/ADP ratio that goes along with catabolization of glucose induces closure of ATP-sensitive transmembrane K^+-channels (K_{ATP}), causing membrane depolarization (347). This, in turn, is thought to activate voltage-gated Ca^{2+}-channels (VGCC) and raise intracellular calcium concentration triggering fusion of pre-stored insulin vesicles with the plasma membrane. Polymorphisms in the Kir6.2 subunit of the K_{ATP} channel were found to predispose to diabetes by reducing K_{ATP} sensitivity to intracellular ATP and decreasing glucose-induced insulin secretion (214). K_{ATP} channels are the targets of sulfonylurea drugs, which like

A

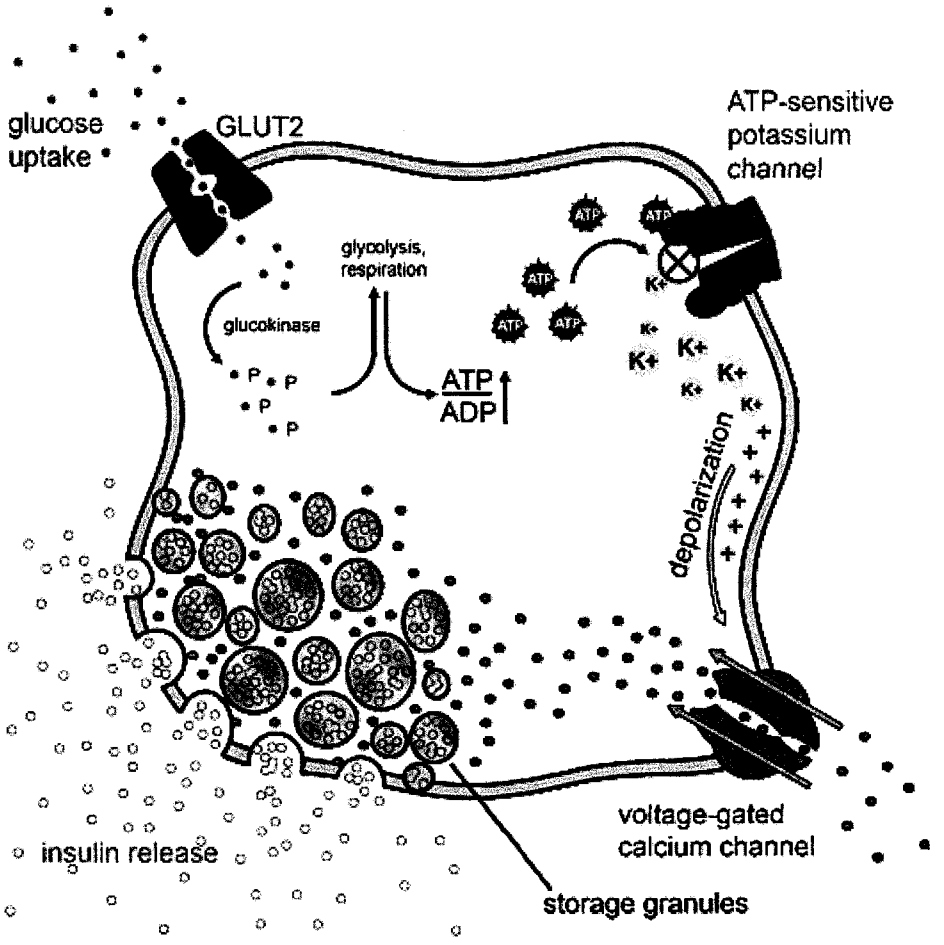

B

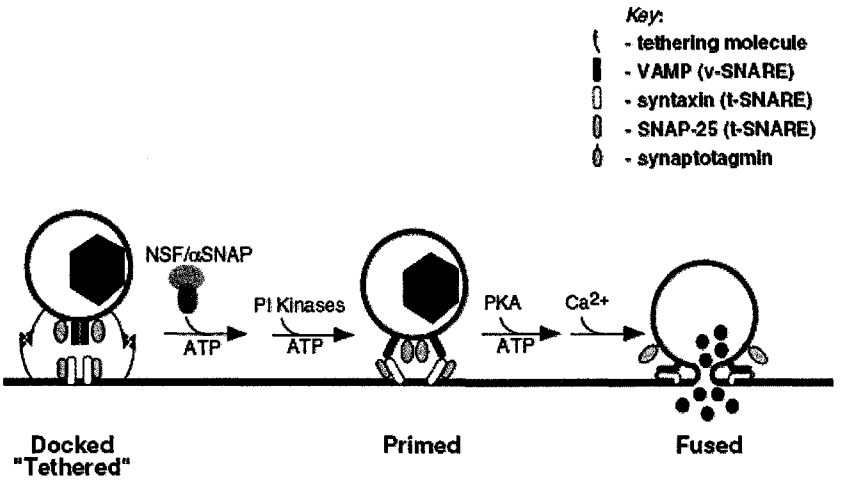

Figure 6. Glucose sensing in pancreatic β-cells

(A) Adapted from http://www.betacell.org/content/articles/print.php?aid=1

(B) Adapted from Easom R.A. (2000) Cell & Developmental Biology 11:253-266

glucose, induce closure of K_{ATP} channels and stimulate insulin secretion (290). For this reason, these agents are commonly prescribed agents in the treatment of T2D.

Insulin is released from pancreatic islet β-cells in two distinct phases in response to glucose stimulation (90). The first phase of insulin release (2-10 min) is elicited by glucose-induced elevation of intracellular calcium levels that trigger fusion of insulin granules pre-docked at the plasma membrane. The second phase of insulin release (10-30 min) requires the amplifying action of glucose and is presumed to require new insulin synthesis (involving both gene transcription and mRNA translation) and mobilization of newly assembled insulin granules close to the plasma membrane. As highlighted above, glucose-induced elevation of cytosolic Ca^{2+} concentration through opening of VGCCs in pancreatic β-cells is central in initiating insulin secretion under physiological conditions. In fact, elevation of Ca^{2+} concentration at the plasma membrane seems to be sufficient to induce fusion of readily releasable pre-primed granules during the first phase of insulin exocytosis (340). On the other hand, the slower second phase of granule mobilization from cytosolic storage was found to be largely dependent on ATP, protein phosphorylation, and actin filaments integrity (6, 90, 233). Recruitment of newly formed insulin granules to the plasma membrane can be separated in three phases: 1) docking, 2) priming, and 3) fusion (Fig. 6B) (90). The docking process involves Ca^{2+}/calmodulin-dependent kinase (CaMK) that phosphorylates cytoskeletal proteins involved in promoting actin mesh dissolution and mobilization or 'docking' of storage insulin granules to the plasma membrane. Priming of insulin granules is mediated by a set of highly conserved membrane v-SNAREs (vesicle soluble NSF attachment protein receptors) such as VAMP2, which interact with a receptor found at the plasma membrane called t-SNARE (composed of SNAP-25 and Syntaxin) (176). These proteins recognize each other in a lock and key fashion to form a multisubunit complex that promotes ATP-dependent granule fusion with the plasma membrane and exocytosis of insulin out of β-cells (90). Relative to the well-studied mechanisms of synaptic vesicle exocytosis from the synapse of neuronal cells, granule exocytosis from β-cells is poorly understood. However, cytoskeleton remodeling regulators such as Rho GTPases Cdc42 and Rac1 or the Ser/Thr protein kinase Pak1 were recently found to control insulin exocytosis by glucose in pancreatic β-cells (287, 288, 439). Depletion of Cdc42 or Pak by RNAi completely abolishes glucose-stimulated insulin release, suggesting that these could represent critical players in insulin secretion and

glucose metabolism *in vivo* (439).

4.3 Glucose uptake by peripheral tissues

The first step by which insulin increases energy storage or utilization in skeletal muscle and fat cells involves the regulated transport of glucose into the cell through the facilitative glucose transporter GLUT4. Insulin increases glucose uptake mainly by enriching the concentration of GLUT4 proteins at the plasma membrane, rather than by increasing the intrinsic activity of the transporter (168, 357, 441). GLUT4 is found in vesicles that continuously cycle from intracellular stores to the plasma membrane. Insulin increases glucose transport by increasing the rate of GLUT4 vesicle exocytosis and by slightly decreasing their rate of internalization (322). The microtubule network and actin cytoskeleton play key roles in GLUT4 trafficking, either by linking signaling components or by directing movement of vesicles from intracellular sites to the plasma membrane in response to insulin (45, 188). In response to elevation of glycaemia, insulin promotes the docking and fusion of GLUT4 vesicles at the plasma membrane through v-SNARE and t-SNARE interactions (322). Although these SNARE interactions are not subjected to regulation by insulin, it was found that accessory proteins associating with SNAREs, such as Munc18c or Synip might be targets of insulin action, although this still needs to be firmly established (178, 405). Of particular interest, however, is the downregulation of GLUT4 expression in adipose tissue of obese subjects (116, 304, 381) and its upregulation in skeletal muscle in response to exercise (164, 218). Since glucose transport is the main step at which insulin action fails in patients affected by obesity and T2D, it suggests that therapeutic strategies based on promoting both GLUT4 expression and translocation may facilitate T2D drug discoveries.

4.4 Signaling from the insulin receptor

The effects of insulin on peripheral tissues are relayed inside the cells through the insulin receptor (IR), a member of the large receptor tyrosine kinase (RTK) family (Fig. 7) (189, 323). The IR belongs to a subfamily of structurally related receptors including the insulin-like growth factor 1 receptor (IGF1R) and orphan IR-related receptor for which no ligand have been found yet (IRR) (134). In its native conformation, the insulin receptor is composed of two α-subunits and two β-subunits covalently linked through intra- and inter-disulfide bonds yielding a $\alpha 2\beta 2$

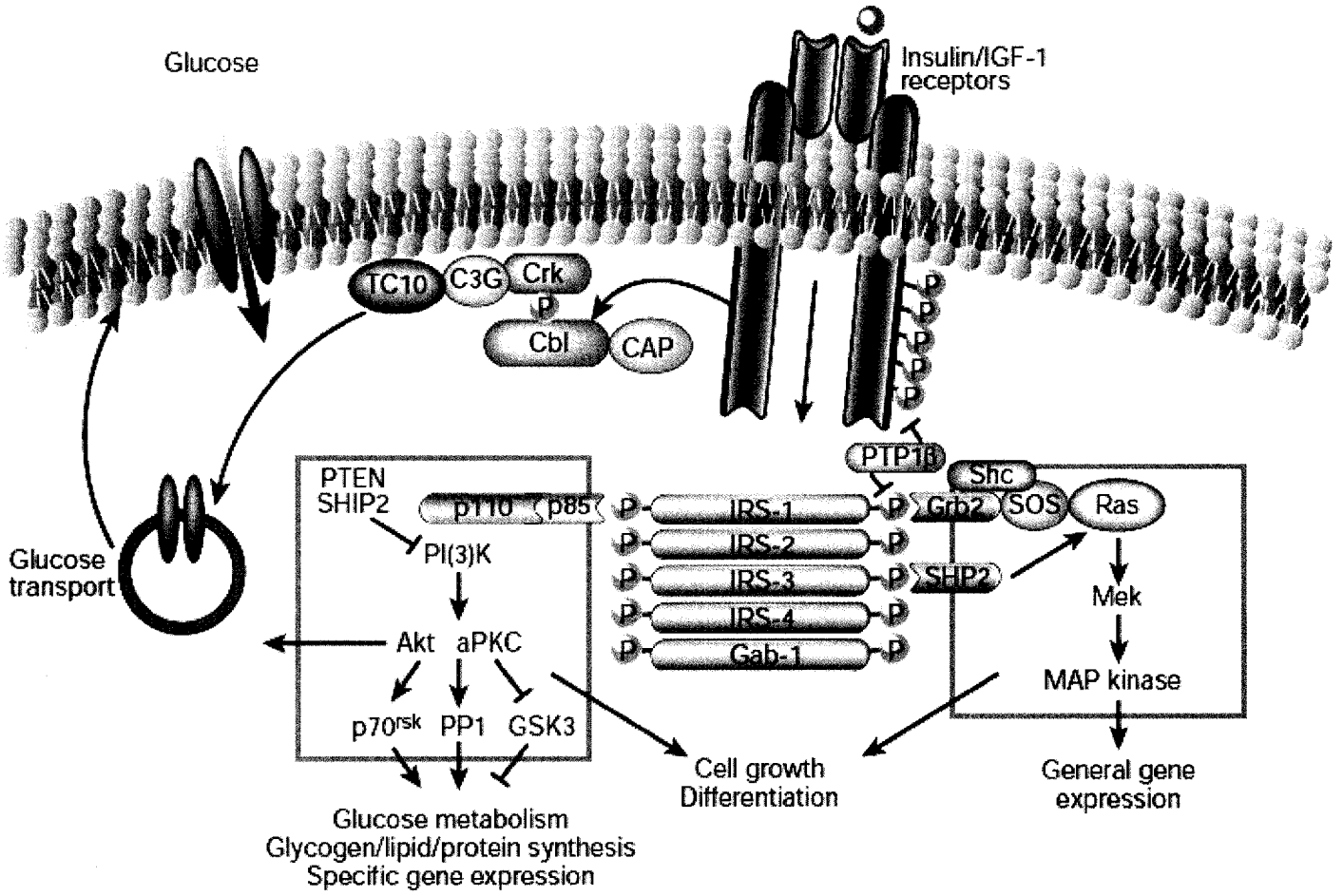

Figure 7. Insulin receptor signaling and GLUT4 translocation
Saltiel A.R. and Kahn R.C. (2001) Nature 414: 799-806

heterotetramer. Each subunit performs a specific function. The extracellular α-subunit contains the insulin recognition sites, whereas the β-subunit possesses an insulin-stimulated catalytic Tyr kinase activity (91, 416). Binding of insulin to the α-subunit induces transphosphorylation of one β subunit by another on specific tyrosine residues in an activation loop resulting in increased catalytic kinase activity (56, 358). The receptor also undergoes autophosphorylation at other tyrosine residues in the juxtamembrane and C-terminal regions. Considerable efforts have been put together to define the role of these phosphorylated tyrosine residues and ultimately, how they determine the biological responses to insulin. What became clear from these investigations is that tyrosine phosphorylation of the IR allows recruitment of various types of proteins, such as signaling adaptors (ex: Grb2, Grb10, CrK, or the p85 subunit of PI3K), docking proteins (IRS-1, Shc) or enzymes (ex: SHP2, Fyn) through either SH2 or PTB phosphotyrosine-recognizing modules (321). The activated IR also phosphorylates tyrosine residues on some of these proteins such as the insulin receptor substrate family, Gab-1, c-Cbl, APS and Shc isoforms (358). Upon phosphorylation, these proteins dock downstream effector molecules and contribute to the formation of large molecular complexes involved in propagating signal from the IR. In fact, recruitment of most signaling proteins occurs indirectly through IRS proteins. For example, IRS-1-mediated recruitment of Grb2 triggers activation of the ERK pathway, which mediates the transcriptional effects of insulin and is mainly involved in modulation of cell growth. By contrast, IRS-1-mediated recruitment of PI3K p85 regulatory subunit which converges on the activation of PI3K and is preferentially involved in the metabolic actions of insulin through targeting of GLUT4 at the plasma membrane (see below) (56, 358).

Among IR substrates, the best characterized are the IRS family of proteins (IRS-1, -2, -3, -4, -5). Although IRS proteins share a high degree of homology, studies in knockout mice and cell lines indicate specific roles for IRS proteins in insulin/IGF1 action (221, 446). IRS-1 knockout mice are growth retarded and do not appear to develop diabetes, but are insulin resistant in peripheral tissues with defective glucose tolerance (399). IRS-2 knockout mice develop T2D due to insulin resistance in muscle, fat and liver and decreased pancreatic β-cell function (447). Therefore, both IRS-1 and IRS-2 function in peripheral glucose metabolism, but IRS-2 is more critical for β-cell development (cell growth) and compensation of peripheral insulin resistance through its ability to transduce signals from IGF1R (446). IRS-1 is composed

of a Pleckstrin homology (PH) and a phosphotyrosine-binding (PTB) domain. At the molecular level, IR activation by insulin promotes binding of IRS-1 PTB domain specifically to phosphotyrosine 960 (NPxY) in the juxtamembrane domain of the IR β-subunit (using rat IR numbering), while the PH domain contributes at stabilizing IRS-1 at the membrane by mediating phospholipid interactions. IRS-1 contains several potential tyrosine phosphorylation sites. In response to insulin, IRS-1 becomes tyrosine phosphorylated on Tyr608 and Tyr628, which generate the major docking sites for the p85 regulatory subunit of PI3K (100). Association of IRS-1 with p85 PI3K leads to the targeting and activation of the enzyme. PI3K generates the lipid product phosphatidylinositol 3,4,5-trisphosphate (PIP3), which regulates the localization and activity of numerous proteins such as AKT (98). PI3K triggers activation of the protein kinase AKT through the action of two intermediate protein kinases, Rictor/mTORC2 (mammalian target of rapamycin complex 2) and PDK1 (362, 422). First, the Rictor/mTORC2 phosphorylates AKT on Ser473 stimulating subsequent phosphorylation of AKT on Thr308 by PDK1. Activated AKT can then activate or deactivate a myriad of substrates via phosphorylation. The PI3K signaling pathway plays an essential role in glucose uptake and GLUT4 translocation. Inhibition of PI3K with pharmacological inhibitors, such as wortmannin, completely blocks the stimulation of glucose uptake by insulin (302). In addition, overexpression of dominant-interfering forms of PI3K blocks GLUT4 translocation and glucose uptake, while overexpression of constitutively active forms of PI3K partially mimics insulin action (267, 373). Mice heterozygote for genes encoding the p110α and p110β catalytic subunits of PI3K show mild glucose intolerance (35). Recently, siRNA knockdown experiments in cultured cells, confirmed the requirement for AKT2, rather than AKT1 or AKT3 isoforms in GLUT4 trafficking in muscle and adipose cells (10, 181), and *in vivo* in mice (64). Given that it is still not clear how the PI3K signaling cascade promotes GLUT4 translocation, active investigation of potential PI3K and AKT2 substrates within the intracellular membrane trafficking system of cells is being performed. Recent evidence shows that atypical Protein kinase C λ/ζ (101) and the recycling RabGAP proteins (168, 187) are substrates of AKT2 and relay insulin signals to GLUT4 translocation. Although these need further clarification, such information should help at getting a better picture of GLUT4 glucose transport in cells.

Stimulation of glucose uptake by insulin also involves PI3K-independent pathways (Fig. 7). The most studied is certainly the CAP (c-Cbl-associated protein)-mediated recruitment and phosphorylation of c-Cbl by the IR (56, 357, 358). Cell culture-based assays showed that translocation of tyrosine phosphorylated c-Cbl recruits the adapter protein CrkII to lipid rafts via interaction of the SH2 domain of CrkII with phospho-Cbl (61). Once c-Cbl is translocated into lipid rafts, C3G comes into proximity and specifically activates the TC10 small GTPase (61). Once activated, TC10 seems to provide a second signal to the GLUT4 protein that functions in parallel with the activation of the PI3K pathway (61). This could involve the stabilization of cortical actin, which seems to be important in GLUT4 vesicle translocation to the plasma membrane. Based on these findings, one could predict that deletion of the *cap* gene in mice would result in insulin resistance. However, whole-body deletion of CAP unexpectedly led to an insulin-sensitive phenotype and protection from HFD-induced insulin resistance (232), as seen in c-Cbl$^{-/-}$ mice (278). Although the contribution of the CAP/c-Cbl/TC10 pathway to whole body insulin sensitivity still needs to be scrutinized, authors suggested that the insulin sensitizing effect of *cap* gene inactivation in macrophage is the underlying cause of improved insulin sensitivity and protection from high fat diet-induced insulin resistance in Cap$^{-/-}$ mice (232).

5 INSULIN RESISTANCE

5.1 IRS-1 Ser phosphorylation and insulin resistance

Obesity is a major risk factor for developing insulin resistance and T2D. In the past decade, a large number of endocrine, inflammatory, neural and cell-intrinsic pathways have been shown to be dysregulated in obesity, which directly impact on glucose metabolism. At the molecular level, impaired glucose uptake caused by decrease in IRS-1 tyrosine phosphorylation and PI3K activation (and thus reduced GLUT4 translocation) was found to be a common issue in animal models of insulin resistance and Type 2 diabetic patients (371). While the mechanisms involved in decreasing IRS-1 tyrosine phosphorylation have not been firmly established, the involvement of IRS-1 serine phosphorylation in the desensitization of insulin actions has been pointed out by numerous groups over the last decade (128, 371). This suggests that a delicate balance between 'positive' IRS-1 tyrosine phosphorylation vs. 'negative' IRS-1 serine phosphorylation could regulate IRS-1 functions and that modification of this equilibrium could

lead to insulin resistance. In obese subjects, elevated levels of plasma free fatty acids (FFAs) and inflammatory biomarkers such as tumor necrosis factor alpha (TNFα) and interleukin-6 (IL-6) associated with massive expansion of the fat mass directly impacts on the sensitivity of peripheral tissues to insulin by activating several ser/thr protein kinases that increase IRS-1 serine phosphorylation. Phosphopeptide mapping, mutational analysis and phosphospecific antibodies revealed that TNFα and FFA induced phosphorylation of IRS-1 on Ser307 (corresponding to Ser312 in human) located at the end of the PTB domain (3). Aguirre *et al.* demonstrated that phosphorylation of IRS-1 on Ser307 markedly reduced the interaction between IRS-1 and the IR and that mutation of Ser307 to alanine impaired the inhibitory effect of TNFα on insulin-induced IRS-1 tyrosine phosphorylation (3, 4). From this study, it was proposed that phosphorylation of Ser307 induces a conformational change in the PTB domain of IRS-1 reducing its affinity for the IR (4). In fact, this model still stands true today. Among the ser/thr kinases activated by TNFα I is JNK, which has been shown to be involved in IRS-1 Ser307 phosphorylation and obesity-induced insulin resistance (3). Interestingly, phosphorylation of IRS-1 Ser307 is increased in liver, skeletal muscle and fat of wild-type mice maintained on high-fat diet (HFD) as compared to control diet (159). JNK1, but not JNK2, knockout mice present decreased adiposity, improved insulin sensitivity due to enhanced IR signaling capacity and are protected from the development of obesity-induced insulin resistance (159). Likewise, JNK-interacting protein 1 (JIP1), which binds components of JNK signaling module, is essential for JNK activation and inhibition of IRS-1 functions in adipose tissue of obese mice (175). Altogether, these results highlight JNK as a potential drug target for the treatment of obesity or T2D. On the other hand, it appears that in addition to the JNK-dependent mechanisms, other ser/thr kinases such as PKC (Protein kinase C) (203, 241) and the inhibitor of NF-κB kinase (IKKβ) (113, 466) can promote obesity-induced Ser307 IRS-1 phosphorylation.

Interestingly, expression of IRS-1, but not IRS-2, was found to be regulated through the proteasome-dependent degradation pathway in cultured cells in response to chronic exposure to insulin, thereby representing an alternative regulatory mechanism modulating insulin signaling (469). Although the exact molecular requirement for activation of the IRS-1 proteasome degradation pathway remains controversial, Ser307 phosphorylation of IRS-1 was found to induced proteasomal degradation of IRS-1 (124). mTOR, a downstream target of the insulin

pathway transducing the effects of insulin on protein synthesis in part by activating S6 kinases has been shown to phosphorylate IRS-1 and stimulate IRS-1 protein degradation (146, 397, 469). S6K1-deficient mice are resistant to diet-induced obesity and insulin resistance due increased insulin signaling (417). At the molecular level, $S6K1^{-/-}$ mice kept on HFD show impaired IRS-1 Ser307 phosphorylation, demonstrating that S6K1 contributes to insulin resistance *in vivo* through IRS-1 Ser307 phosphorylation (417). Surprisingly, however, IRS-1 levels were not altered in S6K1-deficient mice, suggesting that the role of mTOR in IRS-1 proteasomal degradation occurs independently of S6K1 and that the relation between IRS-1 Ser307 phosphorylation and degradation might not be that straightforward. The situation is further complicated by recent evidence showing that modulation of IRS-1 expression by mTOR occurs mainly through S6K-dependent IRS-1 inhibition of gene transcription rather than increased IRS-1 degradation (144). In any case, it is believed IRS-1 downregulation is part of a negative feedback mechanism regulating IR signaling under conditions of nutrient saturation54Given that chronic insulin treatment can induce insulin resistance in healthy human subjects and rats (78, 172, 213, 276), it suggests that decreased expression of IRS-1 could represents an important mechanism of insulin resistance in major insulin-sensitive tissues.

5.2 ER stress-mediated insulin resistance

One of the most important breakthroughs in the field of T2D came in 2004 when it was discovered that the metabolic and inflammatory stresses associated with obesity disrupt operation of the ER in peripheral tissues and promotes insulin resistance (Fig. 8) (311, 411). Both genetic and dietary models of murine obesity show increased levels of PERK activation (PERK Thr980 phosphorylation) and eIF2α Ser51 phosphorylation as well as upregulation of the ER chaperone BiP in both liver and adipose tissues, but not in skeletal muscle. Importantly, this was accompanied by IRE1-mediated JNK activation, which uncoupled IR activation from IRS-1 through phosphorylation of IRS-1 on Ser307 (311). In embryonic fibroblasts derived from IRE1-deficient mice ($IRE1^{-/-}$ MEFs), chemical ER stressors were unable to activate JNK and consequently, cells were protected against insulin resistance (311). In order to substantiate the importance of the ER stress response in the development of obesity-induced insulin resistance *in vivo*, glucose homeostasis of $XBP\text{-}1^{+/-}$ mice kept on high fat diet (HFD) was investigated with the reasoning that modulation of $XBP\text{-}1^{s}$ levels, a critical regulator of ER chaperone gene

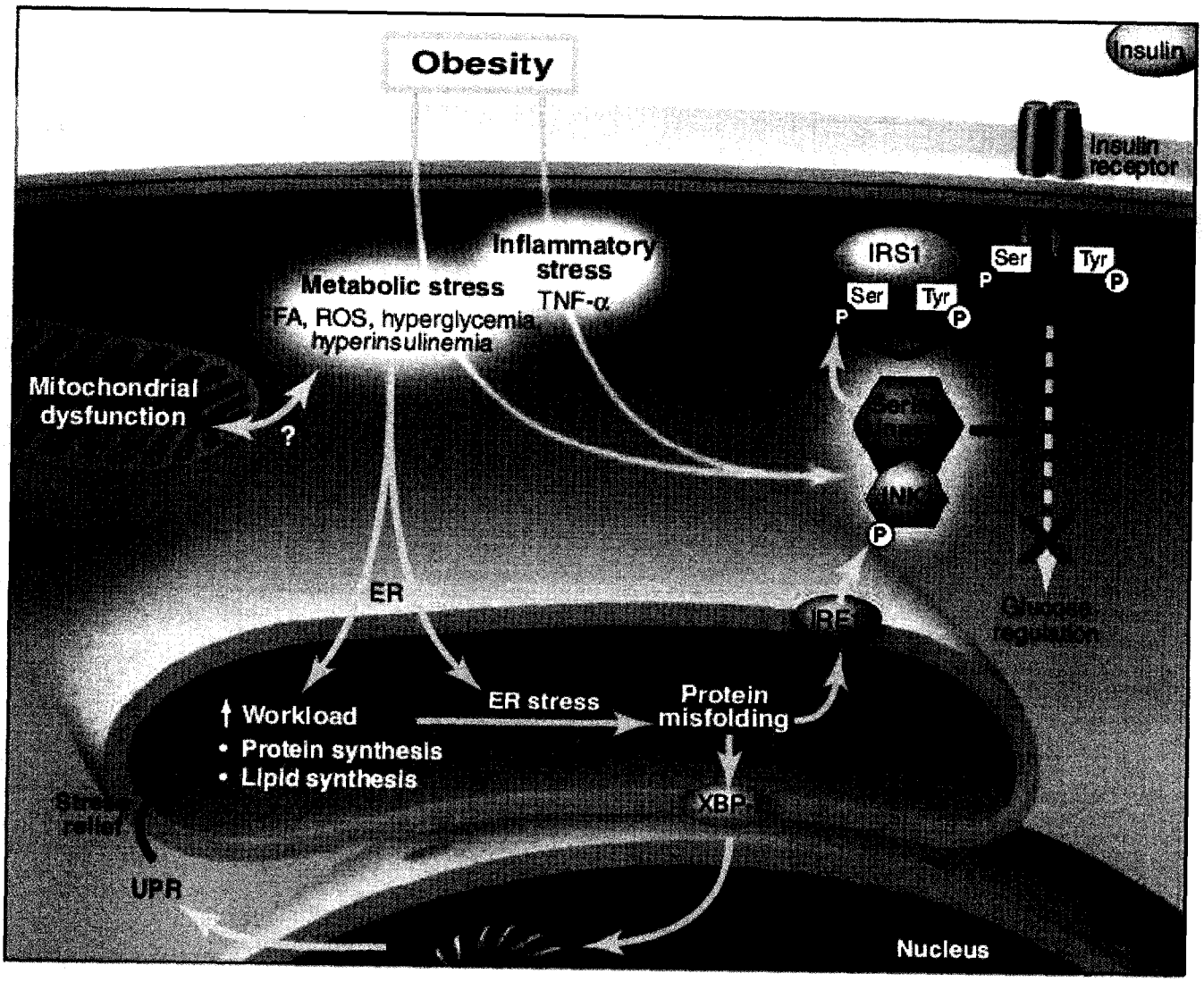

Figure 8. Crosstalk between the UPR and the insulin receptor signaling
Muoio D.M. and Newgard C.B. (2004) Science 306:425-426

expression, would alter insulin action via its impact on the magnitude of the ER stress responses. Obese XBP-$1^{+/-}$ mice were hyperglycaemic and developed progressive hypoinsulinaemia as compared to control mice, and this was associated with significant glucose intolerance due to impaired hypoglycemic response to insulin in peripheral tissues. At the molecular level, XBP-$1^{+/-}$ mice show increased levels of PERK Thr980 and eIF2α Ser51 phosphorylation, as well as increased JNK-mediated IRS-1 Ser307 phosphorylation (311). Importantly, no defects in pancreatic morphology or function were noted in these mice, demonstrating that an important signaling component of obesity-induced insulin resistance originates from stressed ER in liver and adipose tissues. Interestingly, the use of chemical chaperones such as 4-phenyl butyric acid (PBA) or endogenous bile acids derivatives such as ursodeoxycholic acid and its taurine-conjugated derivative (TUDCA) resulted in normalization of hyperglycemia, restoration of systemic insulin sensitivity, resolution of fatty liver disease (hepatic steatosis), and enhancement of insulin action in liver, muscle, and adipose tissues (312). These results demonstrate that chemical chaperones enhance the adaptive capacity of the ER and could act as potent antidiabetic modalities with potential application in the treatment of T2D.

One essential question raised by these studies is how does obesity causes damage to the ER? Increased serum triacylglycerol (TAG) levels associated with obesity and T2D contribute to lipid accumulation in many nonadipose tissues such as liver. Intriguingly, and as briefly stated in section 3.1 and 3.2, the enzymes responsible for excess lipid processing include several integral membrane proteins residing in the ER. Through the process of lipotoxicity, this inappropriate accumulation of excess lipid can lead to cellular dysfunction and even cell death (419). Recently, palmitate was found to directly impair ER functions by being rapidly incorporated into saturated phospholipid and triglyceride species in microsomal membranes (33). The resulting membrane remodeling was associated with dramatic dilatation of the ER and redistribution of protein-folding chaperones to the cytosol (33). This suggests that impairment of the structure and function of this organelle could be involved in the cellular response to lipid overload. Future investigations should increase our knowledge on the link between obesity, lipotoxicity and perturbation of the ER environment.

The complexity of clinical diabetes is matched, if not exceeded, by the complexity of insulin-mediated intracellular signaling elements. In reality, defects at either IR or IRS-1 levels and even downstream in the insulin cascade at the level of GLUT4 translocation were found to contribute to establish insulin resistance. However, recent evidence pointing to a major role of the ER is sensing metabolic stresses associated with obesity suggest that defects in other pathways are likely to impact on insulin sensitivity in peripheral tissues. Although, IRE1-mediated activation of JNK was initially identified as the main causative element of defective IR signaling in obese mice, addressing the importance of PERK and ATF6 sensor proteins in this process is fundamental. Characterization of mice deficient in component of these two arms of the UPR should be considered as an initial and logical step toward unraveling their role in whole body glucose homeostasis and obesity. Alternatively, assessing the importance of UPR activation in biopsies from human diabetic subjects could represent an important step toward understanding the significance of ER stress in T2D.

6 Objective of the Study

Dr. S. Kebache, a previous Ph.D. student in Dr. L. Larose laboratory, identified and characterized the interaction between Nck and eIF2β (198). He provided evidence indicating that overexpression of Nck increases translation rates in cells by decreasing levels of eIF2α Ser51 phosphorylation (197). In addition, he reported that modulation of eIF2α phosphorylation state by Nck is prevented by Calyculin A, a PP1c/PP2A ser/thr phosphatase inhibitor (197). Together, these results suggest the involvement of a phosphatase in mediating Nck effects on mRNA translation and eIF2α phosphorylation. The goal of the study was to delineate the molecular mechanism underlying the regulation of eIF2α Ser51 phosphorylation and mRNA translation by Nck adaptors.

CHAPTER II

Nck in a Complex Containing PP1c Regulates eIF2α Signaling and Cell Survival to Endoplasmic Reticulum Stress.

Reproduced with permission from Mathieu Latreille and Louise Larose.
Nck in a Complex Containing PP1c Regulates eIF2α signaling and Cell Survival to Endoplasmic Reticulum stress.

Journal of Biological Chemistry (2006). **281**: 26633-26644

PREFACE

In previous years, the laboratory of Dr. L. Larose uncovered a novel role for Nck adaptor proteins in mRNA translation. It was established that overexpression of Nck stimulates initiation of mRNA translation through its interaction with eIF2β. Moreover, Nck overexpression decreased PERK-mediated phosphorylation of eIF2α on Ser51, a regulatory mechanism known to attenuate mRNA translation in response to ER stress. However, exactly how Nck overexpression decreased eIF2α phosphorylation remained unclear. One possibility was that Nck decreases levels of eIF2α phosphorylation by assembling and activating a holophosphatase complex dephosphorylating eIF2α on Ser51. Interestingly, treatment with Calyculin A, a PP1c and PP2A protein phosphatase inhibitor, prevented Nck from decreasing eIF2α phosphorylation levels in response to ER stress. Moreover, the PP2A regulatory subunit B56δ was recovered in a yeast-two hybrid screen designed to identify effectors of Nck SH3 domains. Based on these observations, I designed experiments aimed at testing whether Nck mediates its effects on eIF2α phosphorylation and mRNA translation through the PP2A/B56δ protein complex. Unfortunately, after a year of work, I was not successful in establishing a link between the effect of Nck on eIF2α phosphorylation and the PP2A/B56δ complex. Hence, I investigated whether Nck assembles a PP1c-containing eIF2α holophosphatase complex that could dephosphorylates eIF2α. In chapter II, I present additional evidence substantiating a role for Nck adaptors in ER stress signaling and determine that Nck assembles an eIF2α holophosphatase complex containing the PP1c protein phosphatase that dephosphorylates eIF2α on Ser51.

ABSTRACT

Stress imposed on the endoplasmic reticulum (ER) induces the phosphorylation of the α-subunit of the eukaryotic initiation factor 2 (eIF2) on Ser51. This results in transient inhibition of general translation initiation, while concomitantly activating a signaling pathway that promotes the expression of genes whose products improve ER function. Conversely, dephosphorylation of eIF2α Ser51 is accomplished by protein phosphatase 1 (PP1c) complexes containing either the protein CReP or GADD34, which target PP1c to eIF2. Here, we demonstrate that the Src homology (SH) domains-containing adaptor Nck is a key component of a molecular complex that controls eIF2α phosphorylation and signaling in response to ER stress. We show that overexpression of Nck decreases basal and ER stress-induced eIF2α phosphorylation and the attendant induction of ATF4 and CHOP. In contrast, we demonstrate that the mouse embryonic fibroblasts (MEFs) lacking both isoforms of Nck ($Nck1^{-/-}Nck2^{-/-}$) show higher levels of eIF2α phosphorylation and premature induction of ATF4, CHOP and GADD34 in response to ER stress and finally are more resistant to cell death induced by prolonged ER stress conditions. We establish that a significant amount of Nck protein localizes at the ER and is in a complex with eIF2 subunits. Further analysis of this complex revealed that it also contains the ser/thr phosphatase PP1c, its regulatory subunit CReP and dephosphorylates eIF2α on Ser51 *in vitro*. Overall, we demonstrate that Nck as a component of the CReP/PP1c holophosphatase complex contributes to maintain eIF2α in a hypophosphorylated state. In this manner, Nck modulates translation and eIF2α signaling in response to ER stress.

INTRODUCTION

Nck is part of a family of adaptor proteins composed almost exclusively of Src homology 2 (SH2) and 3 (SH3) domains (231). Like other members of this family, Nck is believed to couple activated receptor tyrosine kinases (RTKs) at the plasma membrane and/or their substrates to downstream effectors through its various SH domains (273). In the past decade, identification of molecules interacting with the different SH domains of Nck has mainly implicated this adaptor in signaling processes regulating actin cytoskeleton reorganization (47, 239, 273). In mammals, separate genes encode two Nck molecules (Nck-1 and Nck-2) with 68% amino acid identity (37, 59, 433). Although we cannot totally exclude specific roles for each Nck isoform, their functional redundancy was demonstrated by the knockout of either Nck in mice, which did not present any particular phenotype (25). Nonetheless, early embryonic lethality (9.5 days) of the double Nck knockout has revealed a crucial role for this adaptor during development (25).

In a previous study, we uncovered a novel function for Nck in modulating mRNA translation at the level of initiation, through its direct interaction with the β-subunit of the eukaryotic initiation factor 2 (eIF2) (198). eIF2 is a heterotrimeric complex (α, β, and γ-subunit) that in part drives the initiation of mRNA translation by carrying out the delivery of the methionyl-initiator tRNA to the 40S ribosomal subunit (153). Various cellular insults are known to reduce protein synthesis at the level of initiation by inhibiting the activity of eIF2 through the phosphorylation of its α-subunit on Ser51 by a family of ser/thr kinases, so called eIF2α-kinases (75). This prevents recycling of eIF2 into its active GTP-bound form by the nucleotide exchange factor eIF2B, thereby transiently inhibiting general mRNA translation (350). To date, four eIF2α-kinases have been identified: 1) HRI (heme regulated inhibitor), which couples mRNA translation with heme availability in erythroid cells (57), 2) GCN2 (general control non-derepressible-2), which is activated in response to amino acid deprivation (158), 3) PKR (dsRNA-activated protein kinase), a component of the antiviral response activated by double-strand RNA (193) and 4) PERK (PKR-like endoplasmic reticulum kinase), a type 1 transmembrane protein resident of the endoplasmic reticulum (ER) activated upon accumulation of improperly folded secretory proteins (referred as to ER stress) (137, 142). In this later

condition, attenuation of translation due to eIF2α phosphorylation on Ser51 limits the influx of new proteins into the ER and prevents further buildup of unfolded proteins. On the other hand, reduced eIF2 activity allows the selective translational upregulation of the mRNA encoding the stress-regulated transcription factor ATF4 (137, 365) via a mechanism involving initiation at upstream open reading frames (uORFs) and reinitiation at the downstream ATF4 start codon (250, 423). ATF4 controls a transcriptional program that accounts for the increase in amino acid transporter and redox protein expression observed during ER stress. In this manner, ATF4 contributes to preserve ER homeostasis in stress conditions (140, 143). Among other genes regulated by ATF4 is GADD34, which coordinates the recovery of protein synthesis by interacting with the catalytic subunit of protein phosphatase 1 (PP1c) and targeting PP1c toward eIF2 to promote eIF2α dephosphorylation (295). On the other hand, prolonged ER stress conditions were found to induce programmed cell death (apoptosis) in part through the ATF4-mediated induction of the CHOP/GADD153 gene, a transcriptional activator of the C/EBP protein family with pro-apoptotic properties (reviewed in (308)). CHOP is believed to promote the death of stress cells by increasing the load and oxidation of client proteins in the ER through the upregulation of GADD34 and ERO1α, respectively (264). Together these events downstream of eIF2α phosphorylation occur in response to a broad range of stress conditions and therefore are referred as the integrated stress response (ISR).

In concert with activation of PERK, ER stress also activates two other ER-resident transmembrane proteins: IRE1 (136) and ATF6 (148). IRE1 is a type-I transmembrane ser/thr protein kinase with ribonuclease activity that splices the XBP-1 mRNA (407). The spliced XBP-1 mRNA encodes a transcription factor that migrates to the nucleus where it upregulates a subset of genes that contribute to overcome damage at the ER (227). On the other hand, ATF6 activation occurs via proteolytic cleavage, which likes XBP-1 splicing, generates a functional transcriptional regulator (374, 460). Together IRE1 and ATF6 transduce signals leading to the upregulation of genes encoding ER chaperones such as BiP/Grp78 and degrading enzymes, which enhance ER function and alleviate ER stress. Collectively, these events are integrated in a cellular response called the unfolded protein response (UPR), which protects cells against the deleterious effects of proteotoxicity in the ER. Functional defects in some players of the UPR have been associated with metabolic or neurologic pathological manifestations. For example,

patients affected by the Wolcott-Rallison Syndrome, which results in neonatal insulin-dependent diabetes, show mutations in the *perk/eif2ak3* gene (174). Similarly, mice lacking expression of PERK (139) or harboring an eIF2α that escapes phosphorylation (eIF2α Ser51 for Ala) (365) further illustrate a central role for PERK and eIF2α phosphorylation in pancreatic β-cells function.

We recently provided strong evidence that Nck has an essential function in regulating the UPR (197, 289). We demonstrated that overexpression of Nck strongly impairs cell survival to Thapsigargin (Tg), a pharmacological inducer of ER stress by preventing phosphorylation of eIF2α Ser51 and attenuation of translation that normally occur in these conditions (197). In parallel, we also showed that Nck regulates IRE-1-mediated ERK-1 activation in response to the protein misfolding inducer azetidine-2-carboxylic acid (Azc) (289). In the present study, we further exemplify the concept that Nck regulates signaling from the ER by showing that mouse embryonic fibroblasts (MEFs) deleted of Nck ($Nck1^{-/-}Nck2^{-/-}$) present increased eIF2α phosphorylation levels and expression of numerous stress-induced genes. We observed that these cells induce faster and to a higher extent various components of the eIF2α–dependent arm of the UPR and cope better with ER stress. We provide various lines of evidence demonstrating that Nck, as an adaptor protein, assembles a molecular complex containing the ser/thr phosphatase PP1c, its regulatory subunit CReP and components of eIF2. From these, we conclude that Nck, by being a component of an eIF2α holophosphatase complex, significantly contributes to accurate controls of eIF2α phosphorylation and eIF2-dependent signaling in response to ER stress. Finally, our study sheds light on a potential mechanism by which Nck adaptors regulate initiation of translation.

EXPERIMENTAL PROCEDURES

Cells. HeLa cells were cultured at 37°C in 5% CO_2 in Minimal Essential Medium Eagle (Sigma) containing 10% fetal bovine serum (FBS, Invitrogen) while Dubelcco's Modified Eagle's Medium (Invitrogen) was used for MEFs and HEK 293 cells. Thapsigargin (Tg, Sigma), tunicamycin (Tm, Sigma) or Hydrogen peroxide (H_2O_2, Sigma) treatments were as indicated.

Antibodies. Protein-A-purified pan-Nck (1793) and eIF2β (2087) antibodies were previously described (198, 254). Nck (C-19), eIF2α (Fl-315), eIF2β (P-3), CREB2/ATF4 (C-20), GADD34 (H-193), Gadd153/CHOP (F-168), PP1c (E-9) antibodies were from Santa Cruz. pSer51 eIF2α antibody was from BioSource International. The KDEL antibody (10C3) that detects Grp94 and BiP was from Stressgen. Calnexin (clone 37) antibody was from BD Transduction Laboratories. Caspase-3 (9662) and PARP (9542) antibodies were from Cell signaling. β-actin antibody (AC-74), anti-rabbit IgG FITC-conjugated and anti-Mouse IgG TRITC-conjugated were from Sigma.

Constructs, transfection, and luciferase assays. Human HA-tagged Nck1 and Nck2 constructs generously provided by Dr. Wei Li were described previously (60). Flag-tagged mCReP (aa 24-698) (184), mGADD34 (294) and the ATF4-Luc reporter gene (137) were from Dr. David Ron. GFP-tagged human Nck1 and Nck2 constructs were generated by subcloning the respective Nck cDNAs into pEGFP-C1 (Clontech) using appropriate enzymes restriction digestions. For transfection, cells plated in 60 mm dishes ($3X10^5$ cells) or 100mm dishes ($1X10^6$ cells) were transiently transfected the following day using Lipofectamin Plus reagent (Invitrogen) according to the manufacturer instructions. The amount of plasmid used was normalized with corresponding empty plasmid. For Luciferase assays, 0.5 μg of the ATF4-Luc reporter gene was used in transient transfection of MEFs. The following day, cell lysates prepared in passive lysis buffer (Promega) and normalized for protein content were used (in triplicates) to assess luciferase activity using the Luciferase Assay system (Promega).

Western Blot. MEFs plated in 100 mm dishes ($1X10^6$ cells) and treated the next day with ER stressors at 37°C were washed in ice-cold phosphate-buffered saline (PBS) and lysed in RIPA buffer (50 mM HEPES pH 7.4, 150 mM NaCl, 10% Glycerol, 1% Triton X-100, 0.1% SDS, 1% Sodium Deoxycholate, 1.5 mM $MgCl_2$, 1 mM EGTA, 10 mM Sodium Pyrophosphate, 1 mM

Sodium Orthovanadate, 100 mM Sodium Fluoride, 17.5 mM β-Glycerophosphate) containing protease inhibitors (2 μg ml^{-1} Leupeptin, 4 μg ml^{-1} Aprotinin, 1 mM Benzamidine, 100 μg ml^{-1} Pefabloc SC PLUS). Cell lysates were passed through a 26g syringe and clarified by centrifugation. For immunoprecipitation, cell lysates were prepared in lysis buffer (10 mM Tris-HCl pH 7.5, 50 mM KCl, 2 mM $MgCl_2$, 1% Triton X-100, and 1 mM Dithiothreitol, supplemented with protease inhibitors). 30-50 μg of proteins from clarified cell lysates were resolved on 10% SDS-PAGE, except for GADD34 where 8% gels were used. Proteins transferred onto PVDF membranes were subjected to western blot using specific antibodies and signal detected with enhanced chemiluminescence according to the manufacturer's specification.

Immunofluorescence. HeLa cells plated ($2.5X10^4$) on cover slips were transfected with 50 ng of pEGFP-C1-Nck1 or –Nck2 plasmid. 18h post transfection, cells were washed twice in PBS, fixed in 3% para-formaldehyde/PBS for 10 min, permeabilized for 5 min with 0.2% Triton X-100/PBS, and blocked in 1% bovine serum albumin (BSA)/PBS for 30 min. Primary antibodies (anti-Nck 1793, anti-Calnexin) diluted in PBS were added for 1 h at 37°C. After washing with T-TBS (5 times) and PBS (3 times), cells were incubated with secondary antibodies in PBS for 1 h at room temperature (RT). Cells were washed and DNA stained with 4', 6-diamidino-2-phenylindole (DAPI, Sigma) for 5 min in PBS at RT. Coverslips mounted in MOWIOL were air-dried for 18 h at RT and examined on a Zeiss Axiovert 135 fluorescence microscope (63X). Images were recorded using a digital camera (DVC), analyzed with Northern Eclipse software (Empix Imaging Inc.) and processed using Adobe Photoshop 7.0.

Cell survival. MEFs were plated ($3X10^5$ cells) in 60 mm dishes in triplicates and treated with Tg, Tm or H_2O_2 for 24 h at indicated concentrations. Cell viability was scored by counting the number of cells excluding Trypan blue. Apoptosis associated with classical nuclear changes such chromatin condensation, nuclear shrinkage and formation of apoptotic bodies was monitored under fluorescence microscopy, after appropriate staining of nuclei with DAPI as reported above.

Phosphatase Assay. HeLa cells were plated ($2.5X10^5$ cells) in 60 mm dishes in triplicates and phosphatase activity determined the next day using a ser/thr phosphatase kit (Upstate) according to manufacturer's instructions. Briefly, cells were washed twice in ice-cold phosphate-free buffer

(50 mM HEPES pH 7.5, 150 mM NaCl, 10% Glycerol, 1.5 mM $MgCl_2$, and 1 mM EGTA) and lysed in the same buffer supplemented with 1% Triton-X100 and protease inhibitors. Equal amount of proteins (1-2μg) from clarified cell lysates were processed in triplicate in a reaction containing the phosphorylated peptide (K-R-pT-I-R-R) in a 25μl final volume of phosphatase buffer (19.5mM Tris-HCl pH 7.4 / 39 μM $CaCl_2$). After 10 min at 30°C, the reaction was stopped by adding 100 μl of STOP buffer provided by the manufacturer. Samples were transferred into a 96-wells plate and optical density read at 620 nm. OD of the blank was subtracted from OD of each sample.

***In vitro* eIF2α dephosphorylation assay.** *In vitro* eIF2α dephosphorylation assays were performed using recombinant His-eIF2α P^{32}-labeled by GST-PKR as previously described (475). Free [$-^{32}P$] ATP was removed by gel filtration using Probe Quant G-50 microcolumns (Amersham Pharmacia Biotech). Endogenous Nck (C-19) and PP1c (E-9) immunoprecipitates prepared from HEK 293 cell lysates (1-1.5 mg total protein) were incubated at 30°C for 30 min with radiolabeled His-eIF2α as previously reported (294). At the end of the reaction, levels of P^{32}-eIF2α were determined by submitting 30% of the reaction mixture to SDS-PAGE followed by autoradiography and densitometry for quantitation. Alternatively, *in vitro* eIF2α phosphorylation assays were performed on crude detergent cell lysates following the approach described by David Ron's laboratory (142, 184, 294). Briefly, recombinant His-eIF2α (10-50 ng) was radiolabeled in reticulocyte lysates using 50 ng of recombinant bacterially expressed GST-PERK. After gel filtration to get rid of the free [γ–P^{32}]ATP, 2μl of the radiolabeled proteins were incubated at 30°C for 30 min with 5μg of proteins (5μl) from crude detergent lysates of HEK 293 mock transfected cells, HEK 293 cells transiently transfected with plasmids encoding HA-Nck-1, Flag-CReP or Flag-GADD34 in a final reaction volume of 10 μl (dephosphorylation buffer: 20mM Tris-HCl pH 7.4, 50 mM KCl, 2 mM $MgCl_2$, 0.1 mM EDTA, 0.8 mM ATP). The reactions were stopped by adding 2 μl of 6X Laemmli buffer, then boiled and resolved on 10% SDS-PAGE prior to be exposed to autoradiography. Crude detergent cell lysates were obtained by solubilizing the cells in a lysis buffer containing 20 mM Tris-HCl pH 7.4, 0.5% Triton X-100, 50 mM NaCl, 10% glycerol, 0.1 mm EDTA, aprotinin/leupeptin at 10 ug ml^{-1} and PMSF at 100μM.

RESULTS

Nck overexpression downregulates eIF2α phosphorylation-dependent signaling. To determine whether Nck isoforms are functionally redundant in preventing eIF2α phosphorylation in response to ER stress, we overexpressed these proteins in HeLa cells. As we previously reported in HEK 293 cells (197), transient overexpression of HA-Nck1 in HeLa cells completely blocked eIF2α Ser51 phosphorylation induced by cell treatment with tunicamycin (Tm), an inhibitor of N-linked glycosylation perturbing ER function (Fig 1A, upper panels compare lane 4 to 2). We further observed that high levels of Nck1 yield lower basal levels of eIF2α phosphorylated on Ser51 (Fig. 1A, upper panels, compare lanes 3 to 1). Likewise, overexpression of Nck2 also resulted in downregulation of both basal and stress-induced eIF2α Ser51 phosphorylation (Fig. 1A, upper panels, compare lanes 5-6 to lanes 1-2). Furthermore, similar effects were observed in various cell lines (HeLa, HEK 293, N1E-115, NIH 3T3), suggesting that the regulation of eIF2α phosphorylation by Nck is rather ubiquitous than cell specific (data not shown). Interestingly, the effects of overexpressing Nck on eIF2α phosphorylation resemble those observed following CReP and GADD34 overexpression (Fig. 1A, bottom panels), two related PP1c regulatory subunits found in holophosphatase complexes that dephosphorylate eIF2α Ser51 in non-stressed (184) and ER stressed cells (295), respectively. Lower levels of eIF2α phosphorylation in Nck overexpressing cells were still observed up to 24 h treatment with Tm (data not shown) or with the calcium ATPase inhibitor thapsigargin (Tg), which also induces ER stress (Fig. 1B and D), demonstrating that Nck overexpression causes a long lasting inhibition of eIF2α Ser51 phosphorylation. Based on our results, we conclude that both Nck adaptors antagonize the phosphorylation of eIF2α in various cell lines.

eIF2α phosphorylation is known to result in the translational upregulation of the transcriptional activator ATF4 mRNA (137, 365), which mediates the induction of ISR genes. To test whether Nck modulates ISR genes expression, we assessed GADD34 and CHOP expression in Nck1 overexpressing cells subjected to ER stress. As shown in Fig. 1C, transient overexpression of Nck1 attenuated the induction of GADD34 and CHOP in response to Tg treatment. Furthermore, overexpression of Nck results in a long term inhibition of ISR genes

induction as demonstrated by the lower levels of ATF4 and CHOP detected after 24 hours of treatment with Tg in Nck1 overexpressing cells as compared to mock transfected cells (Fig. 1D). We also observed that expression of the Grp94 chaperone protein was considerably reduced in Nck1 overexpressing cells (Fig. 1D). Taken together, these results establish Nck as a regulator of the ER stress-induced eIF2α Ser51 phosphorylation-dependent ISR.

Figure 1. Nck overexpression downregulates eIF2α phosphorylation and eIF2α-dependent signaling. (A) HeLa cells transiently overexpressing Nck1, Nck2, CReP or GADD34 were treated with tunicamycin (Tm; 7.5 μg ml^{-1}) or thapsigargin (Tg; 1μM) for 30 min. Total cell lysates were subjected to western blot analysis using indicated antibodies. Western blots presented are typical of three independent experiments **(B)** HeLa cells transiently overexpressing Nck1 were exposed to thapsigargin (Tg, 1μM) for indicated times, lysed and subjected to western blot analysis with indicated antibodies **(C)** Similar as in **B**, except cells were treated with Tg for 4 and 6 h. Similar results were obtained in three independent experiments. **(D)** Similar as in **B**, except cells were treated for 24 h with Tg. Western blots presented are typical of three independent experiments.

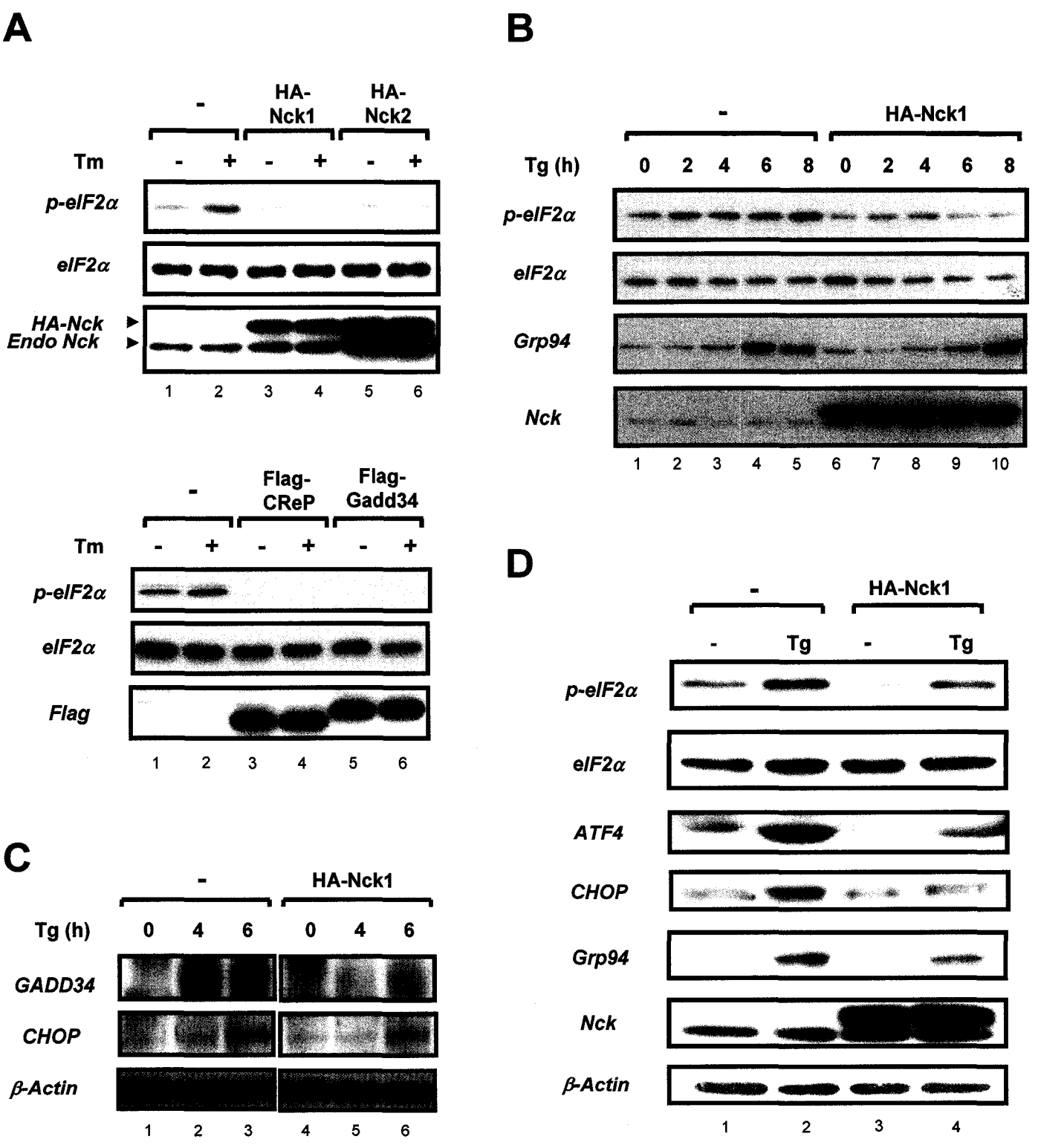
A
-
HA-Nck1
HA-Nck2
Tm
- + - + - +
p-eIF2α
eIF2α
HA-Nck
Endo Nck
1 2 3 4 5 6
-
Flag-CReP
Flag-Gadd34
Tm
- + - + - +
p-eIF2α
eIF2α
Flag
1 2 3 4 5 6
B
-
HA-Nck1
Tg (h)
0 2 4 6 8 0 2 4 6 8
p-eIF2α
eIF2α
Grp94
Nck
1 2 3 4 5 6 7 8 9 10
C
-
HA-Nck1
Tg (h)
0 4 6 0 4 6
GADD34
CHOP
β-Actin
1 2 3 4 5 6
D
-
HA-Nck1
- Tg - Tg
p-eIF2α
eIF2α
ATF4
CHOP
Grp94
Nck
β-Actin
1 2 3 4

Nck localizes at the ER. As phosphorylation of eIF2α by PERK occurs on the cytoplasmic side of the ER and Nck antagonizes PERK-mediated eIF2α phosphorylation, we then used indirect immunofluorescence to determine whether Nck could be detected in the ER area in HeLa cells. Cell staining using a pan-Nck antibody (1793) that recognizes both Nck isoforms revealed a specific and intense reticular signal around the nucleus reminiscent of ER localization (Fig. 2A). Consistent with a role for Nck in receptor tyrosine kinase and integrin signaling, this antiserum also showed enriched local plasma membrane staining (Fig 2A, arrowheads). Similarly, following transient expression of GFP-tagged Nck1 or Nck2 at low levels in HeLa cells, we detected both Nck proteins at the ER (green) as judged by their extensive colocalization with the cytoplasmic domain of calnexin (red), a specific ER marker (Fig. 2B). Since neither Nck1 nor Nck2 amino acid sequence predicts the presence of a signal peptide nor ER retention/retrieval motifs, and thus are not expected to be synthesized and translocated across the Sec61 translocon, we believe the staining for Nck at the ER most likely represents Nck proteins recruited on the cytosolic face of the ER rather than in the ER lumen. These results support our previous findings showing that Nck is detected in enriched calnexin-purified ER fractions (120) and further demonstrate that Nck adaptors localize at the ER, in agreement with their ability to regulate signaling responses from this compartment.

Figure 2. Nck adaptors are detected at the ER. (A) Indirect immunofluorescence in HeLa cells using a pan-Nck antibody (1793) or normal rabbit serum (control). Third panel on the right represents higher magnification of the area selected in the second panel. Bar,10μm. **(B)** HeLa cells transiently transfected with 50 ng of pEGFP-Nck1 or -Nck2 (green) were monitored for Nck expression by direct fluorescence (green) and processed for calnexin detection by indirect immunofluorescence (red). Nucleus staining with DAPI (blue).

A

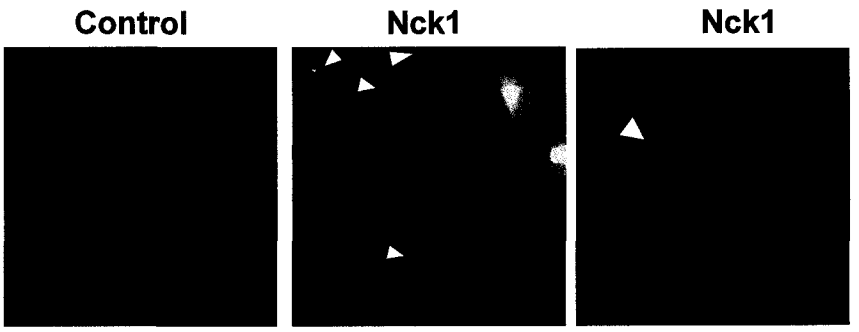

B

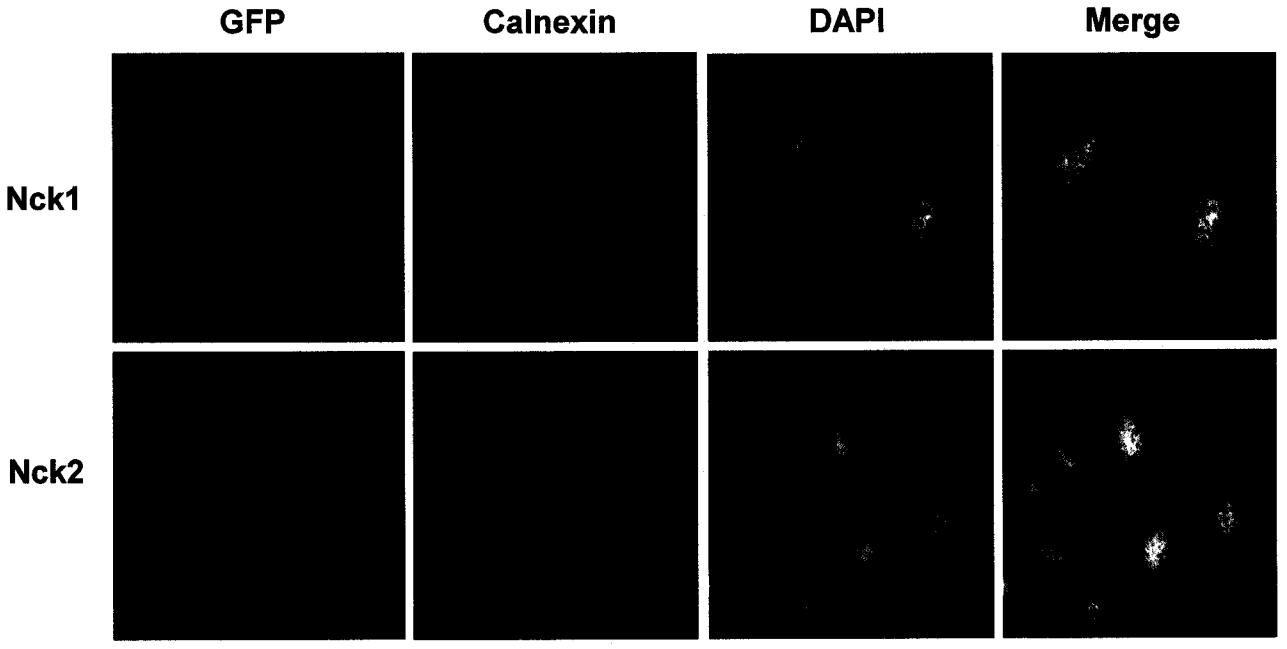

Genetic inactivation of Nck expression establishes spontaneous induction of eIF2α-dependent signaling events. Having shown that overexpression of Nck profoundly impaired phosphorylation of eIF2α and expression of ER stress-related genes, we wished to determine whether deletion of Nck expression promotes activation of components of the ISR. Supported by our previous observation that deletion of Nck in mouse embryonic fibroblasts (MEFs) results in increased phosphorylation of eIF2α Ser51 (197), we addressed eIF2α-dependent signaling events in these cells first in unstressed conditions. As presented in Fig. 3, mutant MEFs presented spontaneous increased levels of ATF4 along with increased induction of its target gene GADD34 (triplicate plates of each cell lines). In addition, Grp94 is also extensively induced in these cells. Although the mutant cells show a primed eIF2α-dependent signaling in absence of exogenous stress, we excluded the possibility that these are continuously experiencing ER stress since BiP, a marker of the UPR downstream of IRE1 and ATF6 activation, is expressed at comparable levels in both cell lines (Fig. 3). This supports our previous observations reporting no constitutive IRE1-dependent events (XBP-1 mRNA levels and splicing) leading to BiP induction in untreated MEFs lacking Nck (289). Overall, our results show that the spontaneous increased levels of eIF2α phosphorylation found in cells genetically deleted of Nck (197) correlates with upregulation of ATF4 and activation of IRS target genes.

Figure 3. Genetic inactivation of Nck expression results in spontaneous induction of components of the ISR in unstressed cells. (A) Equal amount of cell lysate proteins prepared from three separate dishes of early passages of MEFs were analyzed by western blot for indicated proteins using commercial specific antibodies. +/+: MEFs Wt, -/-: MEFs $Nck1^{-/-}Nck2^{-/-}$

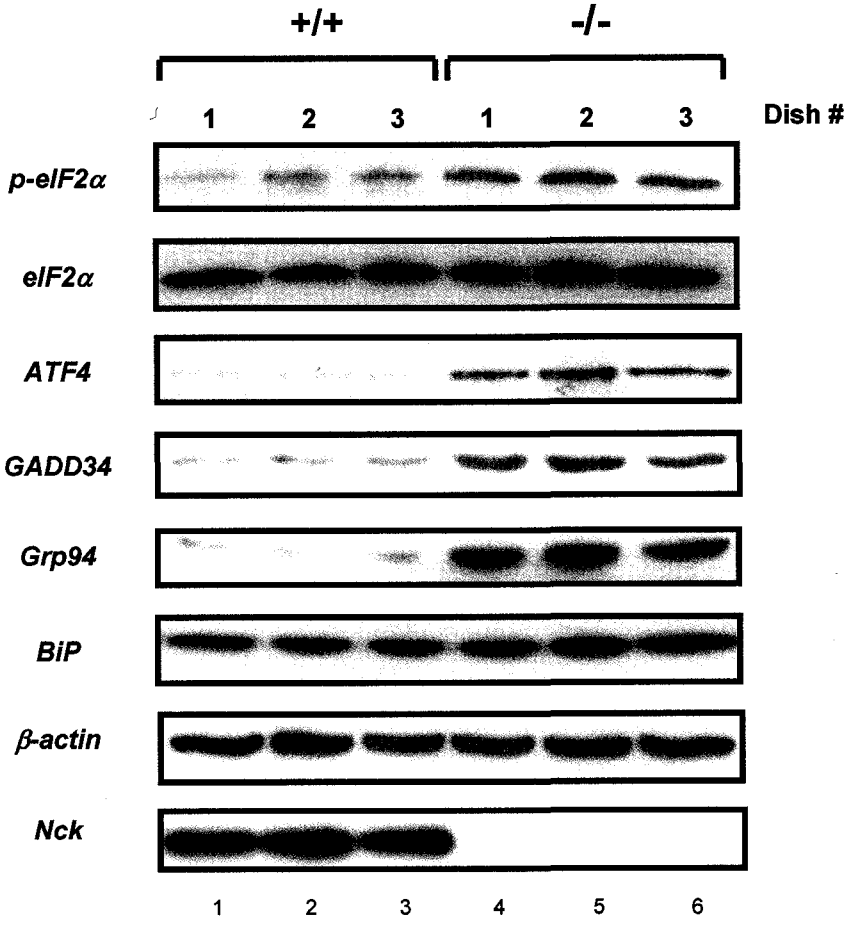
+/+
-/-
1
2
3
1
2
3
Dish #
p-eIF2α
eIF2α
ATF4
GADD34
Grp94
BiP
β-actin
Nck
1
2
3
4
5
6

Genetic inactivation of Nck expression results in higher levels of ER stress-induced eIF2α phosphorylation and premature induction of eIF2α-dependent signaling events, and protects cells from ER stress. We then postulated that Nck adaptors by regulating the phosphorylation of eIF2α Ser51 participate in the accurate control of the timing and intensity of the ISR upon ER stress. To explore this hypothesis, MEFs wt or lacking Nck were subjected to Tm treatment and analyzed for eIF2α phosphorylation (Fig. 4). Western blot analysis revealed greater levels of phosphorylated eIF2α Ser51 in MEFs devoid of Nck, both in dose- (Fig. 4A) and time-dependent (Fig. 4B) manner compared to MEFs wt. At 2.5μg ml^{-1} of Tm, eIF2α phosphorylation is induced by 3.1 fold in MEFs lacking Nck compared to 1.7 fold in MEFs wt (Fig. 4A). After 90 min of treatment with Tm, eIF2α phosphorylation is induced by 2.1 fold in mutant MEFs while being increased by only 1.6 fold in MEFs wt (Fig. 4B). These results suggest that the mechanism regulating the phosphorylation of eIF2α Ser51 in response to ER stress are defective in MEFs lacking Nck.

Figure 4. Genetic inactivation of Nck expression enhances eIF2α Ser51 phosphorylation in response to ER stress. (A) Dose response to Tm. MEFs were treated with indicated concentrations of Tm for 90 min. Cell lysates normalized for protein content were analyzed by western blot with specific pSer51 and total eIF2α antibodies. **(B)** Time-course of eIF2α Ser51 phosphorylation to Tm (2.5 μg ml-1) in MEFs. Upon treatment, cell lysates were processed and analyzed as described in (A).

A

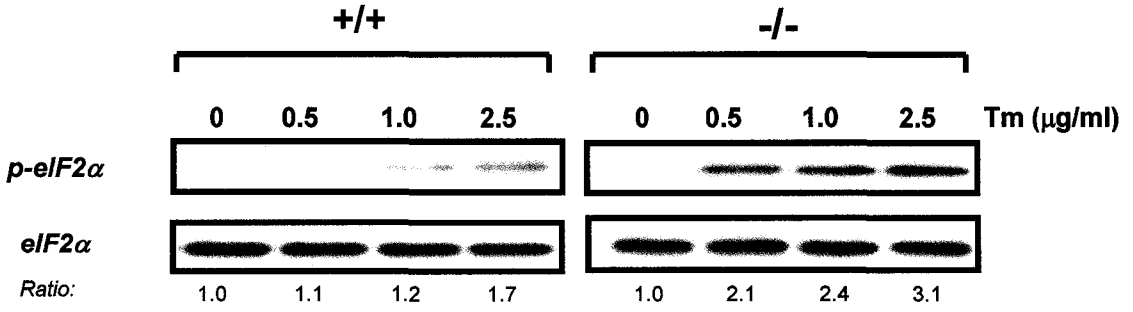
+/+
-/-
0 0.5 1.0 2.5
0 0.5 1.0 2.5
Tm (μg/ml)
p-eIF2α
eIF2α
Ratio:
1.0 1.1 1.2 1.7
1.0 2.1 2.4 3.1

B

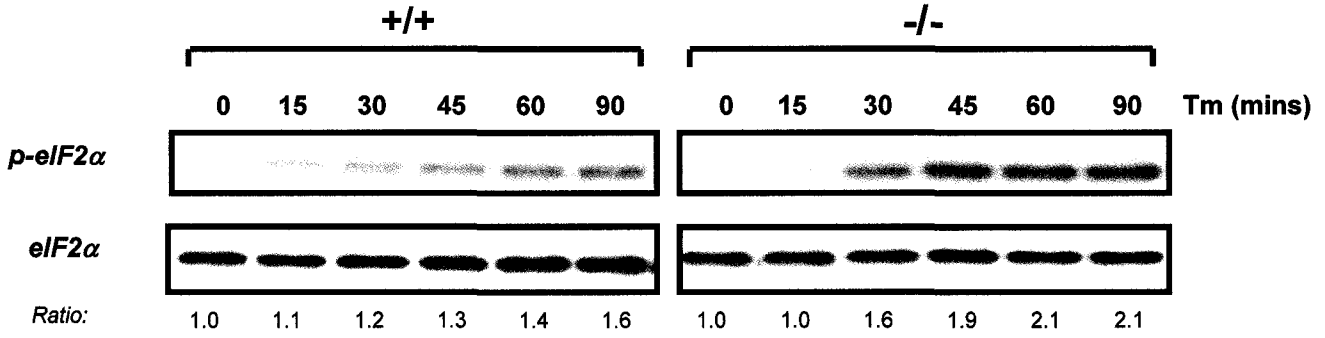
+/+
-/-
0 15 30 45 60 90
0 15 30 45 60 90
Tm (mins)
p-eIF2α
eIF2α
Ratio:
1.0 1.1 1.2 1.3 1.4 1.6
1.0 1.0 1.6 1.9 2.1 2.1

We next examined the kinetics of induction of eIF2α-dependent signaling events in wt and mutant MEFs subjected to ER stress. As shown in Fig 5, MEFs lacking Nck are more responsive to ER stress. First, both ATF4 and CHOP are readily induced at very low concentrations of Tm in mutant MEFs, while being detected only at much higher concentrations in wt MEFs (Fig. 5A). Second, using an ATF4-Luc reporter vector that is a measure of ATF4 translation, we observed that Tg treatment for 6 h resulted in 5-fold induction of the ATF4-Luc reporter in mutant MEFs, while only 2-fold in wt MEFs (Fig. 5B). Finally, the induction of ISR effectors downstream of eIF2α occurs much faster and to a higher extent in mutant MEFs compared to wt (Fig. 5C and D). In particular, ATF4 and CHOP proteins appear within 4 to 6 h upon treatment with Tg in control cells, while being easily detected between 1 and 2 h in mutant cells (Fig. 5C). As shown in Fig. 5D, this prominent signaling persists up to 24 h after initiating ER stress. β-actin levels were very similar among the different MEFs lysates showing that equivalent amount of total proteins were analyzed in each condition. Noteworthy, no change in Nck levels was observed upon exposure of wt MEFs to either Tm or Tg (Fig. 5C and D). Moreover, we noticed that BiP and Grp94 are induced at higher extent in mutant MEFs and in a manner very similar to effectors of the ISR (Fig. 5C and D). As normal XBP-1 mRNA splicing has been reported in ER-stressed MEFs lacking Nck (289), possible crosstalks between PERK and IRE1 and/or ATF6 branches of the UPR can account for the rapid and robust BiP and Grp94 induction we observed in mutant compared to wt MEFs. From these results, we conclude that Nck adaptors modulate the kinetic and robustness of eIF2α-dependent events in response to ER stress.

Figure 5. Genetic inactivation of Nck expression results in premature induction of eIF2α-dependent signaling events in response to ER stress. (A) Dose response to Tm. MEFs were treated with indicated concentrations of Tm for 90 min and cell lysates normalized for protein content were analyzed by western blot using ATF4 and CHOP specific antibodies. β-actin determined also by western blot is used as loading control (**B**) ATF4-Luc reporter activity in MEFs previously transiently transfected with the reporter vector and treated with Tg (250 nM, 6 h). Error bars represent SEM, *P<0.01 by t-test, n=3. **(C)** Time-course of Tg treatment (1 μM) in MEFs. Similar to A, expression of the indicated proteins was followed by western blot using specific antibodies. Close arrowhead: Grp94; open arrowhead: BiP. **(D)** Same as in C, except the time-course was performed over 24 h.

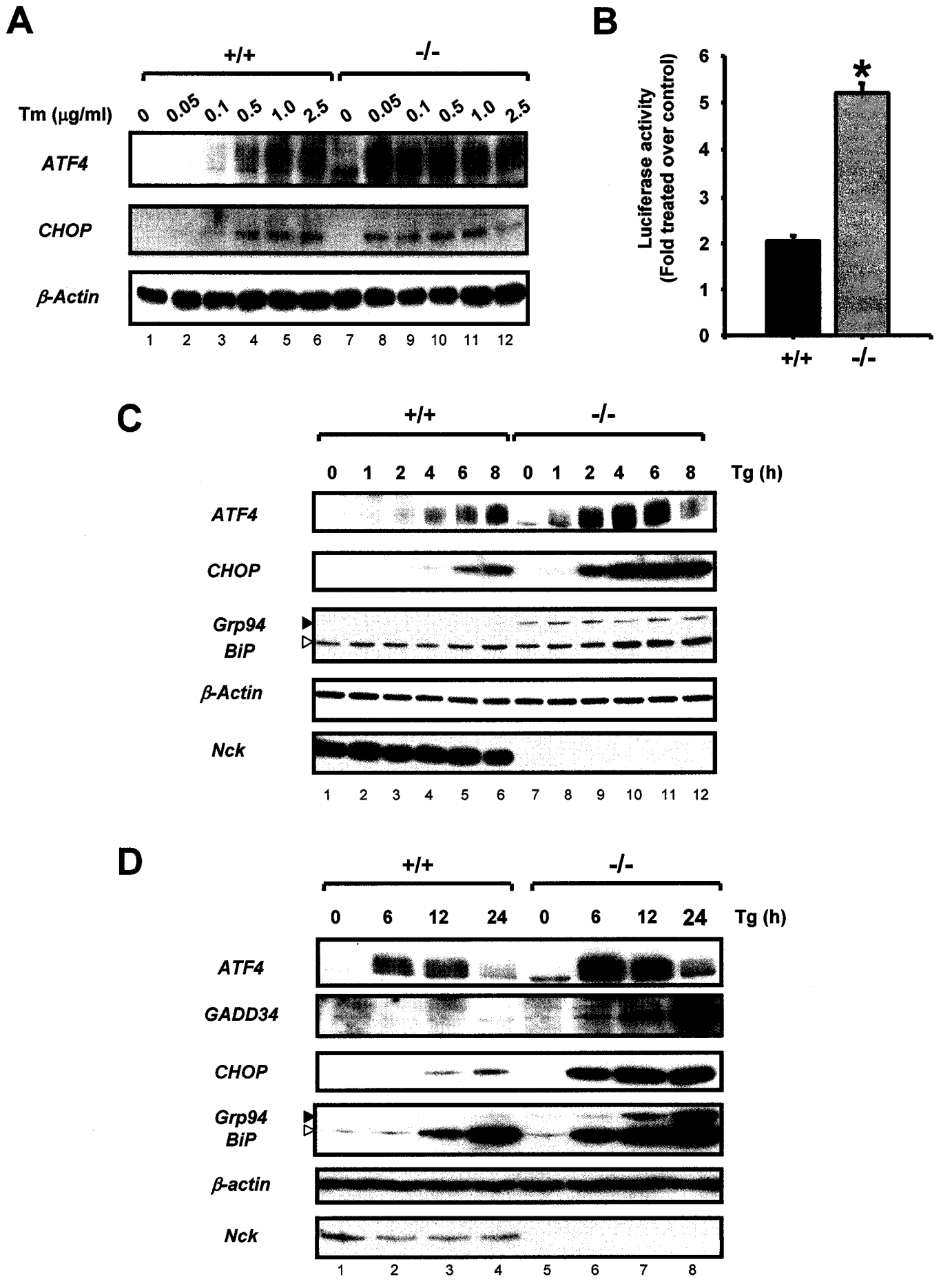
A
+/+
-/-
Tm (μg/ml)
0 0.05 0.1 0.5 1.0 2.5 0 0.05 0.1 0.5 1.0 2.5
ATF4
CHOP
β-Actin
1 2 3 4 5 6 7 8 9 10 11 12
B
Luciferase activity
(Fold treated over control)
0 1 2 3 4 5 6
*
+/+
-/-
C
+/+
-/-
0 1 2 4 6 8 0 1 2 4 6 8 Tg (h)
ATF4
CHOP
Grp94
BiP
β-Actin
Nck
1 2 3 4 5 6 7 8 9 10 11 12
D
+/+
-/-
0 6 12 24 0 6 12 24 Tg (h)
ATF4
GADD34
CHOP
Grp94
BiP
β-actin
Nck
1 2 3 4 5 6 7 8

Phosphorylation of eIF2α on Ser51 serves as a protective mechanism for cells to survive diverse stressful situations including ER stress (184, 251, 289). In opposition, the inability to overcome stress leads to apoptosis through the activation of caspases (334). To directly address the role of Nck in apoptosis induced by chronic ER stress, we treated MEFs wt or deleted of Nck with Tg or Tm for 24 h, and analyzed their morphology and survival at the end of the treatment. Under phase-contrast microscopy, we observed that wt MEFs initially round up and ultimately detached from the surface of the culture dish (Fig. 6A). In contrast, this behavior is less pronounced in cells lacking Nck adaptors, suggesting that these cells are protected from ER stress. This was demonstrated by determining that only 26% of wt MEFs survived to 24 h treatment with Tg, whereas this percentage significantly increased to 57% in mutant MEFs (Fig. 6B). Treatment with Tm yielded similar results, while hydrogen peroxide exposure at doses that had no effect on eIF2α phosphorylation (296), induced much higher levels of cell death in MEFs lacking Nck compared to wt (Fig. 6B). These data demonstrate that the absence of Nck specifically protects cells from ER stress.

To further substantiate our findings, we treated MEFs with different concentrations of Tg or Tm for 24 h and measured the number of apoptotic cells by counting nuclei with condensed chromatin as revealed by DAPI staining (Fig. 6C). We found that the number of apoptotic cells was significantly reduced in mutant MEFs as compared to wt in both Tm and Tg treated conditions, confirming that the MEFs lacking Nck are protected from ER stress-induced cell death. We then assessed caspase-3 and poly(ADP-ribose) polymerase (PARP) processing which normally occur during programmed cell death. As expected, both proteins were preferentially cleaved in a time-dependent manner in wt but not in mutant MEFs (Fig. 6D). Similar results were obtained upon 24 h treatment with Tm (Fig. 6E). In contrast, cleavage of PARP was more pronounced in response to H_2O_2 exposure in MEFs lacking Nck, in agreement with their higher sensitivity to cell death induced by H_2O_2 (Fig. 6F). From these results, we concluded that Nck proteins are required to initiate the events leading to caspases/PARP cleavage and apoptosis in cells experiencing prolonged ER stress.

Figure 6. Improved survival of Nck1$^{-/-}$Nck2$^{-/-}$ MEFs to prolonged ER stress. (A) Phase contrast microscopy of MEFs treated or not for 24 h with Tg (1 μM). **(B)** Quantitative analysis of Tg- and Tm- and H_2O_2-induced cell death in MEFs. MEFs wt (+/+) and Nck1$^{-/-}$Nck2$^{-/-}$ (-/-) were untreated or treated 24 h with Tg (1 μM, n=3), Tm (2.5 μg ml^{-1}, n=7) or 100 μM and 200 μM H_2O_2 (n=3). Cell viability was scored by counting number of cells excluding Trypan Blue. Error bars represent SEM, *P<0.001 and **P=0.002 versus respective MEFs +/+ treated cells by t-test. **(C)** Quantitative analysis of the number of apoptotic nucleus in MEFs treated with indicated concentration of either Tg (n=3) or Tm (n=3). Error bars represent SEM. *P<0.05 by t-test **(D)** Time-course of the induction of caspase-3 and PARP cleavage in MEFs wt (+/+) and Nck1$^{-/-}$ Nck2$^{-/-}$ (-/-) treated for different times with Tg (1 μM). Cell lysates normalized for protein content were analyzed by western blot using appropriate specific antibodies. Close arrowhead: full-length inactive proteins. Open arrowhead: active cleavage product. **(E)** Similar as in **D**, except the MEFs were treated for 24 h with Tg (1 μM) or Tm (2.5 μg ml^{-1}). **(F)** Similar as in **E**, except MEFs were exposed to 100 μM H_2O_2 for 24 h. Panels D, E and F are typical representative of results obtained from three independent experiments.

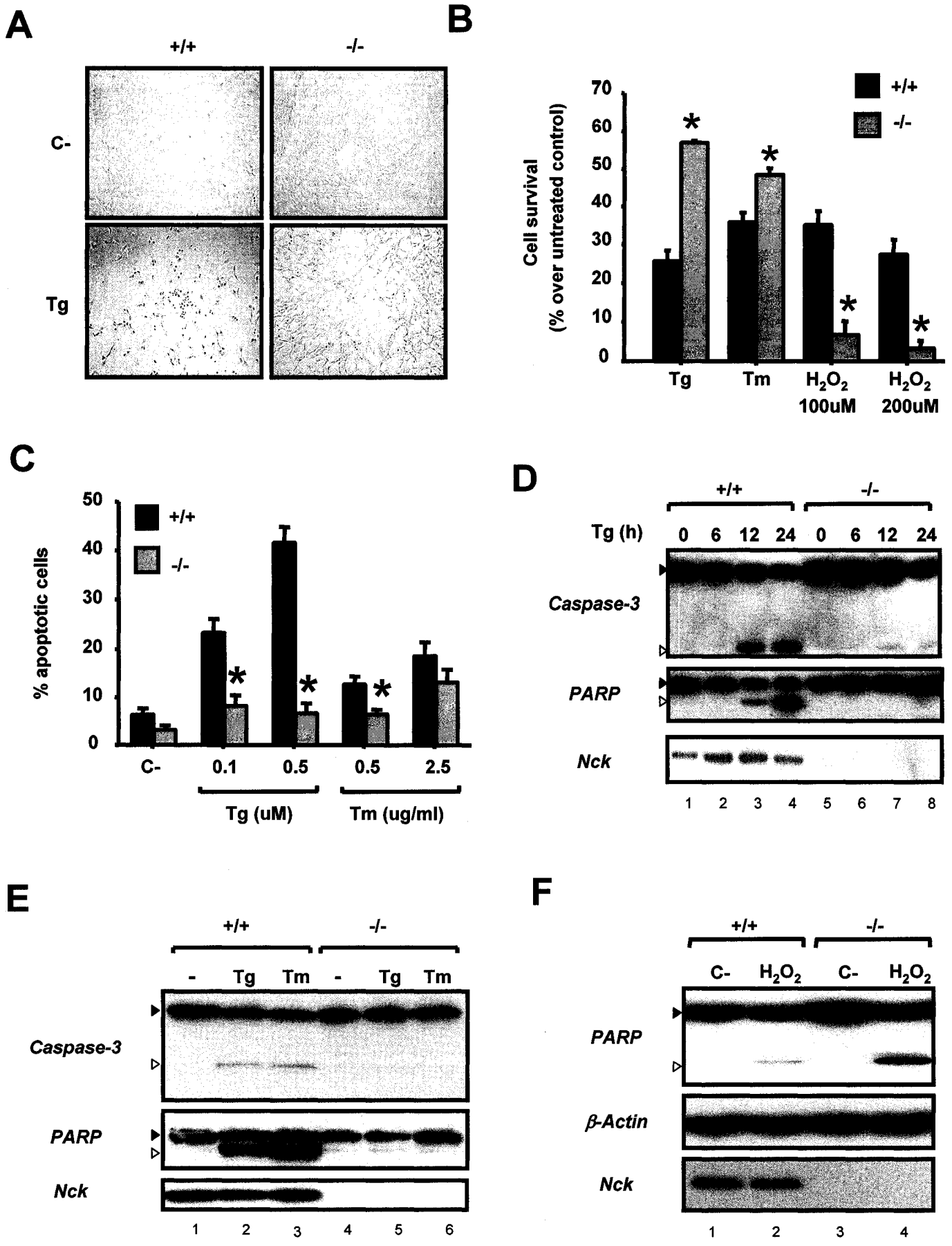
A
+/+
-/-
C-
Tg
B
Cell survival
(% over untreated control)
70
60
50
40
30
20
10
0
+/+
-/-
Tg
Tm
H2O2
100uM
H2O2
200uM
C
% apoptotic cells
50
40
30
20
10
0
+/+
-/-
C-
0.1
0.5
0.5
2.5
Tg (uM)
Tm (ug/ml)
D
+/+
-/-
Tg (h)
0 6 12 24 0 6 12 24
Caspase-3
PARP
Nck
1 2 3 4 5 6 7 8
E
+/+
-/-
- Tg Tm - Tg Tm
Caspase-3
PARP
Nck
1 2 3 4 5 6
F
+/+
-/-
C- H2O2 C- H2O2
PARP
β-Actin
Nck
1 2 3 4

Nck is part of a molecular complex that controls dephosphorylation of eIF2α. The results presented above suggest that Nck adaptors determine the kinetics of eIF2α phosphorylation and the attendant ISR activation in cells undergoing ER stress by being at the center of a mechanism that antagonizes the phosphorylation of eIF2α. However, how Nck downregulates the phosphorylation of eIF2α still remains to be defined. Work from our laboratory demonstrated that Nck regulates translation through its interaction with the β subunit of the eIF2 complex (198). This present study suggests that Nck acts on translation most probably by lowering cellular levels eIF2α phosphorylation. In agreement with this hypothesis, we previously reported that calyculin A, a potent inhibitor of PP1/PP2A activity, prevented Nck from downregulating eIF2α phosphorylation in response to ER stress (197), suggesting that a phosphatase activity mediates the effects of Nck overexpression on eIF2α phosphorylation. To elucidate the mechanism by which Nck controls the phosphorylation state of eIF2α, we initiated a series of experiments aimed to determine whether a protein Ser/Thr phosphatase interacts with Nck. First, using a commercial kit that monitors *in vitro* dephosphorylation of a phosphopeptide by PP1c and PP2A phosphatase activity (KRpTIRR), we detected a ser/thr phosphatase activity of this type in Nck immunoprecipitates prepared from HEK 293 cells (Fig. 7A). Moreover, we found that this phosphatase activity correlated with the presence of PP1c in Nck immunoprecipitates isolated from HEK 293 (Fig. 7B) and HeLa cells (data not shown), while PP2A could not be detected (data not shown). In contrast, PP1c was not detected in normal rabbit IgGs immunoprecipitates (Fig. 7B), further underscoring the specificity of the Nck-PP1c coimmunoprecipitation. As expected Nck immunoprecipitates contain eIF2β and most importantly, eIF2α (Fig. 7B). We confirmed reciprocal coimmunoprecipitations by showing that Nck, PP1c, and eIF2β are all found in an eIF2α immune complex (Fig. 7C) but not in normal rabbit IgG immunoprecipitates (data not shown). Together, these results demonstrate that Nck, PP1c and components of eIF2 are in a common complex.

We further investigate this molecular complex by determining whether CReP, a PP1c interacting protein regulating the dephosphorylation of eIF2α on Ser51 could be found in Nck immune complex. The lack of potent CReP antibody prevented us to sound for endogenous CReP in Nck immunoprecipitates. However, in cells overexpressing a Flag-tagged version of

CReP, we detected CReP, PP1c and eIF2β in Nck immunoprecipitates (Fig. 7D). To clearly establish that Nck is part of an actual eIF2α holophosphatase complex that dephosphorylates eIF2α Ser51, we performed *in vitro* eIF2α dephosphorylating assays using lysates obtained from Nck overexpressing cells. From these assays, we noticed that crude cell lysates prepared from Nck1 overexpressing cells always present higher eIF2α dephosphorylating activity than equivalent mock-transfected cell lysates (Fig. 7E, left panel) and was comparable to the dephosphorylating activity detected in CReP or GADD34 transiently overexpressing cell lysates (Fig. 7E, middle panel). Finally, we found that Nck immunoprecipitate contains an activity that dephosphorylates eIF2α Ser51 as revealed by the decrease of radioactivity associated with eIF2α in Nck immunoprecipitates compared to normal IgGs immunoprecipitates (Fig. 7E, right panel). In these assays, we were surprised to find that the PP1c immunoprecipitates that we used as positive control did not show a robust eIF2α dephosphorylating activity. Although this remains to de determined, to explain this we propose that the specific antibody we used to immunoprecipitates PP1c possibly interferes with the active catalytic site of PP1c, thus reduces PP1c phosphatase activity. On the other hand, we believe the eIF2α dephosphorylating activity detected in Nck immunoprecipitates to be significant since the Nck molecular complex containing PP1c probably represents only a minor fraction of the cellular complexes assembled by Nck adaptors.

Figure 7. Nck assembles an eIF2α holophosphatase complex. (A) PP1c/PP2A phosphatase activity in Nck (C-19) immunoprecipitates. From HeLa cell lysates, equal amount of proteins were subjected to Nck or rabbit control IgG immunoprecipitation and phosphatase activity was evaluated in respective immunoprecipitates using a commercial kit (Upstate) that monitors PP1/PP2A type of phosphatase activity. Results are the mean +/- SEM and represent three independent experiments performed in triplicate. **(B)** Coimmunoprecipitation of PP1c, eIF2β and eIF2α with Nck in HEK 293 cells. TCL: total cell lysate. IgG: Immunoprecipitation with rabbit IgG control. Nck: Immunoprecipitation with Nck antibody (C19). Indicated proteins were detected by western blot using specific antibodies. Similar results were obtained in three independent experiments (**C**) Ectopically expressed HA-Nck1 (close arrowhead); endogenous Nck (open arrowhead), PP1c and eIF2β are detected in eIF2α immunoprecipitates isolated from HEK 293 cell lysates. TCL: total cell lysate. IP eIF2α: Immunoprecipitated eIF2α. Indicated proteins were detected by western blot using specific antibodies. Similar results were obtained in three independent experiments **(D)** Coimmunoprecipitation of Flag-CReP with Nck. Similar as in **A,** except Flag-CReP was transiently expressed in HEK 293 cells. 24 h post transfection, lysates were prepared for Nck immunoprecipitation. Close arrowhead: eIF2β immunoreactive band migrating slightly faster that the IgGs **(E)** I*n vitro* dephosphorylation of His-eIF2α P^{32}-labeled on Ser51 obtained from mock or Ha-Nck1 transiently transfected HEK 293 cells lysates shown in duplicate of transfection (left panel), Reported under the autoradiography are the mean densitometry values of the mock-transfected lysates (set at 100%) and the HA-Nck1 transfected cell lysates. Middle panel: Comparative analysis of the dephosphorylating activity found in lysates prepared from Nck1, CReP and GADD34 transiently overexpressing cells. Left panel: eIF2α dephosphorylating activity found in Nck or PP1c immunoprecipitates prepared from equal amount of proteins from HEK 293 cell lysates. Each reaction was probed by western blot for Nck and PP1c immunoprecipitated (bottom panels). Radioactivity associated with His-eIF2α was monitored by densitometry using the Image Quant program (BioRad) and quantitation shown under the radioautoradiogram. Arrowhead: P^{32}-labeled His-eIF2α Ser51; Asterisk: degradation product of His-P^{32}-labeled eIF2α.

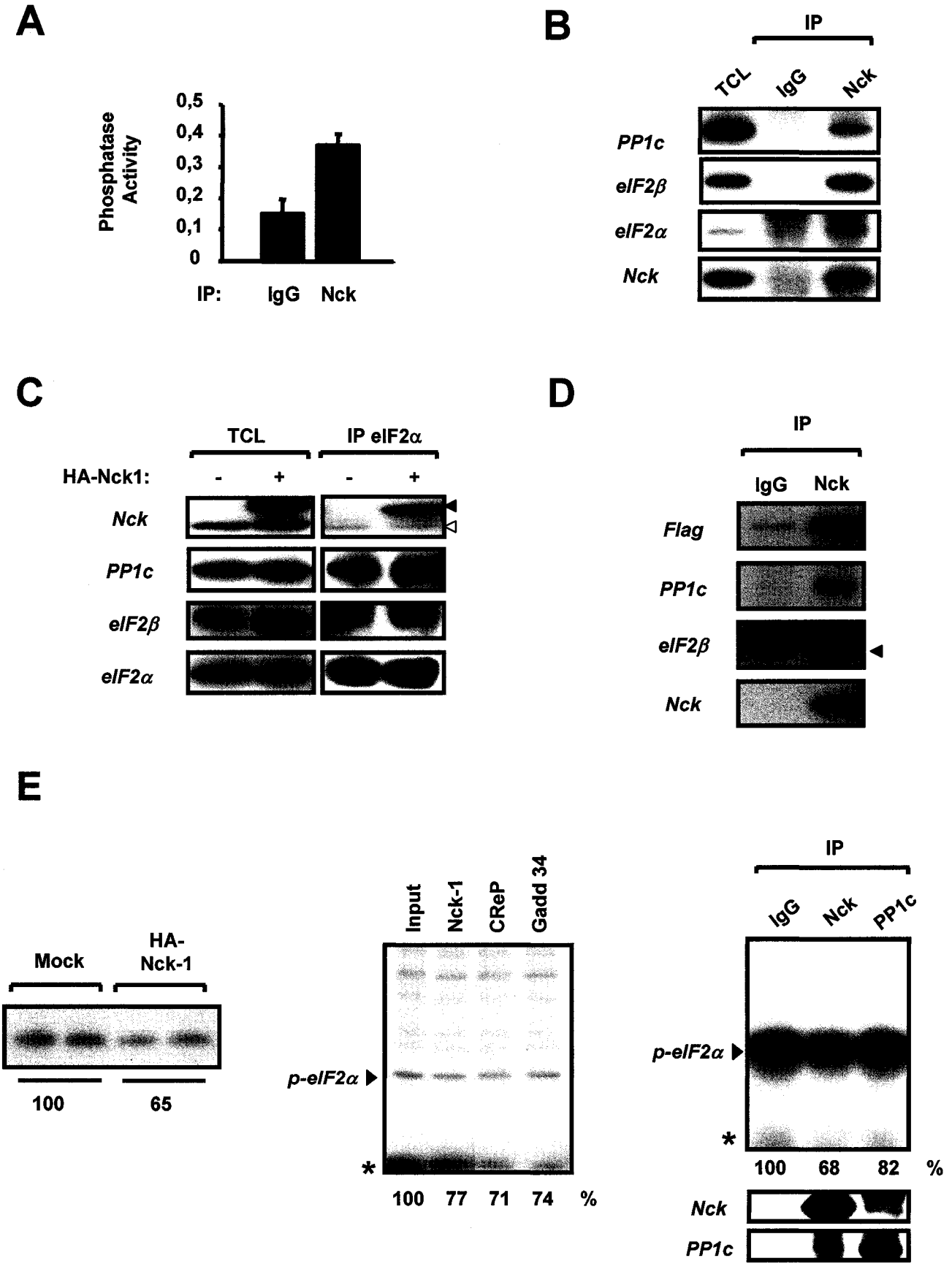
A
Phosphatase Activity
0,5
0,4
0,3
0,2
0,1
0
IP:
IgG
Nck
B
IP
TCL
IgG
Nck
PP1c
eIF2β
eIF2α
Nck
C
TCL
IP eIF2α
HA-Nck1:
-
+
-
+
Nck
PP1c
eIF2β
eIF2α
D
IP
IgG
Nck
Flag
PP1c
eIF2β
Nck
E
Mock
HA-Nck-1
%
100
65
Input
Nck-1
CReP
Gadd 34
p-eIF2α
*
100
77
71
74
%
IP
IgG
Nck
PP1c
p-eIF2α
*
100
68
82
%
Nck
PP1c

Lastly, we reasoned that recruitment of PP1c and eIF2 components in a common complex might be perturbed in absence of Nck proteins. By determining the amount of PP1c detected in eIF2β immunoprecipitates, we observed that it was reduced by approximately 70% in MEFs lacking Nck (Fig. 8). This suggests that Nck plays an important role in maintaining a significant amount of PP1c in the vicinity of eIF2, allowing eIF2α dephosphorylation. All together, our results support the idea that Nck assembles a molecular complex that contains PP1c, CReP and components of eIF2, and in this manner, controls the dephosphorylation of eIF2α. Importantly, defect in this Nck-dependent regulatory mechanism has clear impacts on the cellular response to stress that converge on the phosphorylation of eIF2α as seen in MEFs lacking Nck.

Figure 8. Reduced amounts of PP1c in the eIF2 complex in $Nck1^{-/-}Nck2^{-/-}$ MEFs. Equal amount of proteins from MEFs total cell lysates (TCL) were subjected to eIF2β immunoprecipitation (IP eIF2β) and analyzed by western blot for PP1c, eIF2α and eIF2β content (upper panel). Quantitation of the amount of PP1c in eIF2β immunoprecipitates (bottom panel). Error bars represent SEM. *P<0.05 by t-test, n=3.

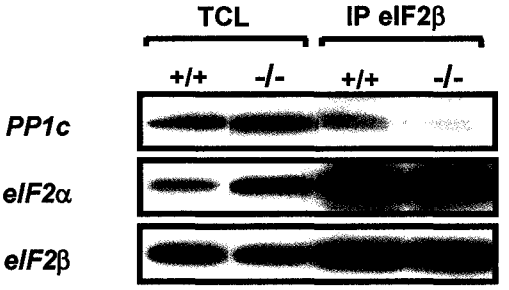
TCL
IP eIF2β
+/+
-/-
+/+
-/-
PP1c
eIF2α
eIF2β

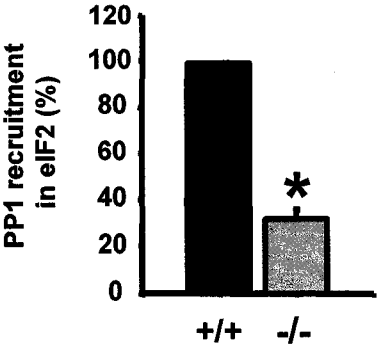
PP1 recruitment in eIF2 (%)
120
100
80
60
40
20
0
*
+/+
-/-

DISCUSSION

Research over the past years has revealed that a number of molecules involved in signaling pathways initiated at the plasma membrane, also transit to endomembrane compartments to transduce signals into different cellular outcomes (63, 248). Our study supports this concept by showing that the SH2/SH3 domains-containing Nck adaptors, not only transduce signal from receptor tyrosine kinases at the plasma membrane (167), but also localize at the ER where they participate in ER signaling regulating cellular response to stress. Thus, Nck adaptors are used by different cellular compartments in various cell conditions to generate specific cellular responses.

It is well documented that other conditions beside ER stress, such as amino acid deprivation (158), viral infection (193) or heme deficiency (57), activate distinct eIF2α kinases that phosphorylate eIF2α on Ser51, resulting in inhibition of mRNA translation. In contrast, in the past years the identification of complexes regulating the dephosphorylation of eIF2α Ser51 revealed the importance of appropriate control of eIF2α-dependent signaling in response to stress. However, our knowledge of the mechanisms regulating eIF2α Ser51 dephosphorylation is still limited to proteins targeting the ser/thr phosphatase PP1c to eIF2α and to the molecular determinants underlying their interaction with PP1c. For example, CReP, the constitutive repressor of eIF2α phosphorylation, is expressed in unstressed cells where it keeps eIF2α hypophosphorylated through its interaction with PP1c (184). Similarly, GADD34 is also known as a PP1c interacting protein that controls dephosphorylation of eIF2α (67). In contrast to CReP, GADD34 expression is induced upon stress and mediates the translational recovery phase of the UPR (67, 256, 294). In addition, some viruses encode products with high homology to GADD34. For example, herpes simplex virus encodes the ICP34.5 protein, which by interacting with PP1c promotes eIF2α dephosphorylation and allows the virus to escape inhibition of protein synthesis occurring upon infection (150, 151). For the most part if not all, PP1c regulatory proteins involved in eIF2α dephosphorylation contain a KVxF motif that was found to mediate their interaction with PP1c (66). While we begin to appreciate the physiological importance of these regulatory checkpoints, other protein components of eIF2α holophosphatase complexes remain to be identified. In this study, we report that the Nck adaptor is part of a CReP-PP1c-containing

molecular complex that dephosphorylates eIF2α and controls the temporal activation of the ISR and cell survival to ER stress.

We established that both Nck1 and Nck2 redundantly modulate eIF2α Ser51 phosphorylation (Fig. 1A). Particularly, we demonstrated that like CReP and GADD34, overexpression of either Nck downregulates both basal and stress-induced eIF2α Ser51 phosphorylation (Fig. 1A and B). In contrast, in MEFs lacking Nck, we previously reported that eIF2α phosphorylation was increased (197) and our present data show that this correlates with a primed eIF2α-signaling (Fig. 3). We believe that this directly impacts on the kinetic and intensity of the ISR (Figs. 4 and 5) and improves cell survival rates to ER stress (Fig. 6). We uncovered that Nck is part a large molecular complex containing CReP, PP1c and subunits of eIF2 that dephosphorylates eIF2α on Ser51 (Fig.7). This complex is required for proper control of eIF2α phosphorylation on Ser51, eIF2α-dependent signaling and an appropriate cell response to ER stress. Importantly, the amount of PP1c found in this complex is dependent on the presence of Nck since it is greatly reduced in MEFs deleted of Nck (Fig. 8). Based on these results, we propose that Nck significantly contributes to the organization and/or stability of this CReP/PP1c-containing complex, regulating the amount of PP1c recruited in close proximity to eIF2 and in this manner, regulates eIF2α dephosphorylation on Ser51 (Fig. 9). Additional experiments are required to dissect the molecular interactions underlying the formation of this complex and to determine its structural organization. Given that the recruitment of PP1c in this complex is perturbed in Nck-deficient MEFs, one possibility is that Nck directly interacts with either PP1c and/or CReP and in this way, contributes to the stability of the complex. In agreement with this is the presence of a potential PP1c binding site (xVxF) (66) in both Nck isoforms and conserved from C. elegans to humans. Alternatively, based on its modular structure, Nck by mediating proline and/or phosphotyrosine-based protein interactions via its SH3 and SH2 domains could be responsible of proper assembly of this molecular complex. Experiments are now being conducted in order to gain insights into the possible interplay existing between Nck and other components of this eIF2α holophosphatase complex.

Figure 9. Schematic model of components of the holophosphatase complex regulating phosphorylation of eIF2α on Ser51 in ER stress. As a component of the CReP/PP1c holophosphatase complex, Nck regulates ER stress-induced eIF2α phosphorylation on Ser51 and attending signaling. This dictates the timing and robustness of ISR signaling and determines cell fate in response to ER stress. Whether Nck is also part of the GADD34/PP1c complex still remains to be demonstrated.

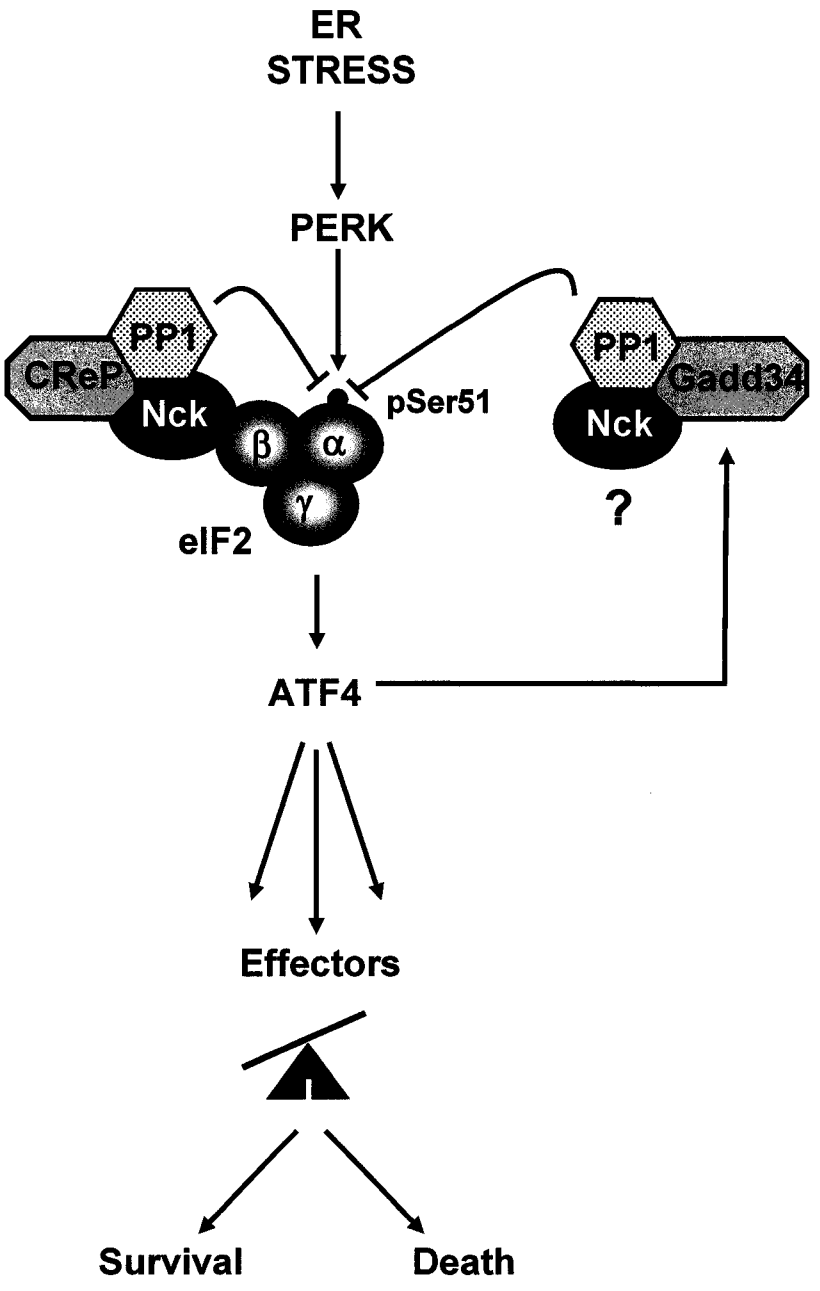
ER
STRESS
PERK
PP1
CReP
Nck
pSer51
β
α
γ
eIF2
PP1
Gadd34
Nck
?
ATF4
Effectors
Survival
Death

As mentioned above, GADD34 has been identified as a regulatory subunit that also targets PP1c to eIF2α and the GADD34-PP1c complex has been shown to act in a coordinated and timely manner to dephosphorylate eIF2α (256, 294). Although we found CReP and Nck in a common complex, it is possible that Nck could also be part of the GADD34 and ICP34.5 eIF2α holophosphatase complex. It is still to be addressed whether Nck could represent a critical component of more than one molecular complex regulating the dephosphorylation of eIF2α in response to diverse stresses. Interestingly, recent data from our group suggest that Nck shows preference or specificity toward stresses activating eIF2α-kinases converging to the phosphorylation of eIF2α, suggesting that its effect is not general to any eIF2α-kinase (unpublished results). Lastly, in a manner very homologous to its adaptor role in translocating specific effectors to activated receptor kinases at the plasma membrane, Nck could target the holophosphatase complexes to specific subcellular compartments to properly control localized mRNA translation and/or eIF2α-dependent signalling. This was proposed in a recent study demonstrating that ER-bound ribosomes are still translationally active during the UPR albeit upregulated eIF2α Ser51 phosphorylation (390), suggesting that spatially restricted mechanisms exist that allow translation of a limited number of mRNA by locally preventing phosphorylation and/or promoting dephosphorylation of eIF2α.

Numerous genes are upregulated by ER stress following phosphorylation of eIF2α. However, how these late events are coordinated among each other over time remains to be determined. Here, we show that MEFs lacking Nck show spontaneous induction of ATF4 and GADD34 (Fig. 3), in addition to primed UPR in response to pharmacological inducers of ER stress (Figs. 4 and 5). Therefore, the Nck-containing eIF2α holophosphatase complex represents an essential regulatory mechanism that restricts signaling from eIF2 in unstressed cells and determines the kinetic and the intensity of this signaling in ER stress conditions. While we anticipated that effectors of the ISR would be modulated by Nck proteins levels, we were surprised to find changes in BiP and Grp94 induction in response to Tg in MEFs lacking Nck (Fig. 5). First, transactivation of the BiP promoter which has been highly investigated is known to be under the control of XBP-1 and ATF6 (227, 229, 455). Second, no change in IRE1-dependent splicing of XBP-1 or BiP mRNA levels were found in Azc-treated MEFs lacking Nck compared to wt (289). Conversely, upregulation of BiP mRNA levels was reduced in MEFs

expressing a non phosphorylated form of eIF2α (eIF2α Ser51 for Ala) (365) and ATF4 overexpression leads to transactivation of the BiP promoter (253). Therefore, increased BiP levels in MEFs lacking Nck could be partially attributed to the higher basal and stress-induced levels of ATF4. Based on these observations, crosstalks between PERK and IRE1 pathways leading to BiP and Grp94 induction likely exist. Alternatively, the discordance in BiP induction upon Azc (289) and Tg (this study) could account on the fact that these drugs do no recapitulate identical ER signaling.

The Nck-dependent regulatory mechanism described in this study appears of major importance as we confirmed that the ability of cells to survive to ER stress inversely correlates with expression levels of Nck (Fig. 6) (197). We found that MEFs lacking Nck show prominent ER stress signaling from eIF2α (Fig. 5). This allows these cells to rapidly clear stress in the ER and escape apoptotic programs (Fig. 6). Noticeably, this closely resembles the behavior of the CReP RNAi cells, which show spontaneous induction of the CHOP promoter, and resistance to stresses that cause eIF2α Ser51 phosphorylation (184). However, we cannot exclude that other ER-induced signaling pathways such as IRE1-mediated ERK1/2 activation also contribute to improve cell survival in absence of Nck (289). Collectively, our results are in accordance with the protective function of eIF2α Ser51 phosphorylation (400), and in agreement with reports demonstrating that preconditioning of cells to stress targeting eIF2 establishes a resistant state toward subsequent challenges (34, 251). It is believed that the temporal induction of the ER stress response strongly influences cellular outcomes, and could underlie the difference in sensitivity of various cell types to ER stress. Our finding that Nck expression levels markedly influence signaling and cells survival to ER stress reveals the interest to search for defects in Nck expression in proteotoxic diseases where uncontrolled ER stress-induced signaling is linked to pathogenesis (138, 220, 311).

Results presented here reinforce the concept that Nck is a bonafide player in such a fundamental cellular process that is mRNA translation and highlights the versatile properties of this protein. More importantly, this study sheds light on the potential mechanism by which Nck adaptors regulate mRNA translation. This could change our understanding of essential biological processes such as development of the central nervous system. Significant evidence has

accumulated in recent years showing that local translation in axons is integral for growth cone navigation in response to environmental cues (326). Concomitantly, Nck has been implicated in photoreceptor cells axon guidance in Drosophila (115, 383) and in signaling downstream of various mammalian axon guidance receptors (68, 240). It is thus possible that Nck might regulate neural network formation by coupling local protein synthesis with guidance receptors activation at the growth cone. Therefore, our study emphasizes the importance of evaluating the role of Nck on translation in biological processes depending on local protein synthesis and simultaneously, opens up new research avenues meant to examine the *in vivo* significance of this novel function of Nck adaptors.

ACKNOWLEDGMENTS

This work was supported by a grant to L.L. from the Canadian Diabetes Association in honor of the late Lilian I. Dale. M.L. was supported by a fellowship and L.L. by an award both from the Fond de la Recherche en Santé du Québec (FRSQ). We thank Tony Pawson for providing the $Nck1^{-/-}Nck2^{-/-}$ MEFs. We also thank Weil Li for Nck1 and Nck-2 expression plasmids and David Ron for the kind gift of the ATF-Luc reporter gene, the pCMV2-Flag-$mCReP_{24\text{-}698}$ and –Flag-mGADD34 plasmids. Finally, we are grateful to Geneviève Bourret for technical assistance, Gaël Jean-Baptiste and Barry I. Posner for critical reading of this manuscript.

CHAPTER III

The Endoplasmic Reticulum Ser/Thr Protein Kinase PERK juxtamembrane domain tyrosine residue 561 is required for Nck adaptor binding and regulation of catalytic kinase activity

Reproduced with permission from Mathieu Latreille and Louise Larose.
The Endoplasmic Reticulum Ser/Thr Protein Kinase PERK juxtamembrane domain tyrosine residue 561 is required for Nck adaptor binding and regulation of catalytic kinase activity

To be submitted for publication

PREFACE

In chapter II, I provided evidence showing that Nck adaptors regulate the signaling associated with the phosphorylation of eIF2α in ER stress conditions: I established that 1) overexpression of Nck downregulates eIF2α-dependent signaling; 2) genetic deficiency of Nck adaptors ($Nck1^{-/-}Nck2^{-/-}$ MEFs) upregulates the eIF2α-dependent signaling. Importantly, I demonstrated that Nck is part of an eIF2α holophosphatase complex containing CReP/PP1c that dephosphorylates eIF2α on Ser51. Surprisingly, however and unlike seen in freshly isolated MEFs, levels of eIF2α were significantly increased in $Nck1^{-/-}Nck2^{-/-}$ MEFs as they were passaged, suggesting that the increased levels of eIF2α phosphorylation and eIF2α-dependent signaling see in these cells could have been caused by reprogramming of eIF2α expression. Therefore, to gain more insights into the function of Nck in the translational arm of the UPR, I have used RNA interference (RNAi) to deplete Nck1 protein from HeLa cells and assessed levels of eIF2α Ser51 phosphorylation and eIF2α-dependent signaling in ER stress conditions. If the true function of Nck is to antagonizes eIF2α phosphorylation, one would predict that depletion of Nck adaptors lead to increased levels of eIF2α phosphorylation as seen in $Nck1^{-/-}Nck2^{-/-}$ MEFs. Surprisingly, however, I found that transfection of Nck1 siRNA (or Nck2) impaired the phosphorylation of eIF2α on Ser51 by ER stress agents. Moreover, I present data demonstrating that Nck adaptors directly interact with the catalytically active PERK cytoplasmic segment via a tyrosine residue located in PERK juxtamembrane domain. Together, the findings presented in this chapter strongly suggest that Nck are required for proper phosphorylation of eIF2α by interacting with the activated form of the PERK protein kinase. The significance of these results is discussed in relation with those obtained using overexpression of Nck in cells and $Nck1^{-/-}$ $Nck2^{-/-}$ MEFs, which suggested instead that Nck antagonizes stress-induced eIF2α Ser51 phosphorylation.

ABSTRACT

The accumulation of misfolded proteins in the endoplasmic reticulum (ER) transiently inhibits mRNA translation through phosphorylation of the eukaryotic initiation factor 2 on its α-subunit (eIF2α) by the ER stress-activated PERK protein kinase. PERK activation is associated with extensive autophosphorylation on ser/thr residues that brings an important conformational change of its cytoplasmic segment increasing PERK catalytic kinase activity and allowing phosphorylation of eIF2α. Herein, we report that Nck adaptor proteins directly interact with PERK cytoplasmic domain through their SH2 domain. We found that tyrosine 561 (Tyr561) in PERK juxtamembrane domain is embedded in a consensus Nck SH2 binding site and its mutation (Y561F) reduces overall tyrosine phosphorylation of PERK and abolishes binding to Nck. Supporting a function for this interaction, we uncover that depletion of Nck proteins in cells decreases ER stress-induced eIF2α phosphorylation, suggesting that Nck is required for PERK-mediated signaling. Moreover, we found that Tyr561 is a regulatory site of PERK catalytic kinase activity as a PERK mutant harboring the Y561F substitution displays increased ability to phosphorylate eIF2α both *in vitro* and *in vivo*. Overall, our findings reveal that PERK Tyr561 is required for the interaction with Nck adaptors and regulation of PERK catalytic activity. We discuss the possibility that phosphorylation of Tyr561 in PERK represents a regulatory mechanism relieving the autoinhibitory function of the juxtamembrane domain and promoting eIF2α phosphorylation and Nck binding.

INTRODUCTION

Proper response to environmental cues is critical for cellular homeostasis. Cells have evolved different mechanisms to detect these extracellular signals, which triggers signaling pathways that modulate gene expression. In some instances, however, these signals originate from various cellular organelles mainly in situation where homeostasis or function is perturbed. For example, an imbalance between the load of client protein facing the ER and the organelle capacity to process that load can lead to the accumulation of improperly folded polypeptide in the ER lumen (i.e. ER stress) and impacts on the survival of cells. In such situations, signaling pathways are turned on to modulate gene transcription and ultimately increase the folding and secretory function of the ER. These signaling events are referred as to the Unfolded Protein Response (UPR) and include three important regulators that transduce ER stress signals: PERK (142), IRE1 (48) and ATF6 (148). These ER transmembrane proteins are activated in ER stress conditions and relay signals to the nucleus to upregulate several genes encoding chaperones, degrading factors or enzymes regulating phospholipid synthesis that increase the size and function of the ER (reviewed in (18)).

Cells undergoing ER stress transiently inhibit protein synthesis through phosphorylation of the eukaryotic initiation factor 2 on Ser51 of its α-subunit (eIF2α) by the ser/thr protein kinase PERK (142). Phosphorylation of eIF2α is thought to reduce the workload imposed on the ER folding machinery, thereby preventing the exacerbation of ER stress (140, 365). This regulatory phosphorylation event converts eIF2α into a competitive inhibitor of eIF2B, the guanine nucleotide exchange factor responsible for recycling eIF2 in a GTP-bound form compatible for translation (350). Given that limiting amounts of eIF2B is present in cells, small changes in the phosphorylation state of eIF2α are thought to bring important changes in the translational activity of stressed cells. The relevance of PERK-mediated phosphorylation of eIF2α is illustrated in mouse embryonic fibroblasts (MEFs) genetically ablated of the *perk/eif2ak3* gene, which are hypersensitive to ER stress agents due to their inability to phosphorylate eIF2α and inhibit mRNA translation (140). Moreover, the importance of PERK is highlighted in patients affected by the Wolcott-Rallison syndrome, a disease characterized by

inactivating mutations in the coding sequence of the *perk/eif2ak3* gene causing permanent neonatal or early infancy insulin-dependent diabetes (22, 79, 370), a phenotype recapitulated in $PERK^{-/-}$ mice (140).

Structurally, PERK resembles to the type I transforming growth factor-β (TGF-β) ser/thr kinase receptors and mechanistically to receptor tyrosine kinases (RTKs), for which ligand binding induces dimerization and regulates cytoplasmic kinase activity. PERK is composed of an N-terminal luminal domain (NLD) connected to a cytoplasmic kinase domain (KD) through a transmembrane (TM) domain. The NLD is a multifunctional domain responsible for detecting the presence of improperly folded proteins in the ER lumen and mediating dimerization of PERK in response to stress (255). Although PERK NLD shares limited sequence homology with the corresponding NLD of IRE1, recent crystallographic studies of IRE1 NLD demonstrated that secondary structures implicated in unfolded protein recognition and dimerization are conserved in PERK, suggesting that IRE1 NLD-associated functions are extendable to PERK (71, 474). Following PERK TM domain and preceding its kinase domain is a region of about 50 amino acids of unknown function. This region is highly conserved between mammalian PERK orthologs, but diverged extensively in size and amino acids composition in *C. elegans* (385) and *D. melanogaster* (328). Interestingly, a similar region defined as the juxtamembrane (JM) domain is found in RTKs such as the insulin receptor (IR), platelet-derived growth factor receptor (PDGFR) and Eph receptor (EphR) (84, 170). Overall analysis of the primary structure of the PERK kinase domain reveals that it folds into a common structure consisting of a smaller N-terminal lobe and a larger C-terminal lobe typical of other protein kinases (134). PERK kinase domain shares features of other eIF2α kinases being more closely related to the double-stranded RNA-dependent kinase PKR (193), and to a lesser extent to HRI (57) and GCN2 (158). Distinctive from other eIF2α kinase, however, is the presence of an unusually large insert loop between strand IV and V of the N-terminal lobe of the kinase domain (142, 263).

The prevailing model for PERK activation suggests that in absence of ER stress, PERK is maintained in a monomeric and inactive state bound to the ER resident chaperone BiP/Grp78 through its NLD (20). In ER stress conditions, BiP/Grp78 dissociates from PERK and

subsequently interacts with misfolded proteins that have accumulated in the ER in the lumen. Concomitantly, this leads to PERK dimerization through the NLDs resulting in a conformational change of its cytoplasmic segment enabling *trans*-autophosphorylation of PERK on a large number of serine and threonine residues. Marciniak et al. reported that during PERK activation, multiple negatively charged phosphate groups are added on ser/thr residues found in its large insert loop, creating an ionic surface that increases PERK affinity for eIF2α (263). Although dispensable for catalytic activity, this loop underlies the structural basis for recruitment of eIF2α to PERK. Phosphorylation of eIF2α is thought to reduce these charge-based interactions, resulting in repulsion and release of eIF2α from PERK. One major difficulty in studying PERK is that there are very few known subtrates besides eIF2α. Therefore, this represents a major limitation in understanding the signaling properties of this protein kinase.

Over the years, we uncovered a role for the SH2/SH3 domain-containing Nck adaptor proteins in signaling events initiated at the ER. We reported that Nck proteins directly interact with the β-subunit of eIF2 (eIF2β) (198) and localize at the ER (224, 289). We established that Nck expression levels modulate eIF2α Ser51 phosphorylation in resting and ER-stressed cells (197, 224), suggesting a role for this adaptor protein in PERK-mediated signaling. Here, we show that Nck directly interacts with PERK in a SH2-dependent manner. We present evidence that Tyr561 in PERK is required for the association of Nck and downregulation of PERK catalytic kinase activity.

MATERIAL AND METHODS

Cells. HeLa cells were cultured in Modified Eagle's Medium (Invitrogen) in 10% fetal bovine serum (FBS), 0.75 mg ml^{-1} penicillin and 0.1 mg ml^{-1} streptomycin at 37°C in 5% CO_2 environment. Cos-1 cells were cultured in the same conditions in Dubelcco's Modified Eagle's Medium (Invitrogen) also containing 10% FBS. MEFs were cultured in Dubelcco's Modified Eagle's Medium supplemented with 0.55 μM β-mercaptoethanol (Sigma) and 10 μM non-essential amid acids (Sigma) and 10% FBS. Thapsigargin (Tg, Sigma) and Dithiothreitol (DTT, Roche) treatments were as indicated in figure legends. The Src-family kinases inhibitor PP2 was purchased from Calbiochem (EMD Chemicals Inc.), while the protein tyrosine phosphatase bpV(phen) was kindly provided by Dr. B. Posner (McGill University, Qc Canada) (329)

Antibodies. PERK antisera obtained after rabbit immunization with a glutathione S-transferase (GST) chimera of the cytoplasmic segment of PERK (aa 537-1114) (142) was Protein A affinity purified and concentrated on Amicon centricon YM-30 centrifugal filter device (Millipore Corp.). The pan Nck antibody was previously described (254). Nck1 and Nck2 specific polyclonal antibodies were generated in rabbits using GST-fusion proteins of each isotype specific amino acid sequence between the third SH3 domain and the SH2 domains. Phospho-Ser51 eIF2α antibody was from BioSource International (Medicorp Inc.). Phospho-Thr980 PERK antibody was obtained from Cell Signaling (Cell Signaling Technology, Inc.). eIF2α (Fl-315), eIF2β (P-3), GADD34 (H-193), phospho-Tyrosine (PY99), GST (B-14), GFP (B-2), and HA (F-7) antibodies were from Santa Cruz. Phospho-ser/thr and Nck antibodies were purchased from BD Transduction Laboratories (BD Biosciences) while β-actin antibody (AC-74) was from Sigma.

Constructs. GST-PERK Wt and Myc-PERK Wt plasmids were provided by Dr. D. Ron (NYU Medical Center, USA). GST-PERK Y561F was generated by overlapping PCR using the following primers: 5'-ACTGACATCGGCACTCACGGAGTCGAATTTACTTTCAGTCTGGC ACTG-3' and 5'-GACCTCCGTGAGTGCCGATGTCAGTG-3'. Myc-PERK Y561F was obtained by site-directed mutagenesis (Mutagenex Inc.). Myc-tagged Nck1 Wt full length cDNA and only the three SH3 domains (3SH3) were generated by subcloning the respective Nck cDNA

sequences into pcDNA 3.1 Myc/His using appropriate restriction enzyme digestions. GFP-tagged Nck1 Wt, 3SH3 (aa 1-267) and SH2 (aa 268-377) were generated by subcloning fragments into XhoI and EcoRI sites of pEGFP-C1 (Clontech). Fv2E PERK Wt, K618A and Y561F chimeras were obtained by first deleting the myristoylation site in pC_4M-Fv2E (ARIAD Pharmaceuticals, Inc.) by inserting a linker (5'-AATCCAGAAGCCGCCACCATGGCTT-3') between EcoRI and XbaI sites. Respective PCR-amplified PERK cytoplasmic segment cDNAs were subcloned at the SpeI site of pC_4M-Fv2E(-myr). All constructs generated in this study were verified by DNA sequencing.

Transfection. Cos-1 cells were plated in 60 mm dishes and transfected 18 h later using Lipofectamine-Plus (Invitrogen) according to manufacturer's recommendations. After 48 h of transfection, cells were lysed for either immunoblotting or immunoprecipitation assays. For RNAi, HeLa cells were plated at $6X10^4$ in 24-wells plate and transfected with siRNAs at a final concentration of 75 nM for 3 h at 37°C in serum-free medium using Lipofectamine-Plus. FBS then was adjusted to 10%, and cells kept at 37°C for 18 h. Cells were then counted and plated at desired density in 60 mm dishes. The following day, cells were exposed to ER stress agents and harvested for immunoblotting analysis. Following are the sequence of siRNAs used in this study: Silencer Negative control siRNA (#1, 5'-CUUCCUCCUUUCUCUCCCUUGUGA-3', Ambion Applied Biosytems) and Silencer pre-designed Nck1 siRNA (#1, 5'GGCACCAAUUUUUACAAGUtt-3', Ambion Applied Biosytems). Nck1 RNAi results were confirmed using Nck1 siRNAs targeting different parts of Nck1 mRNA (#2, 5'-GGUAGCUACAAUGGACAAGUUGGAT-3'; #3, 5'-CGAGAAAAGGAGAUGUAAUG GAUGTT-3'; #4, 5'-GCAGUCGUCAAUAACCUAAAUACTG-3') (Integrated DNA Technologies Inc).

GST Pull-downs and Immunoblotting Blot analysis. Cos-1 cells were plated and treated the next day with chemical agents inducing ER stress at 37°C. Cells were washed in ice-cold phosphate-buffered saline (PBS) and lysed in lysis buffer (10 mM Tris-HCl pH 7.5, 50 mM KCl, 2 mM $MgCl_2$, 1% Triton X-100, 1 mM Dithiothreitol, 10 mM Sodium Pyrophosphate, 1 mM Sodium Orthovanadate, 100 mM Sodium Fluoride, 17.5 mM β-Glycerophosphate) supplemented with protease inhibitors (2 μg ml^{-1} Leupeptin, 4 μg ml^{-1} Aprotinin, 1 mM Benzamidine, 100 μg

ml^{-1} Pefabloc SC PLUS). Purified bacterially expressed GST-PERK (5-10 μg) was used in pull-down experiments performed at 4°C for 3 h. Bound proteins were washed three times in lysis buffer, resuspended in 2X Laemmli buffer and resolved on 10% SDS-PAGE with 30 μg of proteins from clarified cell lysates to provide an evaluation of the input sample. For large scale PERK immunoprecipitations, cells were plated in 150 mm dishes, washed in PBS and lysed in the above lysis buffer containing 1% SDS instead of Triton X-100. Cell lysates was passed through a 26 g needle several times, clarified by centrifugation, boiled for 5 min and clarified again by centrifugation to achieve complete denaturation of proteins. To detected PERK in cell lysates, 100-150 μg of proteins were resolved on 7% SDS-PAGE. Proteins were transferred onto PVDF membranes and subjected to immunoblotting analysis blotting using specific antibodies and final signal detected with enhanced chemiluminescence according to the manufacturer's specifications.

Protein synthesis. Cells were exposed to Nck1 siRNAs as described above. 18h later, cells were deprived of methionine and cysteine for 1 h at 37°C, then treated with 1μM Tg, 1mM DTT or 80 μM sodium arsenite for 30 min, and incubated in presence of 50 μCi/ml of S^{35}-labeled Methionine/Cysteine (TranSlabel [35] Met/Cys, Valeant Pharmaceuticals International) for 10 min. Lysates were prepared and equivalent amounts of proteins were loaded on 10% SDS-PAGE and subjected to autoradiography. IRES-driven mRNA translation was measured using a bicistronic vector containing poliovirus IRES driving expression of Firefly luciferase as described previously (198).

***In vitro* kinase assays and kinetic analysis.** *In vitro* eIF2α phosphorylation assays were performed using recombinant His-eIF2α and purified bacterially expressed GST-PERK cytoplasmic segment. Briefly, GST-PERK fusion proteins (200 ng/reaction) were washed twice in kinase buffer (10 mM Tris-HCl, pH 7.4, 50 mM KCl, 2 mM $MgCl_2$, 1 mM DTT, 0.2 mM phenylmethylsulfonyl fluoride, 2 μg ml^{-1} Leupeptin, 4 μg ml^{-1} Aprotinin). Reactions were supplemented with 300 ng of His-eIF2α and [γ-^{32}P] ATP (10 μCi) in a final volume of 25 μl. The reaction was then incubated at 30°C for 30 min with intermittent mixing every 10 min. Reactions were stopped with Laemmli buffer and loaded on 10% SDS-PAGE. Gels were dried and exposed for autoradiography to reveal phosphoproteins. In experiments to determine the Km

for ATP, His-eIF2α was kept constant at 20 μM. In experiments to determine the $K_{0.5}$ for His-eIF2α, the ATP concentration was fixed at 100 μM. Enzymatic analyses were performed using GraphPad Prism4 software.

Phosphoamino acid analysis. Purified GST–PERK Wt cytoplasmic segment (200 ng/reaction) was subjected to *in vitro* autophosphorylation in presence of [γ-^{32}P] ATP as described above. The reaction was incubated at 30°C for 30 min with intermittent mixing every 10 min. Subsequently, the ^{32}P-labeled GST-PERK was subjected to 10% SDS-PAGE, transferred onto PVDF membrane and upon autoradiography the corresponding phosphorylated band was excised and washed 10 times with H_2O. Hydrolysis was performed for 1 h at 100°C in 6N HCl. Membranes were then discarded, and after centrifugation, supernatants were lyophilized and finally resuspended in buffer at pH 1.9 containing 1mg ml^{-1} phosphoserine, phosphothreonine and phosphotyrosine as internal standards. Phosphoamino acids were separated by two-dimensional electrophoresis (buffer at pH 1.9 and 3.9) on TLC plates (EM Sciences), visualized by autoradiography, and identified by comparing with ninhydrin-stained phosphoamino acids standards.

RESULTS

In previous studies, we established that Nck directly interacts with eIF2β (198) and that overexpression of Nck decreased both basal and ER stress-induced eIF2α phosphorylation (197, 224). As an adaptor protein devoid of catalytic activity, Nck effects are believed to be highly dependent on the stoichiometry existing with its effectors. For this reason, investigating the function of such an adaptor using overexpression studies could be misleading. We decided to investigate the role of Nck on ER stress-induced eIF2α phosphorylation by lowering cellular levels of Nck proteins using RNA interference (RNAi). We initially performed experiments in HeLa cells transfected with a siRNA (siRNA#1) specifically targeting Nck1. Using this approach, we successfully decreased Nck1 protein expression levels by 70% without affecting the levels of Nck2 protein (Fig. 1A). Surprisingly, we observed that depletion of Nck1 decreased eIF2α phosphorylation in unstressed cells (Fig. 1B). Identical results were also obtained in similar experiments performed in HEK 293 cells (data no shown). We then determined translation rates in cells transfected with either control or Nck1 siRNA and found increased ^{S35}Met/Cys incorporation in unstressed cells depleted of Nck1 protein as compared to control cells (Fig. 1C). When these cells were exposed to ER stress-causing agents, we found that Tg treatment modestly inhibited S^{35}Met/Cys incorporation in control cells, while the effect of dithiothreitol (DTT) was much stronger (Fig. 1C). However, Nck1 depletion increased the incorporation of radioactivity into newly synthesized proteins upon Tg or DTT treatment as compared to control cells (Fig.1C). On the other hand, no difference was seen in cells exposed to arsenite, an inducer of oxidative stress also converging on the phosphorylation of eIF2α. Although the vast majority of cellular mRNAs are subjected to cap-dependent initiation of translation, we found that Nck1 depletion increased IRES-dependent translation when measured using a bicistronic reporter gene in which luciferase expression is controlled by poliovirus IRES (data not shown). Furthermore, we found that transfection of Nck1 siRNA #1 decreased the amount of eIF2α phosphorylated at each time point analyzed after Tg treatment (Fig. 1D). We observed that the amplitude, but not the kinetic of eIF2α phosphorylation, was changed in cells depleted of Nck1. Importantly, this effect was also observed using three different siRNAs (siRNA #2, #3 and #4) targeting different parts of the Nck1 mRNA (Fig. 1E). Similar results were obtained in cells treated with other ER stress-inducers such as tunicamycin (Tm) or DTT

(data not shown). We believe that the residual phosphorylation of eIF2α detected in cells transfected with the Nck1 siRNA could relate to the functional redundancy associated with Nck2. In fact, depletion of Nck2 by RNAi also decreased basal and Tg-induced eIF2α phosphorylation (data not shown). Unfortunately, we did not succeed in simultaneously depleting Nck1 and Nck2 in cells, preventing us from investigating the effect of total Nck adaptor depletion on eIF2α phosphorylation. Overall, these depletion experiments strongly suggest that Nck is required for eIF2α phosphorylation and inhibition of mRNA translation in ER-stressed cells.

Inhibition of mRNA translation through eIF2α phosphorylation paradoxically increases the translation of the bZIP transcription factor ATF4. GADD34, an ATF4 target gene, functions as a PP1c regulatory subunit involved in the translational recovery phase of the UPR (256, 294). To complete our analysis, we addressed the effect of Nck1 depletion on Tg-induced GADD34 expression in HeLa cells. We found that Tg-induced eIF2α phosphorylation peaked at 18h of treatment in control cells and paralleled PERK activation status as determined by immunoblotting using a commercially available antisera specific for phospho-PERK Thr980 (Fig 1F). On the other hand, we found decreased levels of eIF2α phosphorylation in Nck1-depleted cells, which intriguingly, inversely correlated with levels of PERK Thr980 phosphorylation (Fig. 1F). This uncoupling between PERK activation and eIF2α phosphorylation suggests that Nck adaptors might play a role in PERK-mediated eIF2α phosphorylation. Importantly, we found lower levels of GADD34 in Nck1-depleted cells exposed to Tg, demonstrating that Nck1 is required for the signaling events downstream of eIF2α phosphorylation.

Figure 1. Depletion of Nck1 by RNA Interference decreases eIF2α phosphorylation and increases mRNA translation. (A) HeLa cells were transiently transfected with Control (C-) or Nck1 siRNA (#1). 24 h later, cells were harvested and Nck1 expression was determined on cell lysates normalized for protein content by immunoblotting analysis using Nck1, Nck2 and β-actin antibodies. The asterisk represents a non-specific band of the Nck2 antiserum immunoblotting. The histogram represents a quantitative analysis of Nck1 expression normalized to β-actin level obtained from three independent experiments. Data are means ± SEM *$p<0.05$ determined by Student t-test **(B)** Same as (A) except cell lysates were probed with phospho-eIF2α Ser51 and total eIF2α antibodies. **(C)** HeLa cells were transiently transfected with Control (C-) or Nck1 siRNAs (#1). 24 h later, cells were exposed to Tg, DTT or Arsenite (As), and labeled with ^{S35}Met/Cyst as described in Materials and Methods. The densitometric values associated with each condition are reported under each lane of the autoradiogram. Shown is a representative experiment of at three independent experiments. Shown below the autoradiogram is the corresponding knockdown experiment **(D)** Time course of eIF2α phosphorylation in HeLa cells transiently transfected with Control (C-) or Nck1 siRNA (#1) and treated with Tg (1 μM) for indicated times. Cells were harvested and cell lysates normalized for protein content were subjected to immunoblotting analysis using antibody against indicated proteins. Quantification of normalized eIF2α phosphorylation levels (eIF2α pSer51/total eIF2α) is reported under each lane **(E)** Cells were transiently transfected with control (C-) or three different Nck1 siRNAs (#2, #3 and #4), and treated with Tg (1 μM)(+) or left untreated (-) for 30 min. Cell lysates normalized for protein content were processed for immunoblotting. Quantification of normalized eIF2α phosphorylation levels (eIF2α pSer51/total eIF2α) is reported under each lane. **(F)** Same as in (D) except cells were treated with 0.25 μM Tg for indicated times. p-PERK immunoblotting analysis was performed using the phospho-PERK Thr980 antibody. Quantification of normalized eIF2α phosphorylation levels (eIF2α pSer51/total eIF2α) is reported under each lane.

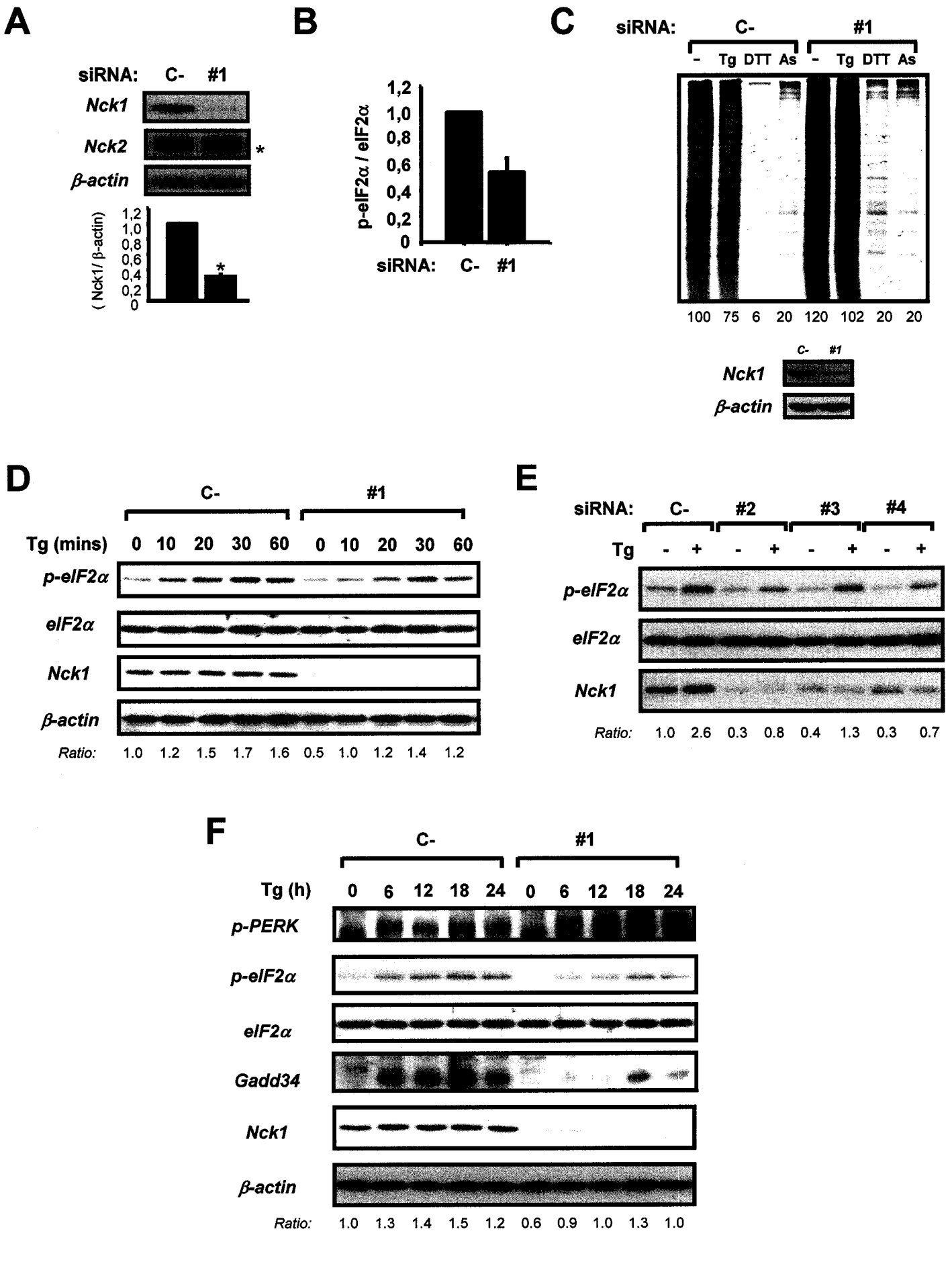
A
siRNA: C- #1
Nck1
Nck2
β-actin
*
(Nck1/ β-actin)
1,2
1,0
0,8
0,6
0,4
0,2
0
*
B
p-eIF2α / eIF2α
1,2
1,0
0,8
0,6
0,4
0,2
0
siRNA: C- #1
C
siRNA: C- #1
- Tg DTT As - Tg DTT As
100 75 6 20 120 102 20 20
C- #1
Nck1
β-actin
D
C- #1
Tg (mins) 0 10 20 30 60 0 10 20 30 60
p-eIF2α
eIF2α
Nck1
β-actin
Ratio: 1.0 1.2 1.5 1.7 1.6 0.5 1.0 1.2 1.4 1.2
E
siRNA: C- #2 #3 #4
Tg - + - + - + - +
p-eIF2α
eIF2α
Nck1
Ratio: 1.0 2.6 0.3 0.8 0.4 1.3 0.3 0.7
F
C- #1
Tg (h) 0 6 12 18 24 0 6 12 18 24
p-PERK
p-eIF2α
eIF2α
Gadd34
Nck1
β-actin
Ratio: 1.0 1.3 1.4 1.5 1.2 0.6 0.9 1.0 1.3 1.0

Based on these results, we hypothesized that Nck could interact with PERK and contribute somehow to regulate eIF2α phosphorylation. To address this point, we first generated an anti-PERK antibody using an antigen corresponding to the cytoplasmic segment of PERK fused to GST. PERK is a large protein of 1,114 amino acids with a predicted size of 124 KDa. However, PERK migrates at a higher molecular weight than its predicted size in immunoblotting analysis due to post-translational modifications, such as glycosylation and phosphorylation (142). In agreement with this, we observed that when overexpressed in Cos-1 cells, PERK Wt and the kinase-dead (K618A) mutant are recognized as proteins of respectively 170 and 150 KDa in immunoblotting experiment using our anti-PERK antibody (Fig. 2A). Moreover, the PERK antibody efficiently immunoprecipitated PERK Wt overexpressed in Cos-1 cells (Fig. 2B). We then determined whether we could immunoprecipitate endogenous PERK using this antibody. We noticed that a substantial amount of PERK, migrating mostly as a single band of 150 KDa, was recovered in large-scale immunoprecipitations (see M&M for details) performed using denatured unstressed Cos-1 cells lysates (Fig. 2C). In response to DTT treatment, the mobility of the PERK immunoreactive band progressively shifted to 170 KDa on SDS-PAGE most likely corresponding to the activated form of PERK, based on the corresponding increase in eIF2α Ser51 phosphorylation (Fig. 2C). Furthermore, we found that this anti-PERK antibody immunoprecipitated endogenous PERK in pancreatic samples. Indeed we detected a major band of approximately 150 KDa in PERK immunoprecipitates performed in this tissue, which was absent in control IgG immunoprecipitates (Fig. 2D).

Figure 2. Development of an anti-PERK polyclonal antibody. (A) Cos-1 cell were transiently transfected with Myc-tagged PERK Wt (lane1) or kinase inactive K618A (lane 2) cDNAs. 48 h later, cells were harvested and lysates normalized for protein content were subjected to anti-PERK immunoblotting. **(B)** Same as in (A) except cells were transfected with increasing amounts of the Myc-tagged PERK Wt cDNA. Cell lysates normalized for protein content were subjected to PERK immunoprecipitations using anti-PERK antibody. Immunoprecipitated PERK was revealed by immunoblotting using an anti-Myc antibody. Also shown are the phosphorylation levels of eIF2α determined using cell lysates determined by immunoblotting with phospho-eIF2α Ser51 and total eIF2α antibodies. **(C)** Cos-1 cells left untreated or treated with DTT (2 mM) for indicated time. Cell lysates were subjected to large-scale denaturing immunoprecipitation of endogenous PERK using anti-PERK antibody. Immunoblotting analysis was performed using anti-PERK antibody. Also shown is the corresponding immunoblot with phospho-eIF2α Ser51 and total eIF2α antibodies. **(D)** PERK immunoprecipitations were conducted using mouse pancreatic tissue homogenates and processed by immunoblotting analysis as reported above. IgG: pre-immune rabbit serum.

A

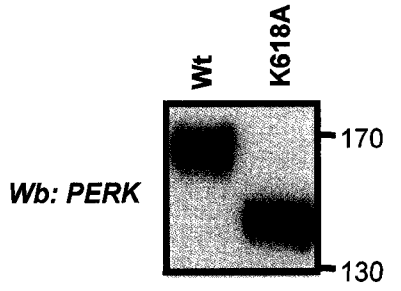
Wt
K618A
Wb: PERK
170
130

B

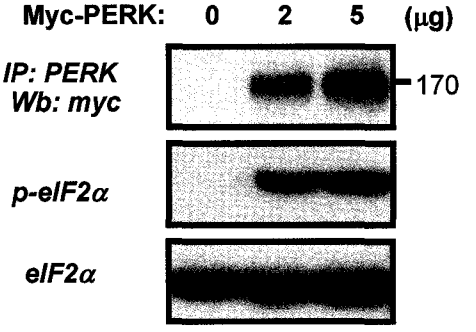
Myc-PERK: 0 2 5 (μg)
IP: PERK
Wb: myc
170
p-eIF2α
eIF2α

C

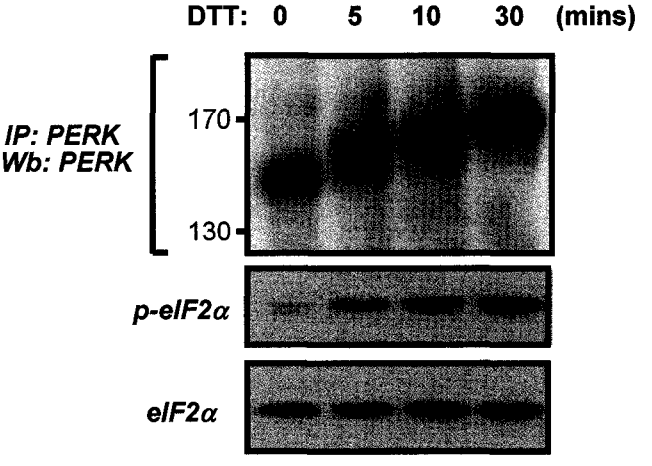
DTT: 0 5 10 30 (mins)
IP: PERK
Wb: PERK
170
130
p-eIF2α
eIF2α

D

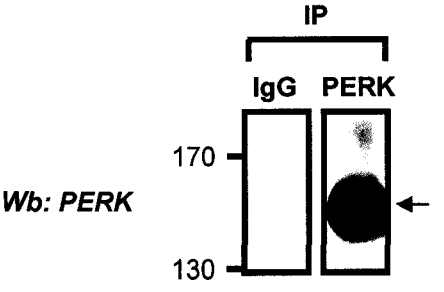
IP
IgG
PERK
170
Wb: PERK
130

We then tested whether Nck adaptors interact with PERK in pull-down assays by incubating purified bacterially expressed GST-fused PERK cytoplasmic segment (containing the JM region and the kinase domain) with recombinant Nck1 and Nck2 proteins. In this experimental setting, the GST moiety of the GST-PERK fusion protein acts as a dimerizing module causing activation of PERK catalytic kinase activity (142). We observed that both Nck1 and Nck2 directly interact with GST-PERK Wt, but not with GST *in vitro* (Fig. 3A). To confirm this interaction, we performed pull-down experiments using GST-PERK Wt incubated with Cos-1 cell lysates. We observed that Nck proteins interact specifically with GST-PERK Wt, but not with the catalytically inactive GST-PERK K618A fusion protein (Fig. 3B). These results indicate that the association of Nck with PERK is dependent on PERK catalytic kinase activity. As reported previously, eIF2α and eIF2β interact only with Wt, but not the K618A mutant (263).

Nck contains three N-terminal SH3 domains recognizing proline-rich motifs, followed by a SH2 domain at its C-terminus engaging phosphotyrosine residues in target proteins (Fig 3C). To characterize the molecular determinants in Nck required for the association with PERK, we expressed GFP-tagged Nck1 Wt and deletion mutants in Cos-1 cells and performed pull-down experiments using GST-PERK Wt. We found that deletion of the SH2 domain of Nck1 (3SH3) completely abrogated binding to PERK, while deletion of the three SH3 domains (SH2) did not affected this interaction (Fig. 3C). This demonstrates that the SH2 domain of Nck1 is sufficient for the interaction with PERK cytoplasmic segment. We then tested whether this interaction exists in cells by performing coimmunoprecipitation analysis in Cos-1 cells coexpressing myc-tagged PERK Wt and Nck1 Wt. We observed that PERK immunoprecipitates contained significant amounts of the myc-Nck1 protein (Fig. 3D), establishing the existence of the PERK/Nck interaction in cells. In addition, we validated that this interaction is dependent on the SH2 domain of Nck as an Nck1 mutant deleted of its SH2 domain (3SH3) was not recovered in PERK immunoprecipitates (Fig. 3D). We could not test whether a mutant deleted of its three SH3 domains interacted with PERK given that it was improperly localized to the nucleus of cells. On the other hand, we ruled out that mislocalization of the SH2-deleted Nck1 mutant was the basis of its inability to interact with PERK by confirming that it still localized at the ER in immunofluorescence microscopy (data not shown). Finally, we found that treatment of cells with bpV(phen), a stable and large spectrum protein tyrosine phosphatase inhibitor (329), resulted in

the recovery of two major bands of 150 and 170 KDa displaying PERK immunoreactivity in anti-Nck immunoprecipitates (Fig.3E). Together, these results strongly support the idea that Nck directly interacts with the cytoplasmic domain of PERK in a kinase activity- and SH2-dependent manner.

Figure 3. Interaction between Nck adaptors and PERK cytoplasmic segment. (A) Binding experiments performed using purified bacterially expressed PERK cytoplasmic segment fused to GST (GST-PERK Wt), and purified bacterially expressed recombinant Nck1 and Nck2. Bound material was revealed by immunoblotting analysis using an anti-Nck antibody. **(B)** Pull-down experiments using GST and indicated GST-PERK fusion proteins incubated with Cos-1 cells lysates. Bound material was revealed by immunoblotting analysis using an anti-Nck antibody. Wt: wild type and catalytically active PERK; K618A: catalytically inactive PERK mutant **(C)** Pull-down experiments using GST or GST-PERK fusion proteins incubated with Cos-1 cell lysates expressing indicated GFP-tagged Nck1 constructs. Bound proteins were revealed by immunoblotting analysis using GFP-antibody. Asterisk: degradation product of the full-length GFP-Nck1 protein. Also shown is a schematic representation of the deletion mutants used in these pull-downs **(D)** Coimmunoprecipitation of Nck1 with PERK in cells. Cos-1 cells were cotransfected with either carrier plasmid (mock), Myc-Nck1 Wt or three SH3 (3SH3) and Myc-PERK. 48 h after, cells were harvested and lysates subjected to immunoprecipitation using anti-PERK antibody. Binding of Nck proteins was revealed by immunoblotting using an Nck antibody. **(E)** Coimmunoprecipitation of Nck and PERK in Cos-1 cells pretreated for 10 min (100 μM) with the protein tyrosine phosphatase inhibitor bpV(phen). Cells were harvested and lysates were subjected to immunoprecipitation using control (IgG) or Nck antibody. Immunoprecipitated material was probed for PERK and Nck using respective antibodies. Two post-translationally modified PERK species (A and B) are recovered in anti-Nck immunoprecipitates prepared from bpV(phen)-treated cells.

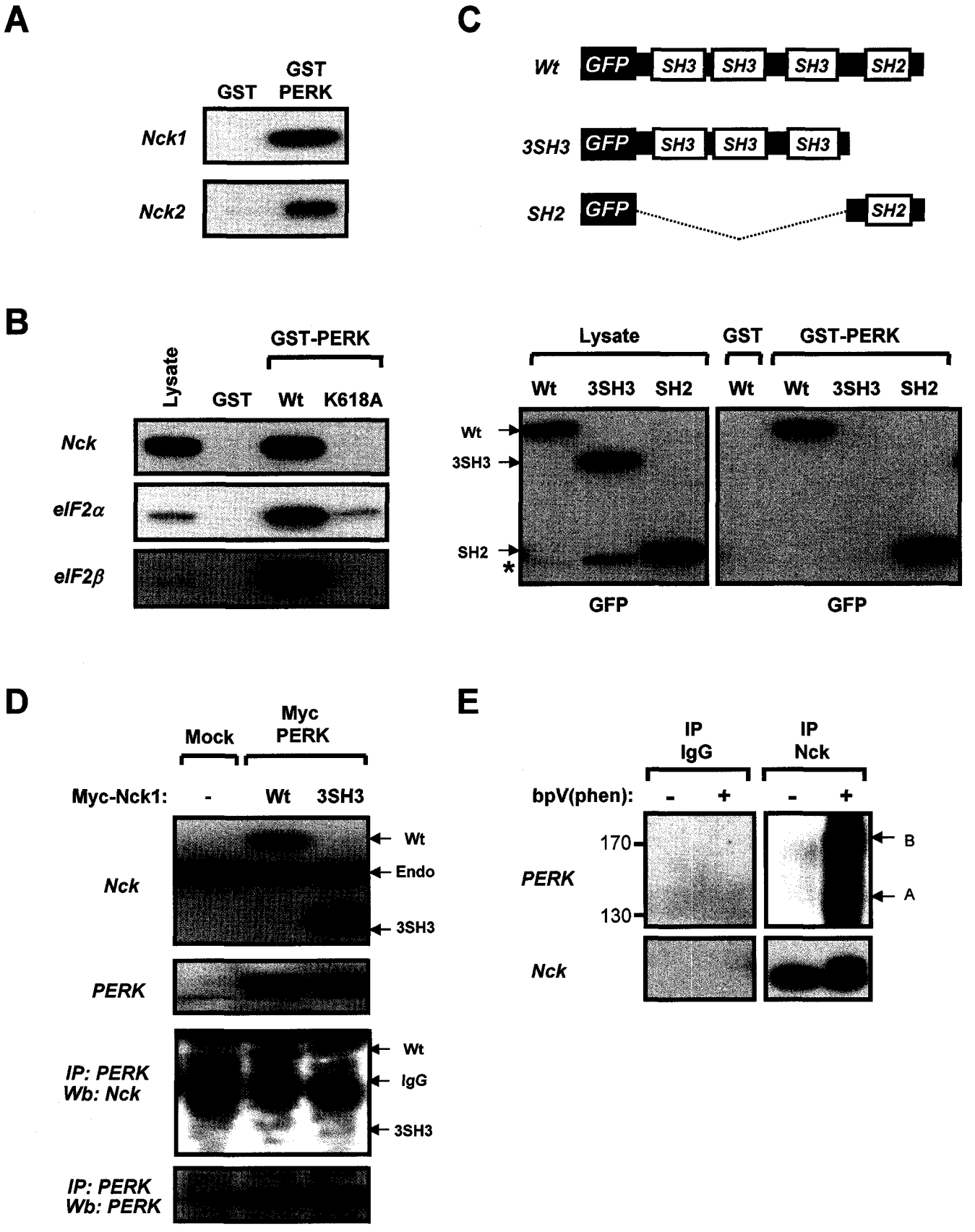
A
GST
GST PERK
Nck1
Nck2
B
Lysate
GST-PERK
GST
Wt
K618A
Nck
eIF2α
eIF2β
C
Wt
GFP
SH3
SH3
SH3
SH2
3SH3
GFP
SH3
SH3
SH3
SH2
GFP
SH2
Lysate
GST
GST-PERK
Wt
3SH3
SH2
Wt
Wt
3SH3
SH2
Wt
3SH3
SH2
GFP
GFP
D
Mock
Myc PERK
Myc-Nck1:
-
Wt
3SH3
Nck
Wt
Endo
3SH3
PERK
IP: PERK
Wb: Nck
Wt
IgG
3SH3
IP: PERK
Wb: PERK
E
IP IgG
IP Nck
bpV(phen):
-
+
-
+
170
130
PERK
B
A
Nck

Although PERK becomes highly phosphorylated on serine and threonine residues upon its activation, little is known about its potential tyrosine phosphorylation. A MALDI-TOF mass spectrometry analysis unexpectedly showed that the bacterially expressed and catalytically active GST-PERK Wt fusion protein was phosphorylated on specific tyrosine residues (257). Our observation that Nck interacts with PERK in a strict SH2 domain dependent manner, both *in vitro* and *in vivo,* strongly suggests that PERK is indeed tyrosine phosphorylated. To investigate this, we examined the tyrosine phosphorylation state of purified bacterially expressed GST-PERK cytoplasmic segment. In immunoblotting performed using anti-phosphotyrosine antibody, we found that catalytically active GST-PERK Wt is strongly phosphorylated on tyrosine residues (Fig. 4A). In contrast, we observed that the catalytically inactive GST-PERK K618A fusion protein was not phosphorylated on tyrosine residues (Fig. 4A). These observations support the idea that PERK tyrosine phosphorylation presumingly results from an autophosphorylation event requiring the intrinsic PERK catalytic kinase activity rather than being catalyzed by a kinase expressed in bacteria. Moreover, this result excludes the possibility that PERK protein contains an epitope that mimics tyrosine phosphorylation. Phosphoamino analysis of purified GST-PERK also indicated the presence of phosphotyrosine, in addition to phosphoserine and phosphothreonine residues (Fig. 4B). Moreover, we observed that, unlike the K618A mutant, GST-PERK Wt autophosphorylated on serine/threonine residues, and most importantly on Thr980, a conserved residue found in the PERK activation loop and critical for kinase activity (Fig. 4A and 4B). Based on these results, we concluded that PERK activity correlates with autophosphorylation of the protein on tyrosine and serine/threonine residues *in vitro*.

Figure 4. *In vitro* analysis of PERK tyrosine phosphorylation. (A) Tyrosine and serine/threonine phosphorylation of purified bacterially expressed GST-PERK (100 ng/lane). Immunoblotting experiments were performed using indicated antibodies. **(B)** Two-dimensional phosphoamino acid analysis of GST-PERK subjected to *in vitro* autophosphorylation in the presence of [γ-^{32}P]ATP. The position of the radioactive phospho-Serine, -Threonine and -Tyrosine residues are indicated. See Experimental procedure for details. A short and long exposure autoradiography are shown.

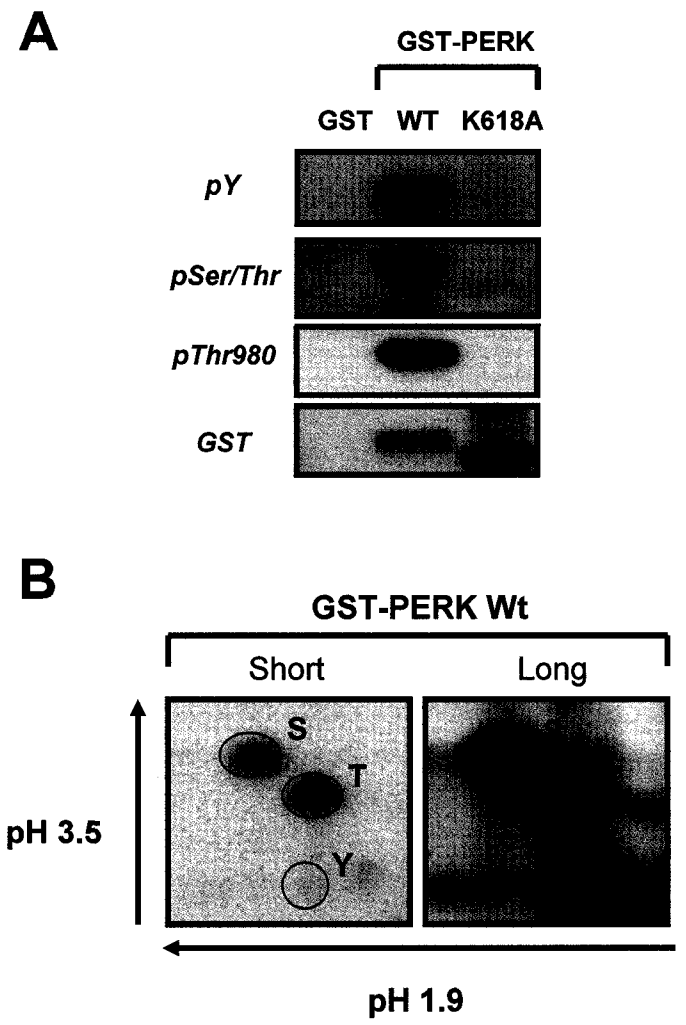
A
GST-PERK
GST
WT
K618A
pY
pSer/Thr
pThr980
GST
B
GST-PERK Wt
Short
Long
S
T
Y
pH 3.5
pH 1.9

To provide evidence of PERK tyrosine phosphorylation *in vivo*, we fused the PERK cytoplasmic segment to an inducible heterologous oligomerizing domain (Fv2E) and addressed tyrosine phosphorylation of this HA-tagged PERK fusion protein in cells treated with the dimerizing drug AP20817. When cells transiently expressing the Fv2E-PERK Wt fusion were exposed to increasing concentrations of AP20187, we found that eIF2α phosphorylation augmented in a dose-dependent manner (Fig. 5A lanes 3-6). Moreover, eIF2α phosphorylation levels correlated with decreased migration of the fusion protein on SDS-PAGE, suggesting that this represents a hyperphosphorylated form of the fusion protein. Importantly, no change in the phosphorylation of eIF2α and migration of the fusion protein was observed in cells expressing Fv2E-PERK K618A (Fig 5A compare lanes 7-10 to 3-6), suggesting that AP20187-induced eIF2α phosphorylation and increased mobility of the Wt fusion protein require PERK catalytic kinase activity. We next verified the tyrosine phosphorylation of Fv2E-PERK Wt and K618A fusion proteins in cells exposed to AP20187 over an increasing period of time. Addition of AP20187 to Fv2E-PERK Wt-expressing cells resulted in rapid activation of PERK kinase activity as reflected in a shift of the Wt fusion protein to a slower mobility form appearing as soon as 10 min of treatment (Fig 5B, top panel lanes 1-4). Although Fv2E-PERK Wt was expressed at high levels in cells, we did not detect any signs of tyrosine phosphorylation in response to AP20187 treatment (Fig. 5B, second panel from the top, lanes 1-4). We hypothesized that tyrosine phosphorylation might be labile and too unstable to be detected by immunoblotting, and therefore tested whether incubation of cells with bpV(phen) would improved detection of PERK tyrosine phosphorylation. We observed that treatment of Fv2E-PERK Wt-expressing cells with bpV(phen) resulted in spontaneous retardation and tyrosine phosphorylation of the fusion protein (Fig. 5B, first and second panels from the top, compare lanes 5). Notably, the slower migrating band aligned perfectly with the band that was tyrosine phosphorylated in HA immunoprecipitates, suggesting that the Fv2E-PERK Wt fusion protein is subjected to tyrosine phosphorylation by exogenous protein tyrosine kinases in these conditions. Interestingly, similar results were obtained with the Fv2E-PERK K618A fusion protein, although tyrosine phosphorylation levels of this later fusion were consistently higher compared to Fv2E-PERK Wt (Fig 5B, second panel from the top, compare lanes 13 to 5). Importantly, addition of AP20187 to Fv2E-PERK Wt-expressing cells pretreated with bpV(phen) resulted in a time-dependent increase in tyrosine phosphorylation of the fusion protein, which correlated with increasing

levels of eIF2α phosphorylation (Fig 5B, second and third panels from the top, lanes 5-8). Supportingly, we found increasing amounts of Fv2E-PERK Wt recovered in anti-phosphotyrosine immunoprecipitates obtained from cells treated with AP20187 for increasing time (Fig. 5C). In contrast, AP20187 treatment caused dephosphorylation of the catalytically inactive Fv2E-PERK K618A over time (Fig. 5B, second panel from the top, lanes 13-16), indicating that the increase in Fv2E-PERK tyrosine phosphorylation induced by the addition of AP20187 requires PERK catalytic kinase activity. Overall, the results presented in this section suggest that monomeric Fv2E-PERKWt and K618A are subjected to tyrosine phosphorylation by exogenous protein tyrosine kinases in cells. Conversely, dimerization of PERK cytoplasmic segment increases its tyrosine phosphorylation in a catalytic kinase activity-dependent manner, which correlates with higher levels of eIF2α phosphorylation.

Figure 5. *In vivo* analysis of PERK tyrosine phosphorylation using a heterologous dimerizing module. (A) Fv2E-fused to WT and K618A PERK cytoplasmic segments were transiently expressed in Cos-1 cells. Cells were treated for 30 min with indicated concentrations of the dimerizer (AP20187), harvested, and subjected to immunoblotting using the antibodies indicated. Note the shift in migration of the Fv2E-PERKWt fusion protein in the presence of AP20187, which is absent in Fv2E-PERK K618A-expressing cells **(B)** Transfected cells were pretreated with the protein tyrosine phosphatase bpV(phen) (100 μM, 10 min) before the addition of AP20187 (100 nM) for indicated times. Cell lysates were prepared and processed by immunoprecipitation using HA antibody. The proteins were revealed by immunoblotting using the indicated antibodies. Also shown are the corresponding levels of eIF2α phosphorylation obtained by immunoblotting using the indicated antibodies (bottom). **(C)** Cos-1 cells transiently transfected with Fv2E-PERK Wt plasmid were treated with AP20187 (100 μM) for the indicated time and harvested for processing. Cell lysates were subjected to immunoprecipitation using an anti-phosphotyrosine antibody (pY). These immunoprecipitates were washed and resolved on SDS-PAGE. Immunoblot analysis was performed using an anti-HA antibody to reveal the presence of the Fv2E PERK fusion protein in the recovered in pY immunoprecipitates (top panel). Also shown is the expression of PERK (second panel form the top). Levels of p-eIF2α (third panel from the top) and total eIF2α (bottom panel) were determined by immunoblotting using the same samples.

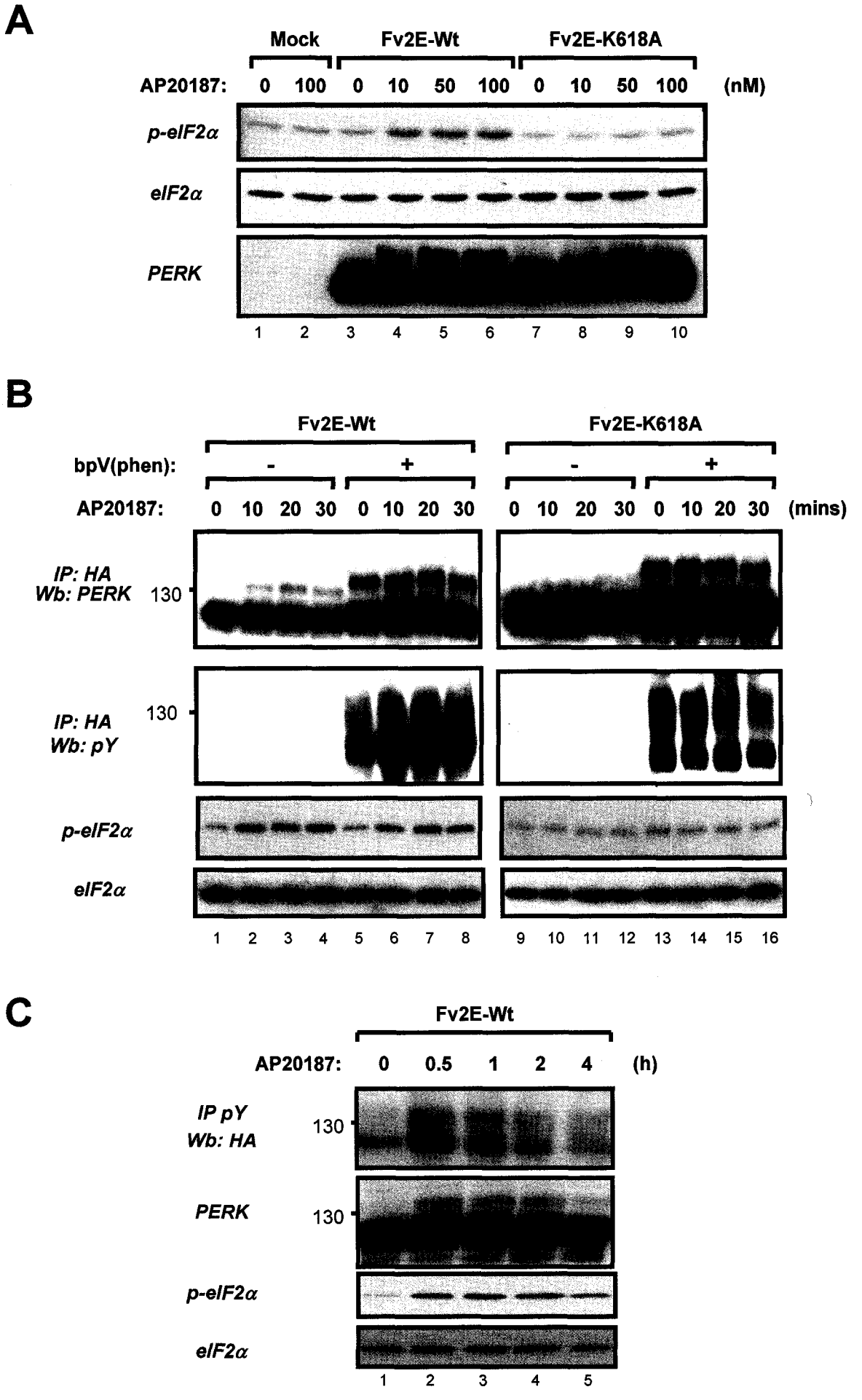
A
Mock
Fv2E-Wt
Fv2E-K618A
AP20187: 0 100 0 10 50 100 0 10 50 100 (nM)
p-eIF2α
eIF2α
PERK
1 2 3 4 5 6 7 8 9 10
B
Fv2E-Wt
Fv2E-K618A
bpV(phen): - + - +
AP20187: 0 10 20 30 0 10 20 30 0 10 20 30 0 10 20 30 (mins)
IP: HA
Wb: PERK
130
IP: HA
Wb: pY
130
p-eIF2α
eIF2α
1 2 3 4 5 6 7 8 9 10 11 12 13 14 15 16
C
Fv2E-Wt
AP20187: 0 0.5 1 2 4 (h)
IP pY
Wb: HA
130
PERK
130
p-eIF2α
eIF2α
1 2 3 4 5

Recently, the phosphopeptide binding profile of both Nck adaptors SH2 domains have been reexamined and found to share equivalent consensus binding sequences (108). Three positions were identified to govern Nck SH2 domain phosphopeptide binding: pTyr, position +1 and +3 (where pTyr represents position 0). Aspartic acid (D) and valine (V) were critical for high affinity binding in position +1 and +3 respectively, with the later dominating the former. We screened the PERK cytoplasmic segment for potential tyrosine residues that could support the Nck SH2 domain binding specificity and found that Tyr565 in human PERK matched the consensus binding sequence for Nck SH2 domain (Fig. 6A). Close examination of Tyr565 surrounding amino acid sequence reveals a high degree of identity with Tyr383, Tyr1217 and Tyr474 Nck SH2 domain binding sequences identified in enteropathogenic *E. coli* Tir, Nephrin or Git-1 proteins, respectively. Tyr565 is localized in the region linking PERK transmembrane helix and kinase domain, corresponding to TGF-β receptors (TβR) family GS-domain or the receptor tyrosine kinases family JM domain (Fig. 7). Interestingly, Tyr565 is highly conserved in mammalian PERK orthologs (Fig. 6A), while being absent in *C. elegans* and *D. melanogaster*, two organisms showing considerable primary structure divergence as compared to mammalian proteins. Likewise, this tyrosine residue is not found in either PKR or the ER stress sensor protein IRE1.

We designed experiments in order to determine the role of this tyrosine residue in PERK by substituting Tyr561, the corresponding Tyr565 residue in mouse PERK, by a non-phosphorylatable phenylalanine (Phe-F). The phenylalanine residue possesses an analogous side chain structure compared to tyrosine, but is devoid of hydroxyl group. Therefore such residue is resistant to the nucleophilic attack by the phoshoryl center of ATP during kinase catalysis. We found that the bacterially expressed GST-PERK Y561F proteins displayed a marked decrease in overall tyrosine phosphorylation as compared to Wt (Fig. 6B), suggesting that this residue contributes to the tyrosine phosphorylation of the PERK cytoplasmic segment. Moreover, phosphorylation of Thr980 in PERK activation loop was completely preserved upon mutation of Tyr561, suggesting that Tyr561 in the PERK JM domain is dispensable for PERK autophosphorylation on Thr980 (Fig. 6B). In fact, we found that this mutant still retained the ability to bind and phosphorylate eIF2α *in vitro* (see below and data not shown). We then tested for Nck binding and found that the Y561F mutation in GST-PERK completely abrogated binding

of Nck proteins in pull-down experiments using Cos-1 cell lysates (Fig. 6C). These results demonstrate that substitution of Tyr561 with a non-phosphorylatable residue in GST-PERK alters global tyrosine phosphorylation and abolishes the interaction with Nck adaptors.

Figure 6. Binding of Nck adaptors to PERK cytoplasmic segment via a conserved residue found in the PERK juxtamembrane domain. (A) Identification of a conserved tyrosine residue in the PERK JM domain (Y565 in human PERK) that matches the consensus motif for Nck SH2 domain binding sequence. Also shown is the comparison between human PERK Tyr565 surrounding sequence and corresponding residues in PERK orthologs, as well as other Nck SH2 binding sites identified in enteropathogenic *E. coli* Tir (Y383), Git-1 (Y474) and Nephrin (Y1217) proteins. Nck SH2 domain consensus binding motif obtained from peptide library screenings is also reported (108)**(B)** Global tyrosine phosphorylation and Thr980 phosphorylation of purified bacterially expressed GST-PERK WT and Y561F fusion proteins (100 ng/lane). Histogram represents the quantitative analysis of global GST-PERK Wt tyrosine phosphorylation profile obtained by immunoblotting analysis. Data are means ± SEM. * $p< 0.001$ by Student t-test from three independent experiments. **(C)** Pull-down experiments using GST and indicated GST-PERK fusion proteins incubated with Cos-1 cell lysates. Bound material was analyzed by immunoblotting analysis using an anti-Nck antibody. Introduction of the Y561F mutation in GST-PERK completely abolished Nck binding.

A

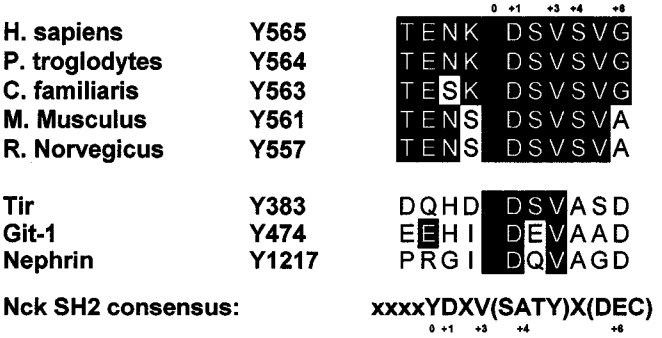
0 +1 +3 +4 +6
H. sapiens Y565 TENK DSVSVG
P. troglodytes Y564 TENK DSVSVG
C. familiaris Y563 TESK DSVSVG
M. Musculus Y561 TENS DSVSVA
R. Norvegicus Y557 TENS DSVSVA
Tir Y383 DQHD DSVASD
Git-1 Y474 EEHI DEVAAD
Nephrin Y1217 PRGI DQVAGD
Nck SH2 consensus: xxxxYDXV(SATY)X(DEC)
0 +1 +3 +4 +6

B

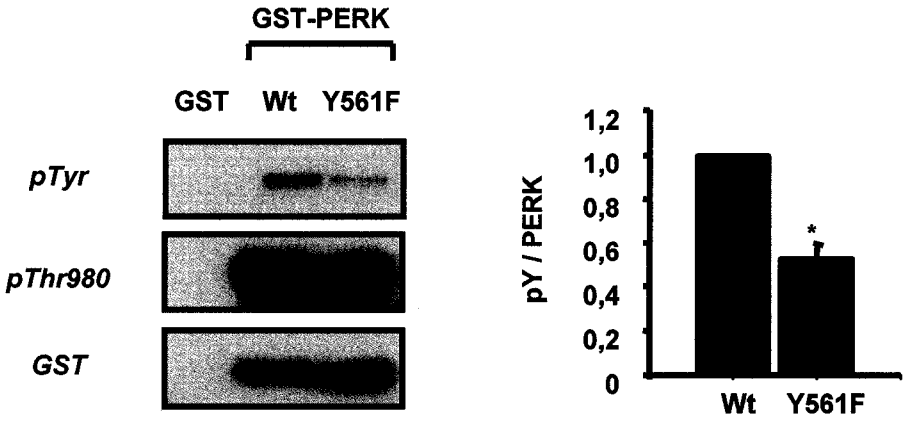
GST-PERK
GST Wt Y561F
pTyr
pThr980
GST
pY / PERK
1,2
1,0
0,8
0,6
0,4
0,2
0
*
Wt Y561F

C

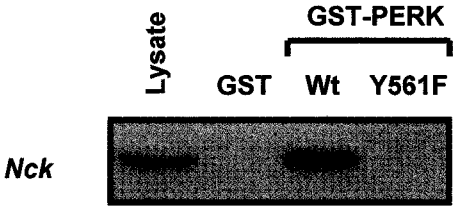
Lysate
GST-PERK
GST Wt Y561F
Nck

Figure 7. Primary structure alignment of mammalian PERK orthologs. PERK primary structure alignment from amino acids 491-715 (based on mouse sequence) of human (*H. sapiens*), chimp (*P. troglodytes*), dog (*C. familiaris*) mouse (*M. musculus*) and rat (*R. norvegicus*). PERK transmembrane domain is underlined. The JM domain encompasses amino acids 537-590. An arrow marks the beginning of the PERK kinase domain. An asterisk marks residue Tyr561 in the JM domain and Lys618 in the N-terminal lobe of the kinase domain. Part of the PERK insert loop is indicated by a dashed line (aa 652-881). The displayed sequence alignment was generated with ClustalW software.

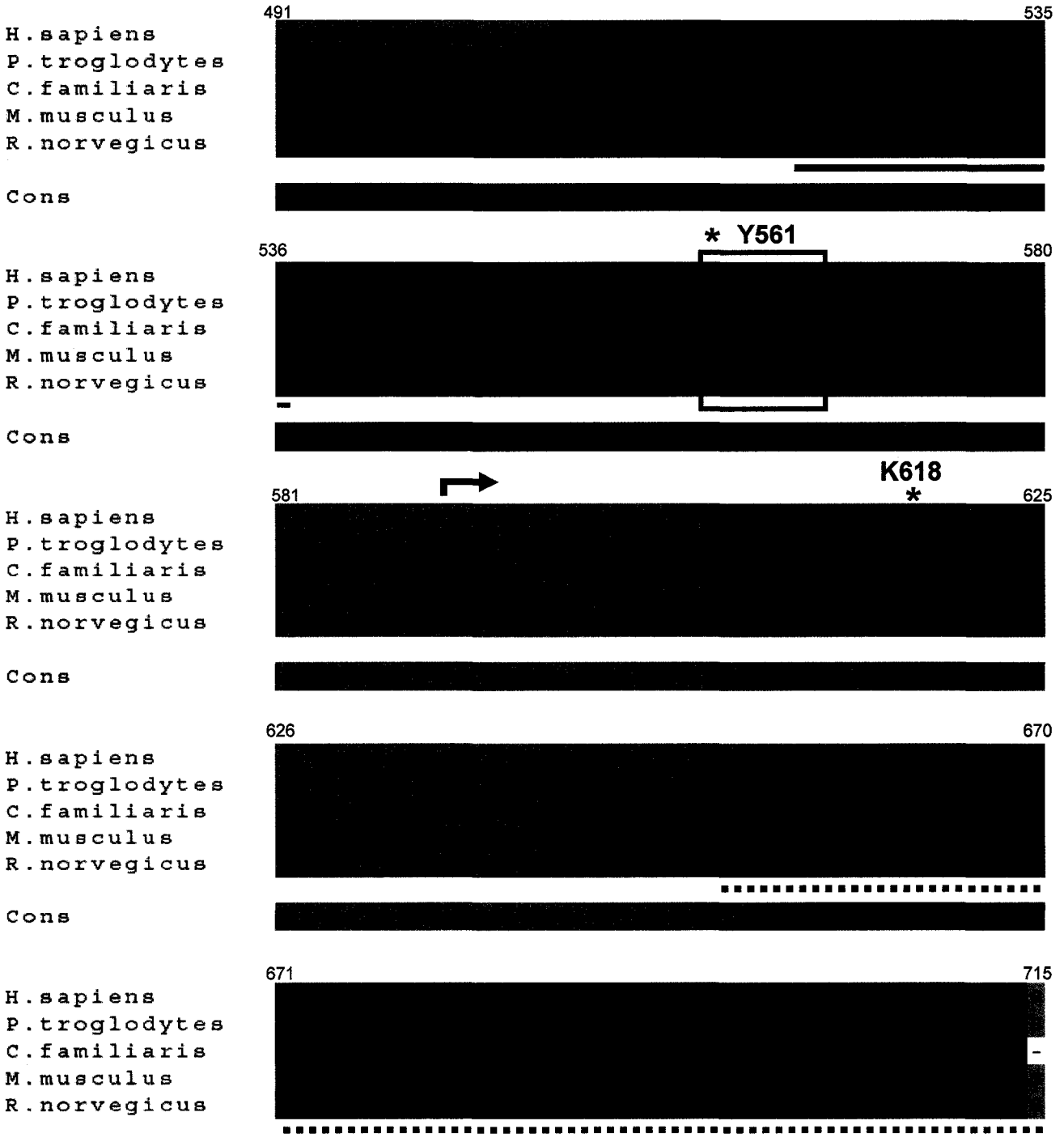
491
535
H.sapiens
P.troglodytes
C.familiaris
M.musculus
R.norvegicus
Cons
* Y561
536
580
H.sapiens
P.troglodytes
C.familiaris
M.musculus
R.norvegicus
Cons
K618
*
581
625
H.sapiens
P.troglodytes
C.familiaris
M.musculus
R.norvegicus
Cons
626
670
H.sapiens
P.troglodytes
C.familiaris
M.musculus
R.norvegicus
Cons
671
715
H.sapiens
P.troglodytes
C.familiaris
M.musculus
R.norvegicus

We then examined the effect of the Y561F mutation on the catalytic kinase activity of purified and bacterially expressed GST-PERK fusion protein. We first noticed that GST-PERK Wt resolved on SDS-PAGE displayed a marked shift in mobility on gel as compared to the catalytically inactive K618A mutant (Fig. 8A), supporting the idea that GST-PERK autophosphorylates *in vitro* (142, 263). Interestingly, we observed that GST-PERK Y561F migrated at the level of GST-PERK Wt (Fig 8A). We also noticed that these GST PERK fusion proteins displayed distinctive sensitivity to proteolytic cleavage when expressed in bacteria. GST-PERK Wt showed less large protease-resistant fragments as compared to the GST-PERK K618A fusion protein (Fig. 8A), supporting the idea that the catalytically active PERK cytoplasmic segment displays a loosened structure rendering it more susceptible to proteolytic cleavage (263). Interestingly, we found that freshly purified GST-PERK Y561F preparation contains less proteolytic fragments as compared to Wt, suggesting that the Y561F substitution in the JM domain of PERK inflicts a conformational change of PERK cytoplasmic segment rendering it more sensitive to proteolysis. We then carried out a comparative analysis of GST-PERK Wt and Y561F catalytic activity by performing *in vitro* kinase assays using the His-tagged eIF2α substrate. Incorporation of radiolabeled phosphate resulting from PERK autophosphorylation was decreased by approximately 30% in GST-PERK Y561F when normalized for fusion protein levels (Fig. 8B). Conversely, we noticed a distinct ability of GST-PERK Y561F to phosphorylate His-tagged eIF2α as compared to Wt. Incorporation of radiolabeled phosphate into His-eIF2α was significantly increased in reactions performed with the mutant fusion protein as compared to Wt (Fig. 8C), suggesting an enhanced catalytic activity of GST-PERK Y561F. We subsequently determined the kinetic parameters of GST-PERK Wt and Y561F fusion proteins. As reported in Fig. 8D, representative Lineweaver-Burk plots demonstrated a significant lower Km value for ATP for the PERK Y561F mutant as compared to Wt (13±3 μM and 35±5 μM, respectively). On the other hand, the kinetics of eIF2α phosphorylation performed in the presence of 100 μM ATP for both proteins did not exhibit typical Michaelis-Menten kinetics as suggested by nonlinear Lineweaver-Burke plots (263). Although the calculated $K_{0.5}$ and V_{max} for eIF2α tend to be higher for GST-PERK Y561F compared to Wt, we could not reach a statistical difference between the two fusion proteins (Fig. 8E). Based on this data, we concluded that PERK Y561F displays altered conformation and increases kinase activity toward eIF2α essentially due to higher affinity for ATP.

Figure 8. *In vitro* analysis of GST-PERK Y561F catalytic kinase activity (A) Purified bacterially expressed GST-PERK proteins (1 μg /lane) were resolved on SDS-PAGE and stained by Coomassie blue. As shown, GST-PERK Y561F migrates at the level of an active PERK protein on SDS-PAGE. **(B)** Decreased overall phosphorylation of GST-PERK Y561F in an *in vitro* autophosphorylating kinase assay. The histogram shows a quantitative analysis of the autophosphorylation of GST-PERK Wt and Y561F proteins normalized for the amount of GST-PERK fusion proteins present in the reaction. Data are means ± SEM * $p<0.02$ by Student t-test from three independent experiments. **(C)** Increased eIF2α phosphorylation by GST-PERK Y561F protein in an *in vitro* kinase assay. The histogram shows a quantitative analysis of the phosphorylation of eIF2α by GST-PERK Wt and Y561F proteins normalized for the amount of His-eIF2α and GST-PERK proteins present in the reactions. Data are means ± SEM. * $p< 0.01$ by t-test in three independent experiments. **(D)** ATP-dependent autophosphorylation of GST-PERK Wt and Y561F in the presence of His-eIF2α. Results were plotted according to Lineweaver-Burk analysis. A representative experiment of three is shown. **(E)** His-eIF2α phosphorylation by GST-PERK WT and Y561F plotted according to Michaelis-Menten analysis. A representative experiment of three is shown. A.U.: Arbitrairy Units.

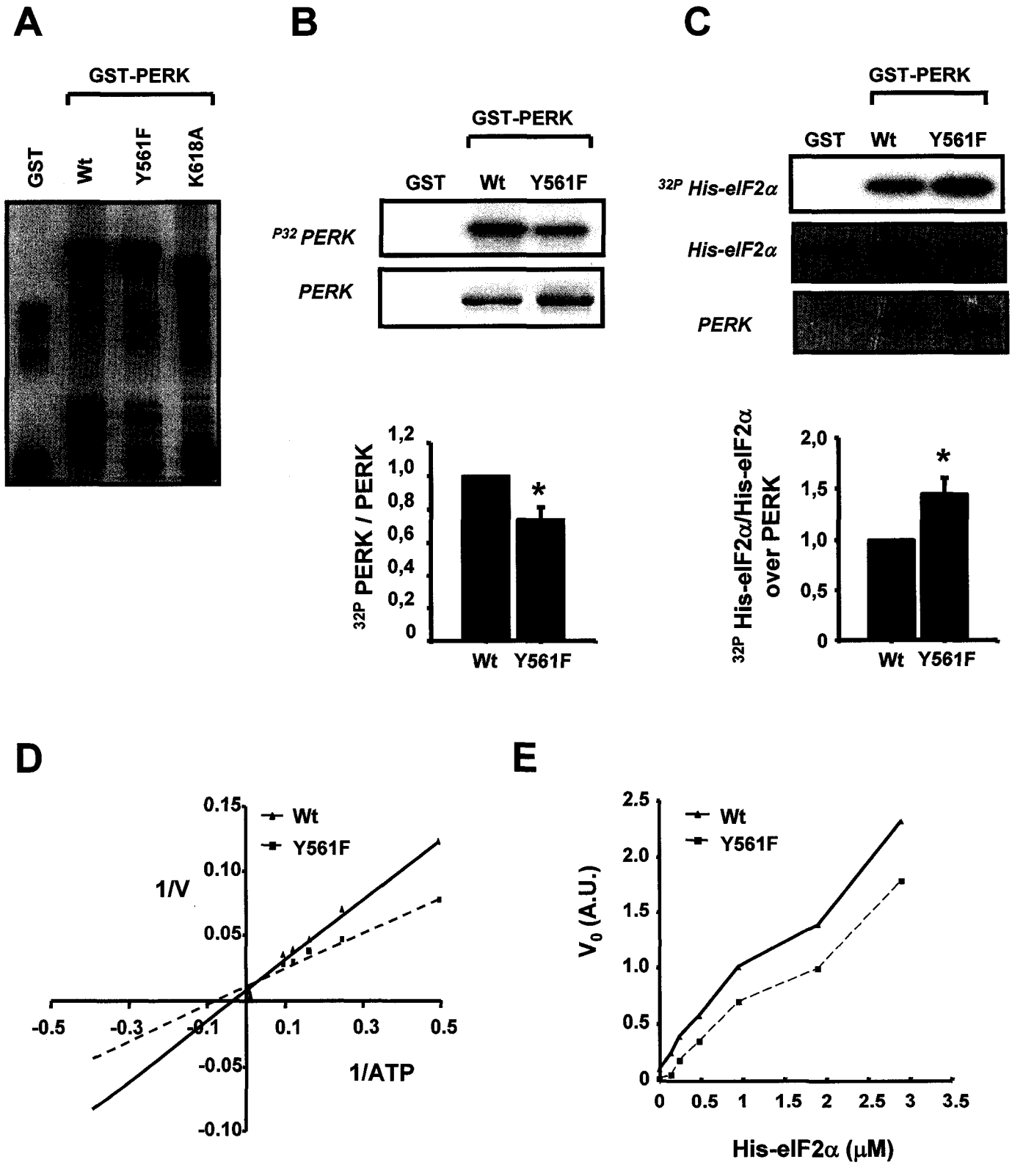
A
GST-PERK
GST
Wt
Y561F
K618A
B
GST-PERK
GST
Wt
Y561F
32P PERK
PERK
32P PERK / PERK
1,2
1,0
0,8
0,6
0,4
0,2
0
Wt
Y561F
C
GST-PERK
GST
Wt
Y561F
32P His-eIF2α
His-eIF2α
PERK
32P His-eIF2α/His-eIF2α over PERK
2,0
1,5
1,0
0,5
0
Wt
Y561F
D
Wt
Y561F
1/V
0.15
0.10
0.05
-0.05
-0.10
-0.5
-0.3
-0.1
0.1
0.3
0.5
1/ATP
E
Wt
Y561F
V0 (A.U.)
2.5
2.0
1.5
1.0
0.5
0
0
0.5
1
1.5
2
2.5
3
3.5
His-eIF2α (μM)

Next, we investigated the effect of the Y561F mutation on ER-stress-induced eIF2α Ser51 phosphorylation *in vivo*. $PERK^{-/-}$ MEFs were transiently transfected with full-length PERK Wt or Y561F cDNAs and the levels of eIF2α phosphorylation in response to DTT treatment were measured by immunoblotting experiment. We observed that treatment with DTT caused higher levels of eIF2α phosphorylation both at 20 and 60 min of treatment in MEFs rescued by PERK Y561F as compared to PERK Wt (Fig. 9A compare lane 7-9 to 4-6; Fig. 9B). In contrast, MEFs expressing the catalytic inactive PERK K618A mutant were completely impaired in inducing eIF2α phosphorylation upon DTT treatment (Fig. 9A, lanes 10-12). As shown in Fig. 9C, MEFs expressing PERK Y561F mutant showed maximal eIF2α phosphorylation one hour after DTT treatment, while this occurred at 2 hours in cells expressing PERK Wt (Fig. 9C-9D). Even after 8h of treatment, PERK Y561F-expressing cells showed reproducibly higher levels of eIF2α phosphorylation compared to PERK Wt-expressing cells. Therefore, mutation of Tyr561 in the PERK JM domain results in faster and prolonged kinetics of eIF2α Ser51 phosphorylation in response to ER stress.

To confirm these findings, we used the Fv2E-PERK reconstituted system and addressed the consequence of the Y561F mutation on eIF2α phosphorylation in response to AP20187 treatment. Addition of increasing concentration of AP20187 to Fv2E-PERK Y561F-expressing MEFs resulted in higher levels of eIF2α phosphorylation as compared to Fv2E-PERK Wt cells (Fig 9E compare lanes 7-10 to 3-6). In agreement with increased eIF2α phosphorylation by PERK Y561F, a time course experiment of AP20187 treatment demonstrated sustained phosphorylation of eIF2α in Fv2E-PERK Y561F-expressing cells as compared to Fv2E-PERK Wt (Fig. 9F). We noticed that the Fv2E-PERK Wt fusion protein migrated as a single band on SDS-PAGE in untreated cells, while the mutant fusion Fv2E-PERK Y561F migrated as a smear (Fig. 9E compare lane 7 to 3). Furthermore, this was frequently associated with increased levels of eIF2α phosphorylation in absence of AP20187, supporting our previous findings suggesting that the Y561F substitution introduces a conformational change in the PERK cytoplasmic segment. Importantly, we estimated that the proportion of fusion protein retarded on SDS-PAGE observed in response to AP20187 treatment (presumingly representing the autophosphorylated and activated form of the fusion protein) was almost 100% for the Fv2E-PERK Y561F, but only 20% for the Wt (Fig 9E and 9F). These observations strongly suggest that the Y561F substitution

introduces a conformational change in the PERK cytoplasmic domain increasing its ability to phosphorylate eIF2α on Ser51. Overall, we provide evidence that Tyr561 in the PERK JM domain is required for Nck binding and regulation of PERK catalytic activity.

Figure 9. *In vivo* analysis of PERK Y561F-mediated eIF2α phosphorylation (A) PERK $^{-/-}$ MEFs were transiently transfected with carrier, full length PERK Wt, Y561F or K618A cDNAs. 48 h later, cells were treated with 1 mM DTT and harvested. Cell lysates normalized for protein content were then subjected to immunoblotting analysis using the indicated antibodies. **(B)** Histogram represents the quantitative analysis of eIF2α phosphorylation in cell lysates prepared from PERK $^{-/-}$ MEFs transiently expressing PERK Wt or Y561F cDNAs and treated with 1 mM DTT for 20 min. Data are means ± SEM. and representative of three independent experiments. **(C)** Same as in (A) except transfected cells were treated with DTT for a longer period of time. **(D)** Densitometry analysis of data presented in C. **(E)** Fv2E-fused PERK WT and Y561F cytoplasmic segments were transiently expressed in Cos-1 cells. 48 h later cells were exposed to the indicated concentrations of the AP20187 dimerizer. Cells were harvested and lysates normalized for protein content were used for immunoblotting analysis using the indicated antibodies. Note the complete mobility shift of the PERK Y561F fusion protein as compared to Wt. **(F)** Same as in (E) except a time course of eIF2α phosphorylation in response to AP20187 treatment (100 μM) was performed.

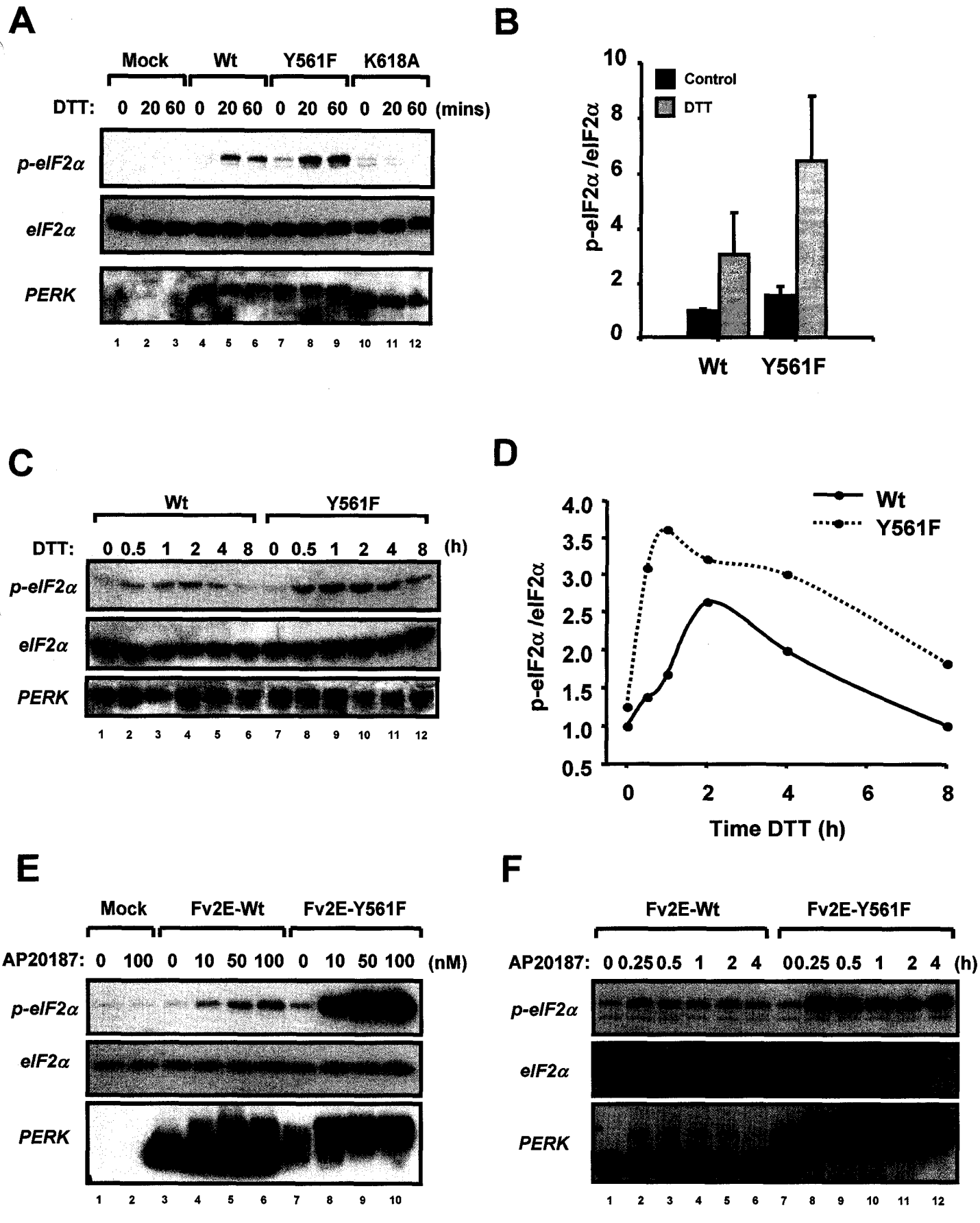
A
Mock
Wt
Y561F
K618A
DTT: 0 20 60 0 20 60 0 20 60 0 20 60 (mins)
p-eIF2α
eIF2α
PERK
1 2 3 4 5 6 7 8 9 10 11 12
B
Control
DTT
p-eIF2α /eIF2α
10
8
6
4
2
0
Wt
Y561F
C
Wt
Y561F
DTT: 0 0.5 1 2 4 8 0 0.5 1 2 4 8 (h)
p-eIF2α
eIF2α
PERK
1 2 3 4 5 6 7 8 9 10 11 12
D
Wt
Y561F
p-eIF2α /eIF2α
4.0
3.5
3.0
2.5
2.0
1.5
1.0
0.5
0 2 4 6 8
Time DTT (h)
E
Mock
Fv2E-Wt
Fv2E-Y561F
AP20187: 0 100 0 10 50 100 0 10 50 100 (nM)
p-eIF2α
eIF2α
PERK
1 2 3 4 5 6 7 8 9 10
F
Fv2E-Wt
Fv2E-Y561F
AP20187: 0 0.25 0.5 1 2 4 0 0.25 0.5 1 2 4 (h)
p-eIF2α
eIF2α
PERK
1 2 3 4 5 6 7 8 9 10 11 12

DISCUSSION

The ER PERK ser/thr kinase plays an important role in the regulation of mRNA translation in response to a growing number of stress conditions impairing ER homeostasis. These include ER stress, hypoxia and viral infection. In all of these cases, PERK activation converges on the phosphorylation of eIF2α on Ser51, which in turn inhibits the initiation of protein synthesis. In the present study, we provide additional evidence that Nck SH2/SH3 domain-containing adaptor proteins are important regulators of PERK-mediated eIF2α phosphorylation in ER stress conditions.

In the past years, we reported a direct interaction between Nck and eIF2β (198). We also demonstrated that overexpression of Nck increases mRNA translation (198) and decreases both basal and ER stress-induced eIF2α phosphorylation levels (197, 224). Although these studies were mainly conducted using overexpression of Nck in cultured cells, one would predict that if these data really reflect Nck function, depletion of Nck proteins in cells should result in increased levels of eIF2α phosphorylation. In this study, we report that RNAi-mediated Nck1 depletion unexpectedly decreases eIF2α phosphorylation levels in resting cells (Fig. 1). Moreover, cells depleted of Nck1 show increased translational rates and impaired phosphorylation of eIF2α induced by ER stress (Fig. 1). How can this discrepancy be explained? It is not unusual in the literature to observe conflicting results on the function of adaptor/scaffolding proteins basically due to limitations in available approaches used to dissect intracellular signaling pathways (165, 431). This reflects the problems associated with the investigation of adapter proteins function using overexpression systems, which create variations in the relative stoichiometry of expressed adaptor protein and individual interacting molecules. If an adaptor serves as a bridge to assemble two or more proteins into a common molecular complex, the stoichiometry of this complex could be disrupted upon transient overexpression of the adaptor, and hence, a positive regulator could appear to act as a negative regulator. Based on this reasoning, increasing Nck expression by a factor of 5- to 10-fold as previously reported (224) is expected to titrate eIF2β away from other limiting components, and in this manner, interfere with the phosphorylation of eIF2α by PERK. Therefore, this problem underscores the need for loss of function approaches to rigorously examine Nck adaptor function in cell biology. Based on the

results presented in this study, we believe that Nck acts as a positive regulator of PERK-mediated eIF2α phosphorylation in ER-stressed cells. In fact, preliminary results obtained in $Nck1^{-/-}$ mice also support this idea (see Chapter IV).

Over the years, few substrates and regulators of the PERK kinase have been identified. In this study, we demonstrate that Nck adaptors represent the third PERK-interacting protein identified after eIF2α (142, 263) and Nrf2 (73). By performing *in vitro* pull-down assays, we established that this interaction is direct and mediated by the PERK cytoplasmic segment. Moreover, we determined that this interaction requires the catalytic activity of PERK and the SH2 domain of Nck (Fig. 3). Finally, we found that Nck is recovered in PERK immunoprecipitates prepared from Cos-1 cells, suggesting that this interaction occurs *in vivo*. Interestingly, preliminary experiments showed that Nck is also phosphorylated by PERK *in vitro* (data not shown), although validation and physiological significance of this observation still remains to be established. Since Nck1 depletion by RNAi reduces levels of eIF2α phosphorylation and increases mRNA translation rates in cells, it suggests that the association of Nck with PERK is important for signaling by this kinase in ER stress conditions.

So far, SH2 domains appear to be uniquely dedicated to pTyr recognition and thus represent key targeting and specificity components of tyrosine kinase signaling. The SH2-dependent interaction of Nck with GST-PERK strongly suggests that PERK cytoplasmic segment is tyrosine phosphorylated at least *in vitro*. It was recently shown that PKR, the closest relative of PERK, autophosphorylates on tyrosine residues (392). PKR autophosphorylation on tyrosine residues impacts on PKR dimerization, catalytic activation, eIF2α phosphorylation and its antiviral properties (74, 83). Furthermore, PKR is able to phosphorylate the tyrosine residue at position 51 in the recombinant eIF2α S51Y protein (249). Crystallographic resolution of the PKR kinase domain structure revealed that the orientation of the P+1 loop in the kinase activation segment closely resembles that of a tyrosine rather than a ser/thr kinase (74). Inspection of the corresponding amino acids in PERK reveals a high degree of identity with PKR in this segment, suggesting that PERK could also behave as a dual-specific kinase. Here, we found that the catalytically active GST-PERK Wt fusion protein is phosphorylated on tyrosine residues when expressed in bacteria (Fig. 4). We presume that this is an autophosphorylation

event given that the catalytically inactive GST-PERK K618A mutant was not tyrosine phosphorylated. Previous mass spectrometry analysis reported that residues Tyr585 and Tyr883 respectively in the N-terminal and C-terminal lobes of the kinase domain of PERK are phosphorylated *in vitro* (257). Here, we reported that PERK Tyr561 is required for binding of Nck adaptors (Fig 7). This highly conserved tyrosine residue is located in the JM domain of the PERK cytoplasmic segment and matches the consensus binding motif for Nck SH2 domain (108, 384). We provided evidence indicating that Tyr561 in GST-PERK is phosphorylated by showing that 1) its substitution with a non-phosphorylatable phenylalanine residue decreases the overall tyrosine phosphorylation of the protein by 50%; and 2) full length Nck1 or isolated Nck1 SH2 domain associates with PERK Wt, but not with the PERK Y561F mutant (Fig. 7). We are aware that introduction of the Y561F mutation could result in a redistribution of phosphorylated tyrosine residues in PERK, and thereby underlie the loss of binding with Nck adaptors. However, introduction of the Y561F mutation in PERK does not abolish the binding of eIF2α and eIF2β in pull-down experiments, suggesting that this substitution does not completely change the conformation and ionic surface of PERK cytoplasmic segment (data not shown). Anyhow, these results demonstrate the importance of Tyr561 in mediating Nck association with PERK *in vitro*.

We noticed that PERK tyrosine phosphorylation was hardly detected *in vivo*, suggesting that this modification is unstable and difficult to detect by conventional immunoblotting analysis using endogenous PERK. Similarly, PERK ser/thr phosphorylation was also difficult to detect in response to treatment with ER stress agents in immunoblotting experiment, although this modification is now recognized as an important regulator of PERK activation and eIF2α phosphorylation (263). We believe that the expression levels of PERK might be too low in cells to monitor its phosphorylation state using phosphospecific antibodies. On the other hand, we found that fusion of the PERK cytoplasmic segment to the Fv2E inducible dimerizing module allowed detection of PERK tyrosine phosphorylation in cells treated with the protein tyrosine phosphatase inhibitor bpV(phen) (Fig. 5). We observed that both Wt and K618A fusion proteins exhibited reduced mobility on SDS-PAGE in cells treated with bpV(phen) and this correlated with tyrosine phosphorylation of the fusion proteins. This indicates that the PERK cytoplasmic segment is subjected to tyrosine phosphorylation by exogenous kinases independent of its catalytic kinase activity. On the other hand, we found that AP20187-mediated dimerization

increased tyrosine phosphorylation of Fv2E-PERK Wt, but decreased that of Fv2E-PERK K618A over time in cells pre-treated with bpV(phen). These results demonstrate that PERK dimerization promotes its tyrosine phosphorylation in a catalytic kinase activity-dependent manner. The autophosphorylation of PERK on tyrosine residues still needs to be tested on endogenous PERK, but our results indicating that GST-PERK Wt, but not the K618A mutant, is phosphorylated on tyrosine residues *in vitro* strongly suggests that PERK also autophosphorylates on tyrosine residues *in vivo*. Therefore, a phosphotyrosine regulatory switch might accompany PERK activation and eIF2α phosphorylation in conditions of ER stress. In unstressed cells, phosphorylation by exogenous tyrosine kinases could bring repulsive electrostatic interactions preventing stochastic dimerization and activation of PERK. Alternatively, this tyrosine phosphorylation may create high affinity binding sites recruiting proteins maintaining PERK in an inactive state. On the other hand, the catalytic activity-dependent tyrosine phosphorylation of PERK induced by dimerization could represent a regulatory mechanism contributing to loosen the conformation of its cytoplasmic segment allowing substrate recruitment and catalysis of eIF2α phosphorylation.

Our results indicate that substitution of Tyr561 in the PERK JM domain to a non-phosphorylatable phenylalanine residue increases PERK catalytic kinase activity and eIF2α phosphorylation both *in vitro* and *in vivo* (Fig. 8-9). These results lead us to consider two potential roles for Tyr561 in the PERK kinase. First, phosphorylation of Tyr561 (autophosphorylation or phosphorylation by an exogenous kinase) is part of a negative regulatory mechanism downregulating PERK catalytic kinase activity. Phosphorylation of Tyr561 could create a binding site for a negative regulatory protein involved in fine-tuning the activity of PERK and/or the phosphorylation of eIF2α, thereby avoiding deregulated signaling in response to ER stress. Second, phosphorylation of PERK on Tyr561 is part of a positive regulatory mechanism that accompanies PERK activation and required for the phosphorylation of eIF2α. The catalytic activity of several protein kinases is regulated by *cis*-acting elements that prevent deregulated activation through spontaneous conformational changes giving free access to either ATP or substrates. Well-characterized examples of such a mode of regulation include RTKs, whose catalytic clefts are occluded by their disorganized activation loop (171, 277). In response to stimuli, phosphorylation of specific residues in the activation loop of most protein kinases is

required for full-scale activation, substrate binding and phosphorylation (293). By looking at the function of the JM domain in TβR or RTK family of transmembrane kinases, we noticed that this region played a critical autoinhibitory function on catalytic activity (170). In the absence of ligand, the unphosphorylated JM segment of both TβR and RTK binds a site near the substrate-binding site in the kinase domain, interfering with substrate binding. TβR and RTK activation results in the phosphorylation of either serine/threonine or tyrosine residues in the JM domain in these receptors respectively, thereby relieving the intrinsic autoinhibitory function to this domain and promoting receptor activation and signaling (125, 170). The importance of the JM in regulating RTKs activity is illustrated by PDGFR family members Kit and Flt3 receptors, in which activating mutation in the JM domain is associated with gastrointestinal stromal tumors and one third of the human acute myeloid leukemia, respectively (125, 152, 160).

Such autoinhibitory function of the JM domain also takes place in the IR. The conserved JM domain residue Tyr984 in the IR is buried in a hydrophobic cleft and performs multiple interactions via its side chain hydroxyl group with other residues located at the junction of five-stranded anti-parallel β-sheets and the α-C helix in the N-terminal lobe (235). These interactions provide steric restraints preventing α-C helix from assuming its catalytically competent position. Substitution of Tyr984 with residues devoid of hydroxyl group in their side chain such as phenylalanine or alanine results in increased ligand-independent and ligand-dependent receptor activation due disengagement of the proximal JM segment from the β-sheet/α-C helix cleft, causing reorientation of α-C helix in a catalytically competent position as seen in the activated IR (169, 235). Based on the increased catalytic activity of IR Y984A mutant, it is believed that hydroxyl group disengagement or deletion, rather than addition of a negatively charged phosphate group at position 984 in the IR is responsible for relieving the autoinhibitory function of the JM domain. Although phosphorylation of Tyr984 still remains to be firmly demonstrated *in vivo*, phosphorylation of this residue might represent the mechanism utilized by the IR to disturb electrostatic bonds carried by the Tyr984 hydroxyl group and disengage the JM domain from the N-terminal lobe. In fact, this mode of regulation has been demonstrated for EphB2 RTKs. The solved X-ray crystal structure of the autoinhibited EphB2 cytoplasmic segment showed that autophosphorylation on Tyr604 and Tyr610 within the highly conserved JM domain generates repulsive electrostatic forces essential for disengagement of tyrosine hydroxyl groups

and expulsion of these residues out of an hydrophobic pocket (452). Importantly, disengagement of these regulatory tyrosine residues by such phosphoregulatory switch is sufficient to disturb the association of the JM domain with the N-terminal lobe of the kinase domain and stimulate kinase activity (452). Interestingly, Holland *et al* (1997) demonstrated that these two tyrosine residues are required for the association of Nck1 SH2 domain (162).

Alignment of PERK with other RTKs JM domain demonstrates that Tyr561 aligns with an equivalent regulatory tyrosine present in the JM domains of several RTKs (Tyr984 in IR, Tyr957 in IGF1R, Tyr572 in PDGFRα, Tyr578 in PDGFRβ), suggesting that a similar phosphoregulatory switch involving Tyr561 could complement the positive regulatory function associated with PERK autophosphorylation on Thr980 in the activation loop. Although PERK autophosphorylates extensively on serine and threonine residues in its kinase insert loop, the JM domain of PERK was found to be phosphorylated only on tyrosine residues Tyr561 (described herein) and Tyr585 (257), but not on serine/threonine as it is usually the case for ser/thr kinase such as type I TβRs. Therefore, the early conformational transition events of the kinase domain occurring during PERK activation might be mainly regulated through tyrosine, rather than serine/threonine phosphorylation of the JM domain. Hence, phosphorylation of Tyr561 in the PERK JM domain could be involved in relieving the autoinhibitory function of the JM domain through disengagement of the Tyr561 side chain hydroxyl group from an inhibitory cleft as found in RTKs and type I TβRs.

Overall, the results obtained in this study led us favor that phosphorylation of Tyr561 is a positive regulatory mechanism promoting PERK activation and phosphorylation of eIF2α mainly for two reasons: First, Tyr561 is found within the PERK JM domain and is required for the association of Nck with the catalytically active form of PERK. Second, RNAi-mediated Nck depletion attenuates ER stress-induced eIF2α phosphorylation, indicating that binding of Nck adaptors to PERK Tyr561 does not result in the targeting of negative regulatory proteins restraining PERK activation. Therefore, as seen for EphRs, Nck adaptors could represent important proteins promoting signal transduction from PERK in ER stress conditions through binding of Tyr561 in the PERK JM domain. In unstressed cells, PERK is found in a monomeric and inactive form, bound to the luminal chaperone BiP/Grp78. Site-specific tyrosine

phosphorylation by exogenous kinases could help prevent stochastic dimerization of PERK and kinase activation in resting cells. Under this configuration, PERK JM domain Tyr561 is engaged in a hydrophobic cleft through interactions of its side chain hydroxyl group with residues in the N-terminal lobe of the kinase domain precluding access to the catalytic site (Fig. 10A). In response to ER stress, PERK autophosphorylates on the Tyr561 side chain hydroxyl group promoting the reorientation of the JM domain, bringing a constitutive "gate-open" conformation of the kinase domain and phosphorylation of eIF2α on Ser51 (Fig. 10A). Importantly, substitution of Tyr561 with residues missing a hydroxyl group in their side chain, such as phenylalanine, would result in increased ability of PERK to phosphorylate eIF2α due to complete disengagement of Tyr561 and reorientation of the JM domain. Therefore, this potential phosphoregulatory switch involving Tyr561 likely plays an important role in the activation of PERK. This regulatory mechanism might also be counteracted by protein tyrosine phosphatases that dephosphorylate Tyr561 and downregulate PERK catalytic kinase activity (Fig. 10B). Accordingly, the constitutive active PERK Y561F mutant would be entirely resistant to the action of protein tyrosine phosphatases partly explaining its decreased mobility on SDS-PAGE and improved ability to phosphorylate eIF2α. In fact, Eph receptors are regulated by a similar mechanism as it was recently demonstrated that the transmembrane protein tyrosine phosphatase receptor type 0 (Ptpro) dephosphorylates Tyr610 in the JM of EphA4 and EphB2 receptors, thereby controlling signal transmission from Eph receptors (379). In this scenario, we can speculate that PTP1B, an ER-localized protein tyrosine phosphatase regulating ER-stress signaling from IRE1, might also regulate the phosphorylation of state of Tyr561 in PERK JM domain (127).

Since we found that Nck adaptors bind in a strict SH2- and Tyr561-dependent manner with PERK and that Nck1 depletion decreases ER stress-induced eIF2α phosphorylation, we propose that Nck, via its interaction with eIF2β, could protect PERK Tyr561 from dephosphorylation, stabilize the [PERK+eIF2α] transition state, and thereby promote phosphorylation of eIF2α (Fig. 10B). In this regard, Nck would represent critical factors setting the activation threshold for the PERK signaling pathway upon ER stress. In fact, the concept of signaling threshold has been found to play important roles in signaling from the EGF receptor during development (107), and could underlie a differential regulation of PERK signaling during

acute or chronic ER stress as observed with the IRE1 sensor protein (245). Overall, we provide evidence demonstrating a positive role for Nck adaptors in transducing signaling form PERK in ER stress conditions. Moreover, we found that Tyr561 in the PERK JM domain is required for association of Nck adaptors. Finally, our results suggest that Tyr561 is involved in an autoinhibitory mechanism restricting PERK activation and eIF2α Ser51 phosphorylation. We believe that the present model should provide the reader with a basis for testing hypotheses based on existing data, although we are aware that crystallographic studies of PERK cytoplasmic segment would greatly complement this model.

Figure 10. PERK activation and signaling. (A) Model illustrating the role of the juxtamembrane Tyr561 in regulating PERK activation. LEFT: In unstressed cells, ER-localized PERK is found in a monomeric and inactive form bound to the luminal chaperone BiP/Grp78. In this condition, Tyr561 in the juxtamembrane (JM) domain is engaged through its side chain hydroxyl (OH) group in intramolecular interactions contributing to maintain PERK in an inactive state (see red circle). RIGHT: Phosphorylation of Tyr561 disrupts Tyr561-OH-dependent interactions, resulting in a constitutive "gate-open" conformation of the kinase domain and increased PERK activity. Replacement of Tyr561 with a Phe residue (Y561F) lacking an OH group in its side chain also results in a constitutive "open-gate" conformation of PERK kinase domain and increased PERK activity **(B) Model illustrating the role of Nck in mediating PERK signaling.** (1) In unstressed cells, ER-localized PERK is found in a monomeric and inactive form bound to the luminal chaperone BiP/Grp78. In such context, we propose that the unphosphorylated Tyr561 residue in the JM domain is engaged through its side chain hydroxyl group (OH) in intramolecular interactions contributing to maintain PERK in an inactive state. (2) In ER stress conditions, BiP/Grp78 is released from PERK luminal domain to promote PERK dimerization and *trans*-autophosphorylation on Tyr561 in the JM domain and various serine/threonine residues in its insert loop. This induces an important change in PERK conformation, relieving the autoinhibitory effect of the juxtamembrane domain and allowing recruitment of the eIF2 complex. (3) Binding of the Nck adaptor to phosphorylated Tyr561 residue via its SH2 domain protects Tyr561 from being dephosphorylated by protein tyrosine phosphatases (PTPases) and stabilizes the [PERK+eIF2α] transition state, leading to increased PERK-mediated phosphorylation of eIF2α. Shown at the bottom of the scheme are the levels of PERK activation (p-PERK) and eIF2α phosphorylation (p-eIF2α) corresponding to the different stages of PERK activation and signaling based on the results obtained in the present study.

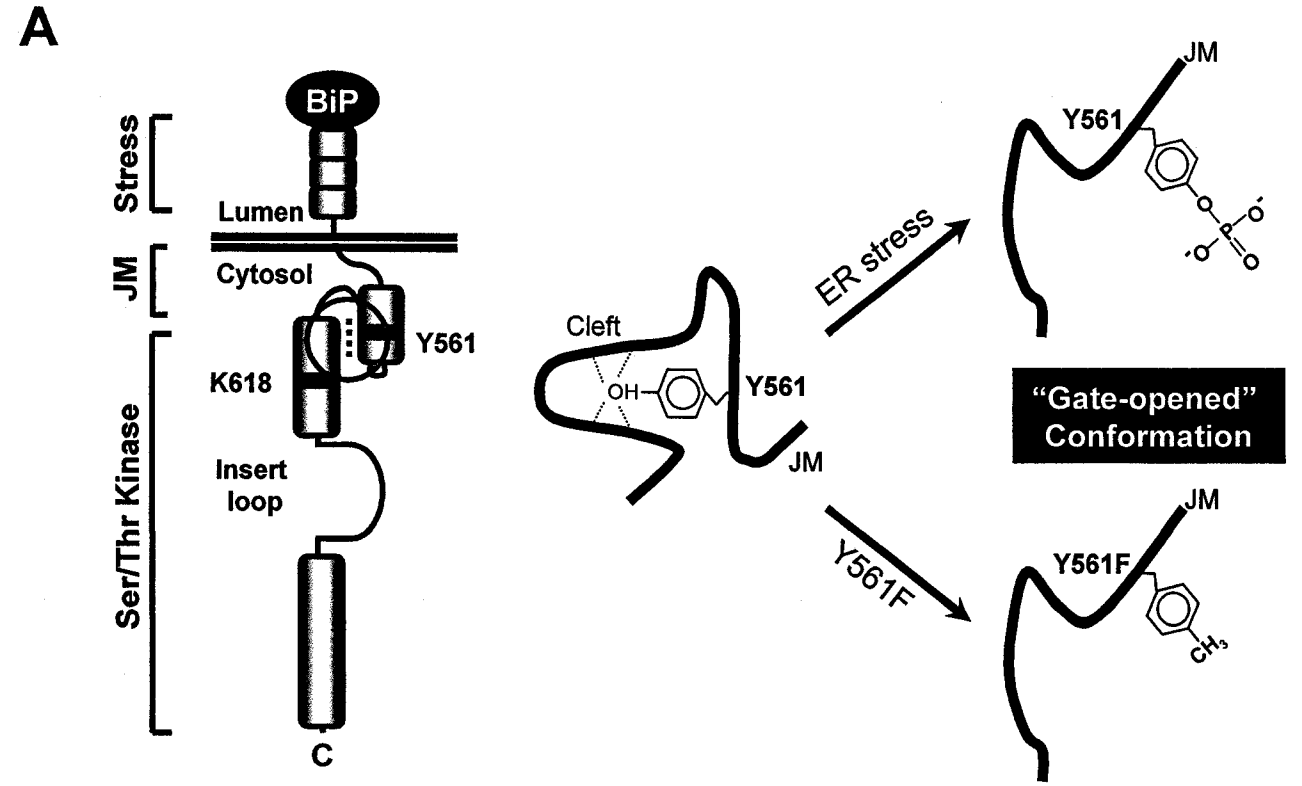
A
BiP
Stress
Lumen
JM
Cytosol
Y561
K618
Ser/Thr Kinase
Insert loop
C
Cleft
OH
Y561
JM
ER stress
Y561F
JM
Y561
Y561F
"Gate-opened" Conformation

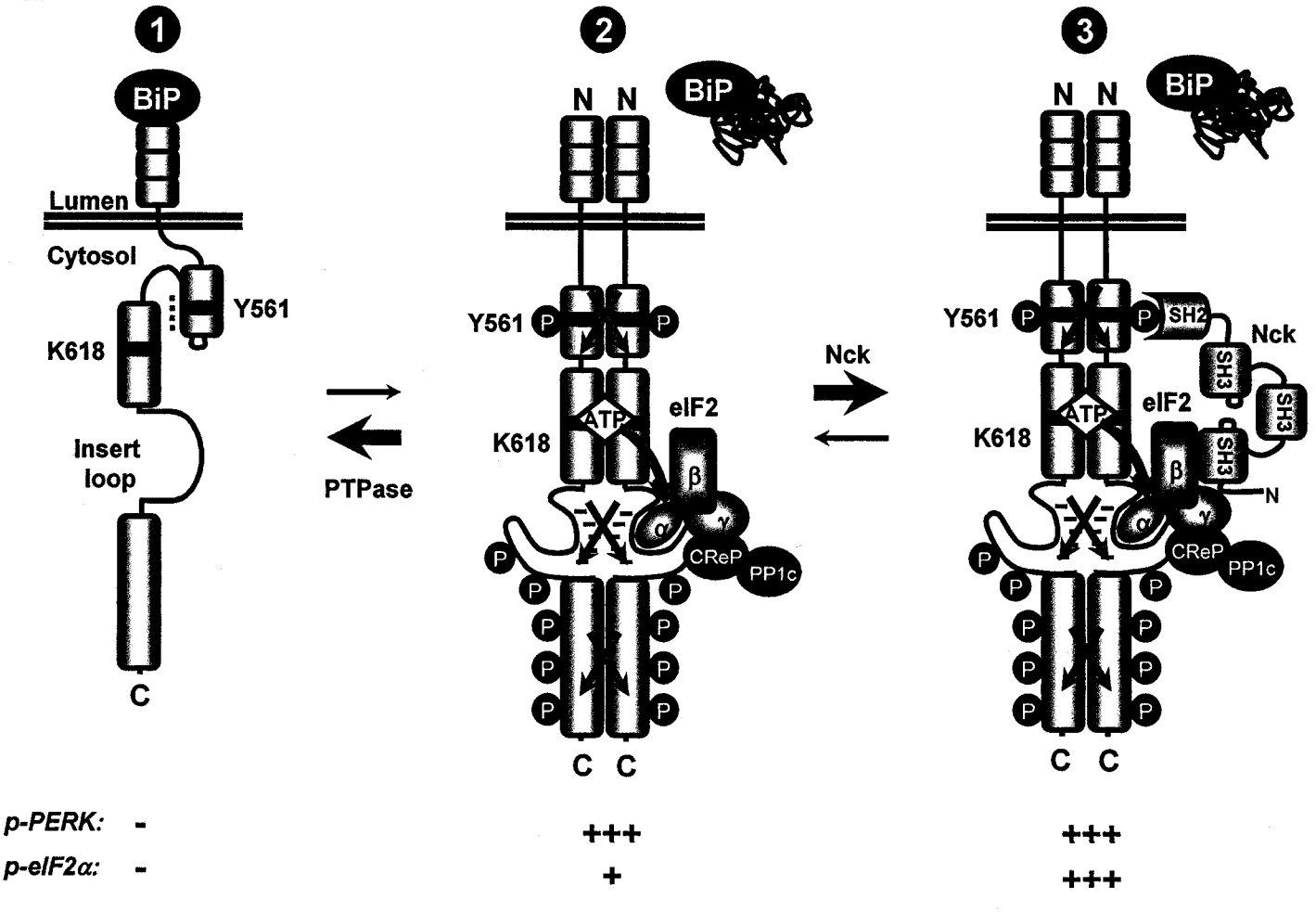
B
1
BiP
Lumen
Cytosol
Y561
K618
Insert loop
C
PTPase
2
N N
BiP
Y561
P
K618
ATP
eIF2
β
α
γ
CReP
PP1c
C C
Nck
3
N N
BiP
Y561
SH2
Nck
SH3
K618
ATP
eIF2
N
C C
p-PERK: - +++ +++
p-eIF2α: - + +++

ACKNOWLEDGMENTS

We thank Dr. D. Ron for providing the GST-PERK Wt and K618A, as well as Myc-PERK Wt and K618A plasmids, and the mouse embryonic fibroblasts (MEFs) PERK$^{-/-}$. We thank ARIAD Pharmaceuticals for supplying the Fv2E expression plasmid and the AP20187 dimerization drug. We thank Genevieve Bourret for her help in generating the PERK antibody. Finally, we thank Salma Ismail for the critical reading of this manuscript. This work was supported by a grant to L.L. from the Canadian Diabetes Association in honor of the late Lilian I. Dale. M.L. was supported by a fellowship from the McGill University Health Center Research Institute (MUHC-RI). L.L. is Chercheur National from the Fond de la Recherche en Santé du Québec (FRSQ).

CHAPTER IV

Mice lacking Nck1 are protected from development of insulin resistance secondary to obesity

Reproduced with permission from Mathieu Latreille, Genevieve Bourret, Marie-Kristine Laberge and Louise Larose.

To be submitted for publication

PREFACE

In chapter III, I determined that Nck directly interacts with PERK in an SH2-dependent manner. Moreover, I reported that depletion of Nck1 from cells reduces the phosphorylation of eIF2α and inhibition of mRNA translation in response to PERK activation by pharmacological ER stress agents. Together, these results suggest that Nck is required for PERK-mediated eIF2α phosphorylation in ER stress conditions by interacting directly with this protein kinase. Recently, murine dietary and genetic models of obesity were found to display signs of ER stress (i.e. phosphorylation of eIF2α on Ser51) in both liver and adipose tissue. To verify whether Nck adaptors are required for phosphorylation of eIF2α *in vivo*, I compared the levels of eIF2α phosphorylation in wild-type and $Nck1^{-/-}$ mice maintained on high fat diet for 18 weeks. Interestingly, I found that preventing Nck1 expression in mice greatly reduced phosphorylation of eIF2α in ER stress conditions secondary to obesity *in vivo*. Moreover, I uncovered that Nck-deficient mice display impair glucose homeostasis when maintained under normal or high fat diet. The results obtained from these molecular and metabolic analyses are presented in the following chapter.

ABSTRACT

Studies on endoplasmic reticulum (ER) overload caused by the accumulation of unfolded proteins have revealed the existence of a complex homeostatic signaling pathway, known as the unfolded protein response (UPR). This pathway increases ER function to maintain a balance between the load of newly synthesized proteins and the capacity of the ER to aid their maturation. Dysfunction of the UPR has been observed in several diseases, such as diabetes. The ER stress sensor protein PERK plays important roles in pancreatic β-cells function through phosphorylation of eIF2α on Ser51, while IRE1 modulates insulin sensitivity in liver and adipose tissues of obese mice through JNK-mediated phosphorylation of IRS-1 on Ser307. Recently, we found that Nck, an SH2/SH3 domain-containing adaptor modulate, modulates both PERK and IRE1 signaling pathways in ER-stressed cells. In this study, we conducted metabolic studies in mice with targeted deletion of the *nck1* gene ($Nck1^{-/-}$) and found that these mice display glucose intolerance, which correlates with reduced pancreatic β-cell mass. On the other hand, when fed a high fat diet, $Nck1^{-/-}$ animals display greater glucose tolerance than control obese mice due to increased insulin sensitivity in liver and adipose tissue. At the molecular level, obese $Nck1^{-/-}$ mice exhibit lower levels of ER stress markers, such as phospho-eIF2α Ser51, phospho-JNK and phospho-IRS-1 Ser307 compared to control obese mice. In accordance with improved insulin sensitivity, we observed significant increase in AKT Ser308 phosphorylation in liver and adipose tissue of $Nck1^{-/-}$ mice challenged with insulin. Overall, these results demonstrate that Nck adaptors are important regulators of glucose homeostasis and provide the first physiological evidence for a role of these adaptors in ER signaling.

INTRODUCTION

Eukaryotic cells have evolved several mechanisms to deal with the accumulation of unfolded protein in the endoplasmic reticulum (ER) assuring that only properly folded and assembled proteins are leaving the secretory pathway. At the center of these processes is the Unfolded Protein Response (UPR), a coordinated quality control network triggered in response to ER stress that culminates in increasing the folding and secretory functions of the ER (367). Three major ER stress transducers of the UPR are found in metazoans: IRE1, ATF6 and PERK. IRE1 transmits stress in the ER to the cytosol by activating its kinase and endoribonuclease activities, which initiates an unconventional mRNA splicing reaction of the XBP1 mRNA that produces an active transcriptional regulator called $XBP1^s$ (48, 229, 460). $XBP1^s$ controls the expression of ER chaperones, degradation factors and enzymes involved in protein folding and lipid biosynthesis, thereby increasing the ability of the ER to fold and process proteins produced through the secretory pathway (227, 461). ATF6 is a transmembrane transcription regulator cleaved by site-1 and site-2 proteases in response to ER stress (374, 375). The cleaved ATF6 N-terminal fragment migrates to the nucleus and activates the transcription of many chaperones genes including Bip/Grp78, which are imported back into the ER lumen to assist protein folding (148). Finally, PERK, is an ER transmembrane ser/thr protein kinase that phosphorylates the α-subunit of the eukaryotic initiation factor 2 (eIF2) on Ser51 in ER stress conditions (142). This event transiently attenuates mRNA translation, thereby decreasing the load of protein translocated at the ER and alleviating stress (140).

The translational arm of the UPR plays an important role in the regulation of glucose homeostasis *in vivo*. In response to elevation of glycaemia, insulin biosynthesis is promoted through targeting of the proinsulin mRNA to the ER. Upon its translocation across the ER, the proinsulin protein is processed by ER quality control systems composed of several chaperone proteins that assure proper folding of secretory proteins. However, the substantial increase in insulin biosynthesis provoke by sustained rise in blood glucose concentration predisposes to ER stress due to the incapacity of the ER to process such secretory load. In these circumstances, ER function is coupled to translation rates by PERK-mediated eIF2α phosphorylation, which attenuates protein synthesis and decreases burden on the ER (142). Phosphorylation of eIF2α is

critical for pancreatic β-cells function as it prevents accumulation of improperly folded polypeptides in the ER and guaranties that only mature insulin is packed into secretory granules for expulsion (365, 366). PERK is specifically required in insulin-secreting β-cells during the fetal and early neonatal period as a prerequisite for postnatal glucose homeostasis (139, 472). $PERK^{-/-}$ mice exhibit severe defects in fetal/neonatal β-cell proliferation and differentiation, resulting in decreased β-cell mass, defects in proinsulin trafficking and abrogation of insulin secretion that culminate in permanent neonatal diabetes (139, 473). The critical role of PERK in humans is underscored by the discovery of inactivating mutations within the *perk/eif2ak3* gene associated with an inherited autosomal recessive disease, called the Wolcott-Rallison syndrome (79). This disease develops in early infancy and is characterized by the destruction of pancreatic β cells (370). The importance of eIF2α phosphorylation in glucose homeostasis is further illustrated by mice harboring serine to alanine substitution at position of 51 in eIF2α (eIF2α S51A). These mice die shortly after birth of severe hypoglycemia caused by defective gluconeogenesis (365). Moreover, heterozygote $eIF2\alpha^{WT/S51A}$ mice maintained on high fat diet (HFD) develop profound glucose intolerance resulting from reduced insulin secretion accompanied by defective trafficking of proinsulin and reduced number of insulin granules in β-cells when maintained on high fat diet (HFD) (366). Together, these highlight the critical role of attenuation of protein synthesis associated with eIF2α phosphorylation on Ser51 in hyperglycaemia-induced insulin biosynthesis in pancreatic β-cells.

The IRE1 branch of the UPR also plays an important role in glucose homeostasis. The metabolic stress associated with obesity was shown to perturb the ER environment and impact on insulin sensitivity in peripheral tissues. Ozcan *et al.* found that genetic and dietary murine models of obesity display signs of ER stress in both liver and adipose tissues (311). Importantly, obesity-induced IRE1 hyperactivation impaired insulin receptor signaling through c-Jun terminal kinase (JNK)-mediated insulin receptor substrate-1 (IRS-1) Ser307 phosphorylation, thereby establishing peripheral insulin resistance. Increasing the folding activity of the ER is believed to prevent the development of insulin resistance based on the profound glucose intolerance of $XBP1^{+/-}$ mice kept on high fat diet (HFD) (311) and the ability of chemical chaperones to restore insulin sensitivity in mouse models of Type 2 diabetes (312).

Nck adaptor proteins are composed of three N-terminal SH3 domains and a C-terminal SH2 domain. In mammals, two genes encode Nck1 and Nck2 isotypes sharing a high degree of identity within the SH domains and therefore, are thought to regulate similar cellular processes (25). Nck were mainly reported to transduce signals from activated plasma membrane receptors to cytosolic effectors involved in actin cytoskeleton remodeling (23). However, we recently found that Nck participate in ER signaling and mRNA translation by regulating the phosphorylation of eIF2α on Ser51 (197, 198, 224). Moreover, we demonstrated that Nck directly associates PERK via its SH2 domain and provide strong evidence that this interaction is dependent on Tyr561 in the PERK juxtamembrane domain (see Chapter III). Moreover, depletion of Nck1 in cells causes decreased phosphorylation of eIF2α in response to pharmacological inducers of ER stress, thereby preventing attenuation of translation. Finally, we found that Nck also regulate ERK-1 signal transduction triggered by the activation of IRE1 in situation of ER stress (289). Although considerable progress has been made over the past few years in identifying effectors proteins that interact with Nck adaptors, the physiological function of these adaptor proteins remains to be firmly established. Based on the close connection between ER stress signaling and glucose homoestasis, we decided to analyze whole-body glucose homeostasis of Nck-deficient mice.

MATERIAL AND METHODS

Mice and diet studies. $Nck1^{-/-}$ and $Nck2^{-/-}$ mice were kindly provided by Dr. T. Pawson (MSH, ON, Canada). These mice were generated and genotyped as previously described (25). All procedures were conducted according to protocols and guidelines approved by the McGill University Animal Committee (#5069). Animals were housed at 21–23 °C with 12-hour light and dark cycles. One month-old $Nck1^{+/+}$ and $Nck1^{-/-}$ littermate male animals were housed pair-wise and provided either a control chow containing 10% fat or a high fat diet containing 45% fat (Research Diets Inc.) for 18 weeks. All studies were performed with 6–10 mice per experimental group and body weight was monitored weekly. Food intake was analyzed by measuring food mass each week during the 18 weeks of diet.

Metabolic studies. Blood glucose and insulin levels were determined respectively by tail and saphenous vein bleeding using OneTouch Ultra Glucometer (LifeScan Canada) and radioimmunoassay (Linco), respectively. We performed glucose tolerance tests on animals after 18-h overnight fast following intraperitoneal injection of 2g D-glucose/kg for mice maintained on chow diet and 1g D-Glucose/kg for mice maintained on high fat diet. Insulin tolerance test were performed on 5h fasted mice fast following intraperitoneal injection of 0.75 Units/kg of Humulin R (Elli Lily, Canada).

Antibodies. PERK polyclonal antibody obtained after rabbit immunization with a glutathione S-transferase (GST) chimera of the cytoplasmic segment of PERK (amino acids 537-1114) (142) was Protein A affinity purified and concentrated on Amicon centricon YM-30 centrifugal filter device (Millipore Corp.). Nck1 and Nck2 specific polyclonal antibodies were generated in rabbits using GST-fusion proteins of an amino acid sequence located between the third SH3 and the SH2 domains of Nck isotypes (Nck1: QNNPLTSGLEPSPPQCD YIRPSLTGKFAGNP; Nck2: VVLSDGPALHPAHA PQISYTGPSSSGRFAGRE) and Protein A affinity purified. The Protein A purified pan-Nck antibody was previously described (415). Phospho-Ser51 eIF2α antibody was from BioSource International (Medicorp Inc.). Insulin (H-86), eIF2α (Fl-315), phospho-tyrosine (PY99), GFP (B-2) and HA (F-7) antibodies were purchased from Santa Cruz. Jnk, phospho-JNK Thr 183/Tyr185, AKT, phospho-Ser308 AKT, and insulin receptor antibodies

were obtained from Cell Signaling. IRS-1 and phospho-Ser307 IRS-1 antibodies were purchased from Upstate. Glucagon antibody (clone K79bB10) was purchased from Sigma.

Tissue preparation and immunoblotting assay. Harvested tissues were snap-frozen in liquid nitrogen and kept at-80°C until further processing. Tissue samples were weighted and homogenized using a Polytron at 20% (w/v) in 5mM Tris-HCl pH 7.4, 0.25 M sucrose, 1 mM $MgCl_2$, 1 mM Dithiothreitol, 10 mM Sodium Pyrophosphate, 1 mM Sodium Orthovanadate, 100 mM Sodium Fluoride, 17.5 mM β-Glycerophosphate) supplemented with protease inhibitors (2 μg ml^{-1} Leupeptin, 4 μg ml^{-1} Aprotinin, 1 mM Benzamidine, 100 μg ml^{-1} Pefabloc SC PLUS). Samples were supplemented with Triton-X100 to a final concentration of 1%, incubated at 4°C for 10 min and centrifuged at 13,000 rpm for 10 min at 4°C. Supernatant were recovered and fractionated at 200,000 *g* for 30 min at 4°C. Resulting supernatants were recovered and subjected to Bradford assay (Bio-Rad) for protein quantification. Immunoprecipitation and immunoblotting experiments on cell lysates were performed respectively with at least 1 mg and 75 μg, without any freeze-thaw cycles from individual aliquots.

Pancreatic *in situ* immunofluorescence, quantitation of β-cell mass and detection of apoptosis. Pancreas were collected, cleared of fat, weighted and fixed for 24 h in formalin solution. Paraffin embedded tissues were sectionized (5 μm) and mounted on slides. Following dewaxing in alcohol, re-hydration and permeabilization (0.1% Triton X-100 / 0.1% NaCitrate), sections were immunostained for α-cells using mouse monoclonal anti-glucagon antibody, while β-cells were immunostained using rabbit anti-insulin antibody. Detection was performed using appropriate rhodamine and fluorescein secondary antibodies (Sigma). Slides were briefly incubated in DAPI (0.01%) to reveal cell nuclei. Acquisition and processing of images was performed using the Metamorph image software (Molecular Devices, Sunnydale, CA). Analysis of pancreatic β-cell mass was calculated by dividing total insulin-positive area by total pancreas section area. Pancreatic apoptotic index was determined using TUNEL assay (Terminal deoxynucleotidyl Transferase Biotin-dUTP Nick End Labeling) according to manufacturer's indications (Roche).

Pancreatic islets isolation and insulin secretion experiments. Pancreatic islets were isolated from one year-old $Nck1^{+/+}$ and $Nck1^{-/-}$ male littermate mice as described (324). Briefly, pancreas were perfused with Liberase (Roche) at 0.25 Unit/ml in HBSS/HEPES and digested at 37 °C. Digested pancreatic preparations were then washed twice with HBSS/HEPES and 0.1% BSA (Sigma), and filtered on cheesecloth. Islets were separated from other pancreatic cells on Histopaque gradient, washed and then hand picked, and incubated for 2 h in RPMI-1640 (Invitrogen) medium containing 2.8 mM glucose, 10 % fetal bovine serum (FBS), 10 mM HEPES, 1 mM sodium pyruvate and 0.75 mg/ml penicillin and 0.1 mg/ml streptomycin at 37 °C in 95 % O_2 - 5% CO_2 environment. In a typical experiment, pancreatic perfusion and islets preparation was done simultaneously using one $Nck1^{+/+}$ and one $Nck1^{-/-}$ mouse on the same day. Glucose-stimulated insulin secretions were conducted in 24-well plate using 8 islets per conditions. Islets were incubated in 500 µl of preincubation medium (Krebs-Ringer bicarbonate buffer containing 10 mM HEPES (KRBH), 0.07 % BSA and 2.8 mM glucose) at 37 °C for 30 min. Insulin secretion experiments were initiated by incubating the islets in 500 µl of fresh KRBH containing 0.5% BSA and supplemented with either 2.8 mM glucose, 16 mM glucose or 50 mM KCl for 1h at 37 °C. At the end of the incubation period, incubation medium was collected and kept at -80 °C until dosage of insulin by radioimmunoassay (Linco Research). For measuring islet insulin content, islets were washed twice with PBS before being subjected to acid-ethanol extraction. (0.2 M HCl in 75 % ethanol). After sonication and centrifugation, supernatants were stored at -80 °C and subsequently analyzed for insulin content by radioimmunoassay as reported above.

Protein and insulin islet content. Isolated pancreatic islets (110-200) were washed twice in PBS and lyzed in TE (Tris-EDTA) containing 0.5% Triton X-100. After centrifugation, clarified supernatants were kept at -80°C until processing. Insulin was measured by radioimmunoassay as reported above. Protein content was measured by Bradford assay (Bio-Rad) and DNA content determined by fluorometry using Cybergreen.

***In vivo* insulin signaling.** Overnight fasted mice were anesthetized with isoflurane and insulin (3.8 U/kg) injected through the jugular vein. Three minutes after insulin injection, liver, hind limb muscle and adipose tissue were collected, frozen in liquid nitrogen and kept at -80°C until

processing. Protein extraction and quantitation was performed as described above.

Statistical analyses: Statistical significance was determined using Student's t test with p values ≤ 0.05. In all tests, two groups with only one changed parameter were compared.

RESULTS

We examined Nck1 and Nck2 protein expression in tissues involved in glucose homeostasis in mice. To perform this, we first developed Nck1 and Nck2 polyclonal antibodies and determined their specificity in immunoblotting using lysates obtained from cells transiently expressing either green fluorescent protein (GFP)-tagged Nck1 and Nck2. We found that these antibodies readily recognize either Nck1 or Nck2 with high specificity and almost no cross reactivity in immunoblotting assay (Fig. 1A). Using these antibodies, we determined that Nck1 is highly expressed in liver, skeletal muscle and pancreas, but at a lower level in the adipose tissue (Fig. 1B). On the other hand, Nck2 protein expression is high in pancreas, low in muscle and not expressed or below the detection limit in liver and adipose tissues (Fig. 1B). As a control, expression of Nck1 is high in the kidney, while Nck2 expression is barely detected in this tissue (Fig. 1B).

Figure 1. Expression of Nck adaptors in mouse tissues. (A) Imunospecificity of polyclonal Nck1 and Nck2 antibodies. Green fluorescent protein (GFP)-tagged Nck1 or Nck2 were transiently expressed in HeLa cells. Corresponding cell lysates were used in immunoblotting assay with either Nck1 or Nck2 antibodies to examine the specificity of each antiserum. Total amount of GFP-tagged proteins was determined using GFP immunoblotting **(B)** Immunoblotting analysis of Nck1 and Nck2 expression levels in wild type mouse tissues using Nck1 and Nck2 antibodies.

A

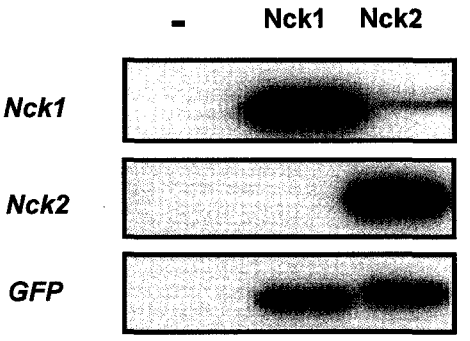
-
Nck1
Nck2
Nck1
Nck2
GFP

B

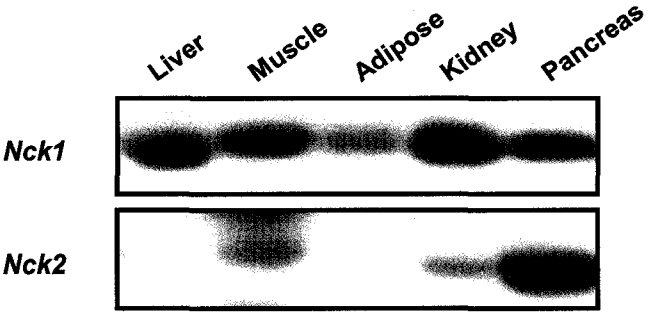
Liver
Muscle
Adipose
Kidney
Pancreas
Nck1
Nck2

Recent studies demonstrated that genetic inactivation of both Nck1 and Nck2 genes in mice ($Nck1^{-/-}Nck2^{-/-}$) is embryonically lethal at day E9.5 (25). In contrast, single $Nck1^{-/-}$ and $Nck2^{-/-}$ knockout mice are viable and fertile with no noticeable abnormalities in general appearance or behavior (25). Hence, we used $Nck1^{-/-}$ and $Nck2^{-/-}$ male animals maintained on chow diet (CD) to investigate the function of Nck adaptors in glucose homeostasis. We first noted a small, but significant, postnatal growth retardation within the first 4 months of age in $Nck1^{-/-}$ mice compared to wild type (Wt) (Fig. 2A). However, no significant difference in major organs weight (Fig. 2B) or food consumption (Fig. 2C) was noticed between the two genotypes. Given that the adipose tissue and skeleton were not included in our analysis, we cannot exclude the possibility that the difference in weight is accounted by the fat and bone mass.

Figure 2. Postnatal growth of Nck1$^{-/-}$ mice. (A) Body weight gain of Nck1$^{+/+}$ and Nck1$^{-/-}$ male littermate mice maintained on normal chow diet (CD) in function of time. Data are means ± SEM. n = 9-10 mice per group. * $p < 0.05$ **(B)** Weight of Nck1$^{+/+}$ and Nck1$^{-/-}$ mice organs normalized for total mice weight. n = 8-10 mice for each organ **(C)** Food intake (g/day/body weight) in Nck1$^{+/+}$ and Nck1$^{-/-}$ mice. Data are means ± SEM of 19 independent food intake measurements. n = 8-10 animals per group

A

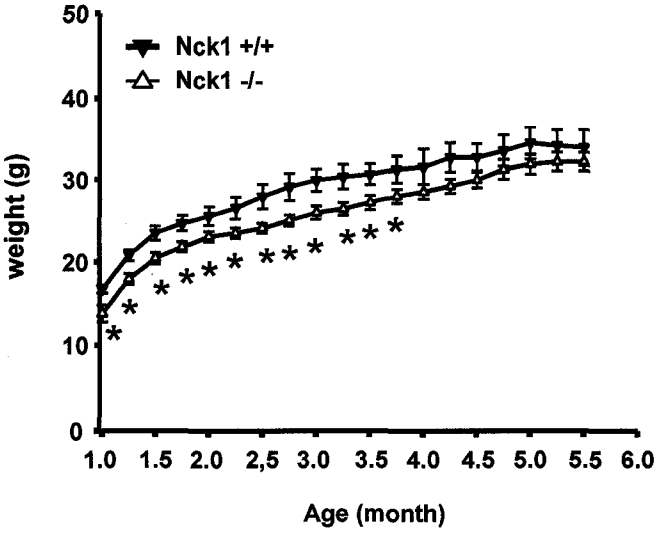
Nck1 +/+
Nck1 -/-
weight (g)
50
40
30
20
10
0
1.0 1.5 2.0 2,5 3.0 3.5 4.0 4.5 5.0 5.5 6.0
Age (month)

B

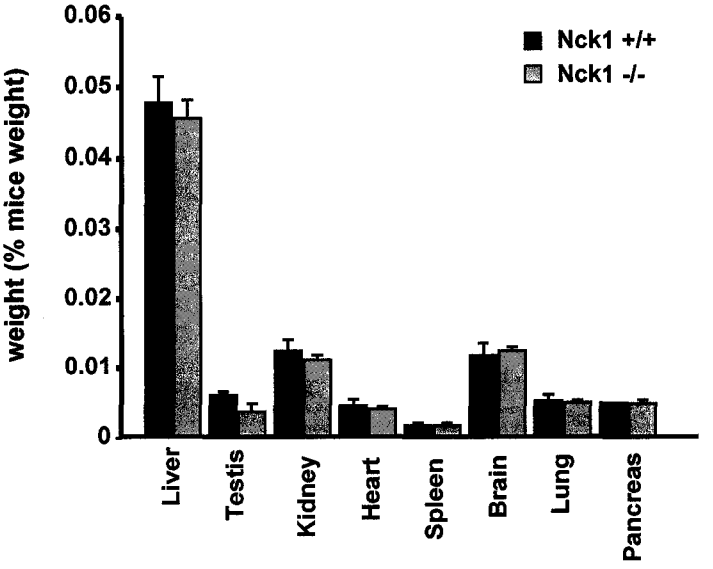
Nck1 +/+
Nck1 -/-
weight (% mice weight)
0.06
0.05
0.04
0.03
0.02
0.01
0
Liver
Testis
Kidney
Heart
Spleen
Brain
Lung
Pancreas

C

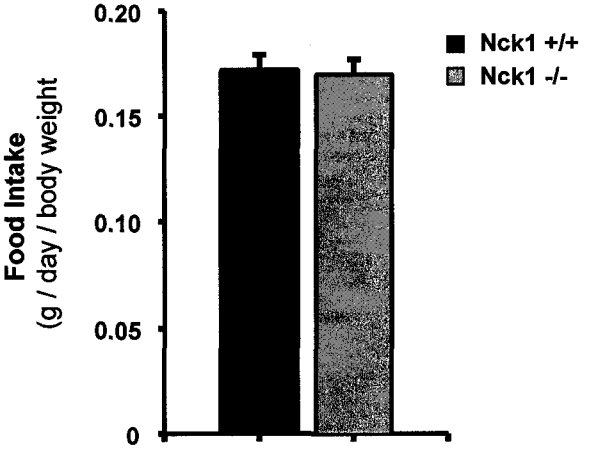
Nck1 +/+
Nck1 -/-
Food Intake
(g / day / body weight
0.20
0.15
0.10
0.05
0

Although fed and fasted blood glucose were nearly normal throughout life of $Nck1^{-/-}$ mice (data not shown), fed insulin levels appeared to be consistently lower in $Nck1^{-/-}$ although statistical significance was not reached (Fig 3A). Therefore, we directly measured $Nck1^{-/-}$ mice glucose disposal using intraperitoneal glucose tolerance test (GTT) in 3 month-old mice. We observed that $Nck1^{-/-}$ mice showed profound impaired ability to clear glucose compared to Wt mice (Fig. 3B). Intriguingly, this anomaly progressed with time as 5 month-old $Nck1^{-/-}$ mice showed even more prominent glucose intolerance (Fig 3C). Moreover, a comparative analysis demonstrated that $Nck2^{-/-}$ mice are also glucose intolerant at both 2 (data not shown) and 5 months (Fig. 3D) of age. The glucose intolerance was evidently severer in $Nck2^{-/-}$ mice as compared to $Nck1^{-/-}$ (compare Fig. 3C and 3D). In contrast, assessment of mice insulin sensitivity using an intraperitoneal insulin tolerance test (ITT) demonstrated that $Nck1^{-/-}$ mice present indistinguishable insulin sensitivity compared to Wt mice (Fig. 3E). Therefore, genetic inactivation of the Nck1 and Nck2 genes causes profound glucose intolerance despite the fact that these mice show normal sensitivity to insulin.

Figure 3. Glucose disposal and insulin sensitivity in Nck1$^{-/-}$ mice. (A) Fed insulin levels in Nck1$^{+/+}$ and Nck1$^{-/-}$ mice at 1 and 5 month of age. Data are means ± SEM. n = 5-9 animals per group. **(B-C)** Glucose tolerance tests were performed after intraperitoneal injection with D-glucose (2g/kg body weight) in 3 (B) and 5 (C) month-old fasted mice. Nck1$^{+/+}$, filled circle and blue colored line; Nck1$^{-/-}$, open circle and red colored line. Data are means values ± SEM. n = 6-9 animals per group. * $p<0.005$, ** $p<0.05$ **(D)** Glucose tolerance tests were performed in 5 month-old Nck2$^{+/+}$ and Nck2$^{-/-}$ mice as in (B-C). Nck2$^{+/+}$, filled circles blue colored line; Nck2$^{-/-}$, open circle red colored line. Data are means ± SEM. n = 6-7 animals per group. * $p<0.001$. **(E)** Insulin tolerance tests were performed after intraperitoneal injection of insulin (0.75 U/kg body weight) in 3 (B) and 5 (C) month-old fasted Nck1$^{+/+}$ and Nck1$^{-/-}$ mice. Wt, filled circles and blue colored line; Nck1$^{-/-}$, open circle and red colored line. Data are means ± SEM. n = 6-9 animals per group. * $p<0.05$.

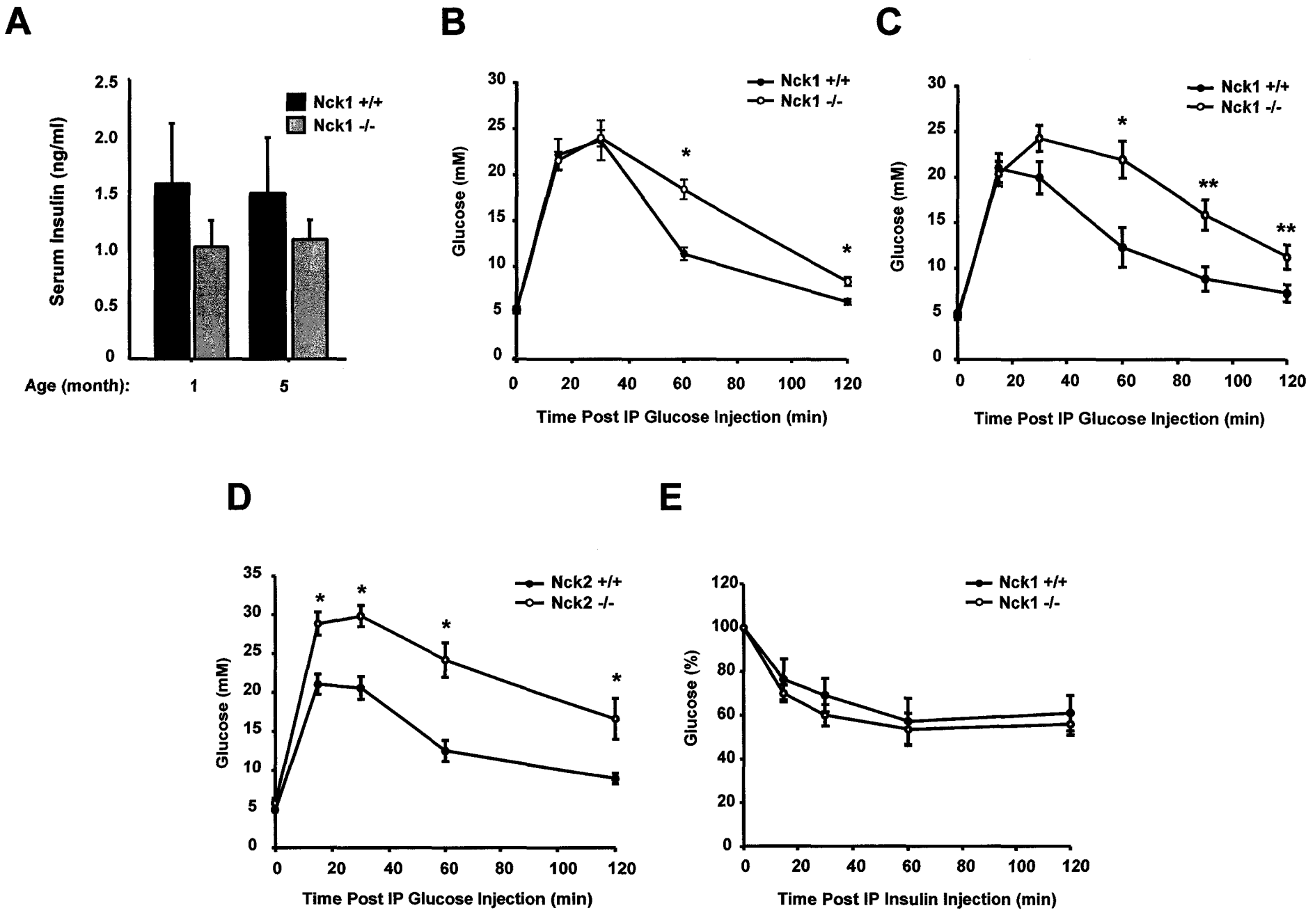
A
Serum Insulin (ng/ml)
2.5
2.0
1.5
1.0
0.5
0
Nck1 +/+
Nck1 -/-
Age (month):
1
5
B
Glucose (mM)
30
25
20
15
10
5
0
Nck1 +/+
Nck1 -/-
*
*
0
20
40
60
80
100
120
Time Post IP Glucose Injection (min)
C
Glucose (mM)
30
25
20
15
10
5
0
Nck1 +/+
Nck1 -/-
*
**
**
0
20
40
60
80
100
120
Time Post IP Glucose Injection (min)
D
Glucose (mM)
35
30
25
20
15
10
5
0
Nck2 +/+
Nck2 -/-
*
*
*
*
0
20
40
60
80
100
120
Time Post IP Glucose Injection (min)
E
Glucose (%)
120
100
80
60
40
20
0
Nck1 +/+
Nck1 -/-
0
20
40
60
80
100
120
Time Post IP Insulin Injection (min)

To delineate the mechanism responsible for impaired glucose tolerance of Nck1-deficient mice, we investigated pancreas architecture and function in $Nck1^{-/-}$ mice. We first determined Nck adaptors expression by performing immunofluorescence staining of Nck proteins on pancreatic sections. This analysis revealed that both Nck1 and Nck2 adaptors (green) are expressed within pancreatic islet of 5-month old mice, but found at very low levels in the surrounding exocrine tissue (Fig. 4A and 4B). Careful analysis of staining revealed that Nck proteins are detected in the central part of pancreatic islets, presumingly in insulin-producing β-cells, and also in glucagon-producing pancreatic α-cells (red) that surround islets (Fig. 4A and 4B). Next, we examined islet morphology and observed no apparent defect in pancreatic islets architecture in both $Nck1^{-/-}$ and $Nck2^{-/-}$ mice compared to controls (Fig. 4C, 4D and data not shown). Moreover, no sign of apoptotic cells was present in islets of either $Nck1^{-/-}$ or $Nck2^{-/-}$ animals (Fig. 5). However, quantitative morphometric analysis revealed a significant decrease in the number of pancreatic islets and β-cells area per pancreatic slides prepared from $Nck1^{-/-}$ mice compared to controls (Fig. 4E-4H). We then evaluated pancreatic β-cell function by measuring acute-phase glucose-stimulated insulin secretion in islets isolated from Wt and $Nck1^{-/-}$ mice. We found no manifest changes in normalized insulin secretion from isolated $Nck1^{-/-}$ islets in response to high glucose (16.7 mM) or KCl, a general depolarizing agent causing insulin release (Fig. 4I). Together, these results strongly suggest that the impaired glucose tolerance of $Nck1^{-/-}$ mice might be ascribed to decreased pancreatic β-cell mass.

Figure 4. Pancreatic islet morphology and insulin secretion in Nck1$^{-/-}$ mice. (A-B) Coimmunostaining for Nck1 or Nck2 and glucagon (red) of pancreatic sections from 5 month-old mice. Permeabilized, paraffin-embedded sections (5 μm) were coincubated with rabbit polyclonal anti-Nck1 (A) or -Nck2 (B) and mouse anti-glucagon antibody. Staining was revealed by fluorescein-conjugated anti-rabbit antibodies and rhodamine-conjugated anti-mouse antibodies. Images of representative fields were captured at a magnification of 10X. **(C-D)** Coimmunostaining of insulin (green) and glucagon (red) in β-cells of pancreas sections from 5 month-old Wt (C) and Nck1$^{-/-}$ (D) mice. Permeabilized, paraffin-embedded sections (5 μm) were incubated with polyclonal anti-insulin and monoclonal anti-glucagon antibodies. Staining was revealed by fluorescein-conjugated anti-rabbit and rhodamine-conjugated anti-mouse antibodies. Images of representative fields were captured at a magnification of 10X. **(E-F)** Light microscopy images of paraffin-embedded and hematoxilin/eosin stained pancreatic sections (5 μm) of Nck1$^{+/+}$ (E) and Nck1$^{-/-}$ (F) mice. Arrows indicate the emplacement of islets surrounded by the exocrine portion of the pancreas. Images of representative fields were captured at a magnification of 10X. **(G-H)** Pancreatic islet number (G) and mass (H) in Nck1$^{+/+}$ and Nck1$^{-/-}$ animals. Data are means ± SEM. n = 3 animals per group. * $p<0.05$. **(I)** Insulin secretion in isolated islets from Nck1$^{+/+}$ and Nck1$^{-/-}$ mice. Freshly isolated islets were incubated with 2.8, 16.7 mM glucose or 50 mM KCl for 1 h. The amount of insulin secreted in the media is expressed as the percentage of total insulin content of the islets measured following acid-ethanol extraction. Data are means ± SEM. n = 15 determinations in 5 independent experiments for glucose and 7 determinations in 2 separate experiments for KCl.

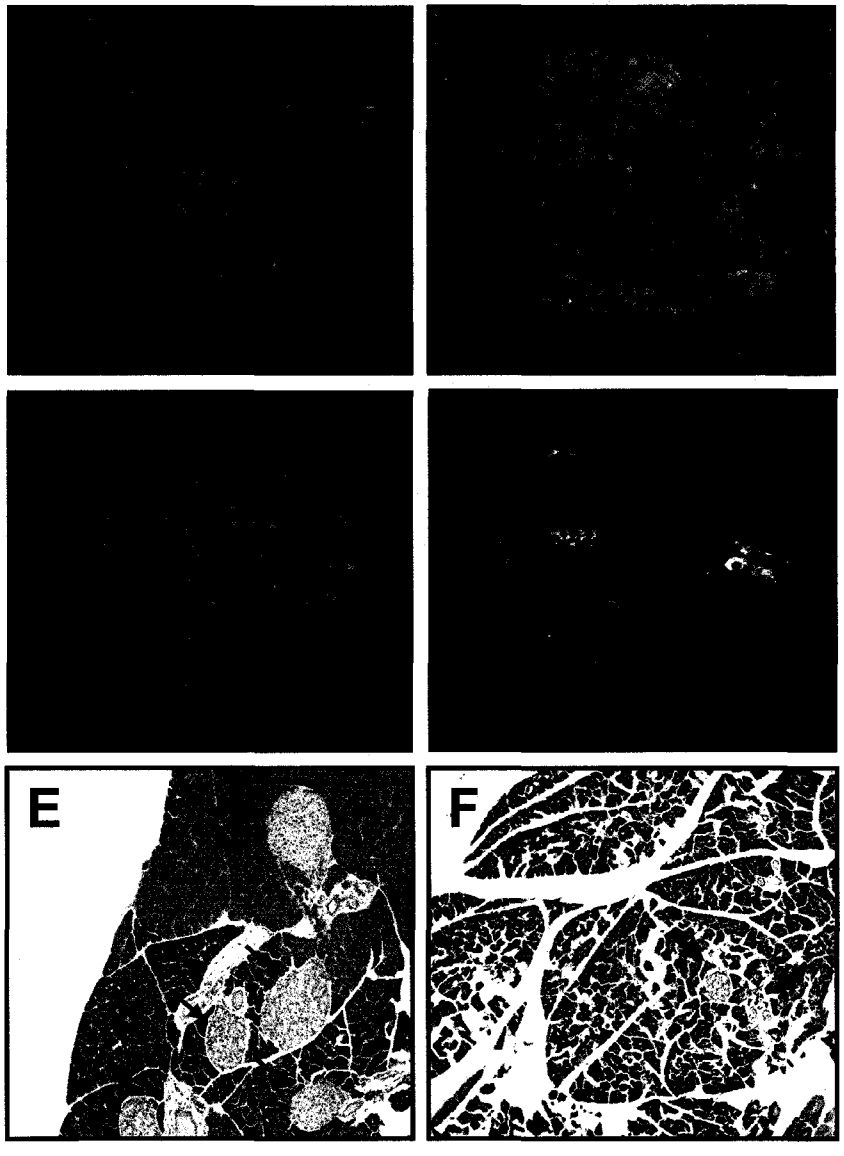
E
F

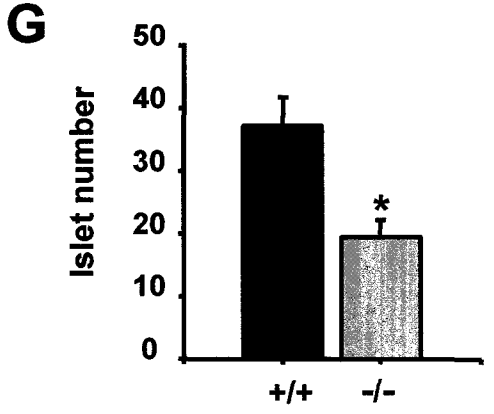
G
Islet number
50
40
30
20
10
0
*
+/+
-/-

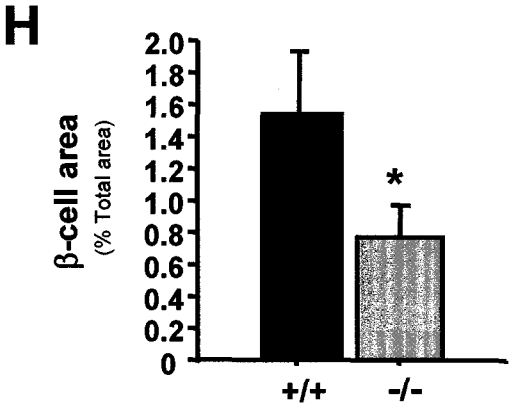
H
β-cell area
(% Total area)
2.0
1.8
1.6
1.4
1.2
1.0
0.8
0.6
0.4
0.2
0
*
+/+
-/-

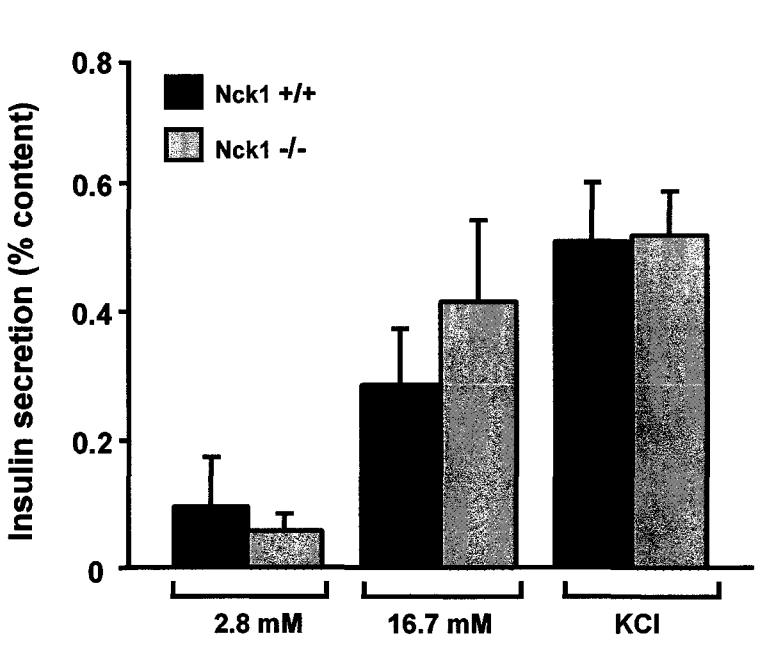
I
Insulin secretion (% content)
0.8
0.6
0.4
0.2
0
Nck1 +/+
Nck1 -/-
2.8 mM
16.7 mM
KCl

Figure 5. Apoptotic index of pancreatic islets in Nck1$^{-/-}$ mice. Apoptotic index of permeabilized, paraffin-embedded pancreas sections (5 μm) from 5 month-old wild type (Wt) mice that were mock (C-) treated (**A-D**) or pretreated with DNAse I (C+) (**E-H**) as a positive control for the TUNEL assay. (**I-L**) Nck1$^{-/-}$ and (**M-P**) Nck2$^{-/-}$ mice pancreatic sections were also subjected to TUNEL staining. TUNEL-positive apoptotic cells (green) within insulin-positive islets (red) were visualized by fluorescence microscopy using TUNEL labeling (see M& M). Nuclei (blue) were revealed by DAPI staining. Merge of TUNEL, β-cells and nuclei is shown on the right.

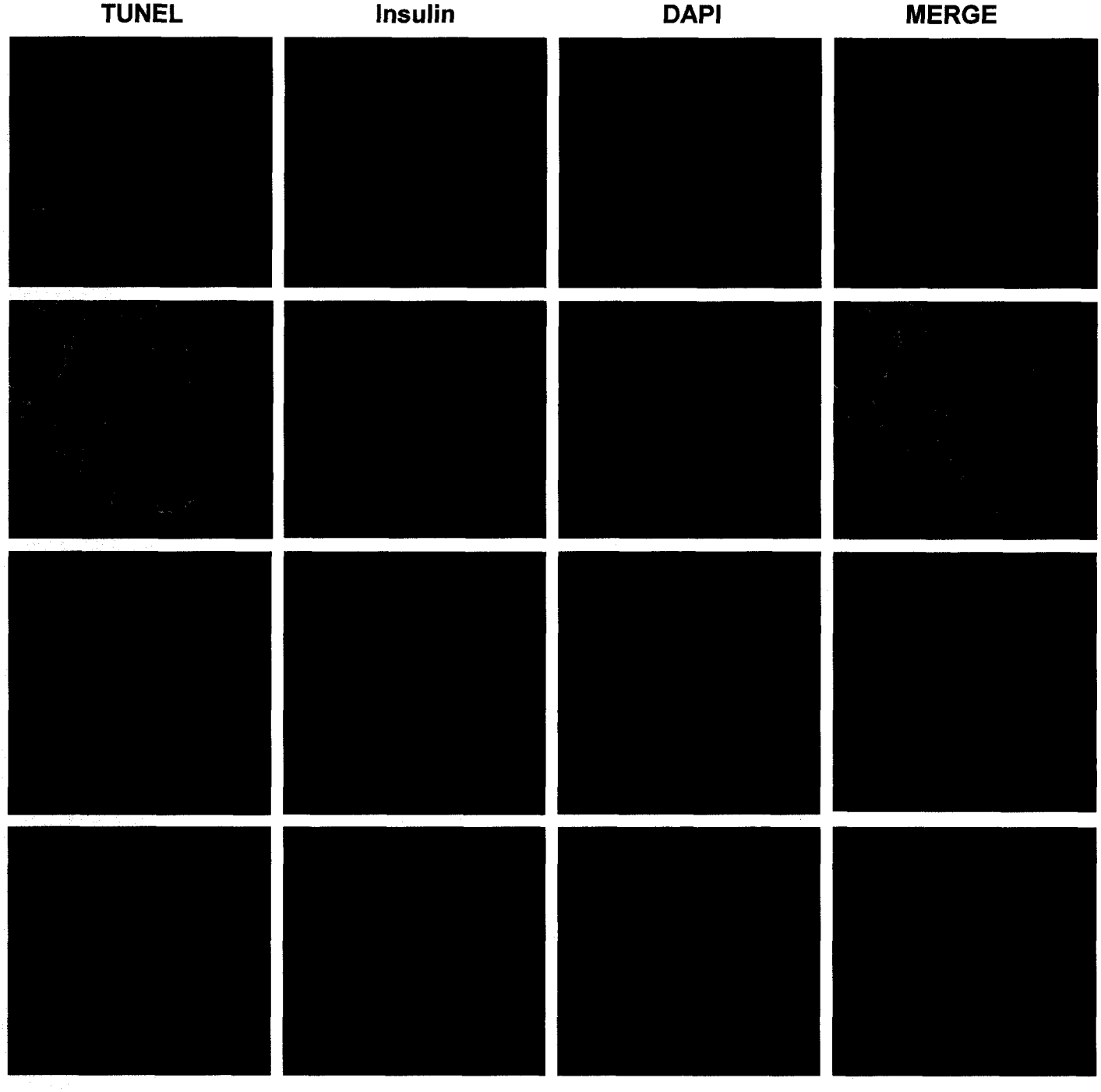
TUNEL
Insulin
DAPI
MERGE

Recent studies revealed that the metabolic stress associated with obesity perturbs the ER environment and leads to the activation of PERK and IRE1 signaling pathways (311). Obesity-induced IRE1 activation was found to converge on JNK activation, which contributes at establishing peripheral insulin resistance via IRS-1 Ser307 phosphorylation (311). Since Nck adaptors are implicated in both PERK and IRE1 signaling pathways, we hypothesized that Nck1$^{-/-}$ mice would be protected against obesity-induced ER stress and insulin resistance. To analyze this, we maintained a cohort of Wt and Nck1$^{-/-}$ littermate male mice under high fat diet (HFD) for 18 weeks. We observed that both Wt and mutant mice gained significantly more weight than mice kept on chow diet (CD) (Fig. 6A). In contrast, no difference was seen in the body weight of Wt and Nck1$^{-/-}$ mice kept on HFD (Fig. 6A). Moreover, Wt and Nck1$^{-/-}$ mice showed comparable hyperinsulinaemia at 18 weeks on HFD (Fig. 6B), suggesting that Wt and Nck1$^{-/-}$ mice counteracted the obesity-induced insulin resistance by similarly increasing insulin biosynthesis and secretion in pancreatic β-cells. Likewise, fed blood glucose concentration was not different between the two groups of mice, but interestingly, Nck1$^{-/-}$ mice displayed significantly lower blood glucose levels after 5 h and 18 h of fasting (Fig. 6C). This suggests that Nck1$^{-/-}$ mice may experience defective hepatic gluconeogenesis in fasting periods, or alternatively, these mice dispose glucose more efficiently. The ability of mice maintained on HFD to manage glucose was then directly assessed by performing GTT. Interestingly, HFD Nck1$^{-/-}$ mice showed markedly improved glucose clearance rates compared to Wt (Fig. 6D). Serum insulin levels of HFD Wt and Nck1$^{-/-}$ mice were not significantly different during a separate glucose tolerance test, indicating that the increased glucose clearance in Nck1$^{-/-}$ mice does not result from enhanced insulin secretion (data no shown). When insulin sensitivity was determined, we noticed that Nck1$^{-/-}$ mice kept on HFD showed slightly better insulin sensitivity as compared to Wt (Fig. 6E). Overall, these results suggest that the improved glucose tolerance of obese Nck1$^{-/-}$ mice is mainly due to an increase in the sensitivity of peripheral tissues to insulin actions.

Figure 6. Glucose disposal and insulin sensitivity in obese Nck1$^{-/-}$ mice. (A) Body weight gain of one-month old Nck1$^{+/+}$ and Nck1$^{-/-}$ male littermate mice maintained on high fat diet (HFD) for 18 weeks. Body weight gain of Nck1$^{+/+}$ and Nck1$^{-/-}$ mice maintained on normal chow diet (CD) is replotted for comparison. Data are means ± SEM. CD: n = 9-10 mice per group. CD vs. HFD $p<0.001$ for both Nck1$^{+/+}$ and Nck1$^{-/-}$ **(B)** Fed insulin levels in Nck1$^{+/+}$ and Nck1$^{-/-}$ mice at 1 month of age before HFD (W0) and after 18 weeks on HFD (W18). Data are means ± SEM. n = 6-9 animals in each group. **(C)** Blood glucose levels in Nck1$^{+/+}$ and Nck1$^{-/-}$ mice maintained on HFD (15-16 weeks) after a 5 h fast or overnight (O/N) fast period. Data are means ± SEM. n = 7-8 mice per group. * $p <0.05$. **(D)** Glucose tolerance tests (GTTs) were performed following intraperitoneal injection with D-glucose (1 kg/kg body weight) on Nck1$^{+/+}$ and Nck1$^{-/-}$ fasted mice kept on HFD for 18 weeks. Nck1$^{+/+}$, filled circles green colored line; Nck1$^{-/-}$, open circle orange colored line. Data are means ± SEM. n = 6-7 animals per group. * $p<0.05$, ** $p<0.001$ **(E)** Insulin tolerance tests (ITTs) were performed following intraperitoneal injection with insulin (0.75 U/kg body weight) in Nck1$^{+/+}$ and Nck1$^{-/-}$ fasted mice maintained on HFD for 18 weeks. Nck1$^{+/+}$, filled circles green colored line; Nck1$^{-/-}$, open circle orange colored line. Data are means ± SEM. n = 7-8 animals per group.

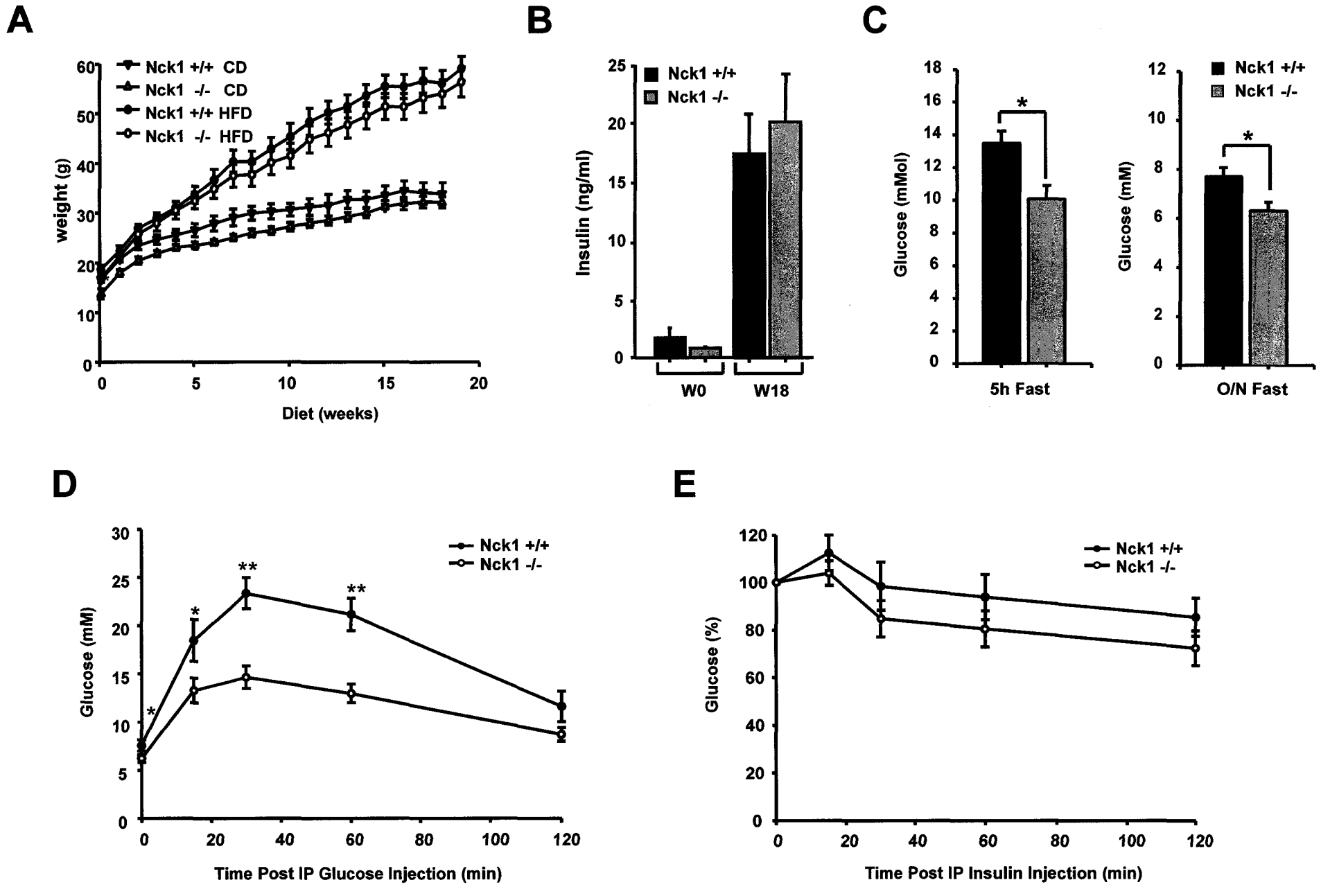
A
Nck1 +/+ CD
Nck1 -/- CD
Nck1 +/+ HFD
Nck1 -/- HFD
weight (g)
Diet (weeks)
B
Nck1 +/+
Nck1 -/-
Insulin (ng/ml)
W0
W18
C
Glucose (mMol)
5h Fast
Glucose (mM)
O/N Fast
D
Glucose (mM)
Time Post IP Glucose Injection (min)
E
Glucose (%)
Time Post IP Insulin Injection (min)

Obesity-induced ER stress signaling was found to impact considerably on the insulin sensitivity of liver and adipose tissues in mice (311). Based on improved glucose tolerance and insulin sensitivity in Nck1$^{-/-}$ mice and the function of Nck adaptors in ER stress signaling, we decided to investigate the relation between ER stress and insulin receptor (IR) signaling in Nck1$^{-/-}$ mice. In agreement with previous studies, we found that HFD induces ER stress in liver and adipose tissue of Wt mice as revealed higher levels of PERK activation, eIF2α Ser51 phosphorylation and ATF4 (Fig. 7A and data not shown). Interestingly, we measured a marked decrease (45%) in the levels of eIF2α Ser51 phosphorylation in liver of Nck1$^{-/-}$ mice maintained on HFD compared to Wt, despite the fact that PERK appears to be activated (based on its mobility on SDS-PAGE) to the same extent in both cohort of mice (Fig. 7A and 7B). Similar results were also obtained in the adipose tissue (data not shown). These results support our previous observations indicating that Nck adaptors are required for PERK-mediated eIF2α phosphorylation in ER stress conditions (see chapter III). In contrast, we did not discerned significant changes in the levels of eIF2α phosphorylation between Wt and Nck1$^{-/-}$ mice kept on CD (Fig. 7A and data now shown). This suggests that Nck adaptors play a role in the regulation of eIF2α phosphorylation in acute ER stress conditions, but not in normal physiological circumstances.

We then addressed IRE1-mediated activation of JNK in animals maintained on HFD. Our observations reveal that JNK activation was greater in mice kept on HFD compared to CD, but this was decreased by 47% in liver of obese Nck1$^{-/-}$ mice (Fig. 7A and 7B). This suggests that the IRE1 signaling branch of the UPR is also impaired in Nck1$^{-/-}$ mice. Intriguingly, we noticed higher expression of IRS-1 in Nck1$^{-/-}$ kept on HFD. Consequently, this resulted in decreased normalized IRS-1 Ser307 phosphorylation levels as compared to Wt (Fig. 7A and 7B). Finally, we studied *in vivo* insulin signaling in obese Nck1$^{-/-}$ mice. We noticed that insulin injection induced greater increase in AKT Ser308 phosphorylation in liver and adipose tissue of obese Nck1$^{-/-}$ mice compared to Wt, despite the fact that levels of IR tyrosine phosphorylation was slightly decreased in mutant animals (Fig. 7C and 7D). Taken together, these results demonstrate that Nck1$^{-/-}$ mice display improved IR signaling, insulin sensitivity and glucose tolerance due to decreased obesity-induced ER stress in liver and adipose tissues.

Figure 7. ER stress and IR signaling in obese Nck1$^{-/-}$ mice. (A) Immunoblotting for ER stress markers on liver samples prepared from mice kept on normal chow diet (CD) or high fat diet (HFD) for 18 weeks. Shown are results obtained with Nck1$^{+/+}$ and Nck1$^{-/-}$ mouse maintained on CD and three Nck1$^{+/+}$ and Nck1$^{-/-}$ mice maintained on HFD. Liver homogenates were subjected to immunoblotting assay using indicated antibodies. Nck immunoblotting was obtained using a pan-Nck antibody **(B)** The histogram represents a quantitative analysis of results presented in (A). A.U.: Arbitrary units Data are means ± SEM. n = 3 mice per group. * $p < 0.05$. **(C)** Insulin-stimulated IR signaling in liver and fat of Nck1$^{+/+}$ and Nck1$^{-/-}$ mice maintained on HFD. Shown are results obtained with one control Wt mice kept on CD, and two Nck1$^{+/+}$ and three Nck1$^{-/-}$ mice maintained on HFD. Tissue homogenates were subjected to immunoblotting with indicated antibodies. Nck immunoblotting was obtained using a pan-Nck antibody **(D)** The histogram represents a quantitative analysis of results presented in (C). A.U.: Arbitrary units. Data are means ± SEM. n = 1-3 mice per group from 3 independent analysis.

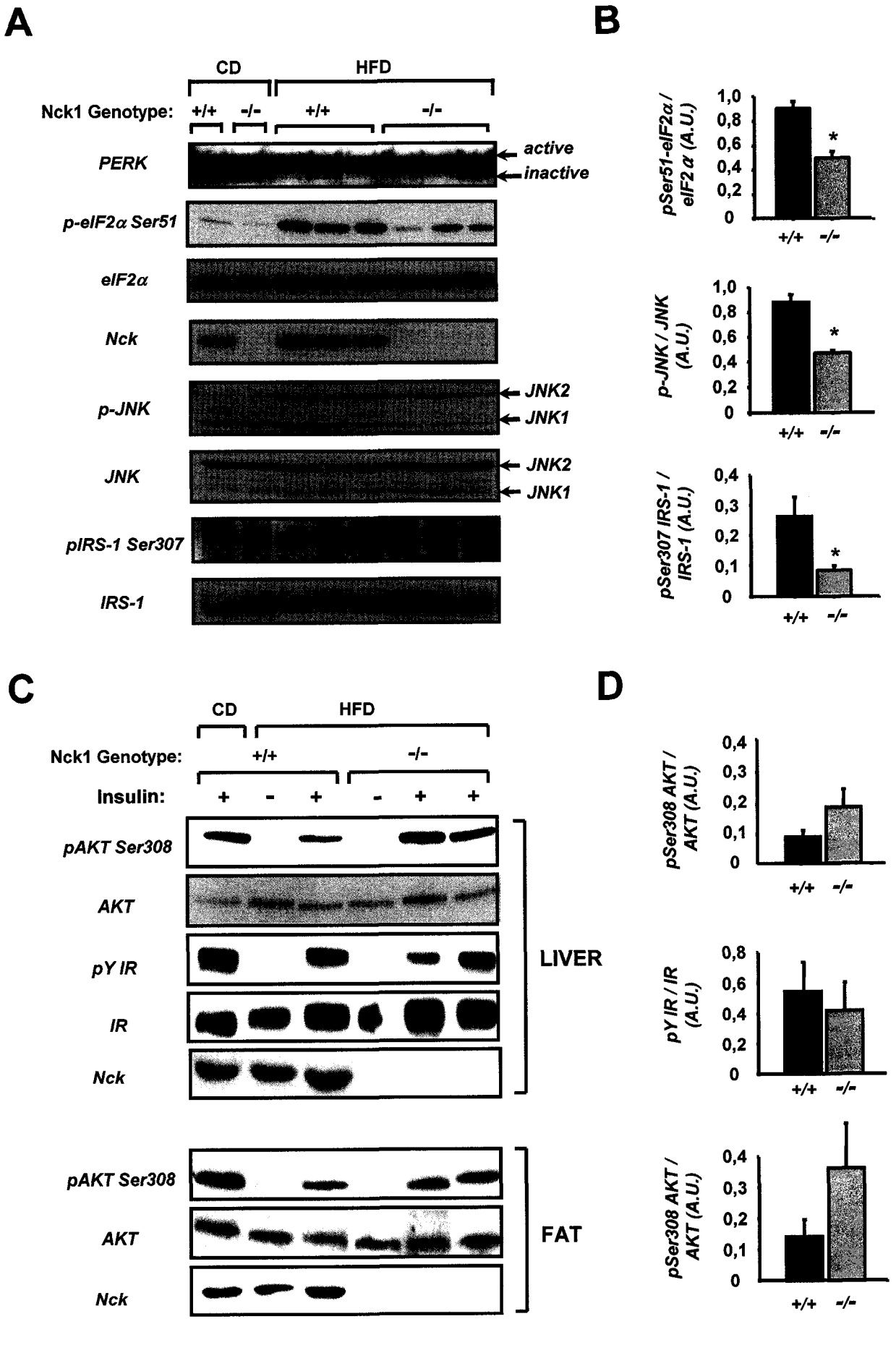
A
CD
HFD
Nck1 Genotype:
+/+
-/-
+/+
-/-
PERK
active
inactive
p-eIF2α Ser51
eIF2α
Nck
p-JNK
JNK2
JNK1
JNK
JNK2
JNK1
pIRS-1 Ser307
IRS-1
B
pSer51-eIF2α / eIF2α (A.U.)
1,0
0,8
0,6
0,4
0,2
0
*
+/+
-/-
p-JNK / JNK (A.U.)
1,0
0,8
0,6
0,4
0,2
0
*
+/+
-/-
pSer307 IRS-1 / IRS-1 (A.U.)
0,4
0,3
0,2
0,1
0
*
+/+
-/-
C
CD
HFD
Nck1 Genotype:
+/+
-/-
Insulin:
+
-
+
-
+
+
pAKT Ser308
AKT
pY IR
IR
Nck
LIVER
pAKT Ser308
AKT
Nck
FAT
D
pSer308 AKT / AKT (A.U.)
0,4
0,3
0,2
0,1
0
+/+
-/-
pY IR / IR (A.U.)
0,8
0,6
0,4
0,2
0
+/+
-/-
pSer308 AKT / AKT (A.U.)
0,4
0,3
0,2
0,1
0
+/+
-/-

DISCUSSION

Ever since the identification of the first mammalian Nck gene (Nck1), tremendous efforts have been put together to identify effectors interacting with Nck SH2 and SH3 domains. In contrast, investigation of Nck physiological functions in mammals is still at its early steps and mainly driven by the generation of mouse with targeted disruption of *nck1* and *nck2* genes (25, 182). In the present study, we provide important piece of information uncovering a role of Nck adaptors in the regulation of glucose homeostasis.

Back in the mid 90's, two reports demonstrated a potential relation between Nck expression levels and diabetes. It was observed that Nck1 expression is significantly decreased in liver of streptozotocin-treated diabetic mice (31), while being strikingly elevated in fat, but not in liver of obese insulin resistant KKA^y mice (32). Here we show that Nck adaptors are important regulators of whole-body glucose homeostasis in mice. On normal chow diet, $Nck1^{-/-}$ and $Nck2^{-/-}$ mice maintain normal fasting and fed glucose, but display glucose intolerance in response to a glucose load. Examination of pancreatic islet morphology and glucose-stimulated insulin release showed virtually no difference between Wt and $Nck1^{-/-}$ mice. Conversely, $Nck1^{-/-}$ mice display significant decreased pancreatic β-cell mass, thus suggesting that this could underly the glucose intolerance of these animals.

During pancreatic organogenesis, endocrine β-cells are generated from a population of pancreatic progenitor cells that eventually differentiate by exiting cell cycle (mitotic quiescence) (94). The early postnatal period is characterized by a massive expansion of the β-cell mass allowing adaptation to metabolic needs. Although major gaps in our knowledge of β-cell development still persist, experiments across several organisms have shown that the number of β-cells during this period is primarily governed by β-cell self-duplication rather than stem cell differentiation (85). Conversely, β-cell replication is counteracted by cell death (apoptosis), thereby establishing the absolute amount of β-cells within pancreatic islets. The cyclin D2 and p27 cell cycle regulators were found to play important role in determining β-cell mass in mice. Neonate cyclin $D2^{-/-}$ mice display dramatically smaller islets and a reduction in β-cell mass, while $p27^{-/-}$ mice exhibit a significant increase in β-cell mass in comparison to Wt littermates

(117, 118). On the other hand, the signals that regulate β-cell differentiation and mass in adulthood remain to be fully defined.

We have observed that Nck1$^{-/-}$ mice show low β-cell mass correlating with marked glucose intolerance. Conversely, no sign of apoptosis was noticed in Nck1$^{-/-}$ mice, pointing to a reduction of β-cell proliferation in these mice. The exact mechanism underlying this low β-cell mass in Nck1-deficient mice still needs further analysis. Interestingly, neonatal PERK-deficient mice display decreased β-cell mass due to a reduction in proliferation rates as assessed by BrdU incorporation and staining for the proliferation marker Ki97 (473). We reported that Nck adaptors interact with PERK and are required for PERK-mediated eIF2α phosphorylation in ER stress conditions (see Chapter II and III). Therefore, it worth evaluating pancreatic β-cell proliferation in Nck1$^{-/-}$ mice (during embryogenesis and adulthood) to get a glimpse at molecular defects underlying the reduced β-cell mass found in these mice. Conversely, we did not notice any defect in glucose-stimulated insulin secretion in pancreatic islets isolated from Nck1$^{-/-}$ mice. In agreement with this, we did not detect any sign of ER stress in pancreatic samples from Nck1$^{-/-}$ mice maintained on CD diet (data not shown). Based on the critical role of PERK and eIF2α phosphorylation in pancreatic β-cell homeostasis, it will be important to address whether Nck deficiency impairs pancreatic β-cell function in obese animals where insulin resistance increases the demand of insulin biosynthesis and secretion (366, 473),.

IRE1 has been linked with glucose homeostasis and insulin resistance through its ability to induce JNK-mediated IRS-1 Ser307 phosphorylation in obese mice (311). Since we previously demonstrated that IRE1 signaling is regulated by Nck adaptors (289), we investigated glucose homeostasis of Nck1$^{-/-}$ mice maintained on HFD. We found that Nck1$^{-/-}$ mice are protected from the development of obesity-induced-insulin resistance even though these mice gained as much weight as controls littermates (Fig 5). Obese Nck1$^{-/-}$ mice show improved glucose tolerance due to improved insulin sensitivity in liver and adipose tissues compare to Wt. Importantly, Wt and Nck1$^{-/-}$ mice show comparable insulin levels on week 4, 9, 12 and 18 on HFD, suggesting that the improved insulin sensitivity in obese Nck1$^{-/-}$ mice is not due to a compensatory increase in insulin release by the pancreas. Unfortunately, we could not compare the glucose tolerance in Nck1$^{-/-}$ mice maintained on HFD and CD since these two groups of mice

were challenged with different amount of glucose due to the profound insulin resistance of obese Wt mice. Whether adipocyte-derived free fatty acids (FFAs) levels are changed in Nck1$^{-/-}$ mice still remains to be investigated, as this is an important factor modulating glucose disposal in mice. However, Nck1$^{-/-}$ mice maintained on HFD did not show changes in hepatic steatosis (fatty liver) as compared to Wt mice (data not shown), suggesting that circulating levels of FFAs are comparable in both animals.

The present study investigating glucose homeostasis in obese Nck1$^{-/-}$ mice allowed us to demonstrate a physiological role for Nck1 at the ER. We confirmed that mice kept on HFD display signs of ER stress in liver and adipose tissues as reflected by increased PERK activation, eIF2α Ser51 phosphorylation, JNK activation and ATF4 levels (Fig. 7 and data not shown). However, the levels of eIF2α phosphorylation were drastically decreased in Nck1$^{-/-}$ mice as compare to Wt mice maintained on HFD. These results confirm our cell culture observations and demonstrate that Nck adaptors are required to transduce signals from PERK in ER stress conditions *in vivo*. Furthermore, our data substantiated that obesity-induced ER stress leads to IRE1-mediated JNK activation and phosphorylation of IRS-1 on Ser307. We established the implication of Nck in IRE1-mediated signaling by reporting that the levels of IRE1-mediated JNK phosphorylation in obese Nck1$^{-/-}$ mice are significantly reduced as compared to Wt (Fig. 7). The exact mechanism by which IRS-1 Ser307 phosphorylation inhibits IR signaling is not totally understood. Some reports show that this blocks IRS-1 recruitment and tyrosine phosphorylation by the IR, while others suggest that IRS-1 Ser307 phosphorylation induces IRS-1 degradation via the ubiquitin-dependent proteasomal pathway (124, 146, 469). Intriguingly, we found higher amounts of IRS-1 in liver of Nck1$^{-/-}$ mice maintained on HFD as compared to Wt, suggesting that Nck1 could be involved in an IR signaling negative feedback mechanism promoting IRS-1 degradation in conditions of nutrient saturation. Importantly, this may have contributed to preserve the sensitivity of obese Nck1$^{-/-}$ mice to insulin. When normalized levels of phospho-IRS-1 Ser307 are measured (phospho-IRS-1 Ser307/total IRS-1), we found over 50% reduction in IRS-1 Ser307 phosphorylation in liver of obese Nck1$^{-/-}$ mice as compared to obese Wt mice (Fig. 7). This correlates with increased levels of insulin-stimulated AKT Ser308 phosphorylation and preserved insulin sensitivity in obese mutant mice. Together, these results indicate that Nck adaptors impact on the IR signaling pathway via their ability to transduce signal from the ER.

However, Nck could also transduce signals from the IR itself and improve signaling to AKT. In fact, Song *et al.* reported that Dock, the Nck orthologue in *Drosophila,* interacts with the insulin receptor (DInR) *in vitro* and *in vivo* (383). Furthermore, Nck1 was found to associate with IRS-1 and IRS-3 (228, 415, 453). Although intense efforts have been put together in our laboratory to try to confirm these findings, we were not able to demonstrate any interaction between Nck and either the IR or IRS proteins (data not shown), suggesting that these might exist only in a subset of insulin responsive tissues. Further work will be required to determine if Nck adaptors regulate insulin sensitivity by being integral components of the IR signaling cascade itself in addition to their function at the ER.

In the past years, the role of ER stress in dietary and genetic models of insulin resistance attracted a lot of attention from the scientific community. The ER stress sensor protein IRE1 was found to transduce inhibitory signals toward the IR via JNK activation (311). However, a link between the translational arm of the UPR and insulin signaling still needs to be demonstrated. TRB3, the mammalian homologue of *Drosophila melanogaster tribble*, was recently characterized as a novel AKT inhibitor protein (87). TRB3 is induced in db/db diabetic mice and its expression promotes hyperglycemia and glucose intolerance in normal mice (87). Furthermore, PPAR γ coactivator-1 (PGC-1) promotes liver insulin resistance through TRB3 upregulation, while hepatic TRB3 knockdown improves glucose tolerance in mice (87, 212). Interestingly, TRB3 gene is also induced in response to ER stress via the PERK-eIF2α-ATF4-CHOP pathway (300), suggesting that PERK activation could negatively regulate the IR signaling pathway through TRB3-mediated AKT inactivation. Based on this reasoning, the marked reduction in eIF2α phosphorylation levels in liver of $Nck1^{-/-}$ mice maintained on high fat diet could result in decreased TRB3 levels. Consequently, this could explain the improved AKT activation and insulin sensitivity in obese $Nck1^{-/-}$ mice. It worth measuring TRB3 levels in $Nck1^{-/-}$ mice to gain more evidence on the role of PERK signaling pathway in obesity and insulin resistance.

Finally, one striking observation made during the course of these experiments is the significant lower blood glucose levels in fasted obese $Nck^{-/-}$ mice (Fig. 5). In fasting periods, glycaemia is maintained through breakdown of glycogen stores (glycogenolysis) and *de novo*

synthesis of glucose (gluconeogenesis) by the liver. Gluconeogenesis is mainly regulated by the transcriptional induction of neoglucogenic enzymes such as phosphoenolpyruvate carboxykinase (PEPCK) or glucose-6-phosphatase (G-6-P). These are induced by glucocorticoids and glucagon in fasting periods, while being repressed by insulin in feeding periods (356). Mice deficient in factors that regulate the neoglucogenic pathway (i.e. PEPCK) exhibit fasting hypoglycemia and improved glucose tolerance (123, 339, 376). In contrast, murine models of insulin resistance and diabetes show increased hepatic glucose output (275). Based on these data, it is possible that Nck1 plays a role in relaying signals increasing transcription of neoglucogenic enzymes. In fact, neonate homozygote $eIF2\alpha^{S51A/S51A}$ mice display lethal hypoglycemia and die soon after birth due to marked reduction in PEPCK activity and impaired gluconeogenesis (365). Therefore, fasting levels and activity of neoglucogenic enzymes in Wt and $Nck1^{-/-}$ mice should be determined in conjunction with the hepatic glycogen content of these mice. Preliminary results indicate that hepatic glycogen content is not different in fed Wt and $Nck1^{-/-}$ mice (data not shown). However, these analyses should also be performed in fasting conditions given that breakdown of glycogen stores often occurs as a compensatory response to defective gluconeogenesis (356). Similarly, analysis of hepatic glucose production using hyperinsulinemic-euglycemic clamp studies should also be envisaged to determine whether this process is altered and modulates glucose homeostasis in $Nck1^{-/-}$ mice.

Overall, we provide strong evidence for a role of Nck adaptor proteins in glucose homeostasis in mice. Analysis of the role of Nck adaptors *in vivo* is complicated by the fact that these adaptors functionally compensate for each other in several signaling pathways (25). We believe that mice with a single allele of either Nck1 or Nck2 ($Nck1^{+/-}Nck2^{-/-}$ and $Nck1^{-/-}Nck2^{+/-}$) or tissues specific inactivation of both Nck1 and Nck2 gene might result in more pronounced effects on glucose metabolism. Studying these knockouts mice should help clarify the mechanism(s) by which Nck adaptor proteins regulate glucose homeostasis.

ACKNOWLEDGMENTS

We thank Dr. T. Pawson for providing the $Nck1^{-/-}$ and $Nck2^{-/-}$ mice. We thank Dr. K. Robinson for help with immunostainings and Dr. M. L. Peyot for help in pancreatic islet isolation and stimulation and insulin secretion experiments. This work was supported by a grant to L.L. in honor of the late Lilian I. Dale from the Canadian Diabetes Association. M.L. was supported by a studentship from the McGill University Hospital Center (MUHC) Research Institute. L.L. is Chercheur National of the Fond de la Recherche en Santé du Québec (FRSQ).

CHAPTER V

General Discussion and Future Perspectives

Significant advances have been made during the past years in identifying and characterizing components of cell signaling cascades involved in increasing the folding and secretory function of the ER in situation of high demands of secretory protein synthesis or ER stress. In this regard, it was found that activation of the PERK signaling cascade converges on the phosphorylation of eIF2α on Ser51 and mediates the transient global translation attenuation associated with the Unfolded Protein Response (UPR) (142). Moreover, phosphorylation of eIF2α triggers reprogramming of cellular gene expression in part through the upregulation of the stress-regulated transcription factor ATF4 that governs the transcription of genes involved in amino acids synthesis and resistance to oxidative stress (137, 143). However, limited information is available on PERK substrates/effectors and regulatory mechanisms controlling the amplitude and temporal activation of the PERK signaling pathway. Given that numerous pathological states have now been linked with deregulated PERK signaling, it is imperative to address these queries in order to understand how this signaling cascade is orchestrated and regulated in cells encountering ER stress.

In 2002, our laboratory uncovered that Nck SH2/SH3 domain-containing adaptor proteins which are involved in transducing signals from RTKs at the plasma membrane to cytoskeleton dynamics also modulate translation rates in cells (198). The first hint that Nck adaptors play a role in mRNA translation came with the finding that the translation initiation factor eIF2β interacts with Nck1 via its SH3 domains (198). Subsequently, it was found that overexpression of Nck1 prevents the phosphorylation of eIF2α on Ser51 and attenuation of translation in response to ER stress (197). Initially, this was correlated with decreased activation of PERK as revealed by decreased levels of Thr980 phosphorylation in the activation loop of the protein kinase (197). Together, these results strongly suggested that Nck would modulate the Integrated Stress Response (ISR) associated with the phosphorylation of eIF2α in response to ER stress, although this still needed to be firmly demonstrated. To investigate this, I overexpressed Nck adaptors in cells and found that this blunted induction of ATF4 and CHOP upon treatment with ER stress agents (Chapter II). In accordance with this, we observed that exposure of $Nck1^{-/-}$ $Nck2^{-/-}$ MEFs to ER stress agents resulted in the premature induction of eIF2α phosphorylation-dependent effectors such as ATF4, GADD34, and CHOP (Chapter II). Importantly, I demonstrated that Nck is part of a CReP/PP1c-containing eIF2α holophosphatase complex that

negatively regulates the phosphorylation of eIF2α and induction of the ISR (184). Together, these results strongly supported the concept that Nck adaptors are negative regulators of the ISR in cells encountering damage to the ER environment through their ability to promote CReP/PP1c-mediated eIF2α dephosphorylation.

Although such reasoning was a logical extension of our previous findings, I subsequently made observations suggesting that this model might not represent exactly how Nck adaptors regulate the phosphorylation of eIF2α and ISR. First, I noticed that when the levels of eIF2α proteins in Wt and $Nck1^{-/-}Nck2^{-/-}$ MEFs are compared side-by-side on a single SDS-PAGE, mutant MEFs displayed significant higher levels of eIF2α as compared to controls (data not shown). This insinuated that the increased eIF2α phosphorylation-dependent signaling observed in these mutant MEFs could have been caused by adaptive remodeling of eIF2α gene expression secondary to Nck gene inactivation. In accordance with this hypothesis, I observed that the overexpression of eIF2α in cells increased basal and ER stress-induced eIF2α phosphorylation and ISR signaling (data not shown). Therefore, these observations suggested that the higher levels of eIF2 phosphorylation found in $Nck1^{-/-}Nck2^{-/-}$ MEFs might not be directly linked with the inactivation of Nck genes, but rather a consequence of the inactivation of Nck genes. Hence, I began to believe that the genetic adaptation of $Nck1^{-/-}Nck2^{-/-}$ MEFs might prevent us from appreciating the true function of Nck adaptors in the PERK signaling pathway. Actually, this situation is not unique to $Nck1^{-/-}Nck2^{-/-}$ MEFs, since MEFs isolated from knockout mice of various players of the UPR also show secondary genetic adaptations that completely alter the behavior of cells (Dr. R.J. Kaufman, personal communication). Having this in mind, I believed that the function of Nck in PERK-mediated eIF2α phosphorylation and mRNA translation needed to be reevaluated by different approaches. Coincidentally, the RNAi approach emerged as a powerful tool for dissecting components and flow of signaling pathways in cells. I taught that such approach might lead to a better understanding of the role of Nck in PERK signaling due to very limited off-target effects associated with RNAi. Surprisingly, I found that depletion of Nck1 or Nck2 by RNAi resulted in decreased levels of eIF2α phosphorylation and ISR activation as compared to controls (Chapter III), thus suggesting that unlike initially conceptualized, Nck adaptors are in fact positive regulators of PERK-mediated eIF2α phosphorylation in ER-stressed cells. Subsequently, I uncovered a direct interaction between Nck and the catalytically active

PERK kinase (Chapter III). Mutation of Tyr561 in the PERK juxtamembrane domain (JM) domain abolished Nck binding, thus shedding light on the molecular basis of this interaction. Finally, I provided strong evidence demonstrating that obese Nck1$^{-/-}$ mice display marked decrease in levels of eIF2α phosphorylation (liver and adipose tissue) as compared to obese Wt mice (Chapter IV). Together, these results strongly suggested that Nck adaptors are required for efficient phosphorylation of eIF2α in ER-stressed cells.

In such circumstances, these results indicate that overexpression of proteins may not be an appropriate approach to study the function of adaptor proteins in cultured cells. As highlighted in several studies, the research methodology used to investigate the biology of adaptor proteins needs to be accurately selected since different approaches lead to different conclusions on adaptor function (165, 431). Overexpression of one or more signaling components often disrupts the physiological stoichiometry of cellular protein complexes and may disrupt protein–protein interactions or even favor others that might not occur under normal circumstances. In such context, interpretation of data derived from function experiments may represent a very complex assignment. For example, overexpression of Grb10 has been shown to inhibit or stimulate insulin/IGF-I signaling depending on the expression levels of the specific isoforms, specific cell context, and/or physiologic endpoint (243). As emphasized by numerous groups, the specific contribution of Grb10 in a signaling complex may depend on the local stochiometric balance of associating mediators, including the ratio of competing signaling proteins (341). In this context a constant cellular level of Grb10 may enhance or restrain a specific signaling mechanism depending on the local distribution and balance of specific Grb10 signaling partners. This concept is compatible with the diverse experimental observations on Grb10 function and emphasizes the importance of the specific cellular context to define the consequences of local changes in Grb10 distribution (341). Based on this, it is possible that the overexpression of Nck (5-10 folds endogenous levels - Chapter II) lead to titration of components of the eIF2 complex preventing PERK from phosphorylating eIF2α and attenuating mRNA translation. Simultaneously, this could have inadvertently impacted on the activation state of PERK and reduced PERK Thr980 phosphorylation (197). One would predict that the overexpression of Nck might also disrupt effectors stoichiometry in other signaling cascades where Nck normally participates. On the other hand, selective RNAi-mediated depletion of Nck1

may also have instituted complex changes in gene expression that inadvertently altered the response of cells of ER stress. Thus, thinking of Nck adaptors as either a positive or negative mediators of signaling cascades such as the eIF2α signaling pathway will be inadequate in reflecting the complexity that underlies the final output of the Nck signal in overexpression and RNAi-mediated depletion experiments.

In Chapter II, I modeled Nck as a component of a CReP/PP1c molecular complex that dephosphorylates eIF2α. On the other hand, in Chapter III and IV, I depicted Nck as a factor required for optimal phosphorylation of eIF2α. At first glance, these concepts could to contradict each other. However, I have come up with a model that integrates data previously obtained in the laboratory and those presented in this thesis. In unstressed cells, a certain amount of Nck protein is found within the CReP/PP1c holophosphatase complex via an SH3-dependent interaction with eIF2β. This molecular complex allows ongoing mRNA translation by contributing to the dephosphorylation of eIF2α on Ser51. In response to ER stress, this molecular complex is targeted to PERK via engagement of the Nck SH2 domain with the phosphorylated Tyr561 residue in PERK JM domain, thereby promoting the phosphorylation of eIF2α on Ser51 and inhibition of mRNA translation. Subsequently, this Nck/eIF2/CReP/PP1c molecular complex is released from PERK triggering the ISR signaling cascade. Future experiments should help refine this model.

The fact that Nck adaptors interact with bacterially produced GST-PERK fusion protein in a SH2- and Tyr561-dependent manner strongly suggests that the Tyr561 residue is autophosphorylated during PERK activation (Chapter III). However, this needs to be demonstrated *in vivo,* as other cellular protein tyrosine kinases could be phosphorylating Tyr561 in the PERK JM domain in response to ER stress. Moreover, we found that replacement of Tyr561 with a non-phosphorylatable phenylalanine (F) residue increases the catalytic kinase activity of PERK both *in vitro* and *in vivo*. This suggests that phosphorylation of Tyr561 could be negatively regulating PERK activity by for example, creating a binding site for an SH2/PTB domain-containing inhibitory protein inactivating PERK catalytic activity *in vivo*. In this case, the charge added by the phosphate group at position 561 in the amino acid sequence of PERK would represent the molecular basis for the inhibition of PERK activity by the Tyr561 residue.

Alternatively, the phosphorylation of PERK on Tyr561 could be positively regulating the overall kinase activity by relieving the autoinhibitory function of the JM domain. In this case, phosphorylation would disrupt intramolecular bonding carried out by the Tyr561 hydroxyl group with residues in the cytoplasmic domain of PERK and promote PERK activation as seen in the activated form of several RTKs and type I TβRs (170). Based on this reasoning, one would expect that substitution of Tyr561 with a phenylalanine residue (Y561F) also increase PERK activity due to the absence of an hydroxyl group in this residue side chain. To discriminate between these two possibilities, one could think of replacing Tyr561 with a negatively charged glutamic acid (E) mimicking the charge brought by the phosphorylation of this tyrosine residue. In the case where phosphorylation of the Tyr561 residue negatively regulates the activity of PERK through the addition of a charged phosphate group, PERK Y561E should display decreased catalytic activity as compared to Wt *in vivo*. On the other hand, if the PERK Y561E mutant still displays as much activity as the Y561F mutant, this would indicate that phosphorylation of Tyr561 is used to displace the hydroxyl group of the tyrosine side chain and relieve the autoinhibitory function of the PERK JM domain. In such context, it is predicted that substitution of Tyr561 with any other amino acids devoid of hydroxyl group in their side chain, such as alanine or serine, should increase PERK catalytic kinase activity in an autonomous manner both *in vitro* and *in vivo*. However, we are aware that unambiguous demonstration of this will require comparative crystallographic studies of catalytically active and inactive PERK cytoplasmic tails. Dr. F. Sicheri group at the University of Toronto previously reported the X-ray crystallographic structure of the catalytic domain of PKR, the closest relative of PERK among eIF2α kinases (74, 83). Although PKR is a cytosolic kinase lacking a JM domain, this work identified important determinants involved in PKR dimerization, autophosphorylation and substrate recruitment, thus demonstrating the utility of such approach to determine the structural properties of eIF2α kinases. Such analyses should provide important information on the mechanism governing PERK activation in response to ER stress and could pave the way to the development of small-molecule inhibitors of PERK. Previous studies demonstrated that Ras^{V12}-driven tumors lacking PERK activity are substantially smaller and compromised in their ability to promote translation of mRNAs involved in angiogenesis and tumor survival (21), suggesting that PERK possesses oncogenic properties. Since I established that the substitution of Tyr561 by a non-phosphorylatable phenylalanine residue increases the catalytic activity of PERK, it would

be interesting to address the phenotype of PERK Y561F knockin mice and determine whether this PERK JM domain mutant displays greater cooperative oncogenic activity in mice.

PERK and eIF2α phosphorylation are required for β-cell function and glucose homeostasis (139, 364, 365, 472, 473). Since Nck adaptors are required for optimal phosphorylation of eIF2α in response to pharmacological inducers of ER stress, I hypothesized that viable Nck-deficient mice would display impaired glucose homeostasis. My results confirm this hypothesis since both $Nck1^{-/-}$ and $Nck2^{-/-}$ mice showed marked glucose intolerance associated with reduced pancreatic β-cell mass (Chapter IV). PERK-deficient mice exhibit severe defects in fetal/neonatal β-cell proliferation and differentiation, resulting in decreased β-cell mass as seen in $Nck1^{-/-}$ mice (473). However, preliminary results suggest that the pancreatic β-cell mass in $Nck1^{-/-}$ mice can still be expanded in situation of nutrient saturation such as in obesity, indicating that signals regulating β-cell replication are still operative in these mutant mice (data not shown). Measuring *in situ* β-cell proliferation by BrdU incorporation or staining for proliferation markers should help validate the function of Nck adaptors in the control of pancreatic β-cell mass. Conversely, we noticed that insulin serum levels in response to intraperitoneal injection of glucose are comparable in Wt and Nck1-deficient mice (data not shown), suggesting that reduced pancreatic β-cell mass of $Nck1^{-/-}$ mice is unlikely to be the sole element underlying the glycaemic dysfunction of these mutant mice. Since we demonstrated that a deficiency in Nck adaptors results in decreased levels of eIF2α phosphorylation and increased translation rates (Chapter III and IV), it is conceivable that such normalization in serum insulin levels could be compensated by increased glucose-stimulated insulin biosynthesis and secretion in $Nck1^{-/-}$ mice. Interestingly, Harding *et al.* (2001) reported increased glucose-stimulated proinsulin biosynthesis in islets isolated from $PERK^{-/-}$ mice (139), thus reinforcing this hypothesis. On the other hand and in light of the role of the PERK signaling cascade in pancreatic β-cell function, I was surprised to find normal pancreatic islet architecture and glucose-stimulated insulin release in $Nck1^{-/-}$ mice given that I found that Nck adaptors are required for PERK-mediated eIF2α phosphorylation upon ER stress. Furthermore, several effectors of Nck adaptors including Pak or NIK, and some cytoskeleton regulators of the Rho GTPases family were recently involved in the control of pancreatic β-cell insulin secretion (287, 288, 401, 439).

Deciphering the mechanism(s) underlying murine phenotype(s) can be a difficult task given that complex genetic interactions between tissues and organs are involved in regulation of glucose metabolism in whole organisms. I established that Nck1 expression is elevated in skeletal muscle and liver, while lower in adipose tissue (Chapter IV). For several years, it was taught that 70-90% of insulin-mediated glucose disposal occurred in skeletal muscle (76). However, muscle-specific inactivation of the IR in mice (MIRKO) did not result in apparent glucose intolerance (275). On the other hand, mice with targeted deletion of the IR in adipose tissue or GLUT4 in muscle display insulin resistance and glucose intolerance (1, 28), demonstrating that both skeletal muscle and adipose tissue are involved in insulin-stimulated glucose uptake in mice. $Nck1^{-/-}$ mice do not show gross defect in insulin sensitivity when assessed by ITT (Chapter IV). However, compensatory effects in different insulin-responsive tissues could mask potential tissue-specific insulin resistance as seen in particular knockout mice. Nck1-deficiency could impair glucose-uptake in skeletal muscle and concomitantly promote insulin-suppressive effects on hepatic glucose production. Together these positive and negative tissue-specific effects could normalize the overall insulin sensitivity of mice analyzed in ITT. Therefore, examining GLUT4 expression or insulin-mediated glucose uptake and metabolism (through 2-deoxy-D-[1-^{14}C]-glucose injection) in skeletal muscle and adipose tissue in $Nck1^{-/-}$ mice should provide valuable information related to the insulin sensitivity of these tissue. In addition, these studies should be supported by the assessment of hepatic glucose production in $Nck1^{-/-}$ mice using the gold standard hyperinsulinemic-euglycemic clamping experiment.

In the second part of Chapter IV, I reported convincing data showing that $Nck1^{-/-}$ mice are protected from the obesity-induced insulin resistance due to decreased ER stress signaling and improved IR signaling in liver and adipose tissue. Remarkably, I found that obese Nck1-deficient mice display decreased levels of IRE-mediated JNK activation in these tissues, suggesting that Nck1 is also required for IRE1 signaling *in vivo*. Importantly, this correlated with increased levels of AKT Ser308 phosphorylation is liver and adipose tissues of $Nck1^{-/-}$ mice, which most likely contributed at improving the insulin sensitivity of these mice. Furthermore, I found decreased eIF2α Ser51 phosphorylation levels in liver and adipose tissue of $Nck1^{-/-}$ mice maintained on HFD as compared to Wt, thus establishing that Nck is a positive regulator of

PERK-mediated eIF2α phosphorylation *in vivo*. Although signaling from IRE1 has been demonstrated to impact directly on the IR signaling pathway and insulin sensitivity (311), it still remains to be determined if and how the PERK signaling pathway modulates the response to insulin in peripheral tissues. Therefore, it is premature to suggest that the reduction in eIF2α signaling observed in obese $Nck1^{-/-}$ mice contributes at preserving the insulin sensitivity in liver and adipose tissue. However and as stated before, the AKT-inhibitory protein TRB3 is induced in obese and diabetic db/db mice, and its hepatic expression promotes hyperglyceamia and glucose intolerance in normal mice (87, 212). Importantly, TRB3 is induced in ER stressed-cells by the ATF4 and CHOP transcriptional regulators (300). Therefore, it is possible that the PERK-eIF2α Ser51 signaling pathway modulates insulin sensitivity in peripheral tissues by promoting induction of TRB3 and preventing AKT activation *in vivo*. It will be important to assess whether TRB3 expression is reduced in obese $Nck1^{-/-}$ mice, since this could provide a direct link between the PERK and IR signaling pathways in obese and diabetic mice.

It is well documented that obesity-induced insulin resistance is accompanied by a compensatory increase in insulin biosynthesis and secretion, which is intended to maintain glycaemia within normal range. On a long term, such insulin resistance directly impacts on β-cell homeostasis (185). $eIF2\alpha^{Wt/S51A}$ mice maintained on HFD display profound glucose intolerance due to decreased insulin secretion caused by perturbation of the ER environment in pancreatic β-cells (366). Interestingly, I did not notice any significant changes in ER stress markers in pancreatic samples obtained from Wt and $Nck1^{-/-}$ mice (data not shown), suggesting that pancreas β-cell homeostasis and function is normal in $Nck1^{-/-}$ mice. Therefore, it will be important to directly evaluate pancreatic islet morphology and function in obese Nck-deficient mice in order to determine whether *nck* gene inactivation impacts on the insulin biosynthetic apparatus within β-cells in situation of high demand in protein synthesis.

The results presented in Chapter IV reveal the implication of Nck adaptors in the regulation of glucose homeostasis in mice. It will be important to substantiate these data by assessing glucose metabolism and pancreatic β-cells function in double heterozygote $Nck1^{+/-}$ $Nck2^{+/-}$ (50% reduction of both Nck1 and Nck2 expression), and single allele-retaining $Nck1^{+/-}$ $Nck2^{-/-}$ and $Nck1^{-/-}Nck2^{+/-}$ mice (75% reduction of total Nck expression) to circumvent the

functional redundancy associated with Nck adaptors. Moreover, tissue-specific inactivation of *nck* genes should help decipher the exact role of these signaling adaptors in different organs and avoid potential compensatory effects elicited by whole animal adaptor deficiency. Finally, since we found that Nck expression levels represent a critical mean of regulating cellular processes such eIF2α phosphorylation, determining whether Nck adaptors expression levels are modulated by metabolic states, for example during fasting periods, should help us understand the role of these adaptors in glucose homeostasis. In fact, it is noteworthy that Nck protein expression is downregulated in a GSK3β- and proteasome-dependent manner in response to serum starvation in cultured cells (Appendix 2 – data not shown). Whether such observations could be extrapolated *in vivo* in mice will require further attention.

CONLUSION

Over the years, Nck adaptors have been recognized as important regulators of plasma membrane RTK signaling pathways converging on remodeling of the cytoskeleton. However, the results presented in this thesis clearly establish that Nck adaptors also transduce signals from transmembrane proteins involved in stress signaling cascades initiated at the ER. In fact, the mechanistic underlying ER signal transduction by Nck adaptor proteins seems to be governed by regulations analogous to those controlling plasma membrane signaling pathways: SH2 domain-mediated binding to phosphotyrosine residues in activated transmembrane proteins and coupling of effector proteins via SH3 domains. Intriguingly, Shc, but not Grb2 or Crk, is also detected at the ER (198, 248, 289), suggesting that this molecule could also be involved in ER stress signaling. We believe that the novel and original work presented in this thesis should open new research avenues in the field of signal transduction and the design of new treatments for an accumulating number of metabolic diseases characterized by aberrant ER stress signaling such as Type 2 diabetes.

CHAPTER VI

Contribution to Original Research

1. The work presented in Chapter II represents a follow up of the work performed by a former graduated Ph.D. student in Dr. L. Larose laboratory. I demonstrated that Nck1 and Nck2 overexpression decreases ER stress-induced eIF2α Ser51 phosphorylation and the attendant induction of ATF4 and CHOP genes. In addition, I found that $Nck1^{-/-}$ and $Nck2^{-/-}$ mouse embryonic fibroblasts (MEFs) show increased expression of ATF4, GADD34 and CHOP and are resistant to apoptosis in prolonged ER stress situation. Using fluorescence microscopy, I demonstrated that a significant amount of Nck1 and Nck2 proteins localizes at the ER and observed that the third SH3 domain of Nck1 is involved in retaining Nck at this organelle. I also demonstrated that Nck is found in a molecular complex containing eIF2α, eIF2β, CReP and PP1c that dephosphorylates eIF2α on Ser51.

2. In Chapter III, I provided strong evidence that Nck adaptors promote the transient inhibition of mRNA translation associated with ER stress-induced eIF2α Ser51 phosphorylation. Furthermore, I demonstrated that the Nck1 adaptor binds directly to the activated form of the PERK protein kinase via its SH2 domain that engages Tyr561 in PERK juxtamembrane domain. This established that Nck represents the third PERK-interacting protein along with eIF2α and Nrf2. Moreover, I found that Tyr561 is at the centre of negative regulatory mechanism involved in downregulation of PERK kinase activity. Together, this study represents a remarkable advance in understanding the proximal events involved in activation of the PERK signaling in ER stress conditions.

3. Finally in Chapter IV, I investigated glucose homeostasis of $Nck1^{-/-}$ and $Nck2^{-/-}$ mice maintained on normal chow diet and high fat diet. I demonstrated that these animals are glucose intolerant due to decreased pancreatic β-cell mass. On the other hand, I determined that $Nck1^{-/-}$ mice maintained on high fat diet display improved glucose tolerance as compared to control animals, due to increased insulin sensitivity in liver and adipose tissue. At le molecular level, I observed significant reduction in levels of eIF2α phosphorylation in obese $Nck1^{-/-}$ mice, thus validating results presented in Chapter III demonstrating that Nck adaptors are required for eIF2α Ser51 phosphorylation in ER stress conditions. Moreover, I found that JNK activation is reduced in obese $Nck^{-/-}$ mice resulting in increased signaling from the insulin receptor in liver and adipose tissue. Importantly, these results represent the first

physiological demonstration of the function of Nck adaptors in ER stress signaling and glucose metabolism *in vivo*.

SUMMARY AND CONCLUSION

SUMMARY AND CONCLUSION

The work described in this thesis supports the function of Nck adaptors in ER signaling. I demonstrated that a significant amount of Nck localizes at the ER and regulates PERK-regulated phosphorylation of eIF2α on Ser51 and induction of ATF4, CHOP and GADD34 in ER stress conditions. However, and unlike previously alleged, Nck is required for efficient phosphorylation of eIF2α on Ser51 and inhibition of mRNA translation. Supportingly, I found that Nck specifically interact with the activated form of PERK through its SH2 domain. Mutation of Tyr561 in the PERK juxtamembrane domain impairs binding of Nck, suggesting that phosphorylation of this residue allows binding of Nck adaptor proteins. I demonstrated that Tyr561 is involved in downregulating PERK catalytic kinase activity as replacement of Tyr561 with a non-phosphorylatable residue (Phe) increases phosphorylation of eIF2α by PERK both *in vitro* and *in vivo*. Ultimately, I described the physiological significance of Nck function in PERK-mediated eIF2α phosphorylation using mice genetically inactivated of Nck adaptors. $Nck1^{-/-}$ mice show impaired glucose homeostasis characterized by marked glucose intolerance correlating with reduced pancreatic β-cell mass. Conversely, I confirmed that obesity induces ER stress in liver and adipose tissues in mice. Importantly, obese $Nck1^{-/-}$ mice display reduced levels of eIF2α Ser51 phosphorylation, demonstrating the critical role of these adaptors in PERK signaling *in vivo*. Furthermore, I found that $Nck1^{-/-}$ mice show improved glucose tolerance and insulin sensitivity due to decreased IRE-1-mediated JNK activation and IRS-1 Ser307 phosphorylation, thus increasing IR-regulated AKT Ser308 phosphorylation.

In conclusion, the work presented in this thesis clearly demonstrate that Nck adaptors are critical signaling proteins involved in both plasma membrane and ER signaling pathways. Importantly, my work sheds light on a physiological role for these adaptor proteins in glucose homeostasis. Future experiments should help improve our knowledge on the role of these adaptor proteins in ER stress signaling and potentially lead to the development of therapeutic agents improving management and prevention of diseases such as Type 2 diabetes.

REFERENCES

1. **Abel, E. D., O. Peroni, J. K. Kim, Y. B. Kim, O. Boss, E. Hadro, T. Minnemann, G. I. Shulman, and B. B. Kahn.** 2001. Adipose-selective targeting of the GLUT4 gene impairs insulin action in muscle and liver. Nature **409:**729-33.

2. **Adams, R. H.** 2002. Vascular patterning by Eph receptor tyrosine kinases and ephrins. Semin Cell Dev Biol **13:**55-60.

3. **Aguirre, V., T. Uchida, L. Yenush, R. Davis, and M. F. White.** 2000. The c-Jun NH(2)-terminal kinase promotes insulin resistance during association with insulin receptor substrate-1 and phosphorylation of Ser(307). J Biol Chem **275:**9047-54.

4. **Aguirre, V., E. D. Werner, J. Giraud, Y. H. Lee, S. E. Shoelson, and M. F. White.** 2002. Phosphorylation of Ser307 in insulin receptor substrate-1 blocks interactions with the insulin receptor and inhibits insulin action. J Biol Chem **277:**1531-7.

5. **Alarcon, C., B. Lincoln, and C. J. Rhodes.** 1993. The biosynthesis of the subtilisin-related proprotein convertase PC3, but no that of the PC2 convertase, is regulated by glucose in parallel to proinsulin biosynthesis in rat pancreatic islets. J Biol Chem **268:**4276-80.

6. **Ammala, C., L. Eliasson, K. Bokvist, P. O. Berggren, R. E. Honkanen, A. Sjoholm, and P. Rorsman.** 1994. Activation of protein kinases and inhibition of protein phosphatases play a central role in the regulation of exocytosis in mouse pancreatic beta cells. Proc Natl Acad Sci U S A **91:**4343-7.

7. **Anderson, P., and N. Kedersha.** 2002. Stressful initiations. J Cell Sci **115:**3227-34.

8. **Anderson, P., and N. Kedersha.** 2002. Visibly stressed: the role of eIF2, TIA-1, and stress granules in protein translation. Cell Stress Chaperones **7:**213-21.

9. **Azfer, A., J. Niu, L. M. Rogers, F. M. Adamski, and P. E. Kolattukudy.** 2006. Activation of endoplasmic reticulum stress response during the development of ischemic heart disease. Am J Physiol Heart Circ Physiol **291:**H1411-20.

10. **Bae, S. S., H. Cho, J. Mu, and M. J. Birnbaum.** 2003. Isoform-specific regulation of insulin-dependent glucose uptake by Akt/protein kinase B. J Biol Chem **278:**49530-6.

11. **Bagrodia, S., and R. A. Cerione.** 1999. Pak to the future. Trends Cell Biol **9:**350-5.

12. **Bagrodia, S., S. J. Taylor, K. A. Jordon, L. Van Aelst, and R. A. Cerione.** 1998. A novel regulator of p21-activated kinases. J Biol Chem **273:**23633-6.

13. **Barda-Saad, M., A. Braiman, R. Titerence, S. C. Bunnell, V. A. Barr, and L. E. Samelson.** 2005. Dynamic molecular interactions linking the T cell antigen receptor to the actin cytoskeleton. Nat Immunol **6:**80-9.

14. **Barone, M. V., A. Crozat, A. Tabaee, L. Philipson, and D. Ron.** 1994. CHOP (GADD153) and its oncogenic variant, TLS-CHOP, have opposing effects on the induction of G1/S arrest. Genes Dev **8:**453-64.

15. **Bassik, M. C., L. Scorrano, S. A. Oakes, T. Pozzan, and S. J. Korsmeyer.** 2004. Phosphorylation of BCL-2 regulates ER Ca2+ homeostasis and apoptosis. Embo J **23:**1207-16.

16. **Becker, E., U. Huynh-Do, S. Holland, T. Pawson, T. O. Daniel, and E. Y. Skolnik.** 2000. Nck-interacting Ste20 kinase couples Eph receptors to c-Jun N-terminal kinase and integrin activation. Mol Cell Biol **20:**1537-45.

17. **Benesch, S., S. Lommel, A. Steffen, T. E. Stradal, N. Scaplehorn, M. Way, J. Wehland, and K. Rottner.** 2002. Phosphatidylinositol 4,5-biphosphate (PIP2)-induced vesicle movement depends on N-WASP and involves Nck, WIP, and Grb2. J Biol Chem **277:**37771-6.

18. **Bernales, S., F. R. Papa, and P. Walter.** 2006. Intracellular signaling by the unfolded protein response. Annu Rev Cell Dev Biol **22:**487-508.

19. **Bertolotti, A., X. Wang, I. Novoa, R. Jungreis, K. Schlessinger, J. H. Cho, A. B. West, and D. Ron.** 2001. Increased sensitivity to dextran sodium sulfate colitis in IRE1beta-deficient mice. J Clin Invest **107:**585-93.

20. **Bertolotti, A., Y. Zhang, L. M. Hendershot, H. P. Harding, and D. Ron.** 2000. Dynamic interaction of BiP and ER stress transducers in the unfolded-protein response. Nat Cell Biol **2:**326-32.

21. **Bi, M., C. Naczki, M. Koritzinsky, D. Fels, J. Blais, N. Hu, H. Harding, I. Novoa, M. Varia, J. Raleigh, D. Scheuner, R. J. Kaufman, J. Bell, D. Ron, B. G. Wouters, and C. Koumenis.** 2005. ER stress-regulated translation increases tolerance to extreme hypoxia and promotes tumor growth. Embo J **24:**3470-81.

22. **Biason-Lauber, A., M. Lang-Muritano, T. Vaccaro, and E. J. Schoenle.** 2002. Loss of Kinase Activity in a Patient With Wolcott-Rallison Syndrome Caused By a Novel Mutation in the EIF2AK3 Gene. Diabetes **51:**2301-2305.

23. **Birge, R. B., B. S. Knudsen, D. Besser, and H. Hanafusa.** 1996. SH2 and SH3-containing adaptor proteins: redundant or independent mediators of intracellular signal transduction. Genes Cells **1:**595-613.

24. **Bixby, J. L., and P. Jhabvala.** 1993. Tyrosine phosphorylation in early embryonic growth cones. J Neurosci **13:**3421-32.

25. **Bladt, F., E. Aippersbach, S. Gelkop, G. A. Strasser, P. Nash, A. Tafuri, F. B. Gertler, and T. Pawson.** 2003. The Murine Nck SH2/SH3 Adaptors Are Important for

the Development of Mesoderm-Derived Embryonic Structures and for Regulating the Cellular Actin Network. Mol. Cell. Biol. **23:**4586-4597.

26. **Blaikie, P., D. Immanuel, J. Wu, N. Li, V. Yajnik, and B. Margolis.** 1994. A region in Shc distinct from the SH2 domain can bind tyrosine-phosphorylated growth factor receptors. J Biol Chem **269:**32031-4.

27. **Blais, J. D., C. L. Addison, R. Edge, T. Falls, H. Zhao, K. Wary, C. Koumenis, H. P. Harding, D. Ron, M. Holcik, and J. C. Bell.** 2006. Perk-dependent translational regulation promotes tumor cell adaptation and angiogenesis in response to hypoxic stress. Mol Cell Biol **26:**9517-32.

28. **Bluher, M., M. D. Michael, O. D. Peroni, K. Ueki, N. Carter, B. B. Kahn, and C. R. Kahn.** 2002. Adipose tissue selective insulin receptor knockout protects against obesity and obesity-related glucose intolerance. Dev Cell **3:**25-38.

29. **Bokoch, G. M., Y. Wang, B. P. Bohl, M. A. Sells, L. A. Quilliam, and U. G. Knaus.** 1996. Interaction of the Nck adapter protein with p21-activated kinase (PAK1). J Biol Chem **271:**25746-9.

30. **Bong, Y. S., Y. H. Park, H. S. Lee, K. Mood, A. Ishimura, and I. O. Daar.** 2004. Tyr-298 in ephrinB1 is critical for an interaction with the Grb4 adaptor protein. Biochem J **377:**499-507.

31. **Bonini, J. A., J. Colca, and C. Hofmann.** 1995. Altered expression of insulin signaling components in streptozotocin-treated rats. Biochem Biophys Res Commun **212:**933-8.

32. **Bonini, J. A., J. R. Colca, C. Dailey, M. White, and C. Hofmann.** 1995. Compensatory alterations for insulin signal transduction and glucose transport in insulin-resistant diabetes. Am J Physiol **269:**E759-65.

33. **Borradaile, N. M., X. Han, J. D. Harp, S. E. Gale, D. S. Ory, and J. E. Schaffer.** 2006. Disruption of endoplasmic reticulum structure and integrity in lipotoxic cell death. J Lipid Res **47:**2726-37.

34. **Boyce, M., K. F. Bryant, C. Jousse, K. Long, H. P. Harding, D. Scheuner, R. J. Kaufman, D. Ma, D. M. Coen, D. Ron, and J. Yuan.** 2005. A selective inhibitor of eIF2alpha dephosphorylation protects cells from ER stress. Science **307:**935-9.

35. **Brachmann, S. M., K. Ueki, J. A. Engelman, R. C. Kahn, and L. C. Cantley.** 2005. Phosphoinositide 3-kinase catalytic subunit deletion and regulatory subunit deletion have opposite effects on insulin sensitivity in mice. Mol Cell Biol **25:**1596-607.

36. **Bradshaw, J. M., V. Mitaxov, and G. Waksman.** 1999. Investigation of phosphotyrosine recognition by the SH2 domain of the Src kinase. J Mol Biol **293:**971-85.

37. **Braverman, L. E., and L. A. Quilliam.** 1999. Identification of Grb4/Nckbeta, a src homology 2 and 3 domain-containing adapter protein having similar binding and biological properties to Nck. J Biol Chem **274:**5542-9.

38. **Brazil, D. P., and B. A. Hemmings.** 2001. Ten years of protein kinase B signalling: a hard Akt to follow. Trends Biochem Sci **26:**657-64.

39. **Brewer, J. W., and J. A. Diehl.** 2000. PERK mediates cell-cycle exit during the mammalian unfolded protein response. PNAS **97:**12625-12630.

40. **Brewer, J. W., L. M. Hendershot, C. J. Sherr, and J. A. Diehl.** 1999. Mammalian unfolded protein response inhibits cyclin D1 translation and cell-cycle progression. PNAS **96:**8505-8510.

41. **Brostrom, C. O., S. B. Bocckino, and M. A. Brostrom.** 1983. Identification of a Ca2+ requirement for protein synthesis in eukaryotic cells. J Biol Chem **258:**14390-9.

42. **Brostrom, C. O., S. B. Bocckino, M. A. Brostrom, and E. M. Galuska.** 1986. Regulation of protein synthesis in isolated hepatocytes by calcium-mobilizing hormones. Mol Pharmacol **29:**104-11.

43. **Brostrom, C. O., C. R. Prostko, R. J. Kaufman, and M. A. Brostrom.** 1996. Inhibition of translational initiation by activators of the glucose-regulated stress protein and heat shock protein stress response systems. Role of the interferon-inducible double-stranded RNA-activated eukaryotic initiation factor 2alpha kinase. J Biol Chem **271:**24995-5002.

44. **Brostrom, M. A., C. R. Prostko, D. Gmitter, and C. O. Brostrom.** 1995. Independent signaling of grp78 gene transcription and phosphorylation of eukaryotic initiator factor 2 alpha by the stressed endoplasmic reticulum. J Biol Chem **270:**4127-32.

45. **Brozinick, J. T., Jr., E. D. Hawkins, A. B. Strawbridge, and J. S. Elmendorf.** 2004. Disruption of cortical actin in skeletal muscle demonstrates an essential role of the cytoskeleton in glucose transporter 4 translocation in insulin-sensitive tissues. J Biol Chem **279:**40699-706.

46. **Brush, M. H., D. C. Weiser, and S. Shenolikar.** 2003. Growth arrest and DNA damage-inducible protein GADD34 targets protein phosphatase 1 alpha to the endoplasmic reticulum and promotes dephosphorylation of the alpha subunit of eukaryotic translation initiation factor 2. Mol Cell Biol **23:**1292-303.

47. **Buday, L., L. Wunderlich, and P. Tamas.** 2002. The Nck family of adapter proteins: Regulators of actin cytoskeleton. Cellular Signalling **14:**723-731.

48. **Calfon, M., H. Zeng, F. Urano, J. H. Till, S. R. Hubbard, H. P. Harding, S. G. Clark, and D. Ron.** 2002. IRE1 couples endoplasmic reticulum load to secretory capacity by processing the XBP-1 mRNA. Nature **415:**92-96.

49. **Campellone, K. G., A. Giese, D. J. Tipper, and J. M. Leong.** 2002. A tyrosine-phosphorylated 12-amino-acid sequence of enteropathogenic Escherichia coli Tir binds the host adaptor protein Nck and is required for Nck localization to actin pedestals. Mol Microbiol **43:**1227-41.

50. **Campellone, K. G., and J. M. Leong.** 2005. Nck-independent actin assembly is mediated by two phosphorylated tyrosines within enteropathogenic Escherichia coli Tir. Mol Microbiol **56:**416-32.

51. **Campellone, K. G., and J. M. Leong.** 2003. Tails of two Tirs: actin pedestal formation by enteropathogenic E. coli and enterohemorrhagic E. coli O157:H7. Curr Opin Microbiol **6:**82-90.

52. **Campellone, K. G., S. Rankin, T. Pawson, M. W. Kirschner, D. J. Tipper, and J. M. Leong.** 2004. Clustering of Nck by a 12-residue Tir phosphopeptide is sufficient to trigger localized actin assembly. J Cell Biol **164:**407-16.

53. **Campellone, K. G., D. Robbins, and J. M. Leong.** 2004. EspFU is a translocated EHEC effector that interacts with Tir and N-WASP and promotes Nck-independent actin assembly. Dev Cell **7:**217-28.

54. **Carlier, M. F., P. Nioche, I. Broutin-L'Hermite, R. Boujemaa, C. Le Clainche, C. Egile, C. Garbay, A. Ducruix, P. Sansonetti, and D. Pantaloni.** 2000. GRB2 links signaling to actin assembly by enhancing interaction of neural Wiskott-Aldrich syndrome protein (N-WASp) with actin-related protein (ARP2/3) complex. J Biol Chem **275:**21946-52.

55. **Celli, J., W. Deng, and B. B. Finlay.** 2000. Enteropathogenic Escherichia coli (EPEC) attachment to epithelial cells: exploiting the host cell cytoskeleton from the outside. Cell Microbiol **2:**1-9.

56. **Chang, L., S. H. Chiang, and A. R. Saltiel.** 2004. Insulin signaling and the regulation of glucose transport. Mol Med **10:**65-71.

57. **Chen, J.** 2000. Heme-regulated eIF2α kinase. In N. Sonenberg, J. W. B. Hershey and M. B. Mathews (ed.), Translational control of gene expression:p529-546.

58. **Chen, J. J., M. S. Throop, L. Gehrke, I. Kuo, J. K. Pal, M. Brodsky, and I. M. London.** 1991. Cloning of the cDNA of the heme-regulated eukaryotic initiation factor 2 alpha (eIF-2 alpha) kinase of rabbit reticulocytes: homology to yeast GCN2 protein kinase and human double-stranded-RNA-dependent eIF-2 alpha kinase. Proc Natl Acad Sci U S A **88:**7729-33.

59. **Chen, M., H. She, E. M. Davis, C. M. Spicer, L. Kim, R. Ren, M. M. Le Beau, and W. Li.** 1998. Identification of Nck family genes, chromosomal localization, expression, and signaling specificity. J Biol Chem **273:**25171-8.

60. **Chen, M., H. She, A. Kim, D. T. Woodley, and W. Li.** 2000. Nckbeta adapter regulates actin polymerization in NIH 3T3 fibroblasts in response to platelet-derived growth factor bb. Mol Cell Biol **20:**7867-80.

61. **Chiang, S. H., C. A. Baumann, M. Kanzaki, D. C. Thurmond, R. T. Watson, C. L. Neudauer, I. G. Macara, J. E. Pessin, and A. R. Saltiel.** 2001. Insulin-stimulated GLUT4 translocation requires the CAP-dependent activation of TC10. Nature **410:**944-8.

62. **Chin, K. V., C. Cade, C. O. Brostrom, E. M. Galuska, and M. A. Brostrom.** 1987. Calcium-dependent regulation of protein synthesis at translational initiation in eukaryotic cells. J Biol Chem **262:**16509-14.

63. **Chiu, V. K., T. Bivona, A. Hach, J. B. Sajous, J. Silletti, H. Wiener, R. L. Johnson, 2nd, A. D. Cox, and M. R. Philips.** 2002. Ras signalling on the endoplasmic reticulum and the Golgi. Nat Cell Biol **4:**343-50.

64. **Cho, H., J. L. Thorvaldsen, Q. Chu, F. Feng, and M. J. Birnbaum.** 2001. Akt1/PKBalpha is required for normal growth but dispensable for maintenance of glucose homeostasis in mice. J Biol Chem **276:**38349-52.

65. **Chong, L. D., E. K. Park, E. Latimer, R. Friesel, and I. O. Daar.** 2000. Fibroblast growth factor receptor-mediated rescue of x-ephrin B1-induced cell dissociation in Xenopus embryos. Mol Cell Biol **20:**724-34.

66. **Cohen, P. T.** 2002. Protein phosphatase 1--targeted in many directions. J Cell Sci **115:**241-56.

67. **Connor, J. H., D. C. Weiser, S. Li, J. M. Hallenbeck, and S. Shenolikar.** 2001. Growth arrest and DNA damage-inducible protein GADD34 assembles a novel signaling complex containing protein phosphatase 1 and inhibitor 1. Mol Cell Biol **21:**6841-50.

68. **Cowan, C. A., and M. Henkemeyer.** 2001. The SH2/SH3 adaptor Grb4 transduces B-ephrin reverse signals. Nature **413:**174-9.

69. **Cox, J. S., R. E. Chapman, and P. Walter.** 1997. The unfolded protein response coordinates the production of endoplasmic reticulum protein and endoplasmic reticulum membrane. Mol Biol Cell **8:**1805-14.

70. **Cox, J. S., C. E. Shamu, and P. Walter.** 1993. Transcriptional induction of genes encoding endoplasmic reticulum resident proteins requires a transmembrane protein kinase. Cell **73:**1197-206.

71. **Credle, J. J., J. S. Finer-Moore, F. R. Papa, R. M. Stroud, and P. Walter.** 2005. Inaugural Article: On the mechanism of sensing unfolded protein in the endoplasmic reticulum. PNAS **102:**18773-18784.

72. **Cullinan, S. B., and J. A. Diehl.** 2006. Coordination of ER and oxidative stress signaling: the PERK/Nrf2 signaling pathway. Int J Biochem Cell Biol **38:**317-32.

73. **Cullinan, S. B., D. Zhang, M. Hannink, E. Arvisais, R. J. Kaufman, and J. A. Diehl.** 2003. Nrf2 Is a Direct PERK Substrate and Effector of PERK-Dependent Cell Survival. Mol. Cell. Biol. **23:**7198-7209.

74. **Dar, A. C., T. E. Dever, and F. Sicheri.** 2005. Higher-order substrate recognition of eIF2alpha by the RNA-dependent protein kinase PKR. Cell **122:**887-900.

75. **de Haro, C., R. Mendez, and J. Santoyo.** 1996. The eIF-2alpha kinases and the control of protein synthesis. Faseb J **10:**1378-87.

76. **DeFronzo, R. A.** 1997. Pathogenesis of type 2 diabetes: Metabolic and molecular implications for identifying diabetes genes. Diabetes Review **5:**177-269.

77. **Deibel, C., S. Kramer, T. Chakraborty, and F. Ebel.** 1998. EspE, a novel secreted protein of attaching and effacing bacteria, is directly translocated into infected host cells, where it appears as a tyrosine-phosphorylated 90 kDa protein. Mol Microbiol **28:**463-74.

78. **Del Prato, S., F. Leonetti, D. C. Simonson, P. Sheehan, M. Matsuda, and R. A. DeFronzo.** 1994. Effect of sustained physiologic hyperinsulinaemia and hyperglycaemia on insulin secretion and insulin sensitivity in man. Diabetologia **37:**1025-35.

79. **Delepine, M., M. Nicolino, T. Barrett, M. Golamaully, G. M. Lathrop, and C. Julier.** 2000. EIF2AK3, encoding translation initiation factor 2-alpha kinase 3, is mutated in patients with Wolcott-Rallison syndrome. Nat Genet **25:**406-9.

80. **Deng, J., H. P. Harding, B. Raught, A. C. Gingras, J. J. Berlanga, D. Scheuner, R. J. Kaufman, D. Ron, and N. Sonenberg.** 2002. Activation of GCN2 in UV-irradiated cells inhibits translation. Curr Biol **12:**1279-86.

81. **Deng, J., P. D. Lu, Y. Zhang, D. Scheuner, R. J. Kaufman, N. Sonenberg, H. P. Harding, and D. Ron.** 2004. Translational Repression Mediates Activation of Nuclear Factor Kappa B by Phosphorylated Translation Initiation Factor 2. Mol. Cell. Biol. **24:**10161-10168.

82. **Derry, J. M., H. D. Ochs, and U. Francke.** 1994. Isolation of a novel gene mutated in Wiskott-Aldrich syndrome. Cell **78:**635-44.

83. **Dey, M., C. Cao, A. C. Dar, T. Tamura, K. Ozato, F. Sicheri, and T. E. Dever.** 2005. Mechanistic link between PKR dimerization, autophosphorylation, and eIF2alpha substrate recognition. Cell **122:**901-13.

84. **DiNitto, J. P., and D. G. Lambright.** 2006. Membrane and juxtamembrane targeting by PH and PTB domains. Biochim Biophys Acta **1761:**850-67.

85. **Dor, Y., J. Brown, O. I. Martinez, and D. A. Melton.** 2004. Adult pancreatic beta-cells are formed by self-duplication rather than stem-cell differentiation. Nature **429:**41-6.

86. **Drucker, D. J.** 2001. Minireview: the glucagon-like peptides. Endocrinology **142:**521-7.

87. **Du, K., S. Herzig, R. N. Kulkarni, and M. Montminy.** 2003. TRB3: a tribbles homolog that inhibits Akt/PKB activation by insulin in liver. Science **300:**1574-7.

88. **Durbin, L., C. Brennan, K. Shiomi, J. Cooke, A. Barrios, S. Shanmugalingam, B. Guthrie, R. Lindberg, and N. Holder.** 1998. Eph signaling is required for segmentation and differentiation of the somites. Genes Dev **12:**3096-109.

89. **DuRose, J. B., A. B. Tam, and M. Niwa.** 2006. Intrinsic capacities of molecular sensors of the unfolded protein response to sense alternate forms of endoplasmic reticulum stress. Mol Biol Cell **17:**3095-107.

90. **Easom, R. A.** 2000. Beta-granule transport and exocytosis. Semin Cell Dev Biol **11:**253-66.

91. **Ebina, Y., L. Ellis, K. Jarnagin, M. Edery, L. Graf, E. Clauser, J. H. Ou, F. Masiarz, Y. W. Kan, I. D. Goldfine, and et al.** 1985. The human insulin receptor cDNA: the structural basis for hormone-activated transmembrane signalling. Cell **40:**747-58.

92. **Eckhart, W., M. A. Hutchinson, and T. Hunter.** 1979. An activity phosphorylating tyrosine in polyoma T antigen immunoprecipitates. Cell **18:**925-33.

93. **Eden, S., R. Rohatgi, A. V. Podtelejnikov, M. Mann, and M. W. Kirschner.** 2002. Mechanism of regulation of WAVE1-induced actin nucleation by Rac1 and Nck. Nature **418:**790-3.

94. **Edlund, H.** 2002. Pancreatic organogenesis--developmental mechanisms and implications for therapy. Nat Rev Genet **3:**524-32.

95. **Edman, J. C., L. Ellis, R. W. Blacher, R. A. Roth, and W. J. Rutter.** 1985. Sequence of protein disulphide isomerase and implications of its relationship to thioredoxin. Nature **317:**267-70.

96. **Ellenberg, J., E. D. Siggia, J. E. Moreira, C. L. Smith, J. F. Presley, H. J. Worman, and J. Lippincott-Schwartz.** 1997. Nuclear membrane dynamics and reassembly in living cells: targeting of an inner nuclear membrane protein in interphase and mitosis. J Cell Biol **138:**1193-206.

97. **Elowe, S., S. J. Holland, S. Kulkarni, and T. Pawson.** 2001. Downregulation of the Ras-mitogen-activated protein kinase pathway by the EphB2 receptor tyrosine kinase is required for ephrin-induced neurite retraction. Mol Cell Biol **21:**7429-41.

98. **Engelman, J. A., J. Luo, and L. C. Cantley.** 2006. The evolution of phosphatidylinositol 3-kinases as regulators of growth and metabolism. Nat Rev Genet **7:**606-19.

99. **Erickson, F. L., L. D. Harding, D. R. Dorris, and E. M. Hannig.** 1997. Functional analysis of homologs of translation initiation factor 2gamma in yeast. Mol Gen Genet **253:**711-9.

100. **Esposito, D. L., Y. Li, A. Cama, and M. J. Quon.** 2001. Tyr(612) and Tyr(632) in human insulin receptor substrate-1 are important for full activation of insulin-stimulated phosphatidylinositol 3-kinase activity and translocation of GLUT4 in adipose cells. Endocrinology **142:**2833-40.

101. **Farese, R. V., M. P. Sajan, and M. L. Standaert.** 2005. Insulin-sensitive protein kinases (atypical protein kinase C and protein kinase B/Akt): actions and defects in obesity and type II diabetes. Exp Biol Med (Maywood) **230:**593-605.

102. **Fawcett, T. W., J. L. Martindale, K. Z. Guyton, T. Hai, and N. J. Holbrook.** 1999. Complexes containing activating transcription factor (ATF)/cAMP-responsive-element-binding protein (CREB) interact with the CCAAT/enhancer-binding protein (C/EBP)-ATF composite site to regulate Gadd153 expression during the stress response. Biochem J **339 (Pt 1):**135-41.

103. **Fels, D. R., and C. Koumenis.** 2006. The PERK/eIF2alpha/ATF4 module of the UPR in hypoxia resistance and tumor growth. Cancer Biol Ther **5:**723-8.

104. **Feng, B., P. M. Yao, Y. Li, C. M. Devlin, D. Zhang, H. P. Harding, M. Sweeney, J. X. Rong, G. Kuriakose, E. A. Fisher, A. R. Marks, D. Ron, and I. Tabas.** 2003. The endoplasmic reticulum is the site of cholesterol-induced cytotoxicity in macrophages. Nat Cell Biol **5:**781-92.

105. **Feng, S., J. K. Chen, H. Yu, J. A. Simon, and S. L. Schreiber.** 1994. Two binding orientations for peptides to the Src SH3 domain: development of a general model for SH3-ligand interactions. Science **266:**1241-7.

106. **Foskett, J. K., C. White, K. H. Cheung, and D. O. Mak.** 2007. Inositol trisphosphate receptor Ca2+ release channels. Physiol Rev **87:**593-658.

107. **Freeman, M., and J. B. Gurdon.** 2002. Regulatory principles of developmental signaling. Annu Rev Cell Dev Biol **18:**515-39.

108. **Frese, S., W. D. Schubert, A. C. Findeis, T. Marquardt, Y. S. Roske, T. E. Stradal, and D. W. Heinz.** 2006. The phosphotyrosine peptide binding specificity of Nck1 and Nck2 Src homology 2 domains. J Biol Chem **281:**18236-45.

109. **Frischknecht, F., V. Moreau, S. Rottger, S. Gonfloni, I. Reckmann, G. Superti-Furga, and M. Way.** 1999. Actin-based motility of vaccinia virus mimics receptor tyrosine kinase signalling. Nature **401:**926-9.

110. **Fukuda, T., K. Chen, X. Shi, and C. Wu.** 2003. PINCH-1 is an obligate partner of integrin-linked kinase (ILK) functioning in cell shape modulation, motility, and survival. J Biol Chem **278:**51324-33.

111. **Gabay, C., and I. Kushner.** 1999. Acute-phase proteins and other systemic responses to inflammation. N Engl J Med **340:**448-54.

112. **Galisteo, M. L., J. Chernoff, Y. C. Su, E. Y. Skolnik, and J. Schlessinger.** 1996. The adaptor protein Nck links receptor tyrosine kinases with the serine-threonine kinase Pak1. J Biol Chem **271:**20997-1000.

113. **Gao, Z., D. Hwang, F. Bataille, M. Lefevre, D. York, M. J. Quon, and J. Ye.** 2002. Serine phosphorylation of insulin receptor substrate 1 by inhibitor kappa B kinase complex. J Biol Chem **277:**48115-21.

114. **Garg, P., R. Verma, and L. B. Holzman.** 2007. Slit diaphragm junctional complex and regulation of the cytoskeleton. Nephron Exp Nephrol **106:**e67-72.

115. **Garrity, P. A., Y. Rao, I. Salecker, J. McGlade, T. Pawson, and S. L. Zipursky.** 1996. Drosophila photoreceptor axon guidance and targeting requires the dreadlocks SH2/SH3 adapter protein. Cell **85:**639-50.

116. **Garvey, W. T., L. Maianu, T. P. Huecksteadt, M. J. Birnbaum, J. M. Molina, and T. P. Ciaraldi.** 1991. Pretranslational suppression of a glucose transporter protein causes insulin resistance in adipocytes from patients with non-insulin-dependent diabetes mellitus and obesity. J Clin Invest **87:**1072-81.

117. **Georgia, S., and A. Bhushan.** 2004. Beta cell replication is the primary mechanism for maintaining postnatal beta cell mass. J Clin Invest **114:**963-8.

118. **Georgia, S., and A. Bhushan.** 2006. p27 Regulates the transition of beta-cells from quiescence to proliferation. Diabetes **55:**2950-6.

119. **German, M. S.** 1993. Glucose sensing in pancreatic islet beta cells: the key role of glucokinase and the glycolytic intermediates. Proc Natl Acad Sci U S A **90:**1781-5.

120. **Gil, D., W. W. Schamel, M. Montoya, F. Sanchez-Madrid, and B. Alarcon.** 2002. Recruitment of Nck by CD3 epsilon reveals a ligand-induced conformational change essential for T cell receptor signaling and synapse formation. Cell **109:**901-12.

121. **Gingras, A. C., B. Raught, and N. Sonenberg.** 1999. eIF4 initiation factors: effectors of mRNA recruitment to ribosomes and regulators of translation. Annu Rev Biochem **68:**913-63.

122. **Goodge, K. A., and J. C. Hutton.** 2000. Translational regulation of proinsulin biosynthesis and proinsulin conversion in the pancreatic beta-cell. Semin Cell Dev Biol **11:**235-42.

123. **Gray, S., B. Wang, Y. Orihuela, E. G. Hong, S. Fisch, S. Haldar, G. W. Cline, J. K. Kim, O. D. Peroni, B. B. Kahn, and M. K. Jain.** 2007. Regulation of gluconeogenesis by Kruppel-like factor 15. Cell Metab **5:**305-12.

124. **Greene, M. W., H. Sakaue, L. Wang, D. R. Alessi, and R. A. Roth.** 2003. Modulation of insulin-stimulated degradation of human insulin receptor substrate-1 by Serine 312 phosphorylation. J Biol Chem **278:**8199-211.

125. **Griffith, J., J. Black, C. Faerman, L. Swenson, M. Wynn, F. Lu, J. Lippke, and K. Saxena.** 2004. The structural basis for autoinhibition of FLT3 by the juxtamembrane domain. Mol Cell **13:**169-78.

126. **Gruenheid, S., R. DeVinney, F. Bladt, D. Goosney, S. Gelkop, G. D. Gish, T. Pawson, and B. B. Finlay.** 2001. Enteropathogenic E. coli Tir binds Nck to initiate actin pedestal formation in host cells. Nat Cell Biol **3:**856-9.

127. **Gu, F., D. T. Nguyen, M. Stuible, N. Dube, M. L. Tremblay, and E. Chevet.** 2004. Protein-tyrosine phosphatase 1B potentiates IRE1 signaling during endoplasmic reticulum stress. J Biol Chem **279:**49689-93.

128. **Gual, P., Y. Le Marchand-Brustel, and J. F. Tanti.** 2005. Positive and negative regulation of insulin signaling through IRS-1 phosphorylation. Biochimie **87:**99-109.

129. **Guillam, M. T., E. Hummler, E. Schaerer, J. I. Yeh, M. J. Birnbaum, F. Beermann, A. Schmidt, N. Deriaz, and B. Thorens.** 1997. Early diabetes and abnormal postnatal pancreatic islet development in mice lacking Glut-2. Nat Genet **17:**327-30.

130. **Haas, I. G., and M. Wabl.** 1983. Immunoglobulin heavy chain binding protein. Nature **306:**387-9.

131. **Hamanaka, R. B., B. S. Bennett, S. B. Cullinan, and J. A. Diehl.** 2005. PERK and GCN2 contribute to eIF2alpha phosphorylation and cell cycle arrest after activation of the unfolded protein response pathway. Mol Biol Cell **16:**5493-501.

132. **Hampton, R. Y.** 2002. Proteolysis and sterol regulation. Annu Rev Cell Dev Biol **18:**345-78.

133. **Han, S., C. P. Liang, T. DeVries-Seimon, M. Ranalletta, C. L. Welch, K. Collins-Fletcher, D. Accili, I. Tabas, and A. R. Tall.** 2006. Macrophage insulin receptor deficiency increases ER stress-induced apoptosis and necrotic core formation in advanced atherosclerotic lesions. Cell Metab **3:**257-66.

134. **Hanks, S. K., and T. Hunter.** 1995. Protein kinases 6. The eukaryotic protein kinase superfamily: kinase (catalytic) domain structure and classification. Faseb J **9:**576-96.

135. **Hansson, G. K.** 2005. Inflammation, atherosclerosis, and coronary artery disease. N Engl J Med **352:**1685-95.

136. **Harding, H. P., M. Calfon, F. Urano, I. Novoa, and D. Ron.** 2002. Transcriptional and translational control in the Mammalian unfolded protein response. Annu Rev Cell Dev Biol **18:**575-99.

137. **Harding, H. P., I. Novoa, Y. Zhang, H. Zeng, R. Wek, M. Schapira, and D. Ron.** 2000. Regulated Translation Initiation Controls Stress-Induced Gene Expression in Mammalian Cells. Molecular Cell **6:**1099-1108.

138. **Harding, H. P., and D. Ron.** 2002. Endoplasmic reticulum stress and the development of diabetes: a review. Diabetes **51 Suppl 3:**S455-61.

139. **Harding, H. P., H. Zeng, Y. Zhang, R. Jungries, P. Chung, H. Plesken, D. D. Sabatini, and D. Ron.** 2001. Diabetes mellitus and exocrine pancreatic dysfunction in perk-/- mice reveals a role for translational control in secretory cell survival. Mol Cell **7:**1153-63.

140. **Harding, H. P., Y. Zhang, A. Bertolotti, H. Zeng, and D. Ron.** 2000. Perk Is Essential for Translational Regulation and Cell Survival during the Unfolded Protein Response. Molecular Cell **5:**897-904.

141. **Harding, H. P., Y. Zhang, S. Khersonsky, S. Marciniak, D. Scheuner, R. J. Kaufman, N. Javitt, Y. T. Chang, and D. Ron.** 2005. Bioactive small molecules reveal antagonism between the integrated stress response and sterol-regulated gene expression. Cell Metab **2:**361-71.

142. **Harding, H. P., Y. Zhang, and D. Ron.** 1999. Protein translation and folding are coupled by an endoplasmic-reticulum-resident kinase. Nature **397:**271-4.

143. **Harding, H. P., Y. Zhang, H. Zeng, I. Novoa, P. D. Lu, M. Calfon, N. Sadri, C. Yun, B. Popko, R. Paules, D. F. Stojdl, J. C. Bell, T. Hettmann, J. M. Leiden, and D. Ron.** 2003. An integrated stress response regulates amino acid metabolism and resistance to oxidative stress. Mol Cell **11:**619-33.

144. **Harrington, L. S., G. M. Findlay, A. Gray, T. Tolkacheva, S. Wigfield, H. Rebholz, J. Barnett, N. R. Leslie, S. Cheng, P. R. Shepherd, I. Gout, C. P. Downes, and R. F.**

Lamb. 2004. The TSC1-2 tumor suppressor controls insulin-PI3K signaling via regulation of IRS proteins. J Cell Biol **166:**213-23.

145. **Hartman, M. G., D. Lu, M.-L. Kim, G. J. Kociba, T. Shukri, J. Buteau, X. Wang, W. L. Frankel, D. Guttridge, M. Prentki, S. T. Grey, D. Ron, and T. Hai.** 2004. Role for Activating Transcription Factor 3 in Stress-Induced {beta}-Cell Apoptosis. Mol. Cell. Biol. **24:**5721-5732.

146. **Haruta, T., T. Uno, J. Kawahara, A. Takano, K. Egawa, P. M. Sharma, J. M. Olefsky, and M. Kobayashi.** 2000. A rapamycin-sensitive pathway down-regulates insulin signaling via phosphorylation and proteasomal degradation of insulin receptor substrate-1. Mol Endocrinol **14:**783-94.

147. **Haze, K., T. Okada, H. Yoshida, H. Yanagi, T. Yura, M. Negishi, and K. Mori.** 2001. Identification of the G13 (cAMP-response-element-binding protein-related protein) gene product related to activating transcription factor 6 as a transcriptional activator of the mammalian unfolded protein response. Biochem J **355:**19-28.

148. **Haze, K., H. Yoshida, H. Yanagi, T. Yura, and K. Mori.** 1999. Mammalian transcription factor ATF6 is synthesized as a transmembrane protein and activated by proteolysis in response to endoplasmic reticulum stress. Mol Biol Cell **10:**3787-99.

149. **He, B.** 2006. Viruses, endoplasmic reticulum stress, and interferon responses. Cell Death Differ **13:**393-403.

150. **He, B., M. Gross, and B. Roizman.** 1998. The gamma134.5 protein of herpes simplex virus 1 has the structural and functional attributes of a protein phosphatase 1 regulatory subunit and is present in a high molecular weight complex with the enzyme in infected cells. J Biol Chem **273:**20737-43.

151. **He, B., M. Gross, and B. Roizman.** 1997. The gamma(1)34.5 protein of herpes simplex virus 1 complexes with protein phosphatase 1alpha to dephosphorylate the alpha subunit of the eukaryotic translation initiation factor 2 and preclude the shutoff of protein synthesis by double-stranded RNA-activated protein kinase. Proc Natl Acad Sci U S A **94:**843-8.

152. **Heinrich, M. C., C. L. Corless, A. Duensing, L. McGreevey, C. J. Chen, N. Joseph, S. Singer, D. J. Griffith, A. Haley, A. Town, G. D. Demetri, C. D. Fletcher, and J. A. Fletcher.** 2003. PDGFRA activating mutations in gastrointestinal stromal tumors. Science **299:**708-10.

153. **Hershey, J. W.** 1991. Translational control in mammalian cells. Annu Rev Biochem **60:**717-55.

154. **Hershey, J. W. a. M., W.C.** 2000. Translation Control in Mammalian Cells. In N. Sonenberg, J. W. B. Hershey and M. B. Mathews (ed.), Translational control of gene expression **CSHL Press, Cold Spring Harbor, N.Y.**

155. **Hetz, C., P. Bernasconi, J. Fisher, A. H. Lee, M. C. Bassik, B. Antonsson, G. S. Brandt, N. N. Iwakoshi, A. Schinzel, L. H. Glimcher, and S. J. Korsmeyer.** 2006. Proapoptotic BAX and BAK modulate the unfolded protein response by a direct interaction with IRE1alpha. Science **312:**572-6.

156. **Higgs, H. N., and T. D. Pollard.** 2001. Regulation of actin filament network formation through ARP2/3 complex: activation by a diverse array of proteins. Annu Rev Biochem **70:**649-76.

157. **Hing, H., J. Xiao, N. Harden, L. Lim, and S. L. Zipursky.** 1999. Pak functions downstream of Dock to regulate photoreceptor axon guidance in Drosophila. Cell **97:**853-63.

158. **Hinnebusch, A. G.** 2000. Mechanism and Regulation of Initiator Methionyl-tRNA Binding to Ribosomes, p. 185-243. In N. Sonenberg, J.W.B. Hershey, M.B. Mathews (ed.), Translational control of gene expression. CSHL Press Cold Spring Harbor, N.Y.

159. **Hirosumi, J., G. Tuncman, L. Chang, C. Z. Gorgun, K. T. Uysal, K. Maeda, M. Karin, and G. S. Hotamisligil.** 2002. A central role for JNK in obesity and insulin resistance. Nature **420:**333-6.

160. **Hirota, S., K. Isozaki, Y. Moriyama, K. Hashimoto, T. Nishida, S. Ishiguro, K. Kawano, M. Hanada, A. Kurata, M. Takeda, G. Muhammad Tunio, Y. Matsuzawa, Y. Kanakura, Y. Shinomura, and Y. Kitamura.** 1998. Gain-of-function mutations of c-kit in human gastrointestinal stromal tumors. Science **279:**577-80.

161. **Hogan, A., S. Heyner, M. J. Charron, N. G. Copeland, D. J. Gilbert, N. A. Jenkins, B. Thorens, and G. A. Schultz.** 1991. Glucose transporter gene expression in early mouse embryos. Development **113:**363-72.

162. **Holland, S. J., N. W. Gale, G. D. Gish, R. A. Roth, Z. Songyang, L. C. Cantley, M. Henkemeyer, G. D. Yancopoulos, and T. Pawson.** 1997. Juxtamembrane tyrosine residues couple the Eph family receptor EphB2/Nuk to specific SH2 domain proteins in neuronal cells. Embo J **16:**3877-88.

163. **Hollien, J., and J. S. Weissman.** 2006. Decay of endoplasmic reticulum-localized mRNAs during the unfolded protein response. Science **313:**104-7.

164. **Holmes, B., and G. L. Dohm.** 2004. Regulation of GLUT4 gene expression during exercise. Med Sci Sports Exerc **36:**1202-6.

165. **Holt, L. J., and R. J. Daly.** 2005. Adapter protein connections: the MRL and Grb7 protein families. Growth Factors **23:**193-201.

166. **Hosokawa, N., I. Wada, K. Hasegawa, T. Yorihuzi, L. O. Tremblay, A. Herscovics, and K. Nagata.** 2001. A novel ER alpha-mannosidase-like protein accelerates ER-associated degradation. EMBO Rep **2:**415-22.

167. **Hu, Q., D. Milfay, and L. T. Williams.** 1995. Binding of NCK to SOS and activation of ras-dependent gene expression. Mol. Cell. Biol. **15:**1169-1174.

168. **Huang, S., and M. P. Czech.** 2007. The GLUT4 glucose transporter. Cell Metab **5:**237-52.

169. **Hubbard, S. R.** 1997. Crystal structure of the activated insulin receptor tyrosine kinase in complex with peptide substrate and ATP analog. Embo J **16:**5572-81.

170. **Hubbard, S. R.** 2004. Juxtamembrane autoinhibition in receptor tyrosine kinases. Nat Rev Mol Cell Biol **5:**464-71.

171. **Hubbard, S. R., L. Wei, L. Ellis, and W. A. Hendrickson.** 1994. Crystal structure of the tyrosine kinase domain of the human insulin receptor. Nature **372:**746-54.

172. **Iozzo, P., T. Pratipanawatr, H. Pijl, C. Vogt, V. Kumar, R. Pipek, M. Matsuda, L. J. Mandarino, K. J. Cusi, and R. A. DeFronzo.** 2001. Physiological hyperinsulinemia impairs insulin-stimulated glycogen synthase activity and glycogen synthesis. Am J Physiol Endocrinol Metab **280:**E712-9.

173. **Iwakoshi, N. N., A. H. Lee, P. Vallabhajosyula, K. L. Otipoby, K. Rajewsky, and L. H. Glimcher.** 2003. Plasma cell differentiation and the unfolded protein response intersect at the transcription factor XBP-1. Nat Immunol **4:**321-9.

174. **Iyer, S., M. Korada, L. Rainbow, J. Kirk, R. M. Brown, N. Shaw, and T. G. Barrett.** 2004. Wolcott-Rallison syndrome: a clinical and genetic study of three children, novel mutation in EIF2AK3 and a review of the literature. Acta Paediatr **93:**1195-201.

175. **Jaeschke, A., M. P. Czech, and R. J. Davis.** 2004. An essential role of the JIP1 scaffold protein for JNK activation in adipose tissue. Genes Dev **18:**1976-80.

176. **Jahn, R., and T. C. Sudhof.** 1999. Membrane fusion and exocytosis. Annu Rev Biochem **68:**863-911.

177. **Jakob, C. A., P. Burda, J. Roth, and M. Aebi.** 1998. Degradation of misfolded endoplasmic reticulum glycoproteins in Saccharomyces cerevisiae is determined by a specific oligosaccharide structure. J Cell Biol **142:**1223-33.

178. **James, D. E.** 2005. MUNC-ing around with insulin action. J Clin Invest **115:**219-21.

179. **Jarosch, E., C. Taxis, C. Volkwein, J. Bordallo, D. Finley, D. H. Wolf, and T. Sommer.** 2002. Protein dislocation from the ER requires polyubiquitination and the AAA-ATPase Cdc48. Nat Cell Biol **4:**134-9.

180. **Jiang, H. Y., and R. C. Wek.** 2005. Phosphorylation of the {alpha}-Subunit of the Eukaryotic Initiation Factor-2 (eIF2{alpha}) Reduces Protein Synthesis and Enhances Apoptosis in Response to Proteasome Inhibition. J Biol Chem **280:**14189-202.

181. **Jiang, Z. Y., Q. L. Zhou, K. A. Coleman, M. Chouinard, Q. Boese, and M. P. Czech.** 2003. Insulin signaling through Akt/protein kinase B analyzed by small interfering RNA-mediated gene silencing. Proc Natl Acad Sci U S A **100:**7569-74.

182. **Jones, N., I. M. Blasutig, V. Eremina, J. M. Ruston, F. Bladt, H. Li, H. Huang, L. Larose, S. S. Li, T. Takano, S. E. Quaggin, and T. Pawson.** 2006. Nck adaptor proteins link nephrin to the actin cytoskeleton of kidney podocytes. Nature **440:**818-23.

183. **Jordan, M. S., A. L. Singer, and G. A. Koretzky.** 2003. Adaptors as central mediators of signal transduction in immune cells. Nat Immunol **4:**110-6.

184. **Jousse, C., S. Oyadomari, I. Novoa, P. Lu, Y. Zhang, H. P. Harding, and D. Ron.** 2003. Inhibition of a constitutive translation initiation factor 2alpha phosphatase, CReP, promotes survival of stressed cells. J Cell Biol **163:**767-75.

185. **Kahn, S. E., R. L. Hull, and K. M. Utzschneider.** 2006. Mechanisms linking obesity to insulin resistance and type 2 diabetes. Nature **444:**840-6.

186. **Kalil, K., and E. W. Dent.** 2005. Touch and go: guidance cues signal to the growth cone cytoskeleton. Curr Opin Neurobiol **15:**521-6.

187. **Kane, S., H. Sano, S. C. Liu, J. M. Asara, W. S. Lane, C. C. Garner, and G. E. Lienhard.** 2002. A method to identify serine kinase substrates. Akt phosphorylates a novel adipocyte protein with a Rab GTPase-activating protein (GAP) domain. J Biol Chem **277:**22115-8.

188. **Kanzaki, M., R. T. Watson, J. C. Hou, M. Stamnes, A. R. Saltiel, and J. E. Pessin.** 2002. Small GTP-binding protein TC10 differentially regulates two distinct populations of filamentous actin in 3T3L1 adipocytes. Mol Biol Cell **13:**2334-46.

189. **Kasuga, M., F. A. Karlsson, and C. R. Kahn.** 1982. Insulin stimulates the phosphorylation of the 95,000-dalton subunit of its own receptor. Science **215:**185-7.

190. **Katayama, T., K. Imaizumi, A. Honda, T. Yoneda, T. Kudo, M. Takeda, K. Mori, R. Rozmahel, P. Fraser, P. S. George-Hyslop, and M. Tohyama.** 2001. Disturbed activation of endoplasmic reticulum stress transducers by familial Alzheimer's disease-linked presenilin-1 mutations. J Biol Chem **276:**43446-54.

191. **Katayama, T., K. Imaizumi, N. Sato, K. Miyoshi, T. Kudo, J. Hitomi, T. Morihara, T. Yoneda, F. Gomi, Y. Mori, Y. Nakano, J. Takeda, T. Tsuda, Y. Itoyama, O. Murayama, A. Takashima, P. St George-Hyslop, M. Takeda, and M. Tohyama.** 1999. Presenilin-1 mutations downregulate the signalling pathway of the unfolded-protein response. Nat Cell Biol **1:**479-85.

192. **Katic, M., and C. R. Kahn.** 2005. The role of insulin and IGF-1 signaling in longevity. Cell Mol Life Sci **62:**320-43.

193. **Kaufman, R. J.** 2000. The double-stranded RNA-activated protein kinase PKR. In N. Sonenberg, J. W. B. Hershey and M. B. Mathews (ed.), Translational control of gene expression:503-527.

194. **Kavanaugh, W. M., and L. T. Williams.** 1994. An alternative to SH2 domains for binding tyrosine-phosphorylated proteins. Science **266:**1862-5.

195. **Kayo, T., and A. Koizumi.** 1998. Mapping of murine diabetogenic gene mody on chromosome 7 at D7Mit258 and its involvement in pancreatic islet and beta cell development during the perinatal period. J Clin Invest **101:**2112-8.

196. **Kazemi, S., Z. Mounir, D. Baltzis, J. F. Raven, S. Wang, J. L. Krishnamoorthy, O. Pluquet, J. Pelletier, and A. E. Koromilas.** 2007. A Novel Function of eIF2{alpha} Kinases as Inducers of the Phosphoinositide-3 Kinase Signaling Pathway. Mol Biol Cell. **9:**3635-44

197. **Kebache, S., E. Cardin, D. T. Nguyen, E. Chevet, and L. Larose.** 2004. Nck-1 Antagonizes the Endoplasmic Reticulum Stress-induced Inhibition of Translation. J Biol Chem **279:**9662-71.

198. **Kebache, S., D. Zuo, E. Chevet, and L. Larose.** 2002. Modulation of protein translation by Nck-1. Proc Natl Acad Sci U S A **99:**5406-11.

199. **Kedersha, N., and P. Anderson.** 2002. Stress granules: sites of mRNA triage that regulate mRNA stability and translatability. Biochem Soc Trans **30:**963-9.

200. **Kedersha, N., S. Chen, N. Gilks, W. Li, I. J. Miller, J. Stahl, and P. Anderson.** 2002. Evidence that ternary complex (eIF2-GTP-tRNA(i)(Met))-deficient preinitiation complexes are core constituents of mammalian stress granules. Mol Biol Cell **13:**195-210.

201. **Kenny, B., R. DeVinney, M. Stein, D. J. Reinscheid, E. A. Frey, and B. B. Finlay.** 1997. Enteropathogenic E. coli (EPEC) transfers its receptor for intimate adherence into mammalian cells. Cell **91:**511-20.

202. **Kesti, T., A. Ruppelt, J. H. Wang, M. Liss, R. Wagner, K. Tasken, and K. Saksela.** 2007. Reciprocal Regulation of SH3 and SH2 Domain Binding via Tyrosine Phosphorylation of a Common Site in CD3{epsilon}. J Immunol **179:**878-85.

203. **Kim, J. K., J. J. Fillmore, M. J. Sunshine, B. Albrecht, T. Higashimori, D. W. Kim, Z. X. Liu, T. J. Soos, G. W. Cline, W. R. O'Brien, D. R. Littman, and G. I. Shulman.** 2004. PKC-theta knockout mice are protected from fat-induced insulin resistance. J Clin Invest **114:**823-7.

204. **Kimata, Y., D. Oikawa, Y. Shimizu, Y. Ishiwata-Kimata, and K. Kohno.** 2004. A role for BiP as an adjustor for the endoplasmic reticulum stress-sensing protein Ire1. J Cell Biol **167:**445-56.

205. **Kimball, S. R., R. L. Horetsky, D. Ron, L. S. Jefferson, and H. P. Harding.** 2003. Mammalian stress granules represent sites of accumulation of stalled translation initiation complexes. Am J Physiol Cell Physiol **284:**C273-84.

206. **Kitamura, T., Y. Kitamura, K. Yonezawa, N. F. Totty, I. Gout, K. Hara, M. D. Waterfield, M. Sakaue, W. Ogawa, and M. Kasuga.** 1996. Molecular cloning of p125Nap1, a protein that associates with an SH3 domain of Nck. Biochem Biophys Res Commun **219:**509-14.

207. **Kobayashi, K., S. Kuroda, M. Fukata, T. Nakamura, T. Nagase, N. Nomura, Y. Matsuura, N. Yoshida-Kubomura, A. Iwamatsu, and K. Kaibuchi.** 1998. p140Sra-1 (specifically Rac1-associated protein) is a novel specific target for Rac1 small GTPase. J Biol Chem **273:**291-5.

208. **Kojima, E., A. TAKEUCHI, M. HANEDA, A. YAGI, T. HASEGAWA, K.-I. YAMAKI, K. TAKEDA, S. AKIRA, K. SHIMOKATA, and K.-I. ISOBE.** 2003. The function of GADD34 is a recovery from a shutoff of protein synthesis induced by ER stress: elucidation by GADD34-deficient mice FASEB J. **17:**1573-1575.

209. **Kondo, S., T. Murakami, K. Tatsumi, M. Ogata, S. Kanemoto, K. Otori, K. Iseki, A. Wanaka, and K. Imaizumi.** 2005. OASIS, a CREB/ATF-family member, modulates UPR signalling in astrocytes. Nat Cell Biol **7:**186-94.

210. **Kondo, S., A. Saito, S. Hino, T. Murakami, M. Ogata, S. Kanemoto, S. Nara, A. Yamashita, K. Yoshinaga, H. Hara, and K. Imaizumi.** 2007. BBF2H7, a novel transmembrane bZIP transcription factor, is a new type of endoplasmic reticulum stress transducer. Mol Cell Biol **27:**1716-29.

211. **Konstantinova, I., G. Nikolova, M. Ohara-Imaizumi, P. Meda, T. Kucera, K. Zarbalis, W. Wurst, S. Nagamatsu, and E. Lammert.** 2007. EphA-Ephrin-A-mediated beta cell communication regulates insulin secretion from pancreatic islets. Cell **129:**359-70.

212. **Koo, S. H., H. Satoh, S. Herzig, C. H. Lee, S. Hedrick, R. Kulkarni, R. M. Evans, J. Olefsky, and M. Montminy.** 2004. PGC-1 promotes insulin resistance in liver through PPAR-alpha-dependent induction of TRB-3. Nat Med **10:**530-4.

213. **Koopmans, S. J., L. Ohman, J. R. Haywood, L. J. Mandarino, and R. A. DeFronzo.** 1997. Seven days of euglycemic hyperinsulinemia induces insulin resistance for glucose metabolism but not hypertension, elevated catecholamine levels, or increased sodium retention in conscious normal rats. Diabetes **46:**1572-8.

214. **Koster, J. C., M. A. Permutt, and C. G. Nichols.** 2005. Diabetes and insulin secretion: the ATP-sensitive K+ channel (K ATP) connection. Diabetes **54:**3065-72.

215. **Koumenis, C., C. Naczki, M. Koritzinsky, S. Rastani, A. Diehl, N. Sonenberg, A. Koromilas, and B. G. Wouters.** 2002. Regulation of protein synthesis by hypoxia via activation of the endoplasmic reticulum kinase PERK and phosphorylation of the translation initiation factor eIF2alpha. Mol Cell Biol **22:**7405-16.

216. **Kozak, M.** 1989. The scanning model for translation: an update. J Cell Biol **108:**229-41.

217. **Kozutsumi, Y., M. Segal, K. Normington, M. J. Gething, and J. Sambrook.** 1988. The presence of malfolded proteins in the endoplasmic reticulum signals the induction of glucose-regulated proteins. Nature **332:**462-4.

218. **Kraniou, Y., D. Cameron-Smith, M. Misso, G. Collier, and M. Hargreaves.** 2000. Effects of exercise on GLUT-4 and glycogenin gene expression in human skeletal muscle. J Appl Physiol **88:**794-6.

219. **Kriz, W.** 2007. Ontogenetic development of the filtration barrier. Nephron Exp Nephrol **106:**e44-50.

220. **Kudo, T., T. Katayama, K. Imaizumi, Y. Yasuda, M. Yatera, M. Okochi, M. Tohyama, and M. Takeda.** 2002. The unfolded protein response is involved in the pathology of Alzheimer's disease. Ann N Y Acad Sci **977:**349-55.

221. **Kulkarni, R. N., M. Holzenberger, D. Q. Shih, U. Ozcan, M. Stoffel, M. A. Magnuson, and C. R. Kahn.** 2002. beta-cell-specific deletion of the Igf1 receptor leads to hyperinsulinemia and glucose intolerance but does not alter beta-cell mass. Nat Genet **31:**111-5.

222. **Ladiges, W. C., S. E. Knoblaugh, J. F. Morton, M. J. Korth, B. L. Sopher, C. R. Baskin, A. Macauley, A. G. Goodman, R. C. Leboeuf, and M. G. Katze.** 2005. Pancreatic {beta}-Cell Failure and Diabetes in Mice With a Deletion Mutation of the Endoplasmic Reticulum Molecular Chaperone Gene P58IPK. Diabetes **54:**1074-81.

223. **Lahdenpera, J., P. Kilpelainen, X. L. Liu, T. Pikkarainen, P. Reponen, V. Ruotsalainen, and K. Tryggvason.** 2003. Clustering-induced tyrosine phosphorylation of nephrin by Src family kinases. Kidney Int **64:**404-13.

224. **Latreille, M., and L. Larose.** 2006. Nck in a complex containing the catalytic subunit of protein phosphatase 1 regulates eukaryotic initiation factor 2alpha signaling and cell survival to endoplasmic reticulum stress. J Biol Chem **281:**26633-44.

225. **Lawe, D. C., C. Hahn, and A. J. Wong.** 1997. The Nck SH2/SH3 adaptor protein is present in the nucleus and associates with the nuclear protein SAM68. Oncogene **14:**223-31.

226. **Lee, A. H., G. C. Chu, N. N. Iwakoshi, and L. H. Glimcher.** 2005. XBP-1 is required for biogenesis of cellular secretory machinery of exocrine glands. Embo J **24:**4368-80.

227. **Lee, A. H., N. N. Iwakoshi, and L. H. Glimcher.** 2003. XBP-1 regulates a subset of endoplasmic reticulum resident chaperone genes in the unfolded protein response. Mol Cell Biol **23:**7448-59.

228. **Lee, C. H., W. Li, R. Nishimura, M. Zhou, A. G. Batzer, M. G. Myers, Jr., M. F. White, J. Schlessinger, and E. Y. Skolnik.** 1993. Nck associates with the SH2 domain-docking protein IRS-1 in insulin-stimulated cells. Proc Natl Acad Sci U S A **90:**11713-7.

229. **Lee, K., W. Tirasophon, X. Shen, M. Michalak, R. Prywes, T. Okada, H. Yoshida, K. Mori, and R. J. Kaufman.** 2002. IRE1-mediated unconventional mRNA splicing and S2P-mediated ATF6 cleavage merge to regulate XBP1 in signaling the unfolded protein response. Genes Dev **16:**452-66.

230. **Legate, K. R., E. Montanez, O. Kudlacek, and R. Fassler.** 2006. ILK, PINCH and parvin: the tIPP of integrin signalling. Nat Rev Mol Cell Biol **7:**20-31.

231. **Lehmann, J. M., G. Riethmuller, and J. P. Johnson.** 1990. Nck, a melanoma cDNA encoding a cytoplasmic protein consisting of the src homology units SH2 and SH3. Nucleic Acids Res **18:**1048.

232. **Lesniewski, L. A., S. E. Hosch, J. G. Neels, C. de Luca, M. Pashmforoush, C. N. Lumeng, S. H. Chiang, M. Scadeng, A. R. Saltiel, and J. M. Olefsky.** 2007. Bone marrow-specific Cap gene deletion protects against high-fat diet-induced insulin resistance. Nat Med **13:**455-62.

233. **Li, G., E. Rungger-Brandle, I. Just, J. C. Jonas, K. Aktories, and C. B. Wollheim.** 1994. Effect of disruption of actin filaments by Clostridium botulinum C2 toxin on insulin secretion in HIT-T15 cells and pancreatic islets. Mol Biol Cell **5:**1199-213.

234. **Li, H., S. Lemay, L. Aoudjit, H. Kawachi, and T. Takano.** 2004. SRC-family kinase Fyn phosphorylates the cytoplasmic domain of nephrin and modulates its interaction with podocin. J Am Soc Nephrol **15:**3006-15.

235. **Li, S., N. D. Covino, E. G. Stein, J. H. Till, and S. R. Hubbard.** 2003. Structural and biochemical evidence for an autoinhibitory role for tyrosine 984 in the juxtamembrane region of the insulin receptor. J Biol Chem **278:**26007-14.

236. **Li, S. S.** 2005. Specificity and versatility of SH3 and other proline-recognition domains: structural basis and implications for cellular signal transduction. Biochem J **390:**641-53.

237. **Li, W., J. Fan, and D. T. Woodley.** 2001. Nck/Dock: an adapter between cell surface receptors and the actin cytoskeleton. Oncogene **20:**6403-17.

238. **Li, W., P. Hu, E. Y. Skolnik, A. Ullrich, and J. Schlessinger.** 1992. The SH2 and SH3 domain-containing Nck protein is oncogenic and a common target for phosphorylation by different surface receptors. Mol Cell Biol **12:**5824-33.

239. **Li, W., and H. She.** 2000. The SH2 and SH3 adapter Nck: a two-gene family and a linker between tyrosine kinases and multiple signaling networks. Histol Histopathol **15:**947-55.

240. **Li, X., M. Meriane, I. Triki, M. Shekarabi, T. E. Kennedy, L. Larose, and N. Lamarche-Vane.** 2002. The adaptor protein Nck-1 couples the netrin-1 receptor DCC (deleted in colorectal cancer) to the activation of the small GTPase Rac1 through an atypical mechanism. J Biol Chem **277:**37788-97.

241. **Li, Y., T. J. Soos, X. Li, J. Wu, M. Degennaro, X. Sun, D. R. Littman, M. J. Birnbaum, and R. D. Polakiewicz.** 2004. Protein kinase C Theta inhibits insulin signaling by phosphorylating IRS1 at Ser(1101). J Biol Chem **279:**45304-7.

242. **Lilley, B. N., and H. L. Ploegh.** 2005. Multiprotein complexes that link dislocation, ubiquitination, and extraction of misfolded proteins from the endoplasmic reticulum membrane. Proc Natl Acad Sci U S A **102:**14296-301.

243. **Lim, M. A., H. Riedel, and F. Liu.** 2004. Grb10: more than a simple adaptor protein. Front Biosci **9:**387-403.

244. **Lin, W., S. L. Bailey, H. Ho, H. P. Harding, D. Ron, S. D. Miller, and B. Popko.** 2007. The integrated stress response prevents demyelination by protecting oligodendrocytes against immune-mediated damage. J Clin Invest **117:**448-56.

245. **Lipson, K. L., S. G. Fonseca, S. Ishigaki, L. X. Nguyen, E. Foss, R. Bortell, A. A. Rossini, and F. Urano.** 2006. Regulation of insulin biosynthesis in pancreatic beta cells by an endoplasmic reticulum-resident protein kinase IRE1. Cell Metab **4:**245-54.

246. **Liu, C. Y., M. Schroder, and R. J. Kaufman.** 2000. Ligand-independent dimerization activates the stress response kinases IRE1 and PERK in the lumen of the endoplasmic reticulum. J Biol Chem **275:**24881-5.

247. **Lommel, S., S. Benesch, K. Rottner, T. Franz, J. Wehland, and R. Kuhn.** 2001. Actin pedestal formation by enteropathogenic Escherichia coli and intracellular motility of Shigella flexneri are abolished in N-WASP-defective cells. EMBO Rep **2:**850-7.

248. **Lotti, L. V., L. Lanfrancone, E. Migliaccio, C. Zompetta, G. Pelicci, A. E. Salcini, B. Falini, P. G. Pelicci, and M. R. Torrisi.** 1996. Shc proteins are localized on endoplasmic reticulum membranes and are redistributed after tyrosine kinase receptor activation. Mol Cell Biol **16:**1946-54.

249. **Lu, J., E. B. O'Hara, B. A. Trieselmann, P. R. Romano, and T. E. Dever.** 1999. The Interferon-induced Double-stranded RNA-activated Protein Kinase PKR Will Phosphorylate Serine, Threonine, or Tyrosine at Residue 51 in Eukaryotic Initiation Factor 2alpha. J. Biol. Chem. **274:**32198-32203.

250. **Lu, P. D., H. P. Harding, and D. Ron.** 2004. Translation reinitiation at alternative open reading frames regulates gene expression in an integrated stress response. J. Cell Biol. **167:**27-33.

251. **Lu, P. D., C. Jousse, S. J. Marciniak, Y. Zhang, I. Novoa, D. Scheuner, R. J. Kaufman, D. Ron, and H. P. Harding.** 2004. Cytoprotection by pre-emptive conditional phosphorylation of translation initiation factor 2. Embo J **23:**169-79.

252. **Lu, R., P. Yang, P. O'Hare, and V. Misra.** 1997. Luman, a new member of the CREB/ATF family, binds to herpes simplex virus VP16-associated host cellular factor. Mol Cell Biol **17:**5117-26.

253. **Luo, S., P. Baumeister, S. Yang, S. F. Abcouwer, and A. S. Lee.** 2003. Induction of Grp78/BiP by translational block: activation of the Grp78 promoter by ATF4 through and upstream ATF/CRE site independent of the endoplasmic reticulum stress elements. J Biol Chem **278:**37375-85.

254. **Lussier, G., and L. Larose.** 1997. A casein kinase I activity is constitutively associated with Nck. J Biol Chem **272:**2688-94.

255. **Ma, K., K. M. Vattem, and R. C. Wek.** 2002. Dimerization and Release of Molecular Chaperone Inhibition Facilitate Activation of Eukaryotic Initiation Factor-2 Kinase in Response to Endoplasmic Reticulum Stress. J. Biol. Chem. **277:**18728-18735.

256. **Ma, Y., and L. M. Hendershot.** 2003. Delineation of a negative feedback regulatory loop that controls protein translation during endoplasmic reticulum stress. J Biol Chem **278:**34864-73.

257. **Ma, Y., Y. Lu, H. Zeng, D. Ron, W. Mo, and T. A. Neubert.** 2001. Characterization of phosphopeptides from protein digests using matrix-assisted laser desorption/ionization time-of-flight mass spectrometry and nanoelectrospray quadrupole time-of-flight mass spectrometry. Rapid Commun Mass Spectrom **15:**1693-700.

258. **Machesky, L. M., and R. H. Insall.** 1999. Signaling to actin dynamics. J Cell Biol **146:**267-72.

259. **Machida, K., and B. J. Mayer.** 2005. The SH2 domain: versatile signaling module and pharmaceutical target. Biochim Biophys Acta **1747:**1-25.

260. **Macias, M. J., M. Hyvonen, E. Baraldi, J. Schultz, M. Sudol, M. Saraste, and H. Oschkinat.** 1996. Structure of the WW domain of a kinase-associated protein complexed with a proline-rich peptide. Nature **382:**646-9.

261. **Macias, M. J., S. Wiesner, and M. Sudol.** 2002. WW and SH3 domains, two different scaffolds to recognize proline-rich ligands. FEBS Lett **513:**30-7.

262. **Manser, E., T. H. Loo, C. G. Koh, Z. S. Zhao, X. Q. Chen, L. Tan, I. Tan, T. Leung, and L. Lim.** 1998. PAK kinases are directly coupled to the PIX family of nucleotide exchange factors. Mol Cell **1:**183-92.

263. **Marciniak, S. J., L. Garcia-Bonilla, J. Hu, H. P. Harding, and D. Ron.** 2006. Activation-dependent substrate recruitment by the eukaryotic translation initiation factor 2 kinase PERK. J Cell Biol **172:**201-9.

264. **Marciniak, S. J., C. Y. Yun, S. Oyadomari, I. Novoa, Y. Zhang, R. Jungreis, K. Nagata, H. P. Harding, and D. Ron.** 2004. CHOP induces death by promoting protein synthesis and oxidation in the stressed endoplasmic reticulum. Genes Dev. **18:**3066-3077.

265. **Margolis, B., O. Silvennoinen, F. Comoglio, C. Roonprapunt, E. Skolnik, A. Ullrich, and J. Schlessinger.** 1992. High-efficiency expression/cloning of epidermal growth factor-receptor-binding proteins with Src homology 2 domains. Proc Natl Acad Sci U S A **89:**8894-8.

266. **Martin, S. K., R. Carroll, M. Benig, and D. F. Steiner.** 1994. Regulation by glucose of the biosynthesis of PC2, PC3 and proinsulin in (ob/ob) mouse islets of Langerhans. FEBS Lett **356:**279-82.

267. **Martin, S. S., T. Haruta, A. J. Morris, A. Klippel, L. T. Williams, and J. M. Olefsky.** 1996. Activated phosphatidylinositol 3-kinase is sufficient to mediate actin rearrangement and GLUT4 translocation in 3T3-L1 adipocytes. J Biol Chem **271:**17605-8.

268. **Masaki, T., M. Yoshida, and S. Noguchi.** 1999. Targeted disruption of CRE-binding factor TREB5 gene leads to cellular necrosis in cardiac myocytes at the embryonic stage. Biochem Biophys Res Commun **261:**350-6.

269. **Matschinsky, F. M., B. Glaser, and M. A. Magnuson.** 1998. Pancreatic beta-cell glucokinase: closing the gap between theoretical concepts and experimental realities. Diabetes **47:**307-15.

270. **Matsumoto, M., M. Minami, K. Takeda, Y. Sakao, and S. Akira.** 1996. Ectopic expression of CHOP (GADD153) induces apoptosis in M1 myeloblastic leukemia cells. FEBS Lett **395:**143-7.

271. **Mayer, B. J.** 2001. SH3 domains: complexity in moderation. J Cell Sci **114:**1253-63.

272. **Mayer, B. J., M. Hamaguchi, and H. Hanafusa.** 1988. A novel viral oncogene with structural similarity to phospholipase C. Nature **332:**272-5.

273. **McCarty, J. H.** 1998. The Nck SH2/SH3 adaptor protein: a regulator of multiple intracellular signal transduction events. Bioessays **20:**913-21.

274. **McCullough, K. D., J. L. Martindale, L. O. Klotz, T. Y. Aw, and N. J. Holbrook.** 2001. Gadd153 sensitizes cells to endoplasmic reticulum stress by down-regulating Bcl2 and perturbing the cellular redox state. Mol Cell Biol **21:**1249-59.

275. **Michael, M. D., R. N. Kulkarni, C. Postic, S. F. Previs, G. I. Shulman, M. A. Magnuson, and C. R. Kahn.** 2000. Loss of insulin signaling in hepatocytes leads to severe insulin resistance and progressive hepatic dysfunction. Mol Cell **6:**87-97.

276. **Miles, P. D., S. Li, M. Hart, O. Romeo, J. Cheng, A. Cohen, K. Raafat, A. R. Moossa, and J. M. Olefsky.** 1998. Mechanisms of insulin resistance in experimental hyperinsulinemic dogs. J Clin Invest **101:**202-11.

277. **Mohammadi, M., J. Schlessinger, and S. R. Hubbard.** 1996. Structure of the FGF receptor tyrosine kinase domain reveals a novel autoinhibitory mechanism. Cell **86:**577-87.

278. **Molero, J. C., T. E. Jensen, P. C. Withers, M. Couzens, H. Herzog, C. B. Thien, W. Y. Langdon, K. Walder, M. A. Murphy, D. D. Bowtell, D. E. James, and G. J. Cooney.** 2004. c-Cbl-deficient mice have reduced adiposity, higher energy expenditure, and improved peripheral insulin action. J Clin Invest **114:**1326-33.

279. **Moremen, K. W., and M. Molinari.** 2006. N-linked glycan recognition and processing: the molecular basis of endoplasmic reticulum quality control. Curr Opin Struct Biol **16:**592-9.

280. **Mori, K., W. Ma, M. J. Gething, and J. Sambrook.** 1993. A transmembrane protein with a cdc2+/CDC28-related kinase activity is required for signaling from the ER to the nucleus. Cell **74:**743-56.

281. **Morris, D. R., and A. P. Geballe.** 2000. Upstream open reading frames as regulators of mRNA translation. Mol Cell Biol **20:**8635-42.

282. **Mullins, R. D.** 2000. How WASP-family proteins and the Arp2/3 complex convert intracellular signals into cytoskeletal structures. Curr Opin Cell Biol **12:**91-6.

283. **Musacchio, A., M. Saraste, and M. Wilmanns.** 1994. High-resolution crystal structures of tyrosine kinase SH3 domains complexed with proline-rich peptides. Nat Struct Biol **1:**546-51.

284. **Nakagawa, T., H. Zhu, N. Morishima, E. Li, J. Xu, B. A. Yankner, and J. Yuan.** 2000. Caspase-12 mediates endoplasmic-reticulum-specific apoptosis and cytotoxicity by amyloid-beta. Nature **403:**98-103.

285. **Nawrocki, S. T., J. S. Carew, K. Dunner, Jr., L. H. Boise, P. J. Chiao, P. Huang, J. L. Abbruzzese, and D. J. McConkey.** 2005. Bortezomib inhibits PKR-like endoplasmic reticulum (ER) kinase and induces apoptosis via ER stress in human pancreatic cancer cells. Cancer Res **65:**11510-9.

286. **Nekrutenko, A., and J. He.** 2006. Functionality of unspliced XBP1 is required to explain evolution of overlapping reading frames. Trends Genet **22:**645-8.

287. **Nevins, A. K., and D. C. Thurmond.** 2005. A direct interaction between Cdc42 and vesicle-associated membrane protein 2 regulates SNARE-dependent insulin exocytosis. J Biol Chem **280:**1944-52.

288. **Nevins, A. K., and D. C. Thurmond.** 2006. Caveolin-1 functions as a novel Cdc42 guanine nucleotide dissociation inhibitor in pancreatic beta-cells. J Biol Chem **281:**18961-72.

289. **Nguyen, D. T., S. Kebache, A. Fazel, H. N. Wong, S. Jenna, A. Emadali, E. H. Lee, J. J. Bergeron, R. J. Kaufman, L. Larose, and E. Chevet.** 2004. Nck-dependent activation of extracellular signal-regulated kinase-1 and regulation of cell survival during endoplasmic reticulum stress. Mol Biol Cell **15:**4248-60.

290. **Nichols, C. G.** 2006. KATP channels as molecular sensors of cellular metabolism. Nature **440:**470-6.

291. **Nishitoh, H., A. Matsuzawa, K. Tobiume, K. Saegusa, K. Takeda, K. Inoue, S. Hori, A. Kakizuka, and H. Ichijo.** 2002. ASK1 is essential for endoplasmic reticulum stress-induced neuronal cell death triggered by expanded polyglutamine repeats. Genes Dev **16:**1345-55.

292. **Nissen, S. E., E. M. Tuzcu, P. Schoenhagen, T. Crowe, W. J. Sasiela, J. Tsai, J. Orazem, R. D. Magorien, C. O'Shaughnessy, and P. Ganz.** 2005. Statin therapy, LDL cholesterol, C-reactive protein, and coronary artery disease. N Engl J Med **352:**29-38.

293. **Nolen, B., S. Taylor, and G. Ghosh.** 2004. Regulation of protein kinases; controlling activity through activation segment conformation. Mol Cell **15:**661-75.

294. **Novoa, I., H. Zeng, H. P. Harding, and D. Ron.** 2001. Feedback Inhibition of the Unfolded Protein Response by GADD34-mediated Dephosphorylation of eIF2{alpha}. J. Cell Biol. **153:**1011-1022.

295. **Novoa, I., Y. Zhang, H. Zeng, R. Jungreis, H. P. Harding, and D. Ron.** 2003. Stress-induced gene expression requires programmed recovery from translational repression. Embo J **22:**1180-7.

296. **O'Loghlen, A., M. I. Perez-Morgado, M. Salinas, and M. E. Martin.** 2003. Reversible inhibition of the protein phosphatase 1 by hydrogen peroxide. Potential regulation of eIF2 alpha phosphorylation in differentiated PC12 cells. Arch Biochem Biophys **417:**194-202.

297. **Oda, Y., T. Okada, H. Yoshida, R. J. Kaufman, K. Nagata, and K. Mori.** 2006. Derlin-2 and Derlin-3 are regulated by the mammalian unfolded protein response and are required for ER-associated degradation. J Cell Biol **172:**383-93.

298. **Ogawa, S., Y. Kitao, and O. Hori.** 2007. Ischemia-induced neuronal cell death and stress response. Antioxid Redox Signal **9:**573-87.

299. **Oh, J., J. Reiser, and P. Mundel.** 2004. Dynamic (re)organization of the podocyte actin cytoskeleton in the nephrotic syndrome. Pediatr Nephrol **19:**130-7.

300. **Ohoka, N., S. Yoshii, T. Hattori, K. Onozaki, and H. Hayashi.** 2005. TRB3, a novel ER stress-inducible gene, is induced via ATF4-CHOP pathway and is involved in cell death. Embo J.**24**: 1243-55

301. **Oikawa, D., Y. Kimata, and K. Kohno.** 2007. Self-association and BiP dissociation are not sufficient for activation of the ER stress sensor Ire1. J Cell Sci **120:**1681-8.

302. **Okada, T., Y. Kawano, T. Sakakibara, O. Hazeki, and M. Ui.** 1994. Essential role of phosphatidylinositol 3-kinase in insulin-induced glucose transport and antilipolysis in rat adipocytes. Studies with a selective inhibitor wortmannin. J Biol Chem **269:**3568-73.

303. **Okamura, K., Y. Kimata, H. Higashio, A. Tsuru, and K. Kohno.** 2000. Dissociation of Kar2p/BiP from an ER sensory molecule, Ire1p, triggers the unfolded protein response in yeast. Biochem Biophys Res Commun **279:**445-50.

304. **Olefsky, J. M., W. T. Garvey, R. R. Henry, D. Brillon, S. Matthaei, and G. R. Freidenberg.** 1988. Cellular mechanisms of insulin resistance in non-insulin-dependent (type II) diabetes. Am J Med **85:**86-105.

305. **Omori, Y., J. Imai, M. Watanabe, T. Komatsu, Y. Suzuki, K. Kataoka, S. Watanabe, A. Tanigami, and S. Sugano.** 2001. CREB-H: a novel mammalian transcription factor belonging to the CREB/ATF family and functioning via the box-B element with a liver-specific expression. Nucleic Acids Res **29:**2154-62.

306. **Orlean, P., and A. K. Menon.** 2007. Thematic review series: lipid posttranslational modifications. GPI anchoring of protein in yeast and mammalian cells, or: how we learned to stop worrying and love glycophospholipids. J Lipid Res **48:**993-1011.

307. **Oyadomari, S., A. Koizumi, K. Takeda, T. Gotoh, S. Akira, E. Araki, and M. Mori.** 2002. Targeted disruption of the Chop gene delays endoplasmic reticulum stress-mediated diabetes. J Clin Invest **109:**525-32.

308. **Oyadomari, S., and M. Mori.** 2004. Roles of CHOP/GADD153 in endoplasmic reticulum stress. Cell Death Differ **11:**381-9.

309. **Oyadomari, S., K. Takeda, M. Takiguchi, T. Gotoh, M. Matsumoto, I. Wada, S. Akira, E. Araki, and M. Mori.** 2001. Nitric oxide-induced apoptosis in pancreatic beta cells is mediated by the endoplasmic reticulum stress pathway. Proc Natl Acad Sci U S A **98:**10845-50.

310. **Oyadomari, S., C. Yun, E. A. Fisher, N. Kreglinger, G. Kreibich, M. Oyadomari, H. P. Harding, A. G. Goodman, H. Harant, J. L. Garrison, J. Taunton, M. G. Katze, and D. Ron.** 2006. Cotranslocational degradation protects the stressed endoplasmic reticulum from protein overload. Cell **126:**727-39.

311. **Ozcan, U., Q. Cao, E. Yilmaz, A. H. Lee, N. N. Iwakoshi, E. Ozdelen, G. Tuncman, C. Gorgun, L. H. Glimcher, and G. S. Hotamisligil.** 2004. Endoplasmic reticulum stress links obesity, insulin action, and type 2 diabetes. Science **306:**457-61.

312. **Ozcan, U., E. Yilmaz, L. Ozcan, M. Furuhashi, E. Vaillancourt, R. O. Smith, C. Z. Gorgun, and G. S. Hotamisligil.** 2006. Chemical chaperones reduce ER stress and restore glucose homeostasis in a mouse model of type 2 diabetes. Science **313:**1137-40.

313. **Palmer, A., M. Zimmer, K. S. Erdmann, V. Eulenburg, A. Porthin, R. Heumann, U. Deutsch, and R. Klein.** 2002. EphrinB phosphorylation and reverse signaling: regulation by Src kinases and PTP-BL phosphatase. Mol Cell **9:**725-37.

314. **Pandey, A., D. F. Lazar, A. R. Saltiel, and V. M. Dixit.** 1994. Activation of the Eck receptor protein tyrosine kinase stimulates phosphatidylinositol 3-kinase activity. J Biol Chem **269:**30154-7.

315. **Park, D., and S. G. Rhee.** 1992. Phosphorylation of Nck in response to a variety of receptors, phorbol myristate acetate, and cyclic AMP. Mol Cell Biol **12:**5816-23.

316. **Paschen, W.** 2001. Dependence of vital cell function on endoplasmic reticulum calcium levels: implications for the mechanisms underlying neuronal cell injury in different pathological states. Cell Calcium **29:**1-11.

317. **Patil, C., and P. Walter.** 2001. Intracellular signaling from the endoplasmic reticulum to the nucleus: the unfolded protein response in yeast and mammals. Curr Opin Cell Biol **13:**349-55.

318. **Paul, A., K. W. Ko, L. Li, V. Yechoor, M. A. McCrory, A. J. Szalai, and L. Chan.** 2004. C-reactive protein accelerates the progression of atherosclerosis in apolipoprotein E-deficient mice. Circulation **109:**647-55.

319. **Pawson, T.** 2004. Specificity in signal transduction: from phosphotyrosine-SH2 domain interactions to complex cellular systems. Cell **116:**191-203.

320. **Pawson, T., G. D. Gish, and P. Nash.** 2001. SH2 domains, interaction modules and cellular wiring. Trends Cell Biol **11:**504-11.

321. **Pawson, T., and P. Nash.** 2003. Assembly of cell regulatory systems through protein interaction domains. Science **300:**445-52.

322. **Pessin, J. E., D. C. Thurmond, J. S. Elmendorf, K. J. Coker, and S. Okada.** 1999. Molecular basis of insulin-stimulated GLUT4 vesicle trafficking. Location! Location! Location! J Biol Chem **274:**2593-6.

323. **Petruzzelli, L. M., S. Ganguly, C. J. Smith, M. H. Cobb, C. S. Rubin, and O. M. Rosen.** 1982. Insulin activates a tyrosine-specific protein kinase in extracts of 3T3-L1 adipocytes and human placenta. Proc Natl Acad Sci U S A **79:**6792-6.

324. **Peyot, M. L., C. J. Nolan, K. Soni, E. Joly, R. Lussier, B. E. Corkey, S. P. Wang, G. A. Mitchell, and M. Prentki.** 2004. Hormone-sensitive lipase has a role in lipid signaling for insulin secretion but is nonessential for the incretin action of glucagon-like peptide 1. Diabetes **53:**1733-42.

325. **Phillips, N., R. D. Hayward, and V. Koronakis.** 2004. Phosphorylation of the enteropathogenic E. coli receptor by the Src-family kinase c-Fyn triggers actin pedestal formation. Nat Cell Biol **6:**618-25.

326. **Piper, M., and C. Holt.** 2004. RNA translation in axons. Annu Rev Cell Dev Biol **20:**505-23.

327. **Plemper, R. K., and D. H. Wolf.** 1999. Retrograde protein translocation: ERADication of secretory proteins in health and disease. Trends Biochem Sci **24:**266-70.

328. **Pomar, N., J. J. Berlanga, S. Campuzano, G. Hernandez, M. Elias, and C. de Haro.** 2003. Functional characterization of Drosophila melanogaster PERK eukaryotic initiation factor 2alpha (eIF2a) kinase. European Journal of Biochemistry **270:**293-306.

329. **Posner, B. I., R. Faure, J. W. Burgess, A. P. Bevan, D. Lachance, G. Zhang-Sun, I. G. Fantus, J. B. Ng, D. A. Hall, and B. S. Lum.** 1994. Peroxovanadium compounds. A new class of potent phosphotyrosine phosphatase inhibitors which are insulin mimetics. J. Biol. Chem. **269:**4596-4604.

330. **Prostko, C. R., M. A. Brostrom, and C. O. Brostrom.** 1993. Reversible phosphorylation of eukaryotic initiation factor 2 alpha in response to endoplasmic reticular signaling. Mol Cell Biochem **127-128:**255-65.

331. **Proud, C. G.** 2005. eIF2 and the control of cell physiology. Semin Cell Dev Biol **16:**3-12.

332. **Puthalakath, H., L. A. O'Reilly, P. Gunn, L. Lee, P. N. Kelly, N. D. Huntington, P. D. Hughes, E. M. Michalak, J. McKimm-Breschkin, N. Motoyama, T. Gotoh, S. Akira, P. Bouillet, and A. Strasser.** 2007. ER stress triggers apoptosis by activating BH3-only protein Bim. Cell **129:**1337-49.

333. **Rabinovich, E., A. Kerem, K. U. Frohlich, N. Diamant, and S. Bar-Nun.** 2002. AAA-ATPase p97/Cdc48p, a cytosolic chaperone required for endoplasmic reticulum-associated protein degradation. Mol Cell Biol **22:**626-34.

334. **Rao, R. V., H. M. Ellerby, and D. E. Bredesen.** 2004. Coupling endoplasmic reticulum stress to the cell death program. Cell Death Differ **11:**372-80.

335. **Rao, Y., and S. L. Zipursky.** 1998. Domain requirements for the Dock adapter protein in growth- cone signaling. Proc Natl Acad Sci U S A **95:**2077-82.

336. **Reimold, A. M., A. Etkin, I. Clauss, A. Perkins, D. S. Friend, J. Zhang, H. F. Horton, A. Scott, S. H. Orkin, M. C. Byrne, M. J. Grusby, and L. H. Glimcher.** 2000. An essential role in liver development for transcription factor XBP-1. Genes Dev **14:**152-7.

337. **Reimold, A. M., N. N. Iwakoshi, J. Manis, P. Vallabhajosyula, E. Szomolanyi-Tsuda, E. M. Gravallese, D. Friend, M. J. Grusby, F. Alt, and L. H. Glimcher.** 2001. Plasma cell differentiation requires the transcription factor XBP-1. Nature **412:**300-7.

338. **Ren, R., B. J. Mayer, P. Cicchetti, and D. Baltimore.** 1993. Identification of a ten-amino acid proline-rich SH3 binding site. Science **259:**1157-61.

339. **Rhee, J., Y. Inoue, J. C. Yoon, P. Puigserver, M. Fan, F. J. Gonzalez, and B. M. Spiegelman.** 2003. Regulation of hepatic fasting response by PPARgamma coactivator-

1alpha (PGC-1): requirement for hepatocyte nuclear factor 4alpha in gluconeogenesis. Proc Natl Acad Sci U S A **100:**4012-7.

340. **Rhodes, C. J., and P. A. Halban.** 1987. Newly synthesized proinsulin/insulin and stored insulin are released from pancreatic B cells predominantly via a regulated, rather than a constitutive, pathway. J Cell Biol **105:**145-53.

341. **Riedel, H.** 2004. Grb10 exceeding the boundaries of a common signaling adapter. Front Biosci **9:**603-18.

342. **Rivera, G. M., C. A. Briceno, F. Takeshima, S. B. Snapper, and B. J. Mayer.** 2004. Inducible clustering of membrane-targeted SH3 domains of the adaptor protein Nck triggers localized actin polymerization. Curr Biol **14:**11-22.

343. **Rivero-Lezcano, O. M., A. Marcilla, J. H. Sameshima, and K. C. Robbins.** 1995. Wiskott-Aldrich syndrome protein physically associates with Nck through Src homology 3 domains. Mol Cell Biol **15:**5725-31.

344. **Rohatgi, R., H. Y. Ho, and M. W. Kirschner.** 2000. Mechanism of N-WASP activation by CDC42 and phosphatidylinositol 4, 5-bisphosphate. J Cell Biol **150:**1299-310.

345. **Rohatgi, R., L. Ma, H. Miki, M. Lopez, T. Kirchhausen, T. Takenawa, and M. W. Kirschner.** 1999. The interaction between N-WASP and the Arp2/3 complex links Cdc42-dependent signals to actin assembly. Cell **97:**221-31.

346. **Rohatgi, R., P. Nollau, H. Y. Ho, M. W. Kirschner, and B. J. Mayer.** 2001. Nck and phosphatidylinositol 4,5-bisphosphate synergistically activate actin polymerization through the N-WASP-Arp2/3 pathway. J Biol Chem **276:**26448-52.

347. **Rolland, F., J. Winderickx, and J. M. Thevelein.** 2001. Glucose-sensing mechanisms in eukaryotic cells. Trends Biochem Sci **26:**310-7.

348. **Romisch, K.** 2005. Endoplasmic reticulum-associated degradation. Annu Rev Cell Dev Biol **21:**435-56.

349. **Ron, D.** 2002. Translational control in the endoplasmic reticulum stress response. J Clin Invest **110:**1383-8.

350. **Rowlands, A. G., R. Panniers, and E. C. Henshaw.** 1988. The catalytic mechanism of guanine nucleotide exchange factor action and competitive inhibition by phosphorylated eukaryotic initiation factor 2. J Biol Chem **263:**5526-33.

351. **Rozelle, A. L., L. M. Machesky, M. Yamamoto, M. H. Driessens, R. H. Insall, M. G. Roth, K. Luby-Phelps, G. Marriott, A. Hall, and H. L. Yin.** 2000. Phosphatidylinositol 4,5-bisphosphate induces actin-based movement of raft-enriched vesicles through WASP-Arp2/3. Curr Biol **10:**311-20.

352. **Ruddock, L. W., and M. Molinari.** 2006. N-glycan processing in ER quality control. J Cell Sci **119:**4373-80.

353. **Rutkowski, D. T., S. M. Arnold, C. N. Miller, J. Wu, J. Li, K. M. Gunnison, K. Mori, A. A. Sadighi Akha, D. Raden, and R. J. Kaufman.** 2006. Adaptation to ER stress is mediated by differential stabilities of pro-survival and pro-apoptotic mRNAs and proteins. PLoS Biol **4:**e374.

354. **Rutkowski, D. T., S. W. Kang, A. G. Goodman, J. L. Garrison, J. Taunton, M. G. Katze, R. J. Kaufman, and R. S. Hegde.** 2007. The Role of p58IPK in Protecting the Stressed Endoplasmic Reticulum. Mol Biol Cell.

355. **Sadowski, I., J. C. Stone, and T. Pawson.** 1986. A noncatalytic domain conserved among cytoplasmic protein-tyrosine kinases modifies the kinase function and transforming activity of Fujinami sarcoma virus P130gag-fps. Mol Cell Biol **6:**4396-408.

356. **Saltiel, A. R.** 2001. New perspectives into the molecular pathogenesis and treatment of type 2 diabetes. Cell **104:**517-29.

357. **Saltiel, A. R., and C. R. Kahn.** 2001. Insulin signalling and the regulation of glucose and lipid metabolism. Nature **414:**799-806.

358. **Saltiel, A. R., and J. E. Pessin.** 2003. Insulin signaling in microdomains of the plasma membrane. Traffic **4:**711-6.

359. **Samelson, L. E.** 2002. Signal transduction mediated by the T cell antigen receptor: the role of adapter proteins. Annu Rev Immunol **20:**371-94.

360. **Santer, R., S. Groth, M. Kinner, A. Dombrowski, G. T. Berry, J. Brodehl, J. V. Leonard, S. Moses, S. Norgren, F. Skovby, R. Schneppenheim, B. Steinmann, and J. Schaub.** 2002. The mutation spectrum of the facilitative glucose transporter gene SLC2A2 (GLUT2) in patients with Fanconi-Bickel syndrome. Hum Genet **110:**21-9.

361. **Santer, R., R. Schneppenheim, A. Dombrowski, H. Gotze, B. Steinmann, and J. Schaub.** 1997. Mutations in GLUT2, the gene for the liver-type glucose transporter, in patients with Fanconi-Bickel syndrome. Nat Genet **17:**324-6.

362. **Sarbassov, D. D., D. A. Guertin, S. M. Ali, and D. M. Sabatini.** 2005. Phosphorylation and regulation of Akt/PKB by the rictor-mTOR complex. Science **307:**1098-101.

363. **Scaplehorn, N., A. Holmstrom, V. Moreau, F. Frischknecht, I. Reckmann, and M. Way.** 2002. Grb2 and Nck act cooperatively to promote actin-based motility of vaccinia virus. Curr Biol **12:**740-5.

364. **Scheper.** 2002. Does phosphorylation of the cap-binding protein eIF4E play a role in translation initiation? Eur. J. Biochem. **269:**- 5350-69.

365. **Scheuner, D., B. Song, E. McEwen, C. Liu, R. Laybutt, P. Gillespie, T. Saunders, S. Bonner-Weir, and R. J. Kaufman.** 2001. Translational Control Is Required for the Unfolded Protein Response and In Vivo Glucose Homeostasis. Molecular Cell **7:**1165-1176.

366. **Scheuner, D., D. Vander Mierde, B. Song, D. Flamez, J. W. Creemers, K. Tsukamoto, M. Ribick, F. C. Schuit, and R. J. Kaufman.** 2005. Control of mRNA translation preserves endoplasmic reticulum function in beta cells and maintains glucose homeostasis. Nat Med **11:**757-64.

367. **Schroder, M., and R. J. Kaufman.** 2005. The mammalian unfolded protein response. Annu Rev Biochem **74:**739-89.

368. **Schuller, S., Y. Chong, J. Lewin, B. Kenny, G. Frankel, and A. D. Phillips.** 2007. Tir phosphorylation and Nck/N-WASP recruitment by enteropathogenic and enterohaemorrhagic Escherichia coli during ex vivo colonization of human intestinal mucosa is different to cell culture models. Cell Microbiol **9:**1352-64.

369. **Schuppin, G. T., and C. J. Rhodes.** 1996. Specific co-ordinated regulation of PC3 and PC2 gene expression with that of preproinsulin in insulin-producing beta TC3 cells. Biochem J **313 (Pt 1):**259-68.

370. **Senee, V., K. M. Vattem, M. Delepine, L. A. Rainbow, C. Haton, A. Lecoq, N. J. Shaw, J.-J. Robert, R. Rooman, C. Diatloff-Zito, J. L. Michaud, B. Bin-Abbas, D. Taha, B. Zabel, P. Franceschini, A. K. Topaloglu, G. M. Lathrop, T. G. Barrett, M. Nicolino, R. C. Wek, and C. Julier.** 2004. Wolcott-Rallison Syndrome: Clinical, Genetic, and Functional Study of EIF2AK3 Mutations and Suggestion of Genetic Heterogeneity. Diabetes **53:**1876-1883.

371. **Sesti, G., M. Federici, M. L. Hribal, D. Lauro, P. Sbraccia, and R. Lauro.** 2001. Defects of the insulin receptor substrate (IRS) system in human metabolic disorders. Faseb J **15:**2099-111.

372. **Shamu, C. E., and P. Walter.** 1996. Oligomerization and phosphorylation of the Ire1p kinase during intracellular signaling from the endoplasmic reticulum to the nucleus. Embo J **15:**3028-39.

373. **Sharma, P. M., K. Egawa, Y. Huang, J. L. Martin, I. Huvar, G. R. Boss, and J. M. Olefsky.** 1998. Inhibition of phosphatidylinositol 3-kinase activity by adenovirus-mediated gene transfer and its effect on insulin action. J Biol Chem **273:**18528-37.

374. **Shen, J., X. Chen, L. Hendershot, and R. Prywes.** 2002. ER stress regulation of ATF6 localization by dissociation of BiP/GRP78 binding and unmasking of Golgi localization signals. Dev Cell **3:**99-111.

375. **Shen, J., and R. Prywes.** 2005. ER stress signaling by regulated proteolysis of ATF6. Methods **35:**382-9.

376. **Shen, W., L. M. Scearce, J. E. Brestelli, N. J. Sund, and K. H. Kaestner.** 2001. Foxa3 (hepatocyte nuclear factor 3gamma) is required for the regulation of hepatic GLUT2 expression and the maintenance of glucose homeostasis during a prolonged fast. J Biol Chem **276:**42812-7.

377. **Sheth, U., and R. Parker.** 2003. Decapping and decay of messenger RNA occur in cytoplasmic processing bodies. Science **300:**805-8.

378. **Shi, Y., K. M. Vattem, R. Sood, J. An, J. Liang, L. Stramm, and R. C. Wek.** 1998. Identification and characterization of pancreatic eukaryotic initiation factor 2 alpha-subunit kinase, PEK, involved in translational control. Mol Cell Biol **18:**7499-509.

379. **Shintani, T., M. Ihara, H. Sakuta, H. Takahashi, I. Watakabe, and M. Noda.** 2006. Eph receptors are negatively controlled by protein tyrosine phosphatase receptor type O. Nat Neurosci **9:**761-9.

380. **Sifers, R. N., S. Brashears-Macatee, V. J. Kidd, H. Muensch, and S. L. Woo.** 1988. A frameshift mutation results in a truncated alpha 1-antitrypsin that is retained within the rough endoplasmic reticulum. J Biol Chem **263:**7330-5.

381. **Sinha, M. K., C. Raineri-Maldonado, C. Buchanan, W. J. Pories, C. Carter-Su, P. F. Pilch, and J. F. Caro.** 1991. Adipose tissue glucose transporters in NIDDM. Decreased levels of muscle/fat isoform. Diabetes **40:**472-7.

382. **Sokka, A. L., N. Putkonen, G. Mudo, E. Pryazhnikov, S. Reijonen, L. Khiroug, N. Belluardo, D. Lindholm, and L. Korhonen.** 2007. Endoplasmic reticulum stress inhibition protects against excitotoxic neuronal injury in the rat brain. J Neurosci **27:**901-8.

383. **Song, J., L. Wu, Z. Chen, R. A. Kohanski, and L. Pick.** 2003. Axons guided by insulin receptor in Drosophila visual system. Science **300:**502-5.

384. **Songyang, Z., S. E. Shoelson, M. Chaudhuri, G. Gish, T. Pawson, W. G. Haser, F. King, T. Roberts, S. Ratnofsky, R. J. Lechleider, and et al.** 1993. SH2 domains recognize specific phosphopeptide sequences. Cell **72:**767-78.

385. **Sood, R., A. C. Porter, K. Ma, L. A. Quilliam, and R. C. Wek.** 2000. Pancreatic eukaryotic initiation factor-2alpha kinase (PEK) homologues in humans, Drosophila melanogaster and Caenorhabditis elegans that mediate translational control in response to endoplasmic reticulum stress. Biochem J **346 Pt 2:**281-93.

386. **Sriburi, R., S. Jackowski, K. Mori, and J. W. Brewer.** 2004. XBP1: a link between the unfolded protein response, lipid biosynthesis, and biogenesis of the endoplasmic reticulum. J Cell Biol **167:**35-41.

387. **Stahl, M. L., C. R. Ferenz, K. L. Kelleher, R. W. Kriz, and J. L. Knopf.** 1988. Sequence similarity of phospholipase C with the non-catalytic region of src. Nature **332:**269-72.

388. **Stein, E., U. Huynh-Do, A. A. Lane, D. P. Cerretti, and T. O. Daniel.** 1998. Nck recruitment to Eph receptor, EphB1/ELK, couples ligand activation to c-Jun kinase. J Biol Chem **273:**1303-8.

389. **Steiner, D. F., D. Cunningham, L. Spigelman, and B. Aten.** 1967. Insulin biosynthesis: evidence for a precursor. Science **157:**697-700.

390. **Stephens, S. B., R. D. Dodd, J. W. Brewer, P. J. Lager, J. D. Keene, and C. V. Nicchitta.** 2005. Stable ribosome binding to the endoplasmic reticulum enables compartment-specific regulation of mRNA translation. Mol Biol Cell **16:**5819-31.

391. **Stirling, J., and P. O'Hare.** 2006. CREB4, a transmembrane bZip transcription factor and potential new substrate for regulation and cleavage by S1P. Mol Biol Cell **17:**413-26.

392. **Su, Q., S. Wang, D. Baltzis, L. K. Qu, A. H. Wong, and A. E. Koromilas.** 2006. Tyrosine phosphorylation acts as a molecular switch to full-scale activation of the eIF2alpha RNA-dependent protein kinase. Proc Natl Acad Sci U S A **103:**63-8.

393. **Sudol, M., and T. Hunter.** 2000. NeW wrinkles for an old domain. Cell **103:**1001-4.

394. **Szegezdi, E., S. E. Logue, A. M. Gorman, and A. Samali.** 2006. Mediators of endoplasmic reticulum stress-induced apoptosis. EMBO Rep **7:**880-5.

395. **Szymczak, A. L., C. J. Workman, D. Gil, S. Dilioglou, K. M. Vignali, E. Palmer, and D. A. Vignali.** 2005. The CD3epsilon proline-rich sequence, and its interaction with Nck, is not required for T cell development and function. J Immunol **175:**270-5.

396. **Tajiri, S., S. Oyadomari, S. Yano, M. Morioka, T. Gotoh, J. I. Hamada, Y. Ushio, and M. Mori.** 2004. Ischemia-induced neuronal cell death is mediated by the endoplasmic reticulum stress pathway involving CHOP. Cell Death Differ **11:**403-15.

397. **Takano, A., I. Usui, T. Haruta, J. Kawahara, T. Uno, M. Iwata, and M. Kobayashi.** 2001. Mammalian target of rapamycin pathway regulates insulin signaling via subcellular redistribution of insulin receptor substrate 1 and integrates nutritional signals and metabolic signals of insulin. Mol Cell Biol **21:**5050-62.

398. **Takenawa, T., and S. Suetsugu.** 2007. The WASP-WAVE protein network: connecting the membrane to the cytoskeleton. Nat Rev Mol Cell Biol **8:**37-48.

399. **Tamemoto, H., T. Kadowaki, K. Tobe, T. Yagi, H. Sakura, T. Hayakawa, Y. Terauchi, K. Ueki, Y. Kaburagi, S. Satoh, and et al.** 1994. Insulin resistance and growth retardation in mice lacking insulin receptor substrate-1. Nature **372:**182-6.

400. **Tan, S., N. Somia, P. Maher, and D. Schubert.** 2001. Regulation of Antioxidant Metabolism by Translation Initiation Factor 2{alpha}. J. Cell Biol. **152:**997-1006.

401. **Tang, X., A. Guilherme, A. Chakladar, A. M. Powelka, S. Konda, J. V. Virbasius, S. M. Nicoloro, J. Straubhaar, and M. P. Czech.** 2006. An RNA interference-based screen identifies MAP4K4/NIK as a negative regulator of PPARgamma, adipogenesis, and insulin-responsive hexose transport. Proc Natl Acad Sci U S A **103:**2087-92.

402. **Thuerauf, D. J., M. Marcinko, P. J. Belmont, and C. C. Glembotski.** 2007. Effects of the isoform-specific characteristics of ATF6alpha and ATF6beta on ER stress response gene expression and cell viability. J Biol Chem.**282:**22865-78

403. **Thuerauf, D. J., L. Morrison, and C. C. Glembotski.** 2004. Opposing roles for ATF6alpha and ATF6beta in endoplasmic reticulum stress response gene induction. J Biol Chem **279:**21078-84.

404. **Thuerauf, D. J., L. E. Morrison, H. Hoover, and C. C. Glembotski.** 2002. Coordination of ATF6-mediated transcription and ATF6 degradation by a domain that is shared with the viral transcription factor, VP16. J Biol Chem **277:**20734-9.

405. **Thurmond, D. C., M. Kanzaki, A. H. Khan, and J. E. Pessin.** 2000. Munc18c function is required for insulin-stimulated plasma membrane fusion of GLUT4 and insulin-responsive amino peptidase storage vesicles. Mol Cell Biol **20:**379-88.

406. **Ting, C. Y., and C. H. Lee.** 2007. Visual circuit development in Drosophila. Curr Opin Neurobiol **17:**65-72.

407. **Tirasophon, W., K. Lee, B. Callaghan, A. Welihinda, and R. J. Kaufman.** 2000. The endoribonuclease activity of mammalian IRE1 autoregulates its mRNA and is required for the unfolded protein response. Genes Dev **14:**2725-36.

408. **Tirasophon, W., A. A. Welihinda, and R. J. Kaufman.** 1998. A stress response pathway from the endoplasmic reticulum to the nucleus requires a novel bifunctional protein kinase/endoribonuclease (Ire1p) in mammalian†cells. Genes Dev. **12:**1812-1824.

409. **Travers, K. J., C. K. Patil, L. Wodicka, D. J. Lockhart, J. S. Weissman, and P. Walter.** 2000. Functional and genomic analyses reveal an essential coordination between the unfolded protein response and ER-associated degradation. Cell **101:**249-58.

410. **Tryggvason, K., J. Patrakka, and J. Wartiovaara.** 2006. Hereditary proteinuria syndromes and mechanisms of proteinuria. N Engl J Med **354:**1387-401.

411. **Tsiotra, P. C., and C. Tsigos.** 2006. Stress, the endoplasmic reticulum, and insulin resistance. Ann N Y Acad Sci **1083:**63-76.

412. **Tu, B. P., and J. S. Weissman.** 2004. Oxidative protein folding in eukaryotes: mechanisms and consequences. J Cell Biol **164:**341-6.

413. **Tu, Y., F. Li, S. Goicoechea, and C. Wu.** 1999. The LIM-only protein PINCH directly interacts with integrin-linked kinase and is recruited to integrin-rich sites in spreading cells. Mol Cell Biol **19:**2425-34.

414. **Tu, Y., F. Li, and C. Wu.** 1998. Nck-2, a novel Src homology2/3-containing adaptor protein that interacts with the LIM-only protein PINCH and components of growth factor receptor kinase-signaling pathways. Mol Biol Cell **9:**3367-82.

415. **Tu, Y., L. Liang, S. J. Frank, and C. Wu.** 2001. Src homology 3 domain-dependent interaction of Nck-2 with insulin receptor substrate-1. Biochem J **354:**315-22.

416. **Ullrich, A., J. R. Bell, E. Y. Chen, R. Herrera, L. M. Petruzzelli, T. J. Dull, A. Gray, L. Coussens, Y. C. Liao, M. Tsubokawa, and et al.** 1985. Human insulin receptor and its relationship to the tyrosine kinase family of oncogenes. Nature **313:**756-61.

417. **Um, S. H., F. Frigerio, M. Watanabe, F. Picard, M. Joaquin, M. Sticker, S. Fumagalli, P. R. Allegrini, S. C. Kozma, J. Auwerx, and G. Thomas.** 2004. Absence of S6K1 protects against age- and diet-induced obesity while enhancing insulin sensitivity. Nature **431:**200-5.

418. **Underhill, D. M., and H. S. Goodridge.** 2007. The many faces of ITAMs. Trends Immunol **28:**66-73.

419. **Unger, R. H.** 2003. Lipid overload and overflow: metabolic trauma and the metabolic syndrome. Trends Endocrinol Metab **14:**398-403.

420. **Urano, F., X. Wang, A. Bertolotti, Y. Zhang, P. Chung, H. P. Harding, and D. Ron.** 2000. Coupling of Stress in the ER to Activation of JNK Protein Kinases by Transmembrane Protein Kinase IRE1. Science **287:**664-666.

421. **van Huizen, R., J. L. Martindale, M. Gorospe, and N. J. Holbrook.** 2003. P58IPK, a novel endoplasmic reticulum stress-inducible protein and potential negative regulator of eIF2alpha signaling. J Biol Chem **278:**15558-64.

422. **Vanhaesebroeck, B., and D. R. Alessi.** 2000. The PI3K-PDK1 connection: more than just a road to PKB. Biochem J **346 Pt 3:**561-76.

423. **Vattem, K. M., and R. C. Wek.** 2004. Reinitiation involving upstream ORFs regulates ATF4 mRNA translation in mammalian cells. PNAS **101:**11269-11274.

424. **Vaynberg, J., T. Fukuda, K. Chen, O. Vinogradova, A. Velyvis, Y. Tu, L. Ng, C. Wu, and J. Qin.** 2005. Structure of an ultraweak protein-protein complex and its crucial role in regulation of cell morphology and motility. Mol Cell **17:**513-23.

425. **Velyvis, A., J. Vaynberg, Y. Yang, O. Vinogradova, Y. Zhang, C. Wu, and J. Qin.** 2003. Structural and functional insights into PINCH LIM4 domain-mediated integrin signaling. Nat Struct Biol **10:**558-64.

426. **Verma, R., I. Kovari, A. Soofi, D. Nihalani, K. Patrie, and L. B. Holzman.** 2006. Nephrin ectodomain engagement results in Src kinase activation, nephrin phosphorylation, Nck recruitment, and actin polymerization. J Clin Invest **116:**1346-59.

427. **Verma, R., B. Wharram, I. Kovari, R. Kunkel, D. Nihalani, K. K. Wary, R. C. Wiggins, P. Killen, and L. B. Holzman.** 2003. Fyn binds to and phosphorylates the kidney slit diaphragm component Nephrin. J Biol Chem **278:**20716-23.

428. **Vinson, C., M. Myakishev, A. Acharya, A. A. Mir, J. R. Moll, and M. Bonovich.** 2002. Classification of human B-ZIP proteins based on dimerization properties. Mol Cell Biol **22:**6321-35.

429. **Vlisidou, I., F. Dziva, R. M. La Ragione, A. Best, J. Garmendia, P. Hawes, P. Monaghan, S. A. Cawthraw, G. Frankel, M. J. Woodward, and M. P. Stevens.** 2006. Role of intimin-tir interactions and the tir-cytoskeleton coupling protein in the colonization of calves and lambs by Escherichia coli O157:H7. Infect Immun **74:**758-64.

430. **Voeltz, G. K., M. M. Rolls, and T. A. Rapoport.** 2002. Structural organization of the endoplasmic reticulum. EMBO Rep **3:**944-50.

431. **Vogel, S. N., K. A. Fitzgerald, and M. J. Fenton.** 2003. TLRs: differential adapter utilization by toll-like receptors mediates TLR-specific patterns of gene expression. Mol Interv **3:**466-77.

432. **Voges, D., P. Zwickl, and W. Baumeister.** 1999. The 26S proteasome: a molecular machine designed for controlled proteolysis. Annu Rev Biochem **68:**1015-68.

433. **Vorobieva, N., A. Protopopov, M. Protopopova, V. Kashuba, R. L. Allikmets, W. Modi, E. R. Zabarovsky, G. Klein, L. Kisselev, and A. Graphodatsky.** 1995. Localization of human ARF2 and NCK genes and 13 other NotI-linking clones to chromosome 3 by fluorescence in situ hybridization. Cytogenet Cell Genet **68:**91-4.

434. **Wahl, S., H. Barth, T. Ciossek, K. Aktories, and B. K. Mueller.** 2000. Ephrin-A5 induces collapse of growth cones by activating Rho and Rho kinase. J Cell Biol **149:**263-70.

435. **Waksman, G., S. E. Shoelson, N. Pant, D. Cowburn, and J. Kuriyan.** 1993. Binding of a high affinity phosphotyrosyl peptide to the Src SH2 domain: crystal structures of the complexed and peptide-free forms. Cell **72:**779-90.

436. **Wang, J., T. Takeuchi, S. Tanaka, S. K. Kubo, T. Kayo, D. Lu, K. Takata, A. Koizumi, and T. Izumi.** 1999. A mutation in the insulin 2 gene induces diabetes with severe pancreatic beta-cell dysfunction in the Mody mouse. J Clin Invest **103:**27-37.

437. **Wang, X. Z., H. P. Harding, Y. Zhang, E. M. Jolicoeur, M. Kuroda, and D. Ron.** 1998. Cloning of mammalian Ire1 reveals diversity in the ER stress responses. Embo J **17:**5708-17.

438. **Wang, X. Z., and D. Ron.** 1996. Stress-induced phosphorylation and activation of the transcription factor CHOP (GADD153) by p38 MAP Kinase. Science **272:**1347-9.

439. **Wang, Z., E. Oh, and D. C. Thurmond.** 2007. Glucose-stimulated Cdc42 signaling is essential for the second phase of insulin secretion. J Biol Chem **282:**9536-46.

440. **Watabe-Uchida, M., E. E. Govek, and L. Van Aelst.** 2006. Regulators of Rho GTPases in neuronal development. J Neurosci **26:**10633-5.

441. **Watson, R. T., M. Kanzaki, and J. E. Pessin.** 2004. Regulated membrane trafficking of the insulin-responsive glucose transporter 4 in adipocytes. Endocr Rev **25:**177-204.

442. **Webb, B. L., and C. G. Proud.** 1997. Eukaryotic initiation factor 2B (eIF2B). Int J Biochem Cell Biol **29:**1127-31.

443. **Wek, R. C., M. Ramirez, B. M. Jackson, and A. G. Hinnebusch.** 1990. Identification of positive-acting domains in GCN2 protein kinase required for translational activation of GCN4 expression. Mol Cell Biol **10:**2820-31.

444. **Welch, W. J., and C. R. Brown.** 1996. Influence of molecular and chemical chaperones on protein folding. Cell Stress Chaperones **1:**109-15.

445. **Welihinda, A. A., and R. J. Kaufman.** 1996. The unfolded protein response pathway in Saccharomyces cerevisiae. Oligomerization and trans-phosphorylation of Ire1p (Ern1p) are required for kinase activation. J Biol Chem **271:**18181-7.

446. **Withers, D. J., D. J. Burks, H. H. Towery, S. L. Altamuro, C. L. Flint, and M. F. White.** 1999. Irs-2 coordinates Igf-1 receptor-mediated beta-cell development and peripheral insulin signalling. Nat Genet **23:**32-40.

447. **Withers, D. J., J. S. Gutierrez, H. Towery, D. J. Burks, J. M. Ren, S. Previs, Y. Zhang, D. Bernal, S. Pons, G. I. Shulman, S. Bonner-Weir, and M. F. White.** 1998. Disruption of IRS-2 causes type 2 diabetes in mice. Nature **391:**900-4.

448. **Wolcott, C. D., and M. L. Rallison.** 1972. Infancy-onset diabetes mellitus and multiple epiphyseal dysplasia. J Pediatr **80:**292-7.

449. **Wong, W. L., M. A. Brostrom, G. Kuznetsov, D. Gmitter-Yellen, and C. O. Brostrom.** 1993. Inhibition of protein synthesis and early protein processing by thapsigargin in cultured cells. Biochem J **289 (Pt 1):**71-9.

450. **Wu, C.** 1999. Integrin-linked kinase and PINCH: partners in regulation of cell-extracellular matrix interaction and signal transduction. J Cell Sci **112 (Pt 24):**4485-9.

451. **Wu, D. Y., and D. J. Goldberg.** 1993. Regulated tyrosine phosphorylation at the tips of growth cone filopodia. J Cell Biol **123:**653-64.

452. **Wybenga-Groot, L. E., B. Baskin, S. H. Ong, J. Tong, T. Pawson, and F. Sicheri.** 2001. Structural basis for autoinhibition of the Ephb2 receptor tyrosine kinase by the unphosphorylated juxtamembrane region. Cell **106:**745-57.

453. **Xu, P., A. R. Jacobs, and S. I. Taylor.** 1999. Interaction of insulin receptor substrate 3 with insulin receptor, insulin receptor-related receptor, insulin-like growth factor-1 receptor, and downstream signaling proteins. J Biol Chem **274:**15262-70.

454. **Yan, W., C. L. Frank, M. J. Korth, B. L. Sopher, I. Novoa, D. Ron, and M. G. Katze.** 2002. Control of PERK eIF2alpha kinase activity by the endoplasmic reticulum stress-induced molecular chaperone P58IPK. Proc Natl Acad Sci U S A **99:**15920-5.

455. **Ye, J., R. B. Rawson, R. Komuro, X. Chen, U. P. Dave, R. Prywes, M. S. Brown, and J. L. Goldstein.** 2000. ER stress induces cleavage of membrane-bound ATF6 by the same proteases that process SREBPs. Mol Cell **6:**1355-64.

456. **Ye, Y., H. H. Meyer, and T. A. Rapoport.** 2001. The AAA ATPase Cdc48/p97 and its partners transport proteins from the ER into the cytosol. Nature **414:**652-6.

457. **Yoneda, T., K. Imaizumi, K. Oono, D. Yui, F. Gomi, T. Katayama, and M. Tohyama.** 2001. Activation of Caspase-12, an Endoplastic Reticulum (ER) Resident Caspase, through Tumor Necrosis Factor Receptor-associated Factor 2-dependent Mechanism in Response to the ER Stress. J. Biol. Chem. **276:**13935-13940.

458. **Yoshida, H., K. Haze, H. Yanagi, T. Yura, and K. Mori.** 1998. Identification of the cis-acting endoplasmic reticulum stress response element responsible for transcriptional induction of mammalian glucose-regulated proteins. Involvement of basic leucine zipper transcription factors. J Biol Chem **273:**33741-9.

459. **Yoshida, H., T. Matsui, N. Hosokawa, R. J. Kaufman, K. Nagata, and K. Mori.** 2003. A time-dependent phase shift in the mammalian unfolded protein response. Dev Cell **4:**265-71.

460. **Yoshida, H., T. Matsui, A. Yamamoto, T. Okada, and K. Mori.** 2001. XBP1 mRNA is induced by ATF6 and spliced by IRE1 in response to ER stress to produce a highly active transcription factor. Cell **107:**881-91.

461. **Yoshida, H., T. Okada, K. Haze, H. Yanagi, T. Yura, M. Negishi, and K. Mori.** 2000. ATF6 Activated by Proteolysis Binds in the Presence of NF-Y (CBF) Directly to the cis-Acting Element Responsible for the Mammalian Unfolded Protein Response. Mol. Cell. Biol. **20:**6755-6767.

462. **Yoshida, H., T. Okada, K. Haze, H. Yanagi, T. Yura, M. Negishi, and K. Mori.** 2001. Endoplasmic reticulum stress-induced formation of transcription factor complex ERSF including NF-Y (CBF) and activating transcription factors 6alpha and 6beta that activates the mammalian unfolded protein response. Mol Cell Biol **21:**1239-48.

463. **Yoshida, H., M. Oku, M. Suzuki, and K. Mori.** 2006. pXBP1(U) encoded in XBP1 pre-mRNA negatively regulates unfolded protein response activator pXBP1(S) in mammalian ER stress response. J Cell Biol **172:**565-75.

464. **Yoshioka, M., T. Kayo, T. Ikeda, and A. Koizumi.** 1997. A novel locus, Mody4, distal to D7Mit189 on chromosome 7 determines early-onset NIDDM in nonobese C57BL/6 (Akita) mutant mice. Diabetes **46:**887-94.

465. **Yu, H., J. K. Chen, S. Feng, D. C. Dalgarno, A. W. Brauer, and S. L. Schreiber.** 1994. Structural basis for the binding of proline-rich peptides to SH3 domains. Cell **76:**933-45.

466. **Yuan, M., N. Konstantopoulos, J. Lee, L. Hansen, Z. W. Li, M. Karin, and S. E. Shoelson.** 2001. Reversal of obesity- and diet-induced insulin resistance with salicylates or targeted disruption of Ikkbeta. Science **293:**1673-7.

467. **Yusta, B., L. L. Baggio, J. L. Estall, J. A. Koehler, D. P. Holland, H. Li, D. Pipeleers, Z. Ling, and D. J. Drucker.** 2006. GLP-1 receptor activation improves beta cell function and survival following induction of endoplasmic reticulum stress. Cell Metab **4:**391-406.

468. **Zeng, R., J. L. Cannon, R. T. Abraham, M. Way, D. D. Billadeau, J. Bubeck-Wardenberg, and J. K. Burkhardt.** 2003. SLP-76 coordinates Nck-dependent Wiskott-Aldrich syndrome protein recruitment with Vav-1/Cdc42-dependent Wiskott-Aldrich syndrome protein activation at the T cell-APC contact site. J Immunol **171:**1360-8.

469. **Zhande, R., J. J. Mitchell, J. Wu, and X. J. Sun.** 2002. Molecular mechanism of insulin-induced degradation of insulin receptor substrate 1. Mol Cell Biol **22:**1016-26.

470. **Zhang, K., X. Shen, J. Wu, K. Sakaki, T. Saunders, D. T. Rutkowski, S. H. Back, and R. J. Kaufman.** 2006. Endoplasmic reticulum stress activates cleavage of CREBH to induce a systemic inflammatory response. Cell **124:**587-99.

471. **Zhang, K., H. N. Wong, B. Song, C. N. Miller, D. Scheuner, and R. J. Kaufman.** 2005. The unfolded protein response sensor IRE1alpha is required at 2 distinct steps in B cell lymphopoiesis. J Clin Invest **115:**268-81.

472. **Zhang, P., B. McGrath, S. Li, A. Frank, F. Zambito, J. Reinert, M. Gannon, K. Ma, K. McNaughton, and D. R. Cavener.** 2002. The PERK eukaryotic initiation factor 2 alpha kinase is required for the development of the skeletal system, postnatal growth, and the function and viability of the pancreas. Mol Cell Biol **22:**3864-74.

473. **Zhang, W., D. Feng, Y. Li, K. Iida, B. McGrath, and D. R. Cavener.** 2006. PERK EIF2AK3 control of pancreatic beta cell differentiation and proliferation is required for postnatal glucose homeostasis. Cell Metab **4:**491-7.

474. **Zhou, J., C. Y. Liu, S. H. Back, R. L. Clark, D. Peisach, Z. Xu, and R. J. Kaufman.** 2006. The crystal structure of human IRE1 luminal domain reveals a conserved dimerization interface required for activation of the unfolded protein response. PNAS **103:**14343-14348.

475. **Zhu, S., A. Y. Sobolev, and R. C. Wek.** 1996. Histidyl-tRNA Synthetase-related Sequences in GCN2 Protein Kinase Regulate in Vitro Phosphorylation of eIF-2. J. Biol. Chem. **271:**24989-24994.

476. **Zinszner, H., M. Kuroda, X. Wang, N. Batchvarova, R. T. Lightfoot, H. Remotti, J. L. Stevens, and D. Ron.** 1998. CHOP is implicated in programmed cell death in response to impaired function of the endoplasmic reticulum. Genes Dev. **12:**982-995.

APPENDIX 1

Reprints

THE JOURNAL OF BIOLOGICAL CHEMISTRY VOL. 281, NO. 36, pp. 26633–26644, September 8, 2006

Nck in a Complex Containing the Catalytic Subunit of Protein Phosphatase 1 Regulates Eukaryotic Initiation Factor 2α Signaling and Cell Survival to Endoplasmic Reticulum Stress*

Received for publication, December 21, 2005, and in revised form, July 10, 2006 Published, JBC Papers in Press, July 11, 2006, DOI 10.1074/jbc.M513556200

Mathieu Latreille[1] **and Louise Larose**[2]

From the Polypeptide Hormone Laboratory, Department of Medicine, McGill University, Montreal, Quebec H3A 2B2, Canada

Stress imposed on the endoplasmic reticulum (ER) induces the phosphorylation of the α-subunit of the eukaryotic initiation factor 2 (eIF2) on Ser[51]. This results in transient inhibition of general translation initiation while concomitantly activating a signaling pathway that promotes the expression of genes whose products improve ER function. Conversely, dephosphorylation of eIF2αSer[51] is accomplished by protein phosphatase 1 (PP1c) complexes containing either the protein CReP or GADD34, which target PP1c to eIF2. Here, we demonstrate that the Src homology (SH) domain-containing adaptor Nck is a key component of a molecular complex that controls eIF2α phosphorylation and signaling in response to ER stress. We show that overexpression of Nck decreases basal and ER stress-induced eIF2α phosphorylation and the attendant induction of ATF4 and CHOP. In contrast, we demonstrate that the mouse embryonic fibroblasts lacking both isoforms of Nck (Nck1$^{-/-}$Nck2$^{-/-}$) show higher levels of eIF2α phosphorylation and premature induction of ATF4, CHOP, and GADD34 in response to ER stress and finally, are more resistant to cell death induced by prolonged ER stress conditions. We establish that a significant amount of Nck protein localizes at the ER and is in a complex with eIF2 subunits. Further analysis of this complex revealed that it also contains the Ser/Thr phosphatase PP1c, its regulatory subunit CReP, and dephosphorylates eIF2α on Ser[51] *in vitro*. Overall, we demonstrate that Nck as a component of the CReP/PP1c holophosphatase complex contributes to maintain eIF2α in a hypophosphorylated state. In this manner, Nck modulates translation and eIF2α signaling in response to ER stress.

Nck is part of a family of adaptor proteins composed almost exclusively of a Src homology 2 (SH2)[3] and 3 (SH3) domains (1). Like other members of this family, Nck is believed to couple activated receptor tyrosine kinases at the plasma membrane and/or their substrates to downstream effectors through its various SH domains (2). In the past decade, identification of molecules interacting with the different SH domains of Nck has mainly implicated this adaptor in signaling processes regulating actin cytoskeleton reorganization (2–4). In mammals, separate genes encode two Nck molecules (Nck-1 and Nck-2) with 68% amino acid identity (5–7). Although we cannot totally exclude specific roles for each Nck isoform, their functional redundancy was demonstrated by the knock-out of either Nck in mice, which did not present any particular phenotype (8). Nonetheless, early embryonic lethality (9.5 days) of the double Nck knock-out has revealed a crucial role for this adaptor during development (8).

In a previous study, we uncovered a novel function for Nck in modulating mRNA translation at the level of initiation through its direct interaction with the β-subunit of the eukaryotic initiation factor 2 (eIF2) (9). eIF2 is a heterotrimeric complex (α-, β-, and γ-subunit) that in part drives the initiation of mRNA translation by carrying out the delivery of the methionyl-initiator tRNA to the 40 S ribosomal subunit (10). Various cellular insults are known to reduce protein synthesis at the level of initiation by inhibiting the activity of eIF2 through the phosphorylation of its α-subunit on Ser[51] by a family of Ser/Thr kinases, so called eIF2α kinases (11). This prevents recycling of eIF2 into its active GTP-bound form by the nucleotide exchange factor eIF2B, thereby transiently inhibiting general mRNA translation (12). To date, four eIF2α kinases have been identified: 1) HRI (heme-regulated inhibitor), which couples mRNA translation with heme availability in erythroid cells (13), 2) GCN2 (general control non-derepressible-2), which is activated in response to amino acid deprivation (14), 3) PKR (double-stranded RNA-activated protein kinase), a component of the antiviral response activated by double-strand RNA (15), and 4) PERK (PKR-like endoplasmic reticulum kinase), a type 1 transmembrane protein resident of the endoplasmic reticulum (ER) and activated upon accumulation of improperly folded secretory proteins (referred as to ER stress) (16, 17). In this later condition, attenuation of translation due to eIF2α phosphorylation on Ser[51] limits the influx of new proteins into the ER and prevents further buildup of unfolded proteins. On the other hand, reduced eIF2 activity allows the selective translational up-regulation of the mRNA encoding the stress-regulated tran-

* This work was supported by a grant (to L. L.) from the Canadian Diabetes Association in honor of the late Lilian I. Dale. The costs of publication of this article were defrayed in part by the payment of page charges. This article must therefore be hereby marked "*advertisement*" in accordance with 18 U.S.C. Section 1734 solely to indicate this fact.

[1] Supported by a fellowship from Fond de la Recherche en Santé du Québec.

[2] Supported by an award from the Fond de la Recherche en Santé du Québec.
To whom correspondence should be addressed: Polypeptide Laboratory, McGill University, Strathcona Bldg. 3640 University St., Rm. W315 Montreal, Quebec, Canada H3A 2B2. Tel.: 514-398-5844; Fax: 514-398-3923; E-mail: louise.larose@mcgill.ca.

[3] The abbreviations used are: SH, Src homology; eIF2, eukaryotic initiation factor 2; PERK, PKR-like endoplasmic reticulum kinase; ER, endoplasmic reticulum; Tg, thapsigargin; TRITC, tetramethylrhodamine isothiocyanate; PP, protein phosphatase; ISR, integrated stress response; UPR, unfolded protein response; Tg, thapsigargin; MEF, mouse embryonic fibroblast; Tn, tunicamycin; HA, hemagglutinin; PBS, phosphate-buffered saline; WT, wild type.

scription factor ATF4 (16, 18) via a mechanism involving initiation at upstream open reading frames and reinitiation at the downstream ATF4 start codon (19, 20). ATF4 controls a transcriptional program that accounts for the increase in amino acid transporter and redox protein expression observed during ER stress. In this manner, ATF4 contributes to preserve ER homeostasis in stress conditions (21, 22). Among other genes regulated by ATF4 is GADD34, which coordinates the recovery of protein synthesis by interacting with the catalytic subunit of protein phosphatase 1 (PP1c) and targeting PP1c toward eIF2 to promote eIF2α dephosphorylation (23). On the other hand, prolonged ER stress conditions were found to induce programmed cell death (apoptosis) in part through the ATF4-mediated induction of the CHOP/GADD153 gene, a transcriptional activator of the C/EBP protein family with pro-apoptotic properties (for review, see Ref. 24). CHOP is believed to promote the death of stress cells by increasing the load and oxidation of client proteins in the ER through the up-regulation of GADD34 and ERO1α, respectively (25). Together these events downstream of eIF2α phosphorylation occur in response to a broad range of stress conditions and therefore, are referred as the integrated stress response (ISR).

In concert with activation of PERK, ER stress also activates two other ER-resident transmembrane proteins, IRE1 (26) and ATF6 (27). IRE1 is a type-I transmembrane Ser/Thr protein kinase with ribonuclease activity that splices the XBP-1 mRNA (28). The spliced XBP-1 mRNA encodes a transcription factor that migrates to the nucleus where it up-regulates a subset of genes that contribute to overcome damage at the ER (29). On the other hand, ATF6 activation occurs via proteolytic cleavage, which like XBP-1 splicing, generates a functional transcriptional regulator (30, 31). Together, IRE1 and ATF6 transduce signals leading to the up-regulation of genes encoding ER chaperones such as BiP/Grp78 and degrading enzymes, which enhance ER function and alleviate ER stress. Collectively, these events are integrated in a cellular response called the unfolded protein response (UPR), which protects cells against the deleterious effects of proteotoxicity in the ER. Functional defects in some players of the UPR have been associated with metabolic or neurologic pathological manifestations. For example, patients affected by the Wolcott-Rallison syndrome, which results in neonatal insulin-dependent diabetes, show mutations in the PERK/EIF2AK3 gene (32). Similarly, mice lacking expression of PERK (33) or harboring an eIF2α that escapes phosphorylation (eIF2α Ser^{51} for Ala) (18) further illustrate a central role for PERK and eIF2α phosphorylation in pancreatic β-cells function.

We recently provided strong evidence that Nck has an essential function in regulating the UPR (34, 35). We demonstrated that overexpression of Nck strongly impairs cell survival to thapsigargin (Tg), a pharmacological inducer of ER stress, by preventing phosphorylation of eIF2αSer^{51} and attenuation of translation that normally occur in these conditions (34). In parallel, we also showed that Nck regulates IRE1-mediated ERK-1 activation in response to the protein misfolding inducer azetidine-2-carboxylic acid (35). In the present study we further exemplify the concept that Nck regulates signaling from the ER by showing that mouse embryonic fibroblasts (MEFs) deleted of Nck ($Nck1^{-/-}Nck2^{-/-}$) present increased eIF2α phosphorylation levels and expression of numerous stress-induced genes. We observed that these cells induce faster and to a higher extent various components of the eIF2α-dependent arm of the UPR and cope better with ER stress. We provide various lines of evidence demonstrating that Nck, as an adaptor protein, assembles a molecular complex containing the Ser/Thr phosphatase PP1c, its regulatory subunit CReP, and components of eIF2. From these, we conclude that Nck, by being a component of an eIF2α holophosphatase complex, significantly contributes to accurate control of eIF2α phosphorylation and eIF2-dependent signaling in response to ER stress. Finally, our study sheds light on a potential mechanism by which Nck adaptors regulate initiation of translation.

EXPERIMENTAL PROCEDURES

Cells—HeLa cells were cultured at 37 °C in 5% CO_2 in minimal essential Eagle's medium (Sigma) containing 10% fetal bovine serum (Invitrogen), whereas Dulbecco's modified Eagle's medium (Invitrogen) was used for MEFs and HEK293 cells. Tg (Sigma), tunicamycin (Tn, Sigma), or hydrogen peroxide (H_2O_2, Sigma) treatments were as indicated.

Antibodies—Protein A-purified pan-Nck (1793) and eIF2β (2087) antibodies were previously described (9, 36). Nck (C-19), eIF2α (Fl-315), eIF2β (P-3), CREB2/ATF4 (C-20), GADD34 (H-193), Gadd153/CHOP (F-168), and PP1 (E-9) antibodies were from Santa Cruz. $Ser(P)^{51}$ eIF2α antibody was from BioSource International. The KDEL antibody (10C3) that detects Grp94 and BiP was from Stressgen. Calnexin (clone 37) antibody was from BD Transduction Laboratories. Caspase-3 (9662) and poly(ADP-ribose) polymerase (9542) antibodies were from Cell Signaling. β-Actin antibody (AC-74) and anti-rabbit IgG fluorescein isothiocyanate-conjugated and anti-mouse IgG TRITC-conjugated antibodies were from Sigma.

Constructs, Transfection, and Luciferase Assays—Human HA-tagged Nck1 and Nck2 constructs generously provided by Dr. Wei Li were described previously (37). FLAG-tagged mCReP (amino acids 24–698) (38), mGADD34 (39), and the ATF4-Luc reporter gene (21) were from Dr. David Ron. Green fluorescent protein-tagged human Nck1 and Nck2 constructs were generated by subcloning the respective Nck cDNAs into pEGFP-C1 (Clontech) using appropriate enzyme restriction digestions. For transfection, cells plated in 60-mm dishes (3×10^5 cells) or 100-mm dishes (1×10^6 cells) were transiently transfected the following day using Lipofectamine Plus reagent (Invitrogen) according to the manufacturer's instructions. The amount of plasmid used was normalized with corresponding empty plasmid. For luciferase assays, 0.5 μg of the ATF4-Luc reporter gene was used in transient transfection of MEFs. The following day, cell lysates prepared in passive lysis buffer (Promega) and normalized for protein content were used (in triplicates) to assess luciferase activity using the luciferase assay system (Promega).

Western Blot—MEFs plated in 100-mm dishes (1×10^6 cells) and treated the next day with ER stressors at 37 °C were washed in ice-cold phosphate-buffered saline (PBS) and lysed in radioimmune precipitation assay buffer (50 mM HEPES, pH 7.4, 150 mM NaCl, 10% glycerol, 1% Triton X-100, 0.1% SDS, 1% sodium

deoxycholate, 1.5 mM $MgCl_2$, 1 mM EGTA, 10 mM sodium pyrophosphate, 1 mM sodium orthovanadate, 100 mM sodium fluoride, 17.5 mM β-glycerophosphate) containing protease inhibitors (2 μg ml^{-1} leupeptin, 4 μg ml^{-1} aprotinin, 1 mM benzamidine, 100 μg ml^{-1} Pefabloc SC PLUS). Cell lysates were passed through a 26-gauge syringe and clarified by centrifugation. For immunoprecipitation, cell lysates were prepared in lysis buffer (10 mM Tris-HCl, pH 7.5, 50 mM KCl, 2 mM $MgCl_2$, 1% Triton X-100, and 1 mM dithiothreitol, supplemented with protease inhibitors). 30–50 μg of proteins from clarified cell lysates were resolved on 10% SDS-PAGE, except for GADD34, where 8% gels were used. Proteins transferred onto polyvinylidene difluoride membranes were subjected to Western blots using specific antibodies and signals detected with enhanced chemiluminescence according to the manufacturer's specification.

Immunofluorescence—HeLa cells plated (2.5×10^4) on coverslips were transfected with 50 ng of pEGFP-C1-Nck1 or -Nck2 plasmid. 18 h post transfection, cells were washed twice in PBS, fixed in 3% para-formaldehyde, PBS for 10 min, permeabilized for 5 min with 0.2% Triton X-100 PBS, and blocked in 1% bovine serum albumin PBS for 30 min. Primary antibodies (anti-Nck 1793, anti-calnexin) diluted in PBS were added for 1 h at 37 °C. After washing with T-TBS (5 times) and PBS (3 times), cells were incubated with secondary antibodies in PBS for 1 h at room temperature. Cells were washed, and DNA was stained with 4′,6-diamidino-2-phenylindole (Sigma) for 5 min in PBS at room temperature. Coverslips mounted in MOWIOL were air-dried for 18 h at room temperature and examined on a Zeiss Axiovert 135 fluorescence microscope (63×). Images were recorded using a digital camera (DVC), analyzed with Northern Eclipse software (Empix Imaging Inc.), and processed using Adobe Photoshop 7.0.

Cell Survival—MEFs were plated (3×10^5 cells) in 60-mm dishes in triplicate and treated with Tg, Tn, or H_2O_2 for 24 h at the indicated concentrations. Cell viability was scored by counting the number of cells that exclude trypan blue. Apoptosis associated with classical nuclear changes such chromatin condensation, nuclear shrinkage, and formation of apoptotic bodies was monitored under fluorescence microscopy after appropriate staining of nuclei with 4′,6-diamidino-2-phenylindole as reported above.

Phosphatase Assay—HeLa cells were plated (2.5×10^5 cells) in 60-mm dishes in triplicate, and phosphatase activity was determined the next day using a Ser/Thr phosphatase kit (Upstate) according to manufacturer's instructions. Briefly, cells were washed twice in ice-cold phosphate-free buffer (50 mM HEPES, pH 7.5, 150 mM NaCl, 10% glycerol, 1.5 mM $MgCl_2$, and 1 mM EGTA) and lysed in the same buffer supplemented with 1% Triton-X100 and protease inhibitors. Equal amounts of proteins (1–2 μg) from clarified cell lysates were processed in triplicate in a reaction containing the phosphorylated peptide (KRpTIRR; pT is phosphothreonine) in a 25-μl final volume of phosphatase buffer (19.5 mM Tris-HCl, pH 7.4, 39 μM $CaCl_2$). After 10 min at 30 °C, the reaction was stopped by adding 100 μl of STOP buffer provided by the manufacturer. Samples were transferred into a 96-well plate, and optical density was read at 620 nm. Optical density of the blank was subtracted from the optical density of each sample.

In Vitro eIF2α Dephosphorylation Assay—*In vitro* eIF2α dephosphorylation assays were performed using recombinant His-eIF2α ^{32}P-labeled by GST-PKR as previously described (40). Free [γ-^{32}P]ATP was removed by gel filtration using Probe Quant G-50 microcolumns (Amersham Biosciences). Endogenous Nck (C-19) and PP1 (E-9) immunoprecipitates prepared from HEK293 cell lysates (1–1.5 mg of total protein) were incubated at 30 °C for 30 min with radiolabeled His-eIF2α as previously reported (39). At the end of the reaction, levels of ^{32}P-labeled eIF2α were determined by submitting 30% of the reaction mixture to SDS-PAGE followed by autoradiography and densitometry for quantitation. Alternatively, *in vitro* eIF2α phosphorylation assays were performed on crude detergent cell lysates following the approach described by David Ron's laboratory (17, 38, 39). Briefly, recombinant His-eIF2α (10–50 ng) was radiolabeled in reticulocyte lysates using 50 ng of recombinant bacterially expressed GST-PERK. After gel filtration to get rid of the free [γ-^{32}P]ATP, 2 μl of the radiolabeled proteins were incubated at 30 °C for 30 min with 5 μg of proteins (5 μl) from crude detergent lysates of 293 mock-transfected cells, 293 cells transiently transfected with plasmids encoding HA-Nck-1, FLAG-CReP, or FLAG-GADD34 in a final reaction volume of 10 μl (dephosphorylation buffer, 20 mM Tris-HCl, pH 7.4, 50 mM KCl, 2 mM $MgCl_2$, 0.1 mM EDTA, 0.8 mM ATP). The reactions were stopped by adding 2 μl of 6× Laemmli buffer, then boiled and resolved on 10% SDS-PAGE before being exposed to autoradiography. Crude detergent cell lysates were obtained by solubilizing the cells in a lysis buffer containing 20 mM Tris-HCl, pH 7.4, 0.5% Triton X-100, 50 mM NaCl, 10% glycerol, 0.1 mM EDTA, aprotinin/leupeptin at 10 μg ml^{-1}, and phenylmethylsulfonyl fluoride at 100 μM.

RESULTS

Nck Overexpression Down-regulates eIF2α Phosphorylation-dependent Signaling—To determine whether Nck isoforms are functionally redundant in preventing eIF2α phosphorylation in response to ER stress, we overexpressed these proteins in HeLa cells. As we previously reported in HEK293 cells (34), transient overexpression of HA-Nck1 in HeLa cells completely blocked eIF2αSer^{51} phosphorylation induced by cell treatment with Tn, an inhibitor of *N*-linked glycosylation perturbing ER function (Fig. 1*A*, *upper panels* compare *lane 4* to *2*). We further observed that high levels of Nck1 yield lower basal levels of eIF2α phosphorylated on Ser^{51} (Fig. 1*A*, *upper panels*, compare *lanes 3* to *1*). Likewise, overexpression of Nck2 also resulted in down-regulation of both basal and stress-induced eIF2αSer^{51} phosphorylation (Fig. 1*A*, *upper panels*, compare *lanes 5* and *6* to *lanes 1* and *2*). Furthermore, similar effects were observed in various cell lines (HeLa, HEK293, N1E-115, NIH 3T3), suggesting that the regulation of eIF2α phosphorylation by Nck is rather ubiquitous than cell-specific (data not shown). Interestingly, the effects of overexpressing Nck on eIF2α phosphorylation resemble those observed after CReP and GADD34 overexpression (Fig. 1*A*, *bottom panels*), two related PP1c regulatory subunits found in holophosphatase complexes that dephosphorylate eIF2αSer^{51} in non-stressed (38) and ER-stressed cells

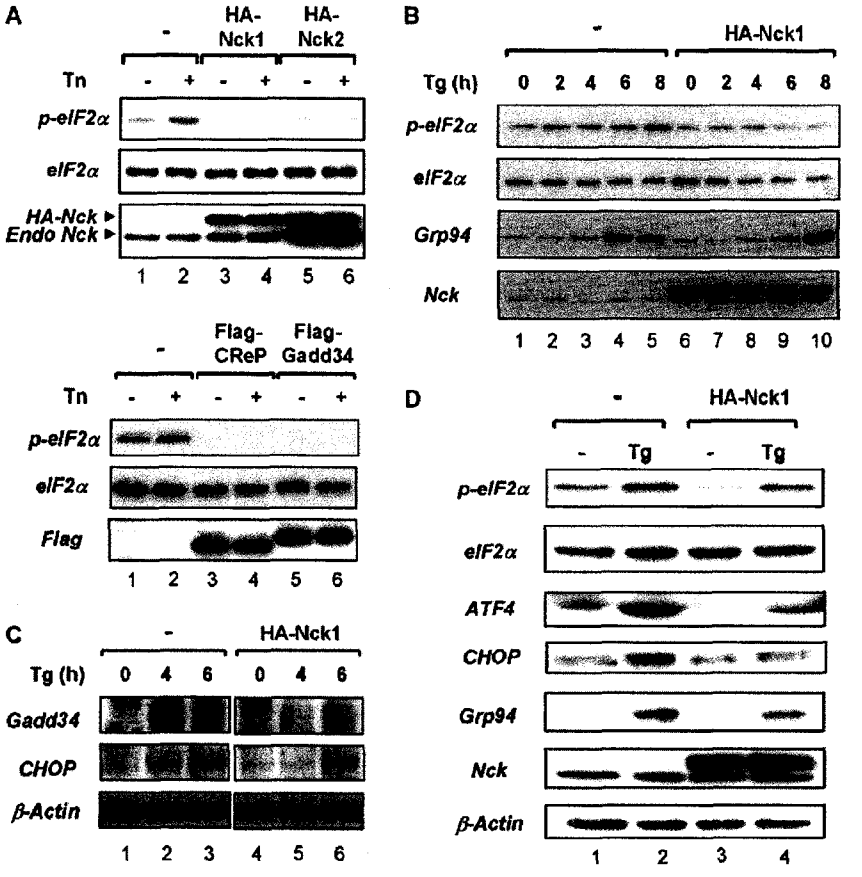

FIGURE 1. **Nck overexpression down-regulates eIF2α phosphorylation and eIF2α-dependent signaling.** *A*, HeLa cells transiently overexpressing Nck1, Nck2, CReP, or GADD34 were treated with Tn (7.5 μg ml^{-1}) for 30 min. Total cell lysates were subjected to Western blot analysis using indicated antibodies. Western blots presented are typical of three independent experiments. *B*, HeLa cells transiently overexpressing Nck1 were exposed to Tg (1 μM) for the indicated times, lysed, and subjected to Western blot analysis with the indicated antibodies. *C*, similar to *B*, except cells were treated with Tg for 4 and 6 h. Similar results were obtained in three independent experiments. *D*, similar to *B*, except cells were treated for 24 h with Tg. Western blots presented are typical of three independent experiments.

(39), respectively. Lower levels of eIF2α phosphorylation in Nck-overexpressing cells were still observed for up to 24 h of treatment with Tn (data not shown) or with the calcium ATPase inhibitor thapsigargin, which also induces ER stress (Tg) (Fig. 1, *B* and *D*), demonstrating that Nck overexpression causes a long-lasting inhibition of eIF2αSer^{51} phosphorylation. Based on our results, we conclude that both Nck adaptors antagonize the phosphorylation of eIF2α in various cell lines.

eIF2α phosphorylation is known to result in the translational up-regulation of the transcriptional activator ATF4 mRNA (16, 18), which mediates the induction of ISR genes. To test whether Nck modulates ISR genes expression, we assessed GADD34 and CHOP expression in Nck1-overexpressing cells subjected to ER stress. As shown in Fig. 1*C*, transient overexpression of Nck1 attenuated induction of GADD34 and CHOP in response to Tg treatment. Furthermore, overexpression of Nck results in a long term inhibition of ISR gene induction as demonstrated by the lower levels of ATF4 and CHOP detected after 24 h of treatment with Tg in Nck1-overexpressing cells as compared with mock-transfected cells (Fig. 1*D*). We also observed that expression of the Grp94 chaperone protein was considerably reduced in Nck1-overexpressing cells (Fig. 1*D*). Taken together, these results establish Nck as a regulator of the ER stress-induced eIF2αSer^{51} phosphorylation-dependent ISR.

Nck Localizes at the ER—Because phosphorylation of eIF2α by PERK occurs on the cytoplasmic side of the ER and Nck antagonizes PERK-mediated eIF2α phosphorylation, we then used indirect immunofluorescence to determine whether Nck could be detected in the ER area in HeLa cells. Cell staining using a pan-Nck antibody (1793) that recognizes both Nck isoforms revealed a specific and intense reticular signal around the nucleus reminiscent of ER localization (Fig. 2*A*). Consistent with a role for Nck in receptor-tyrosine kinase and integrin signaling, this antiserum also showed enriched local plasma membrane staining (Fig. 2*A*, *arrowheads*). Similarly, after transient expression of green fluorescent protein-tagged Nck1 or Nck2 at low levels in HeLa cells, we detected both Nck proteins at the ER (*green*) as judged by their extensive colocalization with calnexin (*red*), a specific ER marker (Fig. 2*B*). Because neither Nck1 nor Nck2 amino acid sequence predicts the presence of a signal peptide nor ER retention/retrieval motifs, and thus, are not expected to be synthesized and translocated across the Sec61 translocon, we believe the staining for Nck at the ER most likely represents Nck proteins recruited on the cytosolic face of the ER rather than in the ER lumen. These results support our previous findings showing that Nck is detected in enriched calnexin-purified ER fractions (35) and further demonstrate that Nck adaptors localize at the ER, in agreement with their ability to regulate signaling responses from this compartment.

Genetic Inactivation of Nck Expression Establishes Spontaneous eIF2α-dependent Signaling Events—Having shown that overexpression of Nck profoundly impaired phosphorylation of eIF2α and expression of ER stress-related genes, we wished to determine whether deletion of Nck expression promotes activation of components of the ISR. Supported by our previous observation that deletion of Nck in MEFs results in increased phosphorylation of eIF2α Ser^{51} (34), we addressed eIF2α-dependent signaling events in these cells first in unstressed conditions. As presented in Fig. 3, mutant MEFs presented spontaneous increased levels of ATF4 along with increased induction of its target gene GADD34 (triplicate plates of each cell lines). In addition, Grp94 is also extensively induced in these cells. Although the mutant cells show a primed eIF2α-dependent sig-

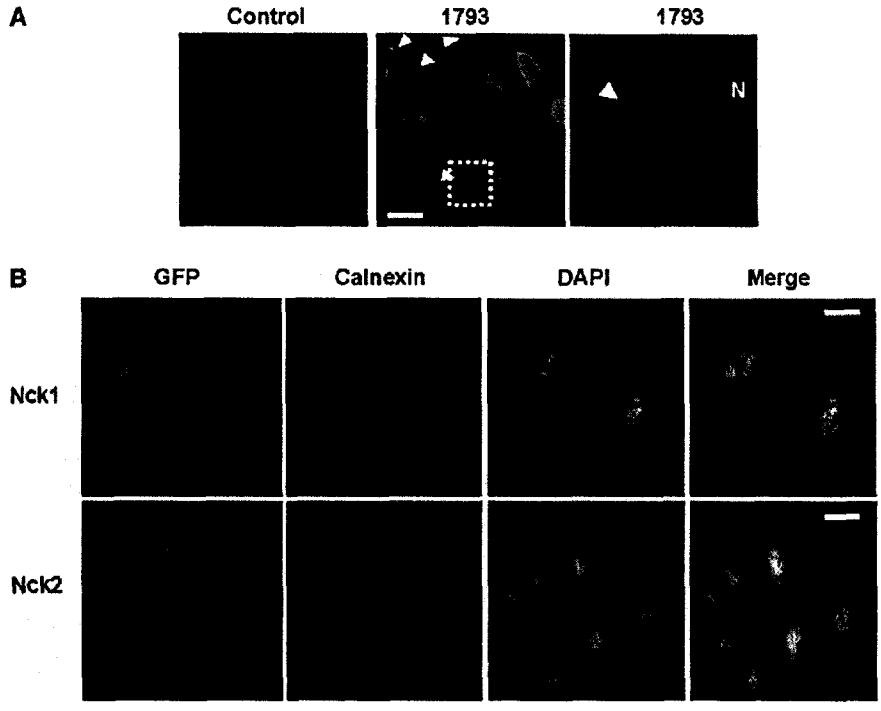

FIGURE 2. **Nck adaptors are detected at the ER.** *A*, indirect immunofluorescence in HeLa cells using a pan-Nck antibody (1793) or normal rabbit serum (control). The *third panel* on the *right* represents higher magnification of the area selected in the *second panel*. *Bar*, 10 μm. *B*, HeLa cells transiently transfected with 50 ng of pEGFP-Nck1 or -Nck2 (*green*) were monitored for Nck expression by direct fluorescence (*green*) and processed for calnexin detection by indirect immunofluorescence (*red*). Nucleus staining with 4′,6-diamidino-2-phenylindole (*DAPI*; *blue*) is shown. *GFP*, green fluorescent protein.

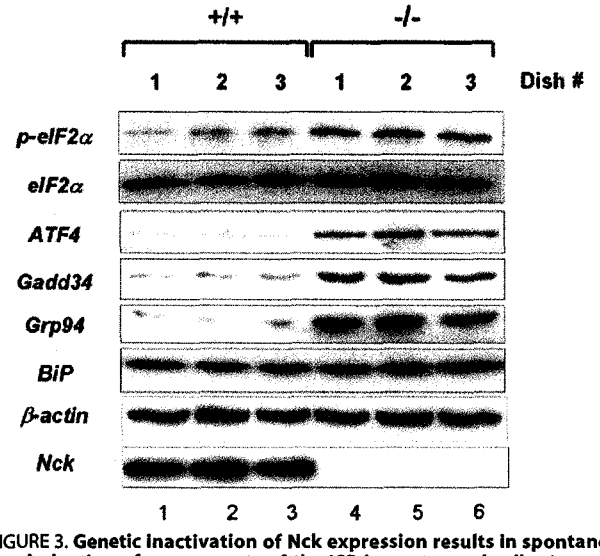

FIGURE 3. **Genetic inactivation of Nck expression results in spontaneous induction of components of the ISR in unstressed cells.** *A*, equal amount of cell lysate proteins prepared from three separate dishes of early passages of MEFs were analyzed by Western blot for indicated proteins using commercial specific antibodies. +/+, MEFs WT; −/−, MEFs Nck1$^{-/-}$Nck2$^{-/-}$. *p*, phosphorylated.

naling in the absence of exogenous stress, we excluded the possibility that these continuously experience ER stress because BiP, a marker of the UPR downstream of IRE1 and ATF6 activation, is expressed at comparable levels in both cell lines (Fig. 3). This supports our previous observations reporting no constitutive IRE1-dependent events (XBP-1 mRNA levels and splicing) leading to BiP induction in untreated MEFs lacking Nck (35). Overall, our results show that the spontaneous increased levels of eIF2α phosphorylation that we previously reported in cells genetically deleted of Nck (34) correlates with up-regulation of ATF4 and activation of IRS target genes.

Genetic Inactivation of Nck Expression Results in Higher Levels of ER Stress-induced eIF2α Phosphorylation and Premature Induction of eIF2α-dependent Signaling Events and Protects Cells from ER Stress—We then postulated that Nck adaptors, by regulating the phosphorylation of eIF2αSer^{51}, participate in the accurate control of the timing and intensity of the ISR upon ER stress. To explore this hypothesis, MEFs WT or lacking Nck were subjected to Tn treatment and analyzed for eIF2α phosphorylation (Fig. 4). Western blot analysis revealed greater levels of phosphorylated eIF2αSer^{51} in MEFs devoid of Nck, both in a dose- (Fig. 4*A*) and time-dependent (Fig. 4*B*) manner compared with MEFs WT. At 2.5 μg ml^{-1} Tn, eIF2α phosphorylation was induced by 3.1-fold in MEFs lacking Nck compared with 1.7-fold in MEFs WT (Fig. 4*A*). After 90 min of treatment with Tn, eIF2α phosphorylation was induced by 2.1-fold in mutant MEFs while being increased by only 1.6-fold in MEFs WT (Fig. 4*B*). These results suggest that the mechanism regulating the phosphorylation of eIF2αSer^{51} in response to ER stress are defective in MEFs lacking Nck.

We next examined the kinetics of induction of eIF2α-dependent signaling events in WT and mutant MEFs subjected to ER stress. As shown in Fig. 5, MEFs lacking Nck are more responsive to ER stress. First, both ATF4 and CHOP are readily induced at very low concentrations of Tn in mutant MEFs but are detected only at much higher concentrations in WT MEFs (Fig. 5*A*). Second, using an ATF4-Luc reporter vector that is a measure of ATF4 translation, we observed that Tg treatment for 6 h resulted in a 5-fold induction of the ATF4-Luc reporter in mutant MEFs but only 2-fold in WT MEFs (Fig. 5*B*). Finally, the induction of ISR effectors downstream of eIF2α occurs much faster and to a higher extent in mutant MEFs compared with WT (Fig. 5, *C* and *D*). In particular, ATF4 and CHOP proteins appear within 4–6 h upon treatment with Tg in control cells but are easily detected between 1 and 2 h in mutant cells (Fig. 5*C*). As shown in Fig. 5*D*, this prominent signaling persists up to 24 h after initiating ER stress. β-Actin levels were very similar among the different MEFs lysates, showing that equivalent amounts of total proteins were analyzed in each con-

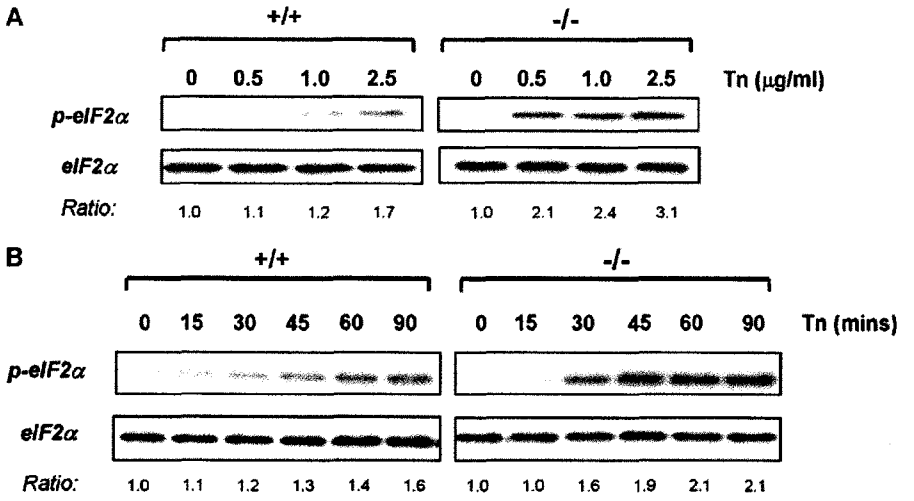

FIGURE 4. **Genetic inactivation of Nck expression enhances eIF2αSer^{51} phosphorylation (*p*) in response to ER stress.** *A*, dose response to Tn. MEFs were treated with indicated concentrations of Tn for 90 min. Cell lysates normalized for protein content were analyzed by Western blot with specific Ser(P)^{51} and total eIF2α antibodies. *B*, time course of eIF2αSer^{51} phosphorylation to Tn (2.5 mg ml^{-1}) in MEFs. Upon treatment, cell lysates were processed and analyzed as described in *A*.

dition. Noteworthy, no change in Nck levels was observed upon exposure of WT MEFs to either Tn or Tg (Fig. 5, *C* and *D*). Moreover, we noticed that BiP and Grp94 are induced at to higher extent in mutant MEFs and in a manner very similar to effectors of the ISR (Fig. 5, *C* and *D*). Because normal XBP-1 mRNA splicing has been reported in ER-stressed MEFs lacking Nck (35), possible cross-talks between PERK and IRE1 and/or ATF6 branches of the UPR can account for the rapid and robust BiP and Grp94 induction we observed in mutant compared with WT MEFs. From these results, we conclude that Nck adaptors modulate the kinetic and robustness of eIF2α-dependent events in response to ER stress.

Phosphorylation of eIF2α on Ser^{51} serves as a protective mechanism for cells to survive diverse stressful situations including ER stress (38, 41). In opposition, the inability to overcome stress leads to apoptosis through the activation of caspases (42). To directly address the role of Nck in apoptosis induced by chronic ER stress, we treated MEFs WT or deleted of Nck with Tg or Tn for 24 h and analyzed their morphology and survival at the end of the treatment. Under phase-contrast microscopy, we observed that WT MEFs initially round up and ultimately detached from the surface of the culture dish (Fig. 6*A*). In contrast, this behavior is less pronounced in cells lacking Nck adaptors, suggesting that these cells are protected from ER stress. This was demonstrated by determining that only 26% of WT MEFs survived to 24 h treatment with Tg, whereas this percentage significantly increased to 57% in mutant MEFs (Fig. 6*B*). Treatment with Tn yielded similar results, whereas hydrogen peroxide exposure at doses that had no effect on eIF2α phosphorylation (43) induced much higher levels of cell death in MEFs lacking Nck compared with WT (Fig. 6*B*). These data demonstrate that the absence of Nck specifically protects cells from ER stress.

To further substantiate our findings, we treated MEFs with different concentrations of Tg or Tn for 24 h and measured the number of apoptotic cells by counting nuclei with condensed chromatin as revealed by 4′,6-diamidino-2-phenylindole staining (Fig. 6*C*). We found that the number of apoptotic cells was significantly reduced in mutant MEFs as compared with WT in both Tn- and Tg-treated conditions, confirming that the MEFs lacking Nck are protected from ER stress-induced cell death. We then assessed caspase-3 and poly(ADP-ribose) polymerase processing, which normally occur during programmed cell death. As expected, both proteins were found to be preferentially cleaved in a time-dependent manner in WT but not in mutant MEFs (Fig. 6*D*). Similar results were obtained upon 24 h of treatment with Tn (Fig. 6*E*). In contrast, cleavage of poly(ADP-ribose) polymerase was more pronounced in response to H_2O_2 exposure in MEFs lacking Nck, in agreement with their higher sensitivity to cell death induced by H_2O_2 (Fig. 6*F*). From these results, we concluded that Nck proteins are required to initiate the events leading to caspases/poly-(ADP-ribose) polymerase cleavage and apoptosis in cells experiencing prolonged ER stress.

Nck Is Part of a Molecular Complex That Controls Dephosphorylation of eIF2α—The results presented above suggest that Nck adaptors determine the kinetics of eIF2α phosphorylation and the attendant ISR activation in cells undergoing ER stress by being at the center of a mechanism that antagonizes the phosphorylation of eIF2α. However, how Nck down-regulates the phosphorylation of eIF2α still remains to be defined. Work from our laboratory demonstrated that Nck regulates translation through its interaction with the β-subunit of the eIF2 complex (9). This present study suggests that Nck acts on translation most probably by lowering cellular levels eIF2α phosphorylation. In agreement with this hypothesis, we previously reported that calyculin A, a potent inhibitor of PP1/PP2A activity, prevented Nck from down-regulating eIF2α phosphorylation in response to ER stress (34), suggesting that a phosphatase activity mediates the effects of Nck overexpression on eIF2α phosphorylation. To elucidate the mechanism by which Nck controls the phosphorylation state of eIF2α, we initiated a series of experiments aimed to determine whether a protein Ser/Thr phosphatase interacts with Nck. First, using a commercial kit that monitors *in vitro* dephosphorylation of a phosphopeptide by PP1 and PP2A phosphatase activity (KRpTIRR), we detected a Ser/Thr phosphatase activity of this type in Nck immunoprecipitates prepared from 293 cells (Fig. 7*A*). Moreover, we found that this phosphatase activity correlated with the presence of PP1c in Nck immunoprecipitates isolated from 293 (Fig. 7*B*) and HeLa cells (data not shown), whereas PP2A could not be detected (data not shown). In contrast, PP1c was not detected in normal rabbit IgG immunoprecipitates (Fig.

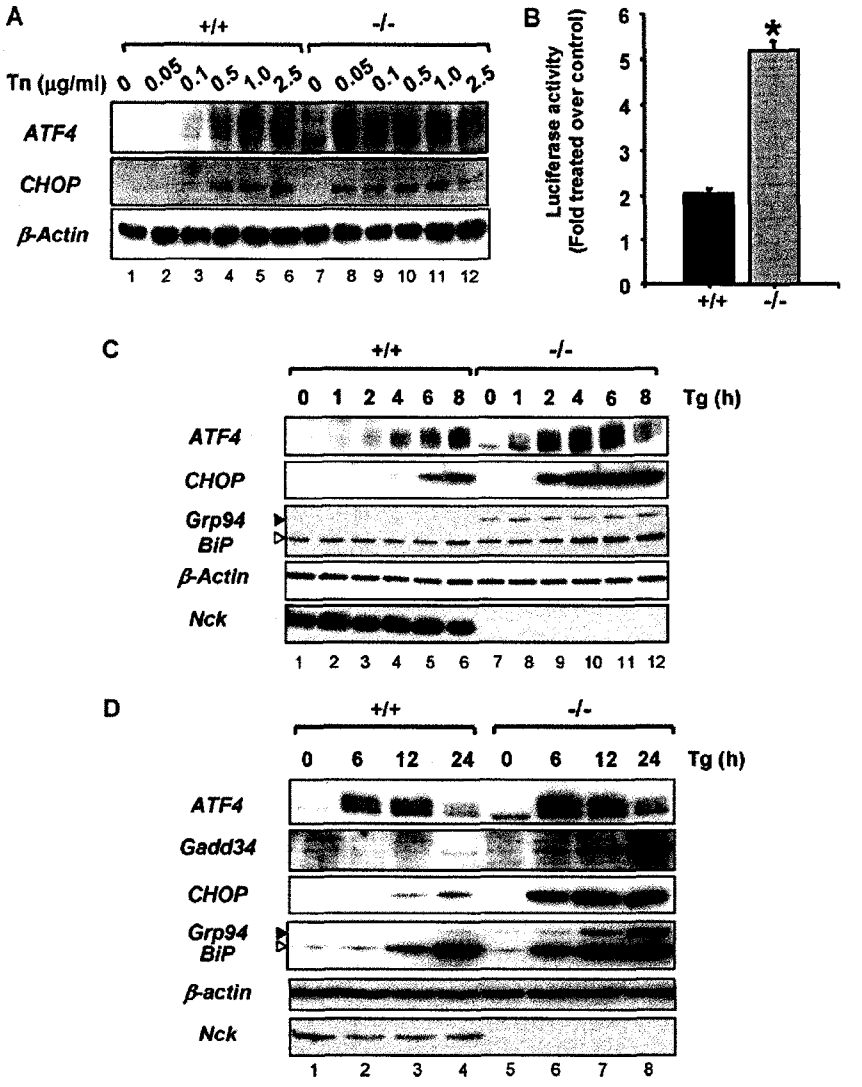

FIGURE 5. **Genetic inactivation of Nck expression results in premature induction of eIF2α-dependent signaling events in response to ER stress.** *A*, dose response to Tn. MEFs were treated with indicated concentrations of Tn for 90 min, and cell lysates normalized for protein content were analyzed by Western blot using ATF4 and CHOP specific antibodies. β-Actin, determined also by Western blot, is used as loading control. *B*, ATF4-Luc reporter activity in MEFs previously transiently transfected with the reporter vector and treated with Tg (250 nM, 6 h). *Error bars* represent S.E.; *, $p < 0.01$ by *t* test, $n = 3$. *C*, time course of Tg treatment (1 μM) in MEFs. Similar to *A*, expression of the indicated proteins was followed by Western blot using specific antibodies. *Closed arrowhead*, Grp94; *open arrowhead*, BiP. *D*, same as in *C*, except the time course was performed over 24 h.

pressing a FLAG-tagged version of CReP, we detected CReP, PP1c, and eIF2β in Nck immunoprecipitates (Fig. 7*D*). To clearly establish that Nck is part of an actual eIF2α holophosphatase complex that dephosphorylates eIF2αSer[51], we performed *in vitro* eIF2α dephosphorylating assays using lysates obtained from Nck-overexpressing cells. From these assays we noticed that crude cell lysates prepared from Nck1-overexpressing cells always present higher eIF2α dephosphorylating activity than equivalent mock-transfected cell lysates (Fig. 7*E*, *left panel*) and was comparable with the dephosphorylating activity detected in CReP or GADD34 transiently overexpressing cell lysates (Fig. 7*E*, *middle panel*). Finally, we found that Nck immunoprecipitate contains an activity that dephosphorylates eIF2αSer[51], as revealed by the decrease of radioactivity associated with eIF2α in Nck immunoprecipitates compared with normal IgGs immunoprecipitates (Fig. 7*E*, *right panel*). In these assays, we were surprised to find that the PP1c immunoprecipitates that we used as a positive control did not show a robust eIF2α dephosphorylating activity. We propose that the antibody we used to immunoprecipitate PP1 possibly interferes with the active catalytic site of PP1c, thus reducing PP1c phosphatase activity. On the other hand, we believe the eIF2α dephosphorylating activity detected in Nck immunoprecipitates to be significant because the Nck molecular complex containing PP1c probably represents only a minor fraction of the cellular complexes assembled by Nck adaptors.

7*B*), further underscoring the specificity of the Nck-PP1c coimmunoprecipitation. As expected, Nck immunoprecipitates contain eIF2β and, most importantly, eIF2α (Fig. 7*B*). We confirmed reciprocal coimmunoprecipitations by showing that Nck, PP1c, and eIF2β are all found in an eIF2α immune complex (Fig. 7*C*) but not in normal rabbit IgG immunoprecipitates (data not shown). Together, these results demonstrate that Nck, PP1c, and components of eIF2 are in a common complex.

We further investigate this molecular complex by determining whether CReP, a PP1c interacting protein regulating the dephosphorylation of eIF2α on Ser[51], could be found in Nck immune complex. The lack of potent CReP antibody prevented us from monitoring the presence of endogenous CReP in Nck immunoprecipitates. However, in cells overex-

Last, we reasoned that recruitment of PP1c and eIF2 components in a common complex might be perturbed in the absence of Nck proteins. In determining the amount of PP1c detected in eIF2β immunoprecipitates, we observed that it was reduced by ~70% in MEFs lacking Nck (Fig. 8). This suggests that Nck plays an important role in maintaining a significant amount of PP1c in the vicinity of eIF2, allowing eIF2α dephosphorylation. All together, our results support the idea that Nck assembles a molecular complex that contains PP1c, CReP, and components of eIF2 and in this manner controls the dephosphorylation of eIF2α. Importantly, a defect in this Nck-dependent regulatory mechanism has clear impacts on the cellular response to stress

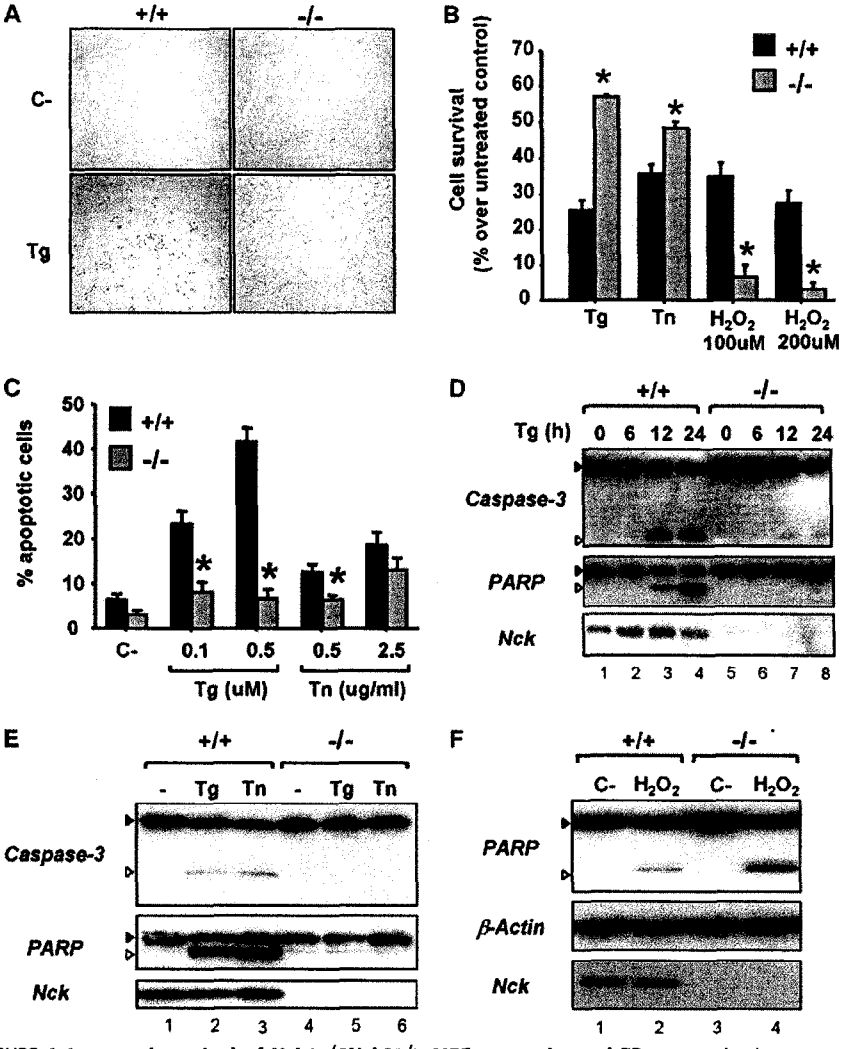

FIGURE 6. **Improved survival of Nck1$^{-/-}$Nck2$^{-/-}$ MEFs to prolonged ER stress.** *A*, phase contrast microscopy of MEFs treated or not for 24 h with Tg (1 μM). *B*, quantitative analysis of Tg-, Tn-, and H_2O_2-induced cell death in MEFs. MEF WT (+/+) and Nck1$^{-/-}$Nck2$^{-/-}$ (−/−) were untreated or treated for 24 h with Tg (1 μM, $n = 3$), Tn (2.5 μg ml^{-1}, $n = 7$), or 100 and 200 μM H_2O_2 ($n = 3$). Cell viability was scored by counting the number of cells that exclude trypan blue. *Error bars* represent S.E.; $p < 0.001$ (*) and $p = 0.002$ (**) *versus* respective MEF-+/+-treated cells by *t* test. *C*, quantitative analysis of the number of apoptotic nucleus in MEFs treated with the indicated concentration of either Tg ($n = 3$) or Tn ($n = 3$). *Error bars* represent S.E. *, $p < 0.05$ by *t* test. *D*, time course of the induction of caspase-3 and poly(ADP-ribose) polymerase (*PARP*) cleavage in MEFs WT (+/+) and Nck1$^{-/-}$Nck2$^{-/-}$ (−/−) treated for different times with Tg (1 μM). Cell lysates normalized for protein content were analyzed by Western blot using appropriate specific antibodies. *Closed arrowhead*, full-length inactive proteins. *Open arrowhead*, active cleavage product. *E*, similar to *D*, except the MEFs were treated for 24 h with Tg (1 μM) or Tn (2.5 μg ml^{-1}). *F*, similar to *E*, except MEFs were exposed to 100 μM H_2O_2 for 24 h. *Panels D–F* are typical and representative of results obtained from three independent experiments.

that converge on the phosphorylation of eIF2α as seen in MEFs lacking Nck.

DISCUSSION

Research over the past years has revealed that a number of molecules involved in signaling pathways initiated at the plasma membrane also transit to endomembrane compartments to transduce signals into different cellular outcomes (44, 45). Our study supports this concept by showing that the SH2/SH3 domain-containing Nck adaptors not only transduce signal from receptor-tyrosine kinases at the plasma membrane (46) but also localize at the ER where they participate in ER signaling regulating cellular response to stress. Thus, Nck adaptors are used by different cellular compartments in various cell conditions to generate specific cellular responses.

It is well documented that other conditions beside ER stress, such as amino acid deprivation (14), viral infection (15), or heme deficiency (13), activate distinct eIF2α kinases that also phosphorylate eIF2α on Ser^{51}, resulting in inhibition of mRNA translation. In contrast, in the past years the identification of complexes regulating the dephosphorylation of eIF2αSer^{51} revealed the importance of appropriate control of eIF2α-dependent signaling in response to stress. However, our knowledge of the mechanisms regulating eIF2αSer^{51} dephosphorylation is still limited to proteins targeting the Ser/Thr phosphatase PP1c to eIF2α and to the molecular determinants underlying their interaction with PP1c. For example, CReP, the constitutive repressor of eIF2α phosphorylation, is expressed in unstressed cells where it keeps eIF2α hypophosphorylated through its interaction with PP1c (38). Similarly, GADD34 is also known as a PP1c interacting protein that controls dephosphorylation of eIF2α (47). In contrast to CReP, GADD34 expression is induced upon stress and mediates the translational recovery phase of the UPR (39, 47, 48). In addition, some viruses encode products with high homology to GADD34. For example, herpes simplex virus encodes the ICP34.5 protein, which by interacting with PP1c, promotes eIF2α dephosphorylation and allows the virus to escape inhibition of protein synthesis occurring upon infection (49, 50). For the most part, PP1c regulatory proteins involved in eIF2α dephosphorylation contain a KVXF motif that was found to mediate their interaction with PP1c (51). Although we begin to appreciate the physiological importance of these regulatory check points, other protein components of eIF2α holophosphatase complexes remain to be identified. In this study we report that the Nck adaptor is part of a CReP-PP1c-containing molecular complex that dephosphorylates eIF2α and controls the temporal activation of the ISR and cell survival to ER stress.

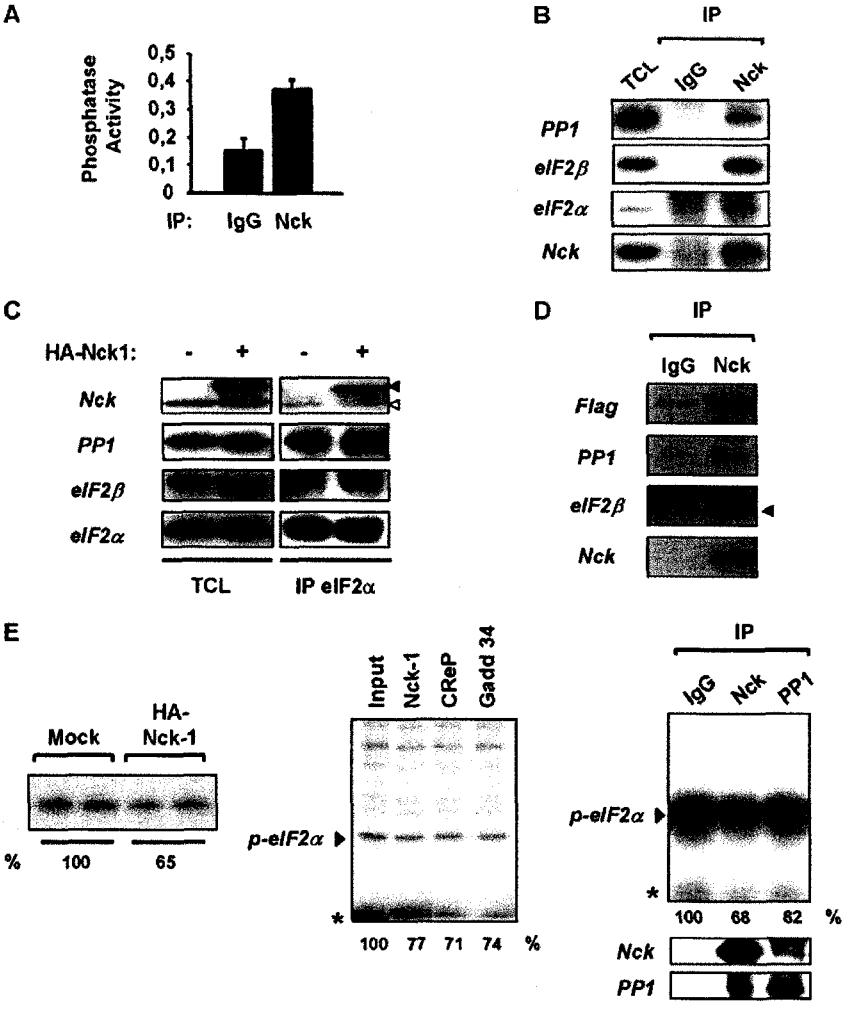

FIGURE 7. **Nck assembles an eIF2α holophosphatase complex.** *A*, PP1c/PP2A phosphatase activity in Nck (C-19) immunoprecipitates. From HeLa cell lysates, equal amount of proteins were subjected to Nck or rabbit control IgG immunoprecipitation (*IP*), and phosphatase activity was evaluated in respective immunoprecipitates using a commercial kit (Upstate) that monitors PP1/PP2A type of phosphatase activity. Results are the mean ± S.E. and represent three independent experiments performed in triplicate. *B*, coimmunoprecipitation of PP1c, eIF2β, and eIF2α with Nck in 293 cells. *TCL*, total cell lysate; *IgG*, immunoprecipitation with rabbit IgG control. *Nck*, immunoprecipitation with Nck antibody (C19). Indicated proteins were detected by Western blot using specific antibodies. Similar results were obtained in three independent experiments. *C*, ectopically expressed HA-Nck1 (*closed arrowhead*) and endogenous Nck (*open arrowhead*) PP1 and eIF2β are detected in eIF2α immunoprecipitates isolated from 293 cell lysates. Indicated proteins were detected by Western blot using specific antibodies. Similar results were obtained in three independent experiments *D*, coimmunoprecipitation of FLAG-CReP with Nck. Similar to *A*, except FLAG-CReP was transiently expressed in 293 cells. 24 h post-transfection lysates were prepared for Nck immunoprecipitation. *Closed arrowhead*, eIF2β immunoreactive band migrated slightly faster that the IgGs. *E*, *in vitro* dephosphorylation of His-eIF2α ^{32}P-labeled on Ser^{51} obtained from mock or Ha-Nck1 transiently transfected 293 cells lysates, shown in duplicates of transfection (*left panel*), Reported under the autoradiography are the mean densitometry values of the mock-transfected lysates (set at 100%) and the HA-Nck1-transfected cell lysates. *Middle panel*, comparative analysis of the dephosphorylating activity found in lysates prepared from Nck1, CReP, and GADD34 transiently overexpressing cells. *Left panel*, eIF2α dephosphorylating activity found in Nck or PP1c immunoprecipitates prepared from equal amount of proteins from 293 cell lysates. Each reaction was probed by Western blot for Nck and PP1-immunoprecipitated (*bottom panels*). Radioactivity associated with His-eIF2α was monitored by densitometry using the ImageQuant program (Bio-Rad) and quantitation shown under the autoradiogram. *Arrowhead*, ^{32}P-labeled His-eIF2αSer51. *Asterisk*, degradation product of His-^{32}P-labeled eIF2α.

We established that both Nck1 and Nck2 redundantly modulate eIF2αSer^{51} phosphorylation (Fig. 1*A*). Particularly, we demonstrated that like CReP and GADD34, overexpression of either Nck down-regulates both basal and stress-induced eIF2αSer^{51} phosphorylation (Fig. 1, *A* and *B*). In contrast, in MEFs lacking Nck, we previously reported that eIF2α phosphorylation was increased (34), and our present data show that this correlates with a primed eIF2α signaling (Fig. 3). We believe that this directly impacts on the kinetic and intensity of the ISR (Figs. 4 and 5) and improves cell survival rates to ER stress (Fig. 6). We uncovered that Nck is part a large molecular complex containing CReP, PP1c, and subunits of eIF2 that dephosphorylate eIF2α on Ser^{51} (Fig. 7). This complex is required for proper control of eIF2α phosphorylation on Ser^{51}, eIF2α-dependent signaling, and an appropriate cell response to ER stress. Importantly, the amount of PP1c found in this complex is dependent on the presence of Nck because it is greatly reduced in MEFs deleted of Nck (Fig. 8). Based on these results, we propose that Nck significantly contributes to the organization and/or stability of this CReP/PP1c-containing complex, regulating the amount of PP1c recruited in close proximity to eIF2 and in this manner regulates eIF2α dephosphorylation on Ser^{51} (Fig. 9). Additional experiments are required to dissect the molecular interactions underlying the formation of this complex and to determine its structural organization. Given that the recruitment of PP1c in this complex is perturbed in Nck-deficient MEFs, one possibility is that Nck directly interacts with either PP1c and/or CReP and in this way contributes to the stability of the complex. In agreement with this is the presence of a potential PP1c binding site (*XVXF*) (51) in both Nck isoforms and conserved from *Caenorhabditis elegans* to humans. Alternatively, based on its modular structure, Nck, by mediating proline and/or phosphotyrosine-based protein interactions via its SH3 and SH2 domains, could be responsible for proper assembly of this molecular complex. Experiments are now being conducted to gain insights into the possible interplay existing between Nck and other components of this eIF2α holophosphatase complex.

As mentioned above, GADD34 has been identified as a

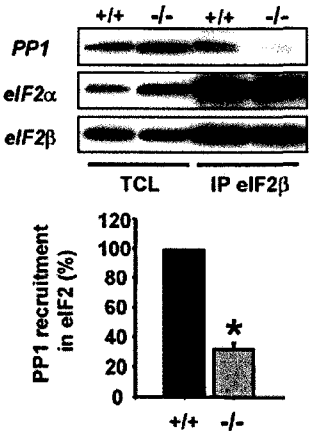

FIGURE 8. **Reduced amounts of PP1c in the eIF2 complex in Nck1$^{-/-}$-Nck2$^{-/-}$ MEFs.** Equal amount of proteins from MEFs total cell lysates (*TCL*) were subjected to eIF2β immunoprecipitation (*IP eIF2β*) and analyzed by Western blot for PP1, eIF2α, and eIF2β content (*upper panel*). Quantitation of the amount of PP1c in eIF2β immunoprecipitates (*bottom panel*). *Error bars* represent S.E. *, $p < 0.05$ by *t* test, $n = 3$.

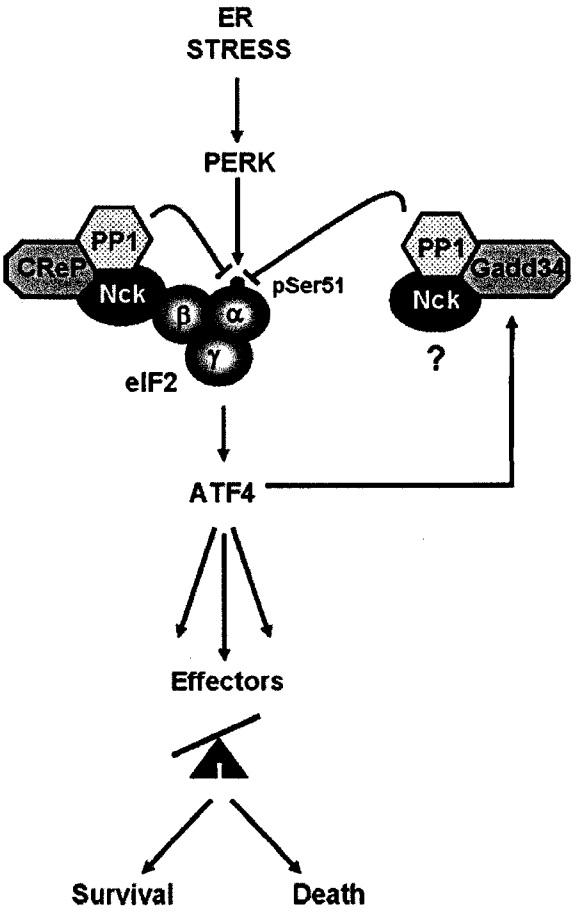

FIGURE 9. **Schematic model of the components of the holophosphatase complex regulating phosphorylation of eIF2α on Ser^{51} in ER stress.** As a component of the CReP/PP1c holophosphatase complex, Nck regulates ER stress-induced eIF2α phosphorylation on Ser^{51} and attending signaling. This dictates the timing and robustness of ISR signaling and determines cell fate in response to ER stress. Whether Nck is also part of the GADD34/PP1c complex still remains to be demonstrated.

regulatory subunit that also targets PP1c to eIF2α, and the GADD34-PP1c complex has been shown to act in a coordinated and timely manner to dephosphorylate eIF2α (39, 48). Although we found CReP and Nck in a common complex, it is possible that Nck could also be part of the GADD34 and ICP34.5 eIF2α holophosphatase complex. It is still to be addressed whether Nck could represent a critical component of more than one molecular complex regulating the dephosphorylation of eIF2α in response to diverse stresses. Interestingly, recent data from our group suggest that Nck shows preference or specificity toward stresses activating eIF2α kinases converging to the phosphorylation of eIF2α, suggesting that its effect is not general to any eIF2α kinase.[4] Last, in a manner very homologous to its adaptor role in translocating specific effectors to activated receptor kinases at the plasma membrane, Nck could target the holophosphatase complexes to specific subcellular compartments to properly control localized mRNA translation and/or eIF2α-dependent signaling. This was proposed in a recent study demonstrating that ER-bound ribosomes are still translationally active during the UPR albeit up-regulated eIF2αSer^{51} phosphorylation (52), suggesting that spatially restricted mechanisms exist that allow translation of a limited number of mRNA by locally preventing phosphorylation and/or promoting dephosphorylation of eIF2α.

Numerous genes are up-regulated by ER stress after phosphorylation of eIF2α. However, how these late events are coordinated among each other over time remains to be determined. Here, we show that MEFs lacking Nck show spontaneous induction of ATF4 and GADD34 (Fig. 3) in addition to primed UPR in response to pharmacological inducers of ER stress (Figs. 4 and 5). Therefore, the Nck-containing eIF2α holophosphatase complex represents an essential regulatory mechanism that restricts signaling from eIF2 in unstressed cells and determines the kinetics and the intensity of this signaling in ER stress conditions. Although we anticipated that effectors of the ISR would be modulated by Nck proteins levels, we were surprised to find changes in BiP and Grp94 induction in response to Tg in MEFs lacking Nck (Fig. 5). First, transactivation of the BiP promoter, which has been highly investigated, is known to be under the control of XBP-1 and ATF6 (29, 53, 54). Second, no change in IRE1-dependent splicing of XBP-1 or BiP mRNA levels were found in azetidine-2-carboxylic acid-treated MEFs lacking Nck compared with WT (35). Conversely, up-regulation of BiP mRNA levels was reduced in MEFs expressing a nonphosphorylated form of eIF2α (eIF2α Ser^{51} for Ala) (18), and ATF4 overexpression leads to transactivation of the BiP promoter (55). Therefore, increased BiP levels in MEFs lacking Nck could be partially attributed to the higher basal and stress-induced levels of ATF4. Based on these observations, cross-talks between PERK and IRE1 pathways leading to BiP and Grp94 induction likely exist. Alternatively, the discordance in BiP induction upon azetidine-2-carboxylic acid (35) and Tg (this study) could account on the fact that these drugs do no recapitulate identical ER signaling.

[4] E. Cardin and L. Larose, unpublished results.

The Nck-dependent regulatory mechanism described in this study appears of major importance as we confirmed that the ability of cells to survive to ER stress inversely correlates with expression levels of Nck (Fig. 6) (34). We found that MEFs lacking Nck show prominent ER stress signaling from eIF2α (Fig. 5). This allows these cells to rapidly clear stress in the ER and escape apoptotic programs (Fig. 6). Noticeably, this closely resembles the behavior of the CReP RNA interference cells, which show spontaneous induction of the CHOP promoter and resistance to stresses that cause eIF2αSer^{51} phosphorylation (38). However, we cannot exclude that other ER-induced signaling pathways such as IRE1-mediated ERK1/2 activation also contribute to improve cell survival in absence of Nck (35). Collectively, our results are in accordance with the protective function of eIF2αSer^{51} phosphorylation (56) and in agreement with reports demonstrating that preconditioning of cells to stress targeting eIF2 establishes a resistant state toward subsequent challenges (41, 57). It is believed that the temporal induction of the ER stress response strongly influences cellular outcomes and could underlie the difference in sensitivity of various cell types to ER stress. Our finding that Nck expression levels markedly influence signaling and cell survival to ER stress reveals the interest in searching for defects in Nck expression in proteotoxic diseases where uncontrolled ER stress-induced signaling is linked to pathogenesis (58–60).

Results presented here reinforce the concept that Nck is a *bona fide* player in such a fundamental cellular process that is mRNA translation and highlights the versatile properties of this protein. More importantly, this study sheds light on the potential mechanism by which Nck adaptors regulate mRNA translation. This could change our understanding of essential biological processes such as development of the central nervous system. Significant evidence has accumulated in recent years showing that local translation in axons is integral for growth cone navigation in response to environmental cues (61). Concomitantly, Nck has been implicated in photoreceptor cell axon guidance in *Drosophila* (62, 63) and in signaling downstream of various mammalian axon guidance receptors (64, 65). It is, thus, possible that Nck might regulate neural network formation by coupling local protein synthesis with guidance receptors activation at the growth cone. Therefore, our study emphasizes the importance of evaluating the role of Nck on translation in biological processes depending on local protein synthesis and simultaneously opens up new research avenues meant to examine the *in vivo* significance of this novel function of Nck adaptors.

Acknowledgments—We thank Tony Pawson for providing the Nck1$^{-/-}$-Nck2$^{-/-}$ MEFs. We also thank Weil Li for Nck1 and Nck-2 expression plasmids and David Ron for the kind gift of the ATF-Luc reporter gene and the pCMV2-FLAG-mCReP$^{24-698}$ and -FLAG-mGADD34 plasmids. Finally, we are grateful to Geneviève Bourret for technical assistance and Gaël Jean-Baptiste and Barry I. Posner for critical reading of this manuscript.

REFERENCES

1. Lehmann, J. M., Riethmuller, G., and Johnson, J. P. (1990) *Nucleic Acids Res.* **18,** 1048
2. McCarty, J. H. (1998) *BioEssays* **20,** 913–921
3. Buday, L., Wunderlich, L., and Tamas, P. (2002) *Cell. Signal.* **14,** 723–731
4. Li, W., and She, H. (2000) *Histol. Histopathol.* **15,** 947–955
5. Braverman, L. E., and Quilliam, L. A. (1999) *J. Biol. Chem.* **274,** 5542–5549
6. Chen, M., She, H., Davis, E. M., Spicer, C. M., Kim, L., Ren, R., Le Beau, M. M., and Li, W. (1998) *J. Biol. Chem.* **273,** 25171–25178
7. Vorobieva, N., Protopopov, A., Protopopov, M., Kashuba, V., Allkimets, R. L., Modi, W., Zabrovsky, E. R., Klein, G., Kisselev, L., and Graphodatsky, A. (1995) *Cytogenet. Cell Genet.* **68,** 91–94
8. Bladt, F., Aippersbach, E., Gelkop, S., Strasser, G. A., Nash, P., Tafuri, A., Gertler, F. B., and Pawson, T. (2003) *Mol. Cell. Biol.* **23,** 4586–4597
9. Kebache, S., Zuo, D., Chevet, E., and Larose, L. (2002) *Proc. Natl. Acad. Sci. U. S. A.* **99,** 5406–5411
10. Hershey, J. W. (1991) *Annu. Rev. Biochem.* **60,** 717–755
11. de Haro, C., Mendez, R., and Santoyo, J. (1996) *FASEB J.* **10,** 1378–1387
12. Rowlands, A. G., Panniers, R., and Henshaw, E. C. (1988) *J. Biol. Chem.* **263,** 5526–5533
13. Chen, J. (2000) *Heme-regulated eIF2α Kinase,* pp. 529–546, Cold Spring Harbor Laboratory Press, Cold Spring Harbor, NY
14. Hinnebusch, A. G. (2000) in *Translational Control of Gene Expression* (Sonenberg, N., Hershey, J. W. B., Mathews, M. B., eds) pp. 185–243, Cold Spring Harbor Laboratory Press, Cold Spring Harbor, NY
15. Kaufman, R. J. (2000) *The Double-stranded RNA-activated Protein Kinase PKR,* Cold Spring Harbor Laboratory Press, Cold Spring Harbor, NY
16. Harding, H. P., Zhang, Y., Bertolotti, A., Zeng, H., and Ron, D. (2000) *Mol. Cell* **5,** 897–904
17. Harding, H. P., Zhang, Y., and Ron, D. (1999) *Nature* **397,** 271–274
18. Scheuner, D., Song, B., McEwen, E., Liu, C., Laybutt, R., Gillespie, P., Saunders, T., Bonner-Weir, S., and Kaufman, R. J. (2001) *Mol. Cell* **7,** 1165–1176
19. Lu, P. D., Harding, H. P., and Ron, D. (2004) *J. Cell Biol.* **167,** 27–33
20. Vattem, K. M., and Wek, R. C. (2004) *Proc. Natl. Acad. Sci. U. S. A.* **101,** 11269–11274
21. Harding, H. P., Novoa, I., Zhang, Y., Zeng, H., Wek, R., Schapira, M., and Ron, D. (2000) *Mol. Cell* **6,** 1099–1108
22. Harding, H. P., Zhang, Y., Zeng, H., Novoa, I., Lu, P. D., Calfon, M., Sadri, N., Yun, C., Popko, B., Paules, R., Stojdl, D. F., Bell, J. C., Hettmann, T., Leiden, J. M., and Ron, D. (2003) *Mol. Cell* **11,** 619–633
23. Novoa, I., Zhang, Y., Zeng, H., Jungreis, R., Harding, H. P., and Ron, D. (2003) *EMBO J.* **22,** 1180–1187
24. Oyadomari, S., and Mori, M. (2004) *Cell Death Differ.* **11,** 381–389
25. Marciniak, S. J., Yun, C. Y., Oyadomari, S., Novoa, I., Zhang, Y., Jungreis, R., Nagata, K., Harding, H. P., and Ron, D. (2004) *Genes Dev.* **18,** 3066–3077
26. Harding, H. P., Calfon, M., Urano, F., Novoa, I., and Ron, D. (2002) *Annu. Rev. Cell Dev. Biol.* **18,** 575–599
27. Haze, K., Yoshida, H., Yanagi, H., Yura, T., and Mori, K. (1999) *Mol. Biol. Cell* **10,** 3787–3799
28. Tirasophon, W., Lee, K., Callaghan, B., Welihinda, A., and Kaufman, R. J. (2000) *Genes Dev.* **14,** 2725–2736
29. Lee, A. H., Iwakoshi, N. N., and Glimcher, L. H. (2003) *Mol. Cell. Biol.* **23,** 7448–7459
30. Shen, J., Chen, X., Hendershot, L., and Prywes, R. (2002) *Dev. Cell* **3,** 99–111
31. Yoshida, H., Matsui, T., Yamammoto, A., Okada, T., and Mori, K. (2001) *Cell* **107,** 881–891
32. Iyer, S., Korada, M., Rainbow, L., Kirk, J., Brown, R. M., Shaw, N., and Barrett, T. G. (2004) *Acta Paediatr.* **93,** 1195–1201
33. Harding, H. P., Zeng, H., Zhang, Y., Jungries, R., Chung, P., Plesken, H., Sabatini, D. D., and Ron, D. (2001) *Mol. Cell* **7,** 1153–1163
34. Kebache, S., Cardin, E., Nguyen, D. T., Chevet, E., and Larose, L. (2004) *J. Biol. Chem.* **279,** 9662–9671
35. Ngyuen, D. T., Kebache, S., Fazel, A., Wong, H. N., Jenna, S., Emaldali, A., Lee, E.-H., Bergeron, J. J. M., Kaufman, R. J., Larose, L., and Chevet, E.

(2004) *Mol. Biol. Cell* **15,** 4248–4260
36. Lussier, G., and Larose, L. (1997) *J. Biol. Chem.* **272,** 2688–2694
37. Chen, M., She, H., Kim, A., Woodley, D. T., and Li, W. (2000) *Mol. Cell. Biol.* **20,** 7867–7880
38. Jousse, C., Oyadomari, S., Novoa, I., Lu, P., Zhang, Y., Harding, H. P., and Ron, D. (2003) *J. Cell Biol.* **163,** 767–775
39. Novoa, I., Zeng, H., Harding, H. P., and Ron, D. (2001) *J. Cell Biol.* **153,** 1011–1022
40. Zhu, S., Sobolev, A. Y., and Wek, R. C. (1996) *J. Biol. Chem.* **271,** 24989–24994
41. Lu, P. D., Jousse, C., Marciniak, S. J., Zhang, Y., Novoa, I., Scheuner, D., Kaufman, R. J., Ron, D., and Harding, H. P. (2004) *EMBO J.* **23,** 169–179
42. Rao, R. V., Ellerby, H. M., and Bredesen, D. E. (2004) *Cell Death Differ* **11,** 372–380
43. O'Loghlen, A., Perez-Morgado, M. I., Salinas, M., and Martin, M. E. (2003) *Arch. Biochem. Biophys.* **417,** 194–202
44. Chiu, V. K., Bivona, T., Hach, A., Sajous, J. B., Silletti, J., Wiener, H., Johnson, R. L., Jr., Cox, A. D., and Philips, M. R. (2002) *Nat. Cell Biol.* **4,** 343–350
45. Lotti, L. V., Lanfrancone, L., Migliaccio, E., Zompetta, C., Pelicci, G., Salcini, A. E., Falini, B., Pelicci, P. G., and Torrisi, M. R. (1996) *Mol. Cell. Biol.* **16,** 1946–1954
46. Hu, Q., Milfay, D., and Williams, L. T. (1995) *Mol. Cell. Biol.* **15,** 1169–1174
47. Connor, J. H., Weiser, D. C., Li, S., Hallenbeck, J. M., and Shenolikar, S. (2001) *Mol. Cell. Biol.* **21,** 6841–6850
48. Ma, Y., and Hendershot, L. M. (2003) *J. Biol. Chem.* **278,** 34864–34873
49. He, B., Gross, M., and Roizman, B. (1997) *Proc. Natl. Acad. Sci. U. S. A.* **94,** 843–848
50. He, B., Gross, M., and Roizman, B. (1998) *J. Biol. Chem.* **273,** 20737–20743
51. Cohen, P. T. W. (2002) *J. Cell Sci.* **115,** 241–256
52. Stephens, S. B., Dodd, R. D., Brewer, J. W., Lager, P. J., Keene, J. D., and Nicchitta, C. V. (2005) *Mol. Biol. Cell* **16,** 5819–5831
53. Lee, K., Tirasophon, W., Shen, X., Michalak, M., Prywes, R., Okada, T., Yoshida, H., Mori, K., and Kaufman, R. J. (2002) *Genes Dev.* **16,** 452–466
54. Ye, J., Rawson, R. B., Komuro, R., Chen, X., Dave, U. P., Prywes, R., Brown, M. S., and Goldstein, J. L. (2000) *Mol. Cell* **6,** 1355–1364
55. Luo, S., Baumeister, P., Yang, S., Abcouwer, S. F., and Lee, A. S. (2003) *J. Biol. Chem.* **278,** 37375–37385
56. Tan, S., Somia, N., Maher, P., and Schubert, D. (2001) *J. Cell Biol.* **152,** 997–1006
57. Boyce, M., Bryant, K. F., Jousse, C., Long, K., Harding, H. P., Scheuner, D., Kaufman, R. J., Ma, D., Coen, D. M., Ron, D., and Yuan, J. (2005) *Science* **307,** 935–939
58. Harding, H. P., and Ron, D. (2002) *Diabetes* **51,** Suppl. 3, 455–461
59. Kudo, T., Katayama, T., Imaizumi, K., Yasuda, Y., Yatera, M., Okochi, M., Tohyama, M., and Takeda, M. (2002) *Ann. N. Y. Acad. Sci.* **977,** 349–355
60. Ozcan, U., Cao, Q., Yilmaz, E., Lee, A. H., Iwakoshi, N. N., Ozdelen, E., Tuncman, G., Gorgun, C., Glimcher, L. H., and Hotamisligil, G. S. (2004) *Science* **306,** 457–461
61. Piper, M., and Holt, C. (2004) *Annu. Rev. Cell Dev. Biol.* **20,** 505–523
62. Garrity, P. A., Rao, Y., Salecker, I., McGlade, J., Pawson, T., and Zipursky, S. L. (1996) *Cell* **85,** 639–650
63. Song, J., Wu, L., Chen, Z., Kohanski, R. A., and Pick, L. (2003) *Science* **300,** 502–505
64. Cowan, C. A., and Henkemeyer, M. (2001) *Nature* **413,** 174–179
65. Li, X., Meriane, M., Triki, I., Shekarabi, M., Kennedy, T. E., Larose, L., and Lamarche-Vane, N. (2002) *J. Biol. Chem.* **277,** 37788–37797

the FEBS Journal

Nck-1 selectively modulates eIF2αSer51 phosphorylation by a subset of eIF2α-kinases

Eric Cardin, Mathieu Latreille, Chamel Khoury, Michael T. Greenwood and Louise Larose

Polypeptide Laboratory, Department of Experimental Medicine, McGill University, Montreal, Canada

Keywords
adaptor proteins; eIF2; eIF2α-kinases; Nck; stress

Correspondence
L. Larose, Polypeptide Laboratory, Department of Experimental Medicine, McGill University, Strathcona Building, 3640 University St., Rm W315, Montreal, QC, Canada H3A 2B2
Fax: +1 514 398 3923
Tel: +1 514 398 5844
E-mail: louise.larose@mcgill.ca

(Received 16 August 2007, accepted 19 September 2007)

doi:10.1111/j.1742-4658.2007.06110.x

Phosphorylation of the α-subunit of the eukaryotic initiation factor 2 (eIF2) on Ser51 is an early event associated with the down-regulation of protein synthesis at the level of translation and initiation of a transcriptional program. This constitutes a potent mechanism to overcome various stress conditions. In mammals, four eIF2α-kinases [PKR-like endoplasmic reticulum kinase (PERK), dsRNA-activated protein kinase (PKR), heme regulated inhibitor (HRI) and general control nonderepressible-2 (GCN2)], activated following specific stresses, have been shown to be involved in this process. In this article, we report that the ubiquitously expressed adaptor protein Nck, composed only of Src homology domains and classically implicated in cell signaling by activated plasma membrane receptor tyrosine kinases, modulates eIF2α-kinase-mediated eIF2αSer51 phosphorylation in a specific manner. Our results show that Nck not only prevents eIF2α phosphorylation upon PERK activation, as reported previously, but also reduces eIF2α phosphorylation in conditions leading to PKR and HRI activation. By contrast, the overexpression of Nck in mammalian cells fails to attenuate eIF2αSer51 phosphorylation in response to amino acid starvation, a stress well known to activate GCN2. This observation is further confirmed by showing that Nck fails to alter eIF2αSer51 phosphorylation in *Saccharomyces cerevisiae*, for which the sole eIF2α-kinase is Gcn2p. Our results suggest the existence of a novel mechanism that specifically modulates the phosphorylation of eIF2α on Ser51 under various stress conditions.

Protein synthesis results from the translation of mRNA into proteins. This process is dependent on numerous translational factors regulating the initiation, elongation and termination of translation (reviewed in [1]). Translation initiation is by far the most complex and is driven in part by the eukaryotic initiation factor 2 (eIF2) composed of three subunits (α, β and γ). When bound to GTP, eIF2 is active and responsible for the transfer of the initiator methionyl tRNA (iMet-tRNA) to the 40S ribosomal subunit [2]. This step in translation is accompanied by the hydrolysis of GTP bound to eIF2 into GDP, with the recycling of the inactive eIF2-GDP into active eIF2-GTP being accomplished by the multimeric subunit-containing guanine nucleotide exchange factor eIF2B [1,3]. In addition, the activity of eIF2 is regulated by the phosphorylation of its α-subunit on Ser51 by eIF2α-kinases [4,5]. Phosphorylation of eIF2αSer51 increases the affinity of eIF2 for eIF2B and converts eIF2 from a substrate to an inhibitor of eIF2B, thus down-regulating protein

Abbreviations
3-AT, 3-amino-1,2,4-triazole; ATF4, activating transcription factor 4; eIF2, eukaryotic initiation factor 2; ER, endoplasmic reticulum; GCN2, general control nonderepressible-2; GST, glutathione *S*-transferase; HRI, heme regulated inhibitor; iMet-tRNA, initiator methionyl tRNA; PERK, PKR-like endoplasmic reticulum kinase; PKR, dsRNA-activated protein kinase; poly IC, polyinosinic-polycytidylic acid; PP1, protein phosphatase-1; RRL, rabbit reticulocyte lysate; SH, Src homology.

synthesis [6,7]. This represents a well-documented cellular mechanism used to down-regulate protein synthesis in various stress conditions and, concomitantly, to initiate a signaling pathway that promotes the expression of specific genes whose products contribute to overcome these different types of cellular stresses (reviewed in [8]).

In mammals, four eIF2α-kinases have been identified (reviewed in [9]). These are heme regulated inhibitor (HRI), which couples mRNA translation with heme availability in erythroid cells [10], general control nonderepressible-2 (GCN2), which is activated in response to amino acid deprivation [2], dsRNA-activated protein kinase (PKR), a component of the antiviral response activated by double-strand RNA [11], and PKR-like endoplasmic reticulum kinase (PERK), a type 1 transmembrane protein resident in the endoplasmic reticulum (ER) which is activated on accumulation of improperly folded secretory proteins in the ER lumen (referred to as ER stress) [12,13]. All eIF2α-kinases consist of a conserved kinase domain linked to different regulatory domains [14] that allow stress-specific activation and cognate an increase in the levels of eIF2α phosphorylation on Ser51. By contrast, the net amount of phosphorylated eIF2αSer51, as well as its eventual dephosphorylation to allow recovery of protein synthesis after stress, mainly depends on molecular complexes harboring eIF2αSer51 phosphatase activity. Such complexes involving the Ser/Thr protein phosphatase-1c (PP1c), associated with regulatory subunits that target PP1c to eIF2, have been identified [15–18].

Previously, we have demonstrated that the overexpression of the Src homology 3/Src homology 2 (SH3/SH2) domain-containing adaptor protein Nck enhances translation through its direct interaction with the β-subunit of eIF2 [19]. In addition, we have reported that increased cellular levels of Nck strongly impair the phosphorylation of eIF2αSer51, attenuation of translation and polysomal dissociation that normally occur in response to pharmacological induction of ER stress leading to PERK activation [20]. In a more recent study, we have provided evidence that Nck promotes dephosphorylation of eIF2αSer51 by being part of a complex containing an eIF2α-phosphatase activity related to PP1c [21]. This suggests that the effect of Nck on eIF2αSer51 phosphorylation may be a general phenomenon rather than being restricted to the phosphorylation of eIF2αSer51 by a specific eIF2α-kinase. Under stress conditions leading to the specific activation of PKR, HRI or GCN2, we show here that Nck modulates eIF2αSer51 phosphorylation in an eIF2α-kinase-specific manner.

Results

Nck attenuates eIF2αSer51 phosphorylation mediated by PKR

We have previously demonstrated a role for Nck in reducing PERK-mediated eIF2α phosphorylation on Ser51. PERK is an ER-resident transmembrane eIF2α protein kinase mediating the unfolded protein response triggered by the accumulation of misfolded proteins in this organelle [20,21]. To further understand the role of Nck in modulating eIF2αSer51 phosphorylation, we investigated whether Nck also impairs the phosphorylation of eIF2αSer51 by other eIF2α-kinases. We first examined the levels of eIF2αSer51 phosphorylation in HeLa cells transiently overexpressing Nck-1 in response to synthetic double-stranded RNA polyinosinic-polycytidylic acid (poly IC) used to activate PKR [22]. Phosphorylation of eIF2αSer51 was observed at the end of a 2 h transfection with poly IC (time zero post-transfection) and was maximal at 2 h post-transfection (Fig. 1A, left panel). In this condition, phosphorylation of eIF2αSer51, although transient, persisted for at least 6 h post-transfection. At 2 h post-transfection, increasing concentrations of poly IC led to parallel increases in eIF2αSer51 phosphorylation up to 0.5 μg of poly IC, where a plateau was reached (Fig. 1A, right panel). Most interestingly, transient overexpression of Nck-1 in HeLa cells strongly inhibited the phosphorylation of eIF2αSer51 induced by poly IC (Fig. 1B). These results show that the modulation of eIF2αSer51 phosphorylation by Nck is not restricted to ER stress conditions activating PERK, as it was also seen in conditions activating PKR.

Nck attenuates eIF2αSer51 phosphorylation mediated by HRI

Sodium arsenite was used to activate HRI in HeLa cells [23]. Phosphorylation of eIF2αSer51 was observed as early as 30 min post-treatment, but was transient and started to decrease after 2 h (Fig. 2A, left panel). Increasing concentrations of sodium arsenite from 1 to 100 μM gradually induced the phosphorylation of eIF2αSer51 (Fig. 2A, right panel). Interestingly, the transient overexpression of Nck-1 strongly inhibited the phosphorylation of eIF2αSer51 in HeLa cells subjected to sodium arsenite exposure (Fig. 2B). However, sodium arsenite is somewhat controversial regarding its specificity towards HRI activation, given that PKR has also been reported to be activated in some conditions [24]. To further confirm the effect of Nck on HRI-mediated eIF2αSer51 phosphorylation, we used

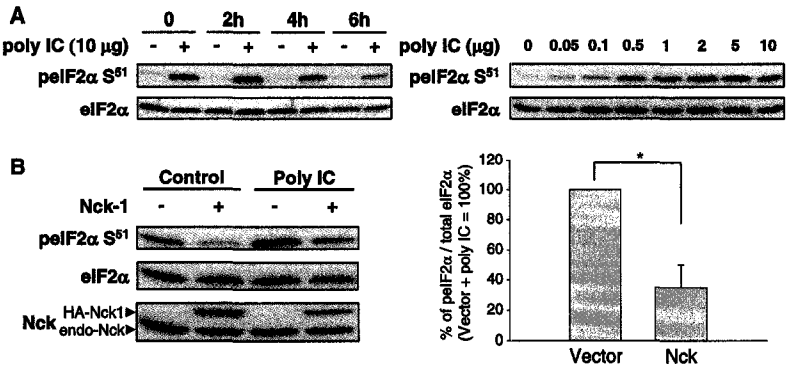

Fig. 1. Overexpression of Nck-1 modulates eIF2αSer51 phosphorylation in stress conditions activating PKR. (A) HeLa cells were transfected with 10 μg of synthetic ds-RNA (poly IC) and cultured for the indicated times post-transfection (left panel), or with increasing amounts of poly IC as indicated and grown for 2 h post-transfection (right panel). Total clarified cell lysates normalized for protein content were subjected to western blot analysis using the indicated specific antibodies. (B) Mock-transfected (–) or transiently overexpressing HA-tagged Nck-1 (+) HeLa cells were transfected with 0.8 μg poly IC, grown for 2 h and western blot analysis was performed on protein extracts as in (A) (left panel). Densitometry and statistical analyses (Student's *t*-test) were performed on the results obtained from four independent experiments, and were plotted as a percentage of phosphorylated eIF2α over total eIF2α for Nck-1 transfected cells compared with empty vector (right panel). Bars represent SEM. $*P < 0.01$.

rabbit reticulocyte lysate (RRL) noncomplemented with hemin, in which HRI is reported to be constitutively activated [25]. The addition of exogenous recombinant glutathione *S*-transferase (GST)–Nck-1 fusion protein to RRL samples, like the addition of the potent HRI inhibitor hemin, resulted in lower levels of phosphorylated eIF2αSer51 at the end of a 30 min incubation at 30 °C, compared with control samples supplemented with an equimolar amount of GST (Fig. 2C). This reveals that the modulation of eIF2αSer51 phosphorylation by Nck is not restricted to a specific stress, but rather is common to stress-activating PERK, PKR or HRI. It also suggests that the effect of Nck on the phosphorylation of eIF2αSer51 is independent of the type of stress condition mediating the activation of eIF2α-kinases.

Nck fails to alter GCN2-mediated eIF2αSer51 phosphorylation

To ascertain that the effect of Nck-1 on eIF2αSer51 phosphorylation by eIF2α-kinases is a general phenomenon, we also investigated the modulation of eIF2α phosphorylation in conditions activating GCN2. As expected, amino acid starvation (deprivation of four amino acids) in HeLa cells resulted in increased eIF2αSer51 phosphorylation (Fig. 3A, lanes 1–3 and lanes 5–7). According to the literature, this is believed to be through the activation of GCN2 [2]. By contrast with the observations in stress conditions activating PERK, PKR or HRI, overexpression of Nck-1 failed to impair GCN2-mediated eIF2αSer51 phosphorylation (Fig. 3A, lanes 3, 4 and 7, 8). To ensure that, in these conditions, the level of overexpressed Nck-1 was not limiting, similar experiments were undertaken in HeLa cells transfected with increasing amounts of Nck-1 to reach higher levels of Nck-1 overexpression. As reported in Fig. 3B, GCN2-mediated eIF2αSer51 phosphorylation was not altered in any case in which Nck-1 was overexpressed in a dose-dependent manner. We then rationalized that perhaps the stress produced by the deprivation of four amino acids was too strong to be attenuated by Nck-1. To address this point, we subjected the cells to only single amino acid starvation (leucine), hoping that this would weaken the stress insult. In mock-transfected HeLa cells, leucine starvation still increased the level of eIF2αSer51 phosphorylation (Fig. 3C, lanes 1–3), although to a lesser extent to that observed in the previous experiments using four amino acid deprivation. These results demonstrate that single amino acid starvation (leucine) induces a weaker stress response compared with the deprivation of four amino acids (glutamine, leucine, lysine and methionine). However, even when using amino acid starvation conditions resulting in only weak eIF2α phosphorylation, Nck-1 had no effect on the levels of eIF2αSer51 phosphorylation in response to GCN2 activation.

We next used yeast cells to further confirm the inability of Nck-1 to modulate eIF2αSer51 phosphorylation mediated by GCN2. Gcn2p is the sole eIF2α-kinase present in *Saccharomyces cerevisiae*, which is

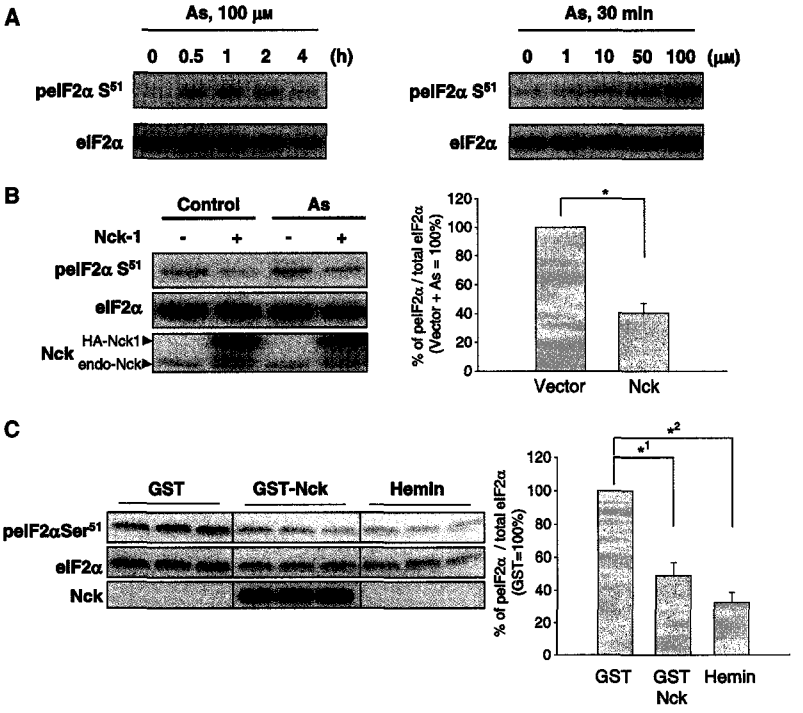

Fig. 2. Overexpression of Nck-1 modulates eIF2αSer51 phosphorylation in stress conditions activating HRI. (A) HeLa cells were treated with 100 μM sodium arsenite (As) for the indicated times (left panel) or with increasing concentrations of As for 30 min (right panel). Cell lysates normalized for protein content were subjected to western blot analysis using the specific antibodies as indicated. (B) Mock-transfected (–) or transiently overexpressing HA-tagged Nck-1 (+) HeLa cells were treated with 25 μM As for 30 min and protein extracts were analyzed by western blot as in (A) (left panel). Densitometry and statistical analyses (Student's *t*-test) were performed on the results obtained from five independent experiments, and were plotted as a percentage of phosphorylated eIF2α over total eIF2α for Nck-1 transfected cells compared with empty vector (right panel). Bars represent SEM. $*P < 0.001$. (C) Triplicates of RRL were incubated at 30 °C for 30 min in buffer containing 25 μM of bacterially purified GST or GST–Nck fusion protein. Hemin (25 μM) was used as a positive control. Data were obtained from western blot analyses performed and treated as in (A). Bar, standard error of the mean. $*^1P < 0.01$, $*^2P < 0.001$.

both functionally and structurally similar to mammalian GCN2 (reviewed in [2]). In yeast, phosphorylation of eIF2α by Gcn2p upon amino acid starvation leads to an increase in the levels of Gcn4p, which, in turn, transcriptionally activates genes implicated in amino acid biosynthesis [26]. This response is absolutely required for yeast cell growth under amino acid starvation imposed by the 3-amino-1,2,4-triazole (3-AT), a competitive inhibitor of the *HIS3* gene product, which limits histidine biosynthesis [2]. We therefore examined whether the expression of Nck-1 would impair Gcn2p-mediated eIF2αSer51 phosphorylation and growth in 3-AT-induced amino acid starvation in *S. cerevisiae*. As shown in Fig. 4A, Nck-1 expression was achieved in galactose-grown yeast transformants harboring a vector driving its expression under the control of a galactose-inducible promoter (lanes 2 and 4). In these conditions, Nck-1 expression failed to modulate unstressed levels of phosphorylated eIF2αSer51 when compared with yeast cells transformed with empty vector (lanes 1 and 2). As expected, phosphorylation of eIF2α on Ser51 was not detected in yeast cells lacking *GCN2* (*GCN2Δ*) (lanes 3 and 4), thus supporting that Gcn2p is the unique eIF2α-kinase in *S. cerevisiae*. This is also in agreement with the observation that wild-type yeast grew on medium containing 3-AT, whereas the growth of *GCN2Δ* yeast cells was severely inhibited (Fig. 4B). Furthermore, consistent with the lack of effect of Nck-1 expression on basal unstressed eIF2αSer51 phosphorylation, expression of Nck-1 in yeast failed to impair Gcn2p-mediated resistance to 3-AT (Fig. 4B). To verify that Nck-1 could modulate eIF2αSer51 phosphorylation in yeast, we cotransformed the *GCN2Δ* yeast strain with plasmids reciprocally encoding human Nck-1 and PKR, both under the regulation of galactose. As seen in Fig. 4C, the expression of Nck-1 effectively modulated eIF2αSer51 phosphorylation in yeast expressing human PKR. However,

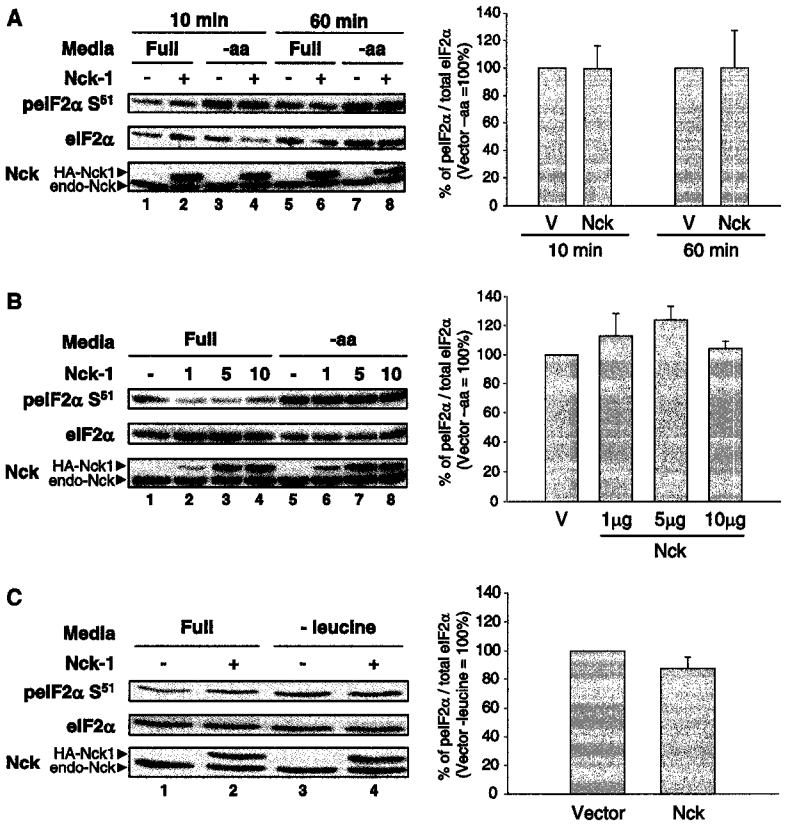

Fig. 3. Overexpression of Nck-1 fails to modulate eIF2αSer51 phosphorylation by GCN2 in mammalian cells. (A) Mock-transfected (–) or transiently overexpressing HA-tagged Nck-1 (+) HeLa cells were grown in complete medium (full) or subjected to four amino acid starvation (– aa) for 10 min or 60 min, as described in Experimental procedures. Total clarified cell lysates normalized for protein content were subjected to western blot analysis using the indicated specific antibodies (left panel). (B) HeLa cells mock-transfected (–) or transfected using increasing amounts (0–10 μg) of Nck-1 cDNA containing plasmid were starved of amino acids for 10 min. (C) Mock-transfected (–) or transiently overexpressing HA-tagged Nck-1 (+) HeLa cells were subjected to L-leucine starvation for 6 h (left panels). Densitometry and statistical analyses (right panels), when appropriate, (Student's *t*-test) were performed on the results obtained from three independent experiments (except two for the data presented in B). The data were plotted as a percentage of phosphorylated eIF2α over total eIF2α for Nck-1 transfected cells (Nck) compared with empty vector (V). Bars represent SEM.

Nck-1 expression increased this phosphorylation, by contrast with the previous observations in mammalian cells (Fig. 1). In agreement with the enhancement of PKR-induced phosphorylation of eIF2αSer51 by Nck-1, we also noticed that Nck-1 enhanced the growth inhibition induced by PKR (Fig. 4D). Together, these results demonstrate that, by contrast with its effect on PERK-, PKR- and HRI-induced eIF2αSer51 phosphorylation, Nck-1 is not a modulator of GCN2-mediated eIF2αSer51 phosphorylation and the related cellular stress response.

Discussion

The regulation of protein synthesis at the level of translation is a well-documented mechanism used by cells to respond to physiological stresses (reviewed in [8]). This process, which involves the phosphorylation of the α-subunit of eIF2 on Ser51, leads to the inhibition of general translation with the concomitant promotion of the translation of specific mRNAs. This is well illustrated by the increased translation of the activating transcription factor 4 (ATF4), a transcription factor that initiates a transcriptional program increasing the expression of specific products involved in stress responses. It is now established that eIF2αSer51 phosphorylation is under the control of eIF2α-kinases activated by specific stress conditions. In mammals, members of this protein kinase family include PERK, PKR, HRI and GCN2. These proteins all share a conserved kinase domain responsible for the phosphorylation of eIF2αSer51, with other domains surrounding

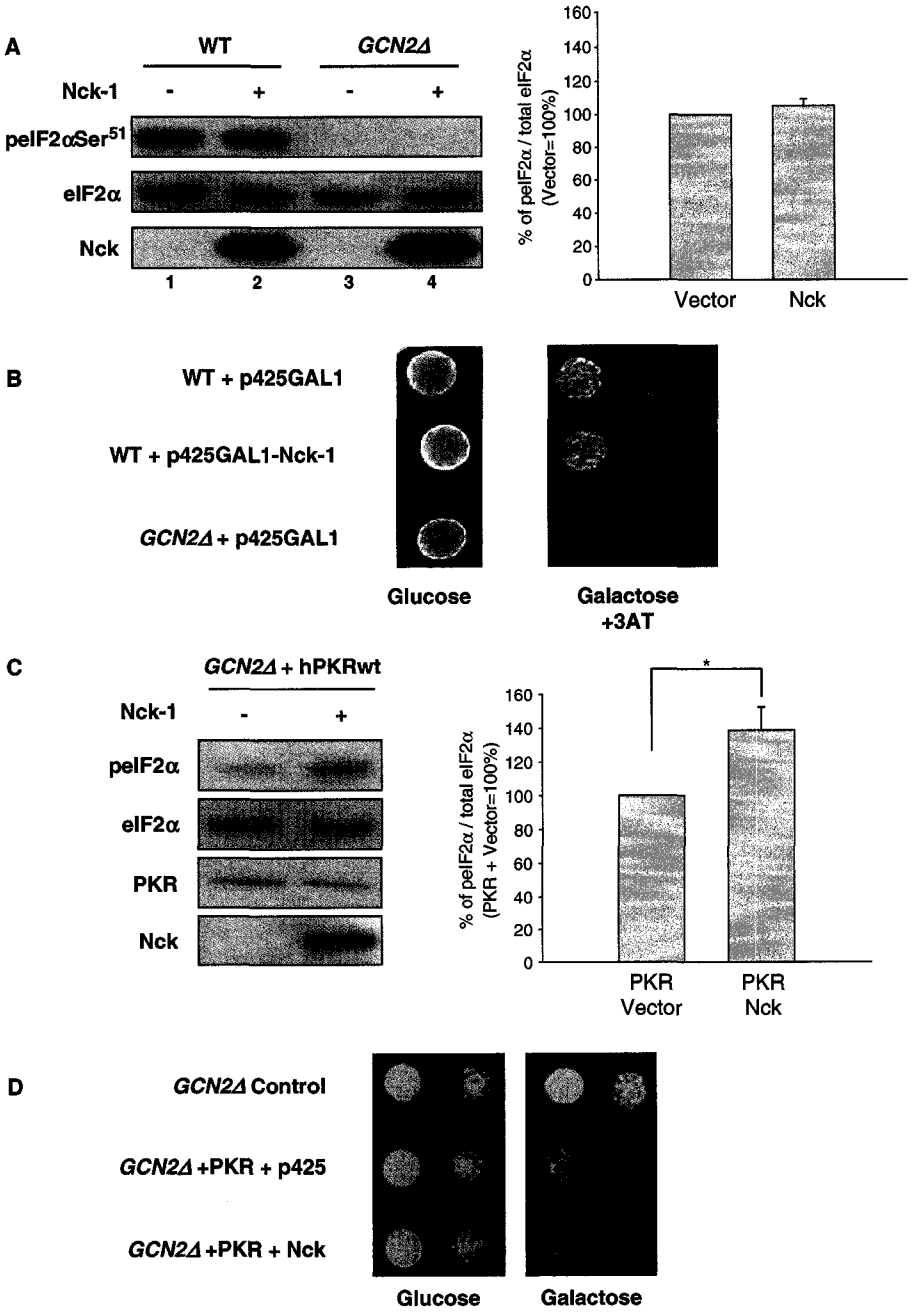

the catalytic core being variable. These various regulatory regions are believed to support the subcellular localization, assembly of molecular complexes and/or stress-specific dependent activation of these proteins. In addition to its regulation by eIF2α-kinases, the levels of eIF2αSer51 phosphorylation are also controlled by eIF2α-phosphatase activities that specifically dephosphorylate this site. This is proposed as a feedback mechanism, allowing translational recovery on cellular stress insults. To date, the eIF2α-phosphatase activities identified essentially engage PP1 in molecular complexes with various regulatory proteins, such as CReP [17], GADD34 [15] or the virulence factor ICP34.5 [16]. Recently, we have reported that the

Fig. 4. In *S. cerevisiae*, the expression of Nck-1 fails to modulate unstressed levels of eIF2αSer51 phosphorylation and Gcn2p-mediated growth in amino acid starvation conditions, but modulates PKR-mediated eIF2αSer51 phosphorylation and growth inhibition. (A) Wild-type and *GCN2Δ* yeast strains transformed with p425GAL1-Nck-1 or empty p425GAL1 vector were grown in galactose medium overnight, and protein extracts were analyzed by western blot. Specific antibodies, as described in Experimental procedures, were used for the detection of Nck, and phosphorylated and total eIF2α (left panel). Densitometry and statistical analyses (Student's *t*-test) were performed on the results obtained from three independent experiments, and were plotted as a percentage of phosphorylated eIF2α over total eIF2α for yeast expressing Nck-1 compared with empty vector (right panel). Bars represent SEM. (B) For the spot assay of yeast strains described in (A), serial dilutions from equivalent amounts of cells were spotted on to agar plates containing synthetic medium with 2% glucose, or 2% galactose and 2% raffinose, and supplemented with 100 mM 3-AT. The results are representative of two independent yeast transformants. (C), *GCN2Δ* yeast strain was cotransformed with p413GAL1-hPKR and either p425GAL1-Nck-1 or empty p425GAL1 vector. Yeast transformants were grown in galactose medium for 4 h and protein extracts were analyzed by western blot as described in (A) (left panel). Densitometry and statistical analyses (Student's *t*-test) were performed on the results obtained from three independent experiments, and were plotted as a percentage of phosphorylated eIF2α over total eIF2α for yeast expressing Nck-1 compared with mock transformed yeast (right panel). Bars represent SEM. $*P < 0.05$. (D), spot assay of *GCN2Δ* yeast strain cotransformed with p426GAL1-hPKR and either p425GAL1-Nck-1 or empty p425GAL1 vector. Serial dilutions from equivalent amounts of cells were spotted on to agar plates containing synthetic medium with 2% glucose, or 2% galactose and 2% raffinose. The results are representative of two independent yeast transformants.

SH2/SH3 domain-containing adaptor protein Nck plays an important role in regulating the levels of phosphorylated eIF2αSer51 in ER stress conditions by being part of an eIF2α-holophosphatase complex containing PP1c [21]. The exact mechanism by which Nck modulates eIF2αSer51 phosphorylation, as well as its role in the holophosphatase complex, still remain to be defined.

In this study, we have shown that, in mammalian cells, the adaptor Nck-1 not only modulates eIF2αSer51 phosphorylation driven by stress conditions preferentially activating PERK, but also PKR and HRI, but not GCN2. The inability of Nck-1 to modulate GCN2-dependent eIF2αSer51 phosphorylation is further supported by our observations in *S. cerevisiae*. eIF2αSer51 phosphorylation under unstressed conditions, as well as during growth under amino acid starvation, both of which depend on Gcn2p activation in yeast, are not impaired by the expression of Nck-1. Given that *S. cerevisiae*, unlike mammalian cells, contains a single eIF2α-kinase (Gcn2p), our results confirm that phosphorylated eIF2αSer51 ascribed to GCN2 activity is resistant to modulation by Nck-1. By contrast, Nck-1 still modulates PKR-mediated eIF2αSer51 phosphorylation in yeast, suggesting that the mechanism by which Nck regulates the phosphorylation of eIF2αSer51 by a subset of eIF2α-kinases can take place in this species. However, different effects of Nck are observed in HeLa cells and yeast, with eIF2αSer51 phosphorylation being decreased in the former and increased in the latter. At the present time, we cannot explain this difference, but, on the basis of the adaptor function of Nck, we suggest that, in yeast and mammalian cells, Nck assembles different molecular complexes which may account for the different effects observed. Nevertheless, these data further support the notion of the specificity in Nck regulation of eIF2αϖ Ser51 phosphorylation by eIF2α-kinases.

Having recently shown that Nck is involved in the maintenance of a significant amount of PP1c in the vicinity of eIF2 [21], it was surprising to find that its effect on eIF2αSer51 phosphorylation was selective amongst eIF2α-kinases. By contrast, we expected that Nck, being part of a complex harboring eIF2α-phosphatase activity, would promote the dephosphorylation of phosphorylated eIF2αSer51 independent of the eIF2α-kinases activated. Nevertheless, the selectivity of the Nck effect on eIF2αSer51 phosphorylation to a subset of eIF2α-kinases could be explained by the innate adaptor function of Nck. For example, Nck is known to translocate specific effectors to a subset of activated receptor tyrosine kinases at the plasma membrane (reviewed in [27]). In an analogous fashion, Nck may target a holophosphatase complex to specific subcellular compartments, where it may modulate pools of eIF2αSer51 phosphorylated by specific eIF2α-kinases. This model implies that, amongst the eIF2α-kinases, GCN2 would phosphorylate a specific restricted pool of eIF2α that is not accessible to the Nck–eIF2α–holophosphatase complex. At the present time, there is no clear evidence for such specificity. Alternatively, it is possible that the effect of Nck on eIF2α phosphorylation could be on eIF2α-kinases by interfering with their activation via a phosphatase or any unknown mechanism. In a previous study, we have reported that PERK phosphorylation following thapsigargin treatment is reduced in cells overexpressing Nck [20]. Regarding the results presented here, Nck would have the capability to interfere with the activation of PERK, PKR and HRI, but not GCN2. It is also possible that cognate structural differences in the eIF2α-kinases may be responsible for Nck

selectivity. GCN2 is by far the largest eIF2α-kinase and, outside the catalytic domain, it does not present a high level of similarity with PERK, PKR or HRI. Indeed, GCN2 harbors multiple domains that are believed to be involved in intra- and intermolecular interactions regulating its activity and subcellular localization [28–31]. Further experiments are required to address whether this could be of importance for Nck-mediated modulation of eIF2αSer51 phosphorylation by eIF2α-kinases.

As observed in Figs 1B, 2B and 3B, the overexpression of Nck-1 reduces basal (unstressed) levels of eIF2αSer51 phosphorylation. This effect is observed in almost all experiments (data presented here and [21]). However, for unknown reasons, in a few experiments it cannot be observed, as shown in Fig. 3A, C. In mammalian cells, all four eIF2α-kinases are present, and their respective resting activity could contribute to basal levels of eIF2αSer51 phosphorylation. Our data demonstrate that Nck modulates PERK-, PKR- and HRI-mediated, but not GCN2-mediated, eIF2α phosphorylation. Therefore, it is expected that Nck-1 overexpression will decrease the basal levels of eIF2α phosphorylation as long as GCN2 is not involved. Supporting this is the fact that Nck failed to modulate the basal levels of eIF2αSer51 phosphorylation in *S. cerevisiae*, in which GCN2 is the sole eIF2α-kinase. We therefore suggest that subtle changes, such as cell type, serum batches, cell density, cell cycle, etc., could affect the nature of the eIF2α-kinase(s) activity under basal conditions. In this context, basal conditions triggering low levels of GCN2 activity would prevent the modulation of basal eIF2αSer51 phosphorylation by Nck-1 overexpression, and could explain why this effect is variable in mammalian cells. However, as the mechanism(s) by which Nck modulates eIF2αSer51 phosphorylation still remains to be completely understood, we cannot exclude other possible factors to explain these uncommon variations.

Although the physiological significance of the specificity of Nck on eIF2αSer51 phosphorylation by eIF2α-kinases remains to be established, we have demonstrated that Nck contributes to the inhibition of eIF2αSer51 phosphorylation by a subset of activated eIF2α-kinases in particular stress conditions. We propose that Nck may contribute to the restriction of eIF2αSer51 phosphorylation by these eIF2α-kinases in specific tissues or at specific stages during embryonic development. Overall, our findings provide new insights into the modulation and complexity of the phosphorylation of eIF2α on Ser51 under various stress conditions. The involvement of the adaptor protein Nck in this process further highlights the versatile properties of SH2/SH3 domain-containing adaptor proteins.

Experimental procedures

Cell culture and transfection

HeLa cells were grown in minimum essential Eagle's medium (Sigma, St Louis, MO, USA) supplemented with 10% fetal bovine serum (Invitrogen, Burlington, Canada) at 37 °C in 5% CO_2/95% O_2. Subconfluent HeLa cells grown in 60 mm dishes were transfected with 1 μg HA-tagged Nck-1 construct (gift from W Li, LA California, previously described [32]) or empty vector (pRK5) using Lipofectamine-Plus reagent (Invitrogen), according to the manufacturer's instructions. After 24 h of transfection, cells were subjected to different treatments to activate eIF2α-kinases.

Activation of eIF2α-kinases in HeLa cells

Individual eIF2α-kinases were activated following specific cell treatments currently reported in the literature. PKR activation was achieved by transfecting cells with 0.8 μg of synthetic double-stranded RNA poly IC (GE Healthcare, Biosciences Corp., Piscataway, NJ, USA) using Lipofectamine-Plus reagent for 2 h. Poly IC transfected cells were then washed and kept in regular fresh medium for an additional 2 h period before being harvested. HRI was activated by treating cells with 25 μM sodium arsenite (Sigma) for 30 min. For GCN2 experiments, cells were grown in Dulbecco's modified Eagle's medium (DMEM)/F-12 base medium (Sigma) reconstituted with L-glutamine (0.37 $g{\cdot}L^{-1}$), L-leucine (0.06 $g{\cdot}L^{-1}$), L-lysine-HCl (0.09 $g{\cdot}L^{-1}$), L-methionine (0.02 $g{\cdot}L^{-1}$), magnesium chloride-6H_2O (0.06 $g{\cdot}L^{-1}$), magnesium sulfate (heptahydrate) (0.10 $g{\cdot}L^{-1}$), calcium chloride (0.15 $g{\cdot}L^{-1}$), sodium bicarbonate (1.2 $g{\cdot}L^{-1}$), supplemented with 10% dialyzed fetal bovine serum (Invitrogen) and 1% antibiotic–antimycotic mixture (Gibco BRL, Gaithersburg, MD, USA). GCN2 was activated by replacing the medium with DMEM/F-12 lacking L-leucine (single amino acid starvation) or lacking L-glutamine, L-leucine, L-lysine and L-methionine (four amino acid starvation).

Assay of effect of Nck-1 on eIF2α phosphorylation by HRI in RRL

Triplicates of hemin (25 μM) or equimolar amounts of bacterially purified GST and GST–Nck-1 were prepared in 95 μL of buffer (50 mM Tris/HCl pH 7.4; 5 mM $MgCl_2$) and preincubated at 30 °C for 10 min. Untreated commercial RRL (5 μL) not supplemented with hemin (Promega, Madison, WI, USA) was added to triplicates, and the reactions were further incubated at 30 °C for

30 min. Reactions were stopped by the addition of Laemmli buffer, and samples were processed for immunoblot analysis as described below.

Immunoblot analysis and antibodies

Treated cells were washed with cold NaCl/P_i and lysed in ice-cold lysis buffer containing 10 mM Tris/HCl (pH 7.4), 50 mM KCl, 2 mM $MgCl_2$, 1% Triton X-100, 3 $\mu g \cdot mL^{-1}$ aprotinin, 1 $\mu g \cdot mL^{-1}$ leupeptin, 1 mM dithiothreitol, 0.1 mM Na_2VO_4 and 0.1 $\mu g \cdot mL^{-1}$ Pefabloc SC (Roche Diagnostic, Basel, Switzerland). Cell lysates were centrifuged at 10 000 *g* for 10 min at 4 °C, and the concentration of proteins in the soluble fractions was determined using a Bio-Rad (Hercules, CA, USA) protein assay based on the Bradford method. Protein concentrations were normalized with lysis buffer and, following the addition of Laemmli buffer, samples were heated at 90 °C for 5 min. Equal amounts of proteins (30–70 μg) were resolved by 10% SDS/PAGE, followed by their transfer onto poly(vinylidene difluoride) membrane (Bio-Rad). Membranes were blocked with 10% nonfat dry milk for 30 min at room temperature, and then incubated with primary antibodies against phosphospecific eIF2αSer51 (BioSource, Camarillo, CA, USA), total eIF2α (Santa Cruz Biotechnology, Santa Cruz, CA, USA), total yeast eIF2α (gracious gift of T. E. Dever, National Institutes of Health, Bethesda, MD, USA) or Nck [33], followed by incubation with specific horseradish peroxidase-conjugated secondary antibodies (Bio-Rad). Signal detection was achieved using ECL plus (Enhanced Chemiluminescence, GE Healthcare) according to the manufacturer's instructions.

Yeast plasmids

Human Nck-1 and human PKR were expressed in yeast under the control of the GAL1 promoter using the plasmids p425GAL1 and p426GAL1, respectively [34]. These plasmids allow the repression of expression by glucose and strong induction by galactose in the growth medium [35]. Nck-1 was amplified by PCR from pcDNA3.1/myc-His Nck-1 DNA. PKR was amplified by PCR from the vector pcDNA3-PKR (generous gift of A. E. Koromilas, McGill University, Montreal, Canada). Nck-1 and PKR PCR products were inserted into *Hin*dIII linearized p425GAL1 or p426GAL1, respectively, by homologous recombination in yeast as described previously [36], to generate p425GAL1-Nck-1 and p426GAL1-PKR. p413GAL1 (generous gift of B. Turcotte, McGill University, Montreal, Canada), a low copy number vector compared with p425GAL1 and p426GAL1, was also used to introduce PKR in yeast. p413GAL1 was generated from p413MET25 by replacing the promoter MET25 by GAL1. p413GAL1-PKR was generated following recovery of PKR cDNA from p426GAL1-PKR with *Bam*HI before subcloning into p413GAL1. All constructs were fully sequenced to confirm the absence of undesirable mutations.

Yeast growth and transformation

Wild-type yeast (*S. cerevisiae*) strain BY4741 (MATα; his3Δ1; leu2Δ0; met15Δ0; ura3Δ0) and the isogenic *GCN2*Δ strain were obtained from Euroscarf (Frankfurt, Germany). Yeasts were grown overnight in yeast complete medium and transformed with different individual plasmids (p425GAL1, p425GAL1-Nck-1, p426GAL1-PKR, p413GAL1-PKR) or cotransformed with p426GAL1-PKR and p425GAL1-Nck-1 or p413GAL1-PKR and p425GAL1-Nck-1 using lithium acetate [37]. Transformants were selected and maintained in synthetic minimal medium lacking their respective amino acid for selection. When necessary, plasmid p423GAL1 was transformed into yeast to make it auxotrophic for histidine [34].

Assays of effect of Nck-1 on eIF2αSer51 phosphorylation by GCN2 and growth under amino acid starvation induced by 3-AT in yeast

To analyze eIF2αSer51 phosphorylation in unstressed conditions, protein extracts were prepared from yeast transformants growing in selective medium as described previously [38]. Briefly, an equal number of yeast cells was treated with NaOH and subsequently heated to 95 °C in Laemmli buffer. Proteins were resolved by SDS/PAGE, transferred to membrane, challenged with specific antibodies and submitted to ECL detection as described above. Spot assay was used to monitor the effect of expression of Nck-1 on the resistance to 100 mM 3-AT growth inhibition mediated through the phosphorylation of eIF2α by GCN2 in *S. cerevisiae* [39]. Briefly, yeast transformants containing p423GAL1 and either p425GAL1 or p425GAL1-Nck-1 were first grown in liquid selective nutriment medium. Saturated cultures were then serially diluted. Corresponding aliquots were spotted on to selective synthetic medium agar plates containing 2% glucose, or on plates containing 2% galactose, 2% raffinose, 100 mM 3-AT and lacking histidine. The plates were then incubated at 30 °C for 3 days.

Assays of effect of Nck-1 on eIF2α phosphorylation by PKR in yeast

To analyze eIF2αSer51 phosphorylation in yeast expressing PKR, protein extracts were prepared from yeast transformants growing in selective medium as described above. The spot assay was used to monitor the effect of expression of Nck-1 on growth inhibition induced by PKR. Yeast transformants containing p413GAL1-PKR and either p425GAL1 or p425GAL1-Nck-1 were grown in liquid

selective nutriment medium. Saturated cultures were then serially diluted. Corresponding aliquots were spotted on to selective synthetic medium agar plates containing 2% glucose or 2% galactose and 2% raffinose. The plates were then incubated at 30 °C for 3 days.

Acknowledgements

We wish to thank Dr B. Turcotte (McGill University, Montreal, Canada) for scientific discussions. This work was supported by the Natural Sciences and Engineering Research Council (NSERC) of Canada (RGPN 250215-02 to LL and RGPN 217502-03 to MTG). EC and ML were supported by the MUHC-RI from McGill University, and LL is a Chercheur National of the Fonds de la Recherche en Santé du Québec.

References

1 Hershey JW (1991) Translational control in mammalian cells. *Annu Rev Biochem* **60**, 717–755.
2 Hinnebusch AG (2000) *Mechanism and Regulation of Initiator Methionyl-tRNA Binding to Ribosomes*. Cold Spring Harbor Laboratory Press, Cold Spring Harbor, New York.
3 Webb BL & Proud CG (1997) Eukaryotic initiation factor 2B (eIF2B). *Int J Biochem Cell Biol* **29**, 1127–1131.
4 Matts RL, Levin DH & London IM (1983) Effect of phosphorylation of the alpha-subunit of eukaryotic initiation factor 2 on the function of reversing factor in the initiation of protein synthesis. *Proc Natl Acad Sci USA* **80**, 2559–2563.
5 Matts RL & London IM (1984) The regulation of initiation of protein synthesis by phosphorylation of eIF-2(alpha) and the role of reversing factor in the recycling of eIF-2. *J Biol Chem* **259**, 6708–6711.
6 Clemens MJ, Pain VM, Wong ST & Henshaw EC (1982) Phosphorylation inhibits guanine nucleotide exchange on eukaryotic initiation factor 2. *Nature* **296**, 93–95.
7 Sudhakar A, Krishnamoorthy T, Jain A, Chatterjee U, Hasnain SE, Kaufman RJ & Ramaiah KV (1999) Serine 48 in initiation factor 2 alpha (eIF2 alpha) is required for high-affinity interaction between eIF2 alpha(P) and eIF2B. *Biochemistry* **38**, 15 398–15 405.
8 Proud CG (2005) eIF2 and the control of cell physiology. *Semin Cell Dev Biol* **16**, 3–12.
9 de Haro C, Mendez R & Santoyo J (1996) The eIF-2alpha kinases and the control of protein synthesis. *Faseb J* **10**, 1378–1387.
10 Chen J (2000) *Heme-Regulated eIF2α Kinase*. Cold Spring Harbor Laboratory Press, Cold Spring Harbor, NY.
11 Kaufman RJ (2000) *The Double-Stranded RNA-Activated Protein Kinase PKR*. Cold Spring Harbor Laboratory Press, Cold Spring Harbor, NY.
12 Harding HP, Zhang Y, Bertolotti A, Zeng H & Ron D (2000) Perk is essential for translational regulation and cell survival during the unfolded protein response. *Mol Cell* **5**, 897–904.
13 Harding HP, Zhang Y & Ron D (1999) Protein translation and folding are coupled by an endoplasmic-reticulum-resident kinase. *Nature* **397**, 271–274.
14 Dever TE (2002) Gene-specific regulation by general translation factors. *Cell* **108**, 545–556.
15 Connor JH, Weiser DC, Li S, Hallenbeck JM & Shenolikar S (2001) Growth arrest and DNA damage-inducible protein GADD34 assembles a novel signaling complex containing protein phosphatase 1 and inhibitor 1. *Mol Cell Biol* **21**, 6841–6850.
16 He B, Gross M & Roizman B (1998) The gamma134.5 protein of herpes simplex virus 1 has the structural and functional attributes of a protein phosphatase 1 regulatory subunit and is present in a high molecular weight complex with the enzyme in infected cells. *J Biol Chem* **273**, 20 737–20 743.
17 Jousse C, Oyadomari S, Novoa I, Lu P, Zhang Y, Harding HP & Ron D (2003) Inhibition of a constitutive translation initiation factor 2alpha phosphatase, CReP, promotes survival of stressed cells. *J Cell Biol* **163**, 767–775.
18 Novoa I, Zeng H, Harding HP & Ron D (2001) Feedback inhibition of the unfolded protein response by GADD34-mediated dephosphorylation of eIF2alpha. *J Cell Biol* **153**, 1011–1022.
19 Kebache S, Zuo D, Chevet E & Larose L (2002) Modulation of protein translation by Nck-1. *Proc Natl Acad Sci USA* **99**, 5406–5411.
20 Kebache S, Cardin E, Nguyen DT, Chevet E & Larose L (2004) Nck-1 antagonizes the endoplasmic reticulum stress-induced inhibition of translation. *J Biol Chem* **279**, 9662–9671.
21 Latreille M & Larose L (2006) Nck in a complex containing the catalytic subunit of protein phosphatase 1 regulates eukaryotic initiation factor 2alpha signaling and cell survival to endoplasmic reticulum stress. *J Biol Chem* **281**, 26 633–26 644.
22 Carter WA & De Clercq E (1974) Viral infection and host defense. *Science* **186**, 1172–1178.
23 McEwen E, Kedersha N, Song B, Scheuner D, Gilks N, Han A, Chen JJ, Anderson P & Kaufman RJ (2005) Heme-regulated inhibitor kinase-mediated phosphorylation of eukaryotic translation initiation factor 2 inhibits translation, induces stress granule formation, and mediates survival upon arsenite exposure. *J Biol Chem* **280**, 16 925–16 933.

24 Patel CV, Handy I, Goldsmith T & Patel RC (2000) PACT, a stress-modulated cellular activator of interferon-induced double-stranded RNA-activated protein kinase, PKR. *J Biol Chem* **275**, 37 993–37 998.
25 Farrell PJ, Balkow K, Hunt T, Jackson RJ & Trachsel H (1977) Phosphorylation of initiation factor eIF-2 and the control of reticulocyte protein synthesis. *Cell* **11**, 187–200.
26 Dever TE, Feng L, Wek RC, Cigan AM, Donahue TF & Hinnebusch AG (1992) Phosphorylation of initiation factor 2 alpha by protein kinase GCN2 mediates gene-specific translational control of GCN4 in yeast. *Cell* **68**, 585–596.
27 McCarty JH (1998) The Nck SH2/SH3 adaptor protein: a regulator of multiple intracellular signal transduction events. *Bioessays* **20**, 913–921.
28 Dong J, Qiu H, Garcia-Barrio M, Anderson J & Hinnebusch AG (2000) Uncharged tRNA activates GCN2 by displacing the protein kinase moiety from a bipartite tRNA-binding domain. *Mol Cell* **6**, 269–279.
29 Garcia-Barrio M, Dong J, Ufano S & Hinnebusch AG (2000) Association of GCN1-GCN20 regulatory complex with the N-terminus of eIF2alpha kinase GCN2 is required for GCN2 activation. *Embo J* **19**, 1887–1899.
30 Padyana AK, Qiu H, Roll-Mecak A, Hinnebusch AG & Burley SK (2005) Structural basis for autoinhibition and mutational activation of eukaryotic initiation factor 2alpha protein kinase GCN2. *J Biol Chem* **280**, 29 289–29 299.
31 Qiu H, Garcia-Barrio MT & Hinnebusch AG (1998) Dimerization by translation initiation factor 2 kinase GCN2 is mediated by interactions in the C-terminal ribosome-binding region and the protein kinase domain. *Mol Cell Biol* **18**, 2697–2711.
32 Chen M, She H, Kim A, Woodley DT & Li W (2000) Nckbeta adapter regulates actin polymerization in NIH 3T3 fibroblasts in response to platelet-derived growth factor bb. *Mol Cell Biol* **20**, 7867–7880.
33 Lussier G & Larose L (1997) A casein kinase I activity is constitutively associated with Nck. *J Biol Chem* **272**, 2688–2694.
34 Mumberg D, Muller R & Funk M (1994) Regulatable promoters of *Saccharomyces cerevisiae*: comparison of transcriptional activity and their use for heterologous expression. *Nucleic Acids Res* **22**, 5767–5768.
35 Johnston M & Davis RW (1984) Sequences that regulate the divergent GAL1-GAL10 promoter in *Saccharomyces cerevisiae*. *Mol Cell Biol* **4**, 1440–1448.
36 Oldenburg KR, Vo KT, Michaelis S & Paddon C (1997) Recombination-mediated PCR-directed plasmid construction in vivo in yeast. *Nucleic Acids Res* **25**, 451–452.
37 Gietz D, St Jean A, Woods RA & Schiestl RH (1992) Improved method for high efficiency transformation of intact yeast cells. *Nucleic Acids Res* **20**, 1425.
38 Kong JL, Panetta R, Song W, Somerville W & Greenwood MT (2002) Inhibition of somatostatin receptor 5-signaling by mammalian regulators of G-protein signaling (RGS) in yeast. *Biochim Biophys Acta* **1542**, 95–105.
39 Li XY, Yang Z & Greenwood MT (2004) Galpha protein dependent and independent effects of human RGS1 expression in yeast. *Cell Signal* **16**, 43–49.

The adaptor protein Nck interacts with Fas ligand: Guiding the death factor to the cytotoxic immunological synapse

Marcus Lettau*, Jing Qian*, Andreas Linkermann*, Mathieu Latreille†, Louise Larose†, Dieter Kabelitz*, and Ottmar Janssen*‡

*Institute for Immunology, University Hospital Schleswig–Holstein Campus Kiel, 24105 Kiel, Germany; and †Polypeptide Laboratory, McGill University, Montreal, QC, Canada H3A 2B2

Edited by Stuart F. Schlossman, Dana–Farber Cancer Institute, Boston, MA, and approved February 21, 2006 (received for review October 3, 2005)

The Fas ligand (FasL) is a key death factor of cytotoxic T lymphocytes and natural killer cells. It is stored intracellularly as a transmembrane protein of secretory lysosomes. Upon activation, these vesicles are transported to the cytotoxic immunological synapse (IS), and FasL becomes exposed to the cell surface to trigger cell death through ligation of its receptor Fas (CD95) on the target cell. We propose that the FasL-associated adaptor protein Nck is involved in the actin-dependent transport of FasL-bearing secretory lysosomes to the IS. Nck binds to the proline-rich portion of FasL and alters its subcellular distribution when coexpressed in 293T cells. In T lymphocytes, endogenous Nck partially colocalizes with lysosome-associated FasL. When T cell clones or lines are exposed to target cells, both proteins and other components of secretory lysosomes (i.e., granzyme B or cathepsin D) are transported to the cell–cell interface. The present data suggest that T cell receptor engagement provokes a rapid, tyrosine kinase- and actin-dependent transport of Nck-associated FasL-carrying lysosomes to the contact area. Our observations support the previous notion that the unique cytoplasmic tail of FasL is crucial for its directed transport to the cell surface and into the assembling cytotoxic IS.

protein–protein interaction | Src homology 3 domain | secretory lysosomes | T lymphocytes

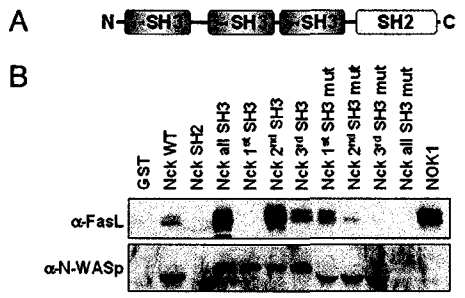

Fig. 1. Nck binding to FasL and N-WASp. (*A*) The modular composition of Nck. Nck contains three N-terminal SH3 domains (from N-terminal to C-terminal, termed first, second, and third SH3 domain, respectively, throughout) and a single C-terminal SH2 domain. (*B*) FasL selectively interacts with the second and third SH3 domains of Nck. The indicated GST fusion proteins on glutathione Sepharose beads were incubated with lysates prepared from KFL-9 cells. Precipitates with anti-FasL mAb NOK-1 served as a positive control and with GST as a negative control. Anti-FasL and anti-N-WASp immunoblots are shown. Note that the fusion proteins were not used at equimolar concentration to allow conclusions on quantitative binding preferences.

IMMUNOLOGY

The Fas ligand (FasL) (CD95L, APO1-L, and TNFSF6) is a type-II transmembrane protein belonging to the TNF family of death factors (1, 2). During primary stimulation of cytotoxic T lymphocytes and natural killer cells, newly synthesized FasL is directed to and stored in specialized secretory lysosomes (3, 4). Thus, in activated human T cells, FasL is a transmembrane component of these lytic granules that also contain granzymes and pore-forming perforin monomers (5). Upon interaction with a target cell, the lipid bilayer of the secretory lysosomes is believed to fuse with the plasma membrane, thereby releasing the soluble factors into the synapse and presenting FasL on the cell surface (4, 6). The molecular mechanisms that regulate the targeting of FasL to secretory lysosomes and the activation-dependent transport of these organelles to the immunological synapse (IS) are so far unknown.

Because the intracellular localization of FasL depends on its proline-rich domain (PRD) (7), the identification and functional analysis of FasL PRD-interacting proteins should provide more information on regulators of the lysosomal association of FasL and its activation-dependent transport to the IS. From the various proteins that were identified as potential FasL interactors (8, 9), the adaptor protein Nck attracted our attention in the context of T cell receptor (TCR)-induced vesicular transport and cytoskeletal reorganization. Nck is an adaptor protein that is built of a C-terminal Src homology (SH) 2 domain and three SH3 domains (Fig. 1*A*). The main function of Nck is the regulation of an activation-dependent actin filament formation through its interactions with components of the TCR/CD3 activation complex and cytoskeletal regulators including the Wiskott–Aldrich syndrome protein (WASp) (10), the WASp-interacting protein WIP (11), and others. In the context of T cell activation, it was proposed that, enabled by a conformational change induced by TCR ligation, Nck might be directly recruited to the ε-chain of the TCR/CD3 complex (12). However, by using molecular imaging and fluorescence resonance energy-transfer techniques, a more recent study demonstrated that the involvement of other adaptors including LAT (Linker for activation of T cells) and SLP-76 (SH2 domain-containing leukocyte protein) is indispensable for the recruitment of Nck and WASp to the activated TCR (13).

With a set of Nck mutants, we investigated the Nck/FasL interaction in detail. We found that two of the three SH3 domains of Nck bind to the FasL proline-rich domain. Coexpression in 293T cells revealed an association of both proteins with lysosomal structures. Moreover, FasL and Nck coprecipitate from double transfectants and are enriched in lysosomal fractions of FasL-transfected Jurkat cells, T cell blasts, and untransformed T cell clones.

Conflict of interest statement: No conflicts declared.

This paper was submitted directly (Track II) to the PNAS office.

Abbreviations: FasL, Fas ligand; IS, immunological synapse; TCR, T cell receptor; WASp, Wiskott–Aldrich syndrome protein; SH, Src homology; siRNA, short interfering RNA; PHA, phytohemagglutinin; lamp-1, lysosome-associated membrane protein 1; EBV, Epstein–Barr virus; B-LCL, lymphoblastoid B cell line.

‡To whom correspondence should be addressed at: Institute for Immunology, University Hospital Schleswig–Holstein Campus Kiel, Michaelisstrasse 5, 24105 Kiel, Germany. E-mail: ojanssen@email.uni-kiel.de.

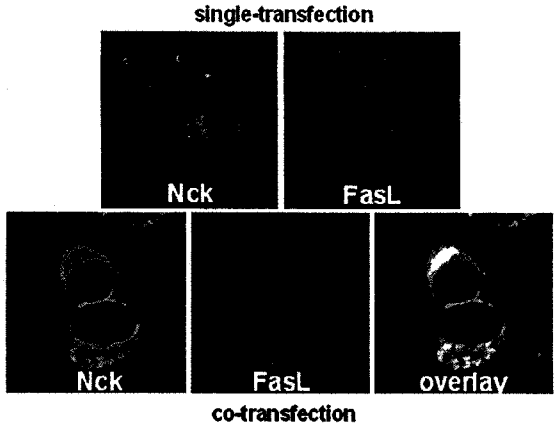

Fig. 2. Colocalization of Nck with FasL in 293T transfectants. GFP-tagged WT Nck and/or FasL was expressed alone or coexpressed in 293T cells. Twenty-four hours after transfection, the cells were fixed, permeabilized, and stained with α-FasL mAb NOK-1 and Alexa Fluor 546-conjugated goat anti-mouse IgG. The samples were analyzed by confocal microscopy. Colocalization of FasL and Nck is evident from the overlay image.

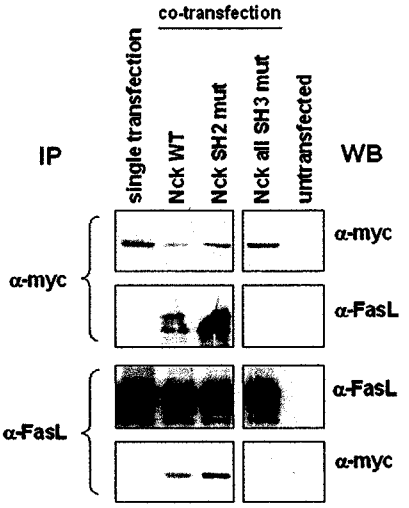

Fig. 3. FasL coprecipitates with Nck from 293T transfectants. Myc-tagged Nck variants were transiently coexpressed with FasL in 293T cells. Cell lysates were prepared 24 h after transfection and split into two aliquots for parallel immunoprecipitation (IP) with anti-myc mAb 9C11 and anti-FasL mAb NOK-1. Proteins were transferred to nitrocellulose membranes, followed by Western blotting (WB). To monitor protein expression in transfectants, the blots were stripped and stained with anti-myc and anti-FasL antibodies. The amount of coprecipitated FasL in anti-myc IPs is due to the different levels of coexpressed myc-tagged Nck variants.

With regard to the potential involvement of Nck in leading FasL to the IS, we demonstrate that, upon contact with target cells, FasL and Nck colocalize to the contact zone. This finding is supported by the presence of active tyrosine kinases in the same area as detected by simultaneous staining for phosphotyrosine. Moreover, other components of secretory lysosomes (i.e., granzyme B and cathepsin D) are concomitantly guided to the developing synapse. Importantly, the transport of FasL-containing lysosomes to the forming IS is blocked in the presence of an overexpressed interaction-deficient Nck mutant and by reducing the intracellular level of Nck by short interfering RNA (siRNA). Our observations further suggest that the receptor-induced Nck-dependent actin remodeling is indispensable for the recruitment of FasL-loaded secretory lysosomes during formation of the cytotoxic IS. Therefore, Nck serves as an important adaptor for the directed FasL transport and surface expression.

Results

FasL Interacts with the Second and Third SH3 Domains of Nck. GST fusion proteins were used to precipitate FasL from stably transfected KFL-9 cells. WT Nck constructs were compared with a panel of variants carrying functional defect mutations within the respective SH3 or SH2 domains. The second and third SH3 domains, the combined SH3 domains, and the full-length protein of Nck efficiently precipitated FasL (Fig. 1*B*). In contrast, no precipitated FasL was seen with the first SH3 domain or the SH2 domain. Individual SH3 domain mutations resulted in reduced FasL association. When all SH3 domains were mutated, FasL (and WASp) precipitation was completely abolished. Interestingly, mutations in individual SH3 domains hardly reduced the presence of WASp in the same precipitates, stressing that all SH3 domains might be capable of binding to WASp but that only the second and third SH3 domains of Nck interact with FasL. The differential migration of WASp in Fig. 1*B* is due to the presence of the full-length fusion proteins in the respective lanes (data not shown). Identical results were obtained by using Jurkat transfectants (JFL). However, in contrast to KFL-9 cells and 293T transfectants, FasL precipitated as a single band from JFL cells or activated untransformed T cells.

FasL and Nck Associate in 293T Transfectants. Full-length GFP-tagged WT Nck was expressed alone or coexpressed with FasL in 293T cells (Fig. 2). Twenty-four hours after transfection, in single transfectants, FasL was detected in the Golgi compartment and partially at the plasma membrane (14), whereas Nck was evenly distributed in the cytosol. In the presence of Nck, FasL was found predominantly in vesicle-like structures. Importantly, in double transfectants, Nck also associated with FasL-loaded vesicles (Fig. 2). Cotransfection of FasL with Nck carrying point mutations in individual SH3 domains did not result in FasL redistribution, indicating that SH3 binding to FasL was functionally required for the observed localization (data not shown).

FasL and Nck Coprecipitate from 293T Transfectants. Myc-tagged Nck constructs were expressed alone or together with FasL in 293T cells (Fig. 3). Twenty-four hours after transfection, cell lysates were subjected to immunoprecipitation with anti-myc or anti-FasL mAbs. The anti-myc immunoprecipitation followed by FasL staining revealed coprecipitation of FasL in the presence of WT or SH2-mutated Nck but not when all SH3 domains of Nck were mutated. Conversely, anti-FasL mAb coprecipitated the WT and SH2-mutated but not the SH3-mutated myc-tagged Nck (Fig. 3).

Lysosomal Association of FasL and Nck in T Cells. We and others have previously noted that most, if not all, *in vitro* propagated T cell lines and clones (irrespective of CD4, CD8, TCR-$\alpha\beta$, or TCR-$\gamma\delta$ expression) store FasL in lysosomal structures (15). We therefore examined the subcellular localization of endogenous Nck and FasL and putative markers for secretory lysosomes in cloned $CD4^+$ T cells (Fig. 4). For practical reasons, we first analyzed that the use of anti-cathepsin D antibodies to visualize the lysosomal compartment was comparable with the lysosome-associated membrane protein 1 (lamp-1) staining widely used for detection of lysosomes (Fig. 4*A*). When we observed the colocalization of granzyme B and cathepsin D (Fig. 4*B*), cathepsin D and FasL (Fig. 4*C*), and Nck and FasL (Fig. 4*D*), we concluded that all proteins directly or indirectly associate with secretory lysosomes. We noted that, although we used a clonal population, the FasL expression was somewhat heterogeneous. Interestingly, colocalization of FasL with Nck was most prominent in cells with high FasL expression, whereas Nck was distributed more evenly in the cytosol when cells expressed lower levels of FasL (data not shown).

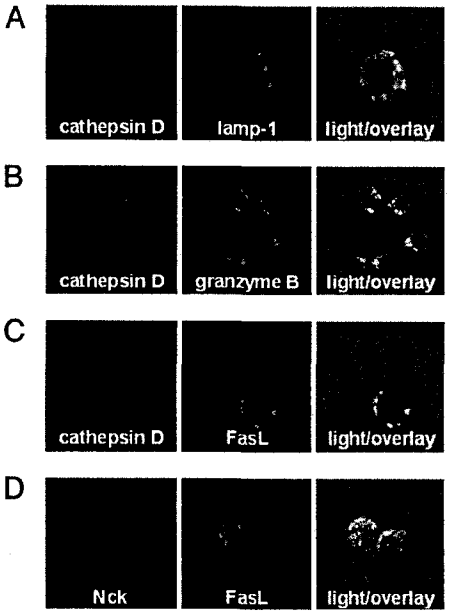

Fig. 4. Subcellular distribution of granzyme B, FasL, and Nck in cloned CD4+ T cells. (*A*) Cathepsin D and lamp-1 staining. Parallel staining for cathepsin D and lamp-1 shows that both markers are suitable for visualization of the lysosomal compartment of the investigated T cells. (*B*) Colocalization of cathepsin D and granzyme B. (*C*) Colocalization of cathepsin D and FasL. (*D*) Colocalization of Nck and FasL. FasL expression is restricted to granular structures, where it colocalizes with Nck. Nck itself is enriched around these granules but also appears to be present in the cytosol.

FasL and Nck Are Enriched in Lysosomal Fractions. Coprecipitation experiments of endogenous molecules with FasL from untransfected cells have failed in many laboratories. To prove the lysosomal association of FasL and Nck biochemically, we fractionated lysates of JFL cells and phytohemagglutinin (PHA)-activated T cell blasts. As demonstrated in Fig. 9, which is published as supporting information on the PNAS web site, JFL transfectants retain the characteristic surface expression of T cell markers, including CD3 and CD2. They express high levels of surface FasL in the absence of Fas. The presence of FasL associated with intracellular vesicles was documented by confocal microscopy. In contrast, polyclonal T cell blasts and T cell clones express little surface FasL and store most of the protein in the lysosomal compartment (15, 16). When individual fractions obtained by density gradient centrifugation of JFL lysates were analyzed by Western blotting, we found an enrichment of FasL in the two fractions (fractions 2 and 3) that exclusively contained the lysosomal marker protein lamp-1 (Fig. 5*A*). Despite the evident differences in FasL surface expression, similar results were obtained with PHA blasts (Fig. 5*B*). Interestingly, in T cell blasts, Nck was detected in all fractions but was clearly enriched in the putative lysosomal fraction 2. Subcellular fractionation by differential centrifugation of cloned CD4+ T cell lysates confirmed the exclusive presence of FasL in the lamp-1-positive organelle fraction (Fig. 5*C*). Again, Nck was slightly enriched in the same fraction.

Actin-Dependent Recruitment of FasL to the Cytotoxic IS. TCR-triggered recruitment of Nck to CD3ε (12) or to other TCR-associated signaling components (i.e., Linker for activation of T cells and SLP-76) (13) seems to be essential for the TCR-induced synapse formation. Thus, our observation that Nck colocalizes with FasL in activated T cells raised the hypothesis that, via FasL, Nck might also connect the cytoskeleton to the transport of secretory lysosomes during T cell–target cell contact. To address this possibility, we examined the actin and FasL distribution in T cells exposed to Epstein–Barr virus (EBV)-transformed target cells in the presence or absence of latrunculin A or cytochalasin D, two inhibitors of actin filament formation. As a control, the intracellular FasL distribution was not affected in the presence of cytochalasin or latrunculin, whereas the detection of actin filaments by phalloidin was dramatically impaired (Fig. 10*A*, which is published as supporting information on the PNAS web site). When clone cells were cocultured with target cells, actin filaments stained by phalloidin and FasL accumulated in the contact area in the absence, but not in the presence, of cytochalasin or latrunculin (Fig. 10*B*). Thus, pretreatment of T cells with both substances abolished transport of FasL and also impaired synapse formation. It should be mentioned that, in the presence of both inhibitors, tyrosine phosphorylation at the contact area was still detectable (data not shown), indicating that early events of T cell activation remained unaffected by the inhibitors.

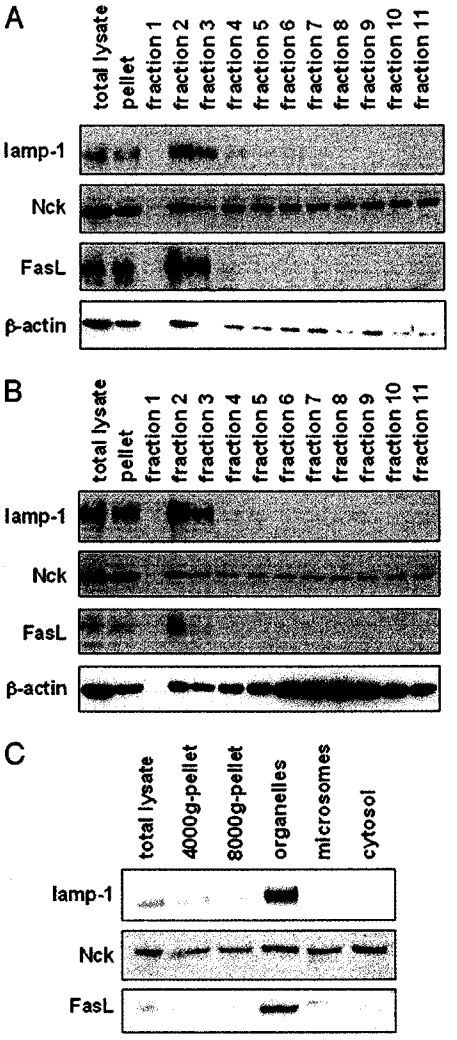

Fig. 5. Enrichment of FasL and Nck in lysosomal fractions. Lysates of unstimulated JFL cells (*A*), PHA blasts (*B*), and cloned CD4+ T cells (*C*) were fractionated by density gradient or differential centrifugation as described in *Materials and Methods*. Equal amounts of protein of each fraction were separated by SDS/PAGE and analyzed by Western blotting. The blots were first stained for FasL and consecutively reprobed for lamp-1, Nck, and β-actin (except in *C*).

Colocalization of Nck, FasL, and Lysosomal Markers at the IS. We next analyzed the distribution of Nck, FasL, granzyme B, and cathepsin

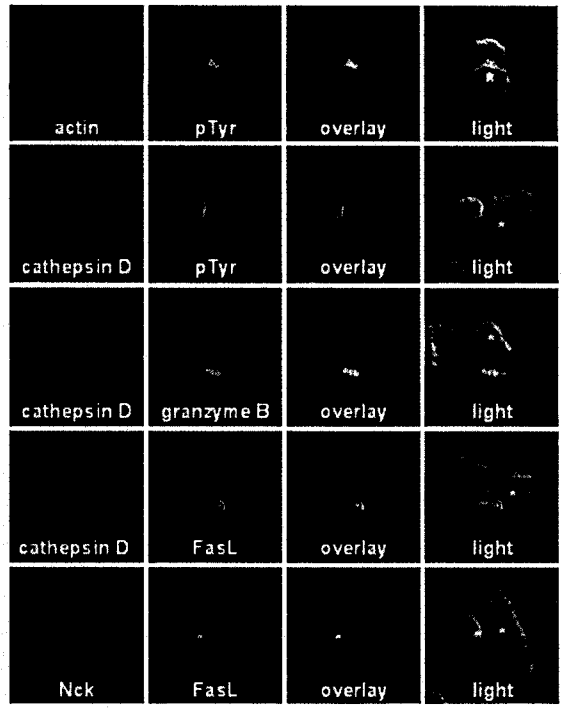

Fig. 6. Colocalization of Nck and FasL in conjugates of cloned T cells and B-LCL. Cloned T cells were cocultured with EBV-transformed B-LCL cells (*) for 30 min before fixation and staining as indicated. The antibody combinations were as follows: anti-pTyr mAb 4G10, anti-granzyme B mAb and anti-FasL mAb NOK-1 with Alexa Fluor 488-conjugated donkey anti-mouse IgG, and polyclonal anti-cathepsin D and anti-Nck Ab-1 with Alexa Fluor 546-conjugated goat anti-rabbit IgG. DAPI was used to stain nuclei, rhodamine-conjugated phalloidin was used to stain actin filaments, and transmitted light was recorded to visualize cell shapes.

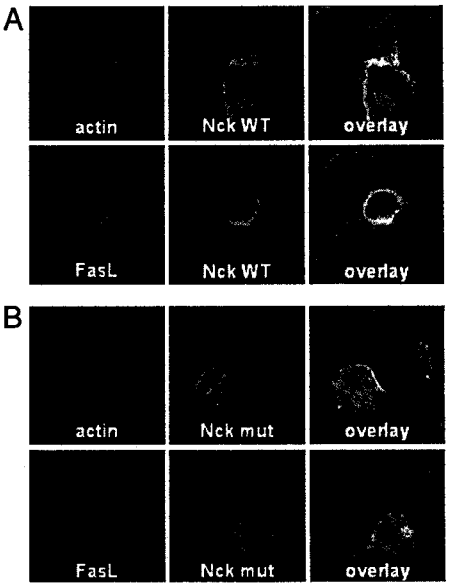

Fig. 7. Colocalization of Nck and FasL in conjugates of JFL and B-LCL. JFL cells were transiently transfected with EGFP-tagged Nck constructs and cocultured with *Staphylococcus* enterotoxin E-pulsed B-LCL cells for 20 min before fixation and staining with rhodamine-phalloidin, anti-FasL mAb NOK-1, and Alexa Fluor 546-conjugated donkey anti-mouse IgG and DAPI. (*A*) Overexpression of WT Nck. Actin filaments, Nck, and FasL accumulate at the IS. (*B*) Overexpression of Nck with mutations in all SH3 domains. Actin filament formation is blocked, Nck is evenly distributed within the cytoplasm, and the FasL-containing vesicles are not transported to the contact area.

D in a T cell–target cell contact situation (Fig. 6). The activation and actin recruitment within the area of the forming IS of cloned T cells was visualized by anti-phosphotyrosine and phalloidin staining, respectively. Under the same conditions, the lysosome-associated proteins cathepsin D and granzyme B were detected in a defined contact area, indicating that the lysosomes were efficiently recruited to the IS within the analyzed time frame. Moreover, FasL colocalized with cathepsin D and with Nck in the cell–cell contact region. These observations were confirmed with $CD8^+$ T cells (data not shown).

Nck and Its Interaction with FasL Is Required for Transport of FasL-Containing Secretory Lysosomes to the Cytotoxic IS. If the interaction between FasL and Nck was essential for transport of secretory lysosomes and the formation of a cytotoxic IS, down-regulation of Nck and interference with FasL/Nck binding should have a major impact in both cases. To address this issue, we used Nck SH3 mutants to abolish the interaction and siRNA to reduce Nck expression. Overexpression of WT Nck constructs in JFL cells (Fig. 7*A*) obviously did not influence the overall protein localization as compared with T cell clones (Fig. 6) or PHA blasts (Fig. 11*A*, which is published as supporting information on the PNAS web site). In contrast, overexpression of the SH3-mutated Nck variant dramatically changed the subcellular distribution of Nck. Moreover, actin filament reorganization was blocked, and synapse formation was impaired. In the presence of superantigen-loaded lymphoblastoid B cell line (B-LCL) target cells, the colocalization of FasL with Nck and its translocation to the IS was abolished (Fig. 7*B*).

A partial knockdown of Nck by siRNA transfection yielded comparable results for PHA blasts (Fig. 8). Although the siRNA delivery was efficient as judged by FACS analysis of labeled control siRNA (Fig. 8*A*), Nck was still detectable by Western blotting. The 50–60% reduction of Nck at the protein level (Fig. 8*B*), however, was sufficient to affect the subcellular localization of FasL. As analyzed by confocal microscopy, in the presence of Nck siRNA, the transport of FasL-containing secretory lysosomes to the site of cell–cell contact was impaired, resulting in a much lower abundance of detectable FasL-associated synapses (Figs. 8*C* and 11*B*).

Discussion

In cytotoxic T cells and natural killer cells, the death factor FasL is safely stored in so-called secretory lysosomes (17). These cell type-specific vesicles obviously combine degrading and secretory functions and also contain other potentially dangerous apoptosis-promoting molecules such as granzymes and perforins (3, 4). The rapid surface expression of FasL, associated with the directed release of the other cytotoxic factors into a cleft between killer and target cells, forms the basis for formation of the cytotoxic IS and is crucial for T and natural killer cell function. Unlike other proteins that are sorted to the lysosomal compartment by dileucine or tyrosine-based sorting motifs (18), targeting of FasL to secretory vesicles was shown by Griffiths and colleagues (7) to require the intracellular proline-rich domain of the molecule. Thus, compared with conventional lysosomes, this mechanism of lysosomal targeting and transport seems to be unique for secretory lysosomes and potentially exclusive for FasL-loaded vesicles. The fact that FasL is a transmembrane element of the secretory vesicles facing with its cytoplasmic tail into the cytosol suggests that FasL might be actively involved in the movement of secretory vesicles by virtue of SH3-mediated protein–protein interactions with cytoskeletal elements.

To link rapid cellular activation and FasL to the lysosomal transport machinery, among the putative FasL interactors identified before, actin cytoskeleton reorganizing molecules attracted our attention. As such, Nck, an adaptor protein consisting of a

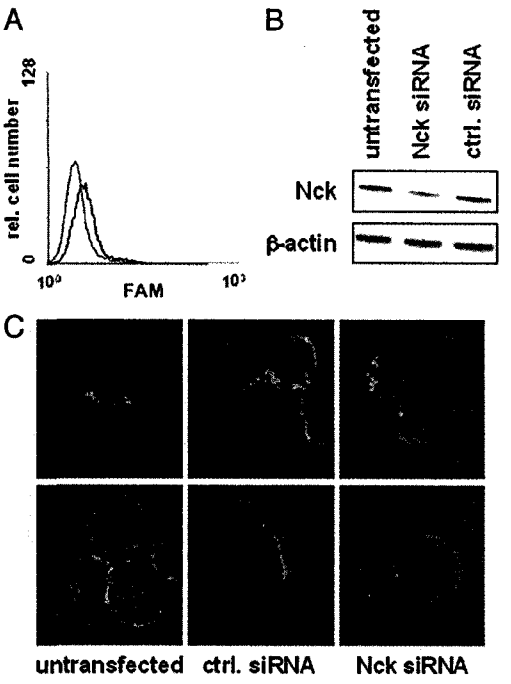

Fig. 8. Partial knockdown of Nck suffices to reduce FasL transport and synapse formation. PHA blasts were left untreated or transfected with control siRNA or siRNA to target Nck by using the Amaxa nucleofection kit for primary human T cells (program X-001). (*A*) Delivery control. Efficient transfection of FAM-labeled control siRNA (dark line) into PHA blasts was monitored by FACS analysis after 24 h. (*B*) Western blot analysis of whole-cell lysates after 72 h. At the protein level, Nck expression was reduced by ≈50–60%. (*C*) FasL distribution in untreated and siRNA-treated T cell blasts. FasL was stained with NOK-1 and Alexa Fluor 488-conjugated donkey anti-mouse IgG.

C-terminal SH2 domain and three SH3 domains, was reported to directly link CD3 signaling subunits of the TCR/CD3 complex to the WASp-activated actin filament formation (12). More recently, it was proposed that, in a multimolecular activation complex, Nck recruitment and WASp activation follow the phosphorylation of adaptor proteins including Linker for activation of T cells and SLP-76 (13). Whether or not Nck represents a direct or indirect link between the TCR/CD3 complex and the cytoskeleton, the presence of distinct binding modules within Nck could allow separate interactions with other molecules, including FasL.

Therefore, we analyzed the interaction between Nck and FasL in detail using different GST fusion proteins. *In vitro* binding was seen with full-length Nck and with the second and third SH3 domain. Interestingly, we observed that, at the same time, all three SH3 domains of Nck precipitated N-WASp. Mutations of the second and third SH3 domain significantly reduced the FasL association. Upon cotransfection, we were able to coprecipitate FasL with myc-tagged Nck and, conversely, Nck with anti-FasL antibodies. We also demonstrated a redistribution of FasL and a colocalization of Nck with FasL to the lysosomal compartment.

Also in untransformed human T cells, without further stimulation, FasL accumulates within larger granular structures. This association is experimentally reflected by the presence and enrichment of FasL (and also Nck) in isolated lamp-1-positive vesicles obtained after density gradient or differential centrifugation and is in agreement with our previous observation that only upon secondary activation do the granules rapidly disintegrate and does FasL appear on the cell surface (16).

Upon TCR stimulation, Nck recruits other proteins to the TCR/CD3 complex, thereby reassembling the cytoskeleton around the IS (12, 13). Therefore, we investigated a potential colocalization of FasL, Nck, granzyme B, and cathepsin D in unstimulated T cells and during T cell–target cell interaction. In unexposed T cells, we observed that the endogenous proteins colocalized at FasL-containing vesicles. When T cells were exposed to EBV-transformed B cells, we could demonstrate a directed relocation of all four molecules to the contact area. At the same time, activation was visualized by anti-pTyr and actin reorganization by phalloidin staining. Importantly, the effective synapse formation and the recruitment of secretory lysosomes, Nck and FasL, to the contact area were sensitive to latrunculin A- or cytochalasin D-induced prevention of actin filament formation. We also demonstrate that the inhibition of the Nck/FasL interaction by different means (siRNA knockdown of Nck and overexpression of mutated variants) abolished FasL transport and impaired formation of the cytotoxic IS.

Taken together, the present data indicate that the Nck-mediated actin reorganization is associated with the TCR/CD3-dependent directed movement of FasL-loaded secretory granules to the cytotoxic IS. This article also explains the biphasic FasL surface expression on T and natural killer cells after activation (16). We suggest that the first peak of FasL expression after TCR stimulation is directly provoked by a rapid and dynamic "TCR-to-secretory-lysosome crosstalk" involving the adaptor Nck. Studies using siRNA approaches that target other FasL-interacting proteins are needed to answer the question of whether Nck serves as the prominent recruitment factor in this scenario or whether other FasL-binding proteins also play a role as potential linkers between actin reorganization and microtubule-dependent lysosomal movement. Ultimately, the establishment of FasL mutant mice lacking different parts of the cytoplasmic tail but retaining the receptor-interacting extracellular part will provide further insight into the regulatory role of FasL in lysosomal transport and formation of the cytotoxic IS.

Materials and Methods

Cells. The human $CD4^+$ T cell clone 12603, PHA-stimulated T cell blasts, and EBV-transformed B-LCLs were established in this laboratory. T cell clones/lines were cultured at 37°C in RPMI medium 1640 with 10% FBS, antibiotics, and recombinant IL-2 (rIL-2) (10 units/ml, Chiron). T cell clones were restimulated periodically with irradiated peripheral blood mononuclear cells and EBV-transformed B-LCL in the presence of PHA (0.5 μg/ml, Burroughs Wellcome) and rIL-2. Dead cells were removed by Ficoll gradient centrifugation, and T cells were further cultured in the presence of rIL-2. KFL-9 cells were stable FasL transfectants established from K562 human erythroleukemia cells by David Kaplan (Case Western Reserve University, Cleveland). 293T (human embryonic kidney, SV40 transformed) cells were used for transient protein expression. JFL cells were established in our laboratory from a Fas-negative Jurkat variant.

Plasmids and Transfection. GST-, Myc-, or EGFP-tagged expression vectors for WT and mutant Nck are described in refs. 9 and 19–21. WT Nck indicates full-length cDNA (GenBank accession no. BC006403); the first SH3 domain represents residues 5–60, the second SH3 domain represents residues 109–164, the third SH3 domain represents residues 193–251, the SH2 domain represents residues 280–362, and all SH3 domains comprise residues 1–251. The first SH3-mutated variant carries an exchange of Trp at residue 38 to Arg (W38K), the second SH3-mutated variant carries a W143K exchange, the third SH3-mutated variant carries a W229K exchange, and the SH2-mutated variant carries an R308K replacement. pGEX4T2 or pGEX2TK vectors (Amersham Pharmacia) were used for expression of GST-tagged proteins, and pCDNA3.1myc.HisA (Invitrogen) was used for expression of myc-tagged proteins. pCB6-based GFP-Nck constructs were kindly provided by Michael Way (London Research Institute, London). A vector encoding full-length FasL (pl217s) was provided by Pascal

Schneider and Margot Thomé (both of University of Lausanne, Epalinges, Switzerland). 293T cells were transfected in bulk (3×10^6) or on coverslips (10^5) by standard calcium phosphate precipitation and used for coprecipitation or immunostaining 24 h after transfection. JFL cells were transfected by using the nucleofection kit for cell line V (program S-018, Amaxa, Gaithersburg, MD), following the manufacturer's instructions.

Precipitation and Western Blotting. For precipitation with fusion proteins, KFL9 cells were lysed in a standard Nonidet P-40 lysis buffer with protease inhibitors. Lysates were incubated with 25 μg of the respective GST fusion protein on beads for 2 h rotating at 4°C. For coimmunoprecipitation, 293T cells were collected and lysed in Nonidet P-40 buffer. Precleared lysates were divided into two aliquots and incubated for 2 h at 4°C with either anti-FasL mAb (NOK-1; BD Pharmingen) or anti-myc mAb (Cell Signaling Technology, Beverly, MA) and protein A-Sepharose beads (Amersham Pharmacia). After vigorous washes, the precipitates were boiled in sample buffer, separated on SDS polyacrylamide gels, and transferred to nitrocellulose membranes. Proteins were analyzed with anti-FasL mAb (G-247.4, BD Pharmingen) and goat anti-mouse horseradish peroxidase (HRP)-conjugated secondary antibody (Amersham Pharmacia) with a polyclonal anti-N-WASp antiserum and HRP-conjugated goat anti-rabbit antibodies (Amersham Pharmacia) or with HRP-conjugated anti-myc mAb (Invitrogen) and ECL (enhanced chemiluminescence) detection reagents (Amersham Pharmacia).

Subcellular Fractionation. For subcellular fractionation and enrichment of lysosomes, T cell blasts or FasL-transfected JFL cells were washed with PBS, resuspended in 1 ml of homogenization buffer (340 mM sucrose/10 mM Hepes, pH 7.3/0.3 mM EDTA), and subjected to two freeze/thaw cycles. The homogenate was centrifuged at $4,000 \times g$ for 10 min at 4°C to pellet nuclei and remaining intact cells. The postnuclear supernatant was collected and applied on a Percoll gradient in the presence of sucrose. The samples were spun at $100,000 \times g$ for 150 min at 4°C in Ultra-Clear centrifugation tubes (Beckman Coulter). The protein content in individual fractions of 150 μl was determined by BCA (bicinchoninic acid) protein assay (Pierce). Twenty-five micrograms of protein per fraction was separated by SDS/PAGE on a 10% gel. Alternatively, clone cells were homogenized as described above in a modified homogenization buffer with 250 mM sucrose. The postnuclear supernatant was subjected to a second centrifugation step at $8,000 \times g$ for 2 min at 4°C to pellet membrane fragments. After centrifugation at $100,000 \times g$ for 2 min, which pellets organelles, the sample was spun at $400,000 \times g$ for 12 min to divide microsomes from cytosol. Five micrograms of protein per fraction was separated by SDS/PAGE on a 4–12% Bis-Tris gel (Invitrogen). The following antibodies were used for Western blot detection: anti-FasL mAb G-247.4, anti-lamp-1 mAb clone 25 (BD Pharmingen), rabbit polyclonal anti-Nck antibody Ab-1 (LabVision, Fremont, CA), and anti-β-actin mAb AC-15 (Sigma).

Antibodies and Reagents for Immunofluorescence Staining. The following reagents were used for immunofluorescence staining: anti-FasL mAb NOK-1, anti-granzyme B mAb, anti-pTyr mAb 4G10, anti-lamp-1 mAb clone 25 (BD Pharmingen), polyclonal rabbit anti-cathepsin D (Calbiochem), polyclonal rabbit anti-Nck Ab-1 (LabVision), rhodamine-conjugated donkey anti-rabbit IgG (Santa Cruz Biotechnology), rhodamine-conjugated phalloidin, Alexa Fluor 546-conjugated goat anti-rabbit IgG, Alexa Fluor 546-conjugated goat anti-mouse IgG, Alexa Fluor 488-conjugated donkey anti-mouse IgG, Alexa Fluor 488-conjugated donkey anti-rabbit IgG (Molecular Probes), and DAPI (Roche). For surface staining, we used phycoerythrin-labeled NOK-1 (Caltag, South San Francisco, CA) and anti-CD3PE, anti-CD2FITC, and anti-CD95PE (BD Pharmingen).

Confocal Microscopy. Cells were fixed with 3% paraformaldehyde in PEM buffer (100 mM Pipes/1 mM $MgCl_2$/1 mM EGTA, pH 6.5) for 5 min followed by 3% paraformaldehyde in borate buffer (100 mM $Na_2B_4O_7$/1 mM EGTA, pH 11) for 10 min and permeabilized with 1% Triton X-100 in PBS for 15 min. After three washes with PBS, the coverslips were treated two times with $NaBH_4$ (1 mg/ml in PBS) for 10 min to reduce reactive aldehydes. The samples were washed with PBS and blocked with 0.2% BSA/PBS followed by incubation with chromophore-conjugated antibodies or dyes. Stained samples were mounted with antifade (Molecular Probes) or MobiGLOW (Mobi-Tec, Göttingen, Germany) mounting media and analyzed on a laser scanning microscope (LSM 510, Zeiss).

Analyses of T Cell–Target Cell Interactions. T cells and B-LCL target cells were mixed at a ratio of 2:1 and cocultured for 10–30 min in 1 ml of culture medium at 37°C before transfer to poly(L-lysine)-pretreated coverslips. For JFL cells, B-LCL cells were pretreated with *Staphylococcus* enterotoxin E; for T cell blasts, B-LCL cells were pretreated with a mixture of *Staphylococcus* enterotoxins A, B, C, D, and E. After 10 min on ice, the cells were washed with PBS and processed for fixation as described above. To block actin filament formation, T cells were cultured in medium supplemented with 10 μM cytochalasin D (Calbiochem) or 5 nM latrunculin A (Sigma-Aldrich) for 30 min before exposure to target cells.

siRNA Transfection of T Cell Blasts. To knock down Nck in T cell blasts, the cells were transfected with control siRNA (Silencer Negative Control no. 1 siRNA) or siRNA to target Nck (Silencer Predesigned siRNA, 144183, 144184, and 144185, Ambion, Austin, TX) by using the Amaxa nucleofection kit for primary human T cells (program X-001). Transfection efficacy was tested in parallel with a FAM-labeled control siRNA (Silencer FAM-labeled Negative Control no. 1 siRNA), and reduction of protein expression was monitored by Western blotting of whole-cell lysates.

We thank Alyn Beyer and Graziella Podda for expert technical assistance and our collaborators for providing essential reagents for this study. This work was supported by German Research Council Grant SFB415, A9 and the Medical Faculty of Christian–Albrechts University (Kiel, Germany) (O.J.).

1. Suda, T., Takahashi, T., Golstein, P. & Nagata, S. (1993) *Cell* **75**, 1169–1178.
2. Linkermann, A., Qian, J., Kabelitz, D. & Janssen, O. (2003) *Signal Transduct.* **3**, 33–46.
3. Blott, E. J. & Griffiths, G. M. (2002) *Nat. Rev. Mol. Cell Biol.* **3**, 122–131.
4. Trambas, C. M. & Griffiths, G. M. (2003) *Nat. Immunol.* **4**, 399–403.
5. Bossi, G., Stinchcombe, J. C., Page, L. J. & Griffiths, G. M. (2000) *Eur. J. Cell Biol.* **79**, 539–543.
6. Stinchcombe, J. C., Bossi, G., Booth, S. & Griffiths, G. M. (2001) *Immunity* **15**, 751–761.
7. Blott, E. J., Bossi, G., Clark, R., Zvelebil, M. & Griffiths, G. M. (2001) *J. Cell Sci.* **114**, 2405–2416.
8. Ghadimi, M. P., Sanzenbacher, R., Thiede, B., Wenzel, J., Jing, Q., Plomann, M., Borkhardt, A., Kabelitz, D. & Janssen, O. (2002) *FEBS Lett.* **519**, 50–58.
9. Wenzel, J., Sanzenbacher, R., Ghadimi, M., Lewitzky, M., Zhou, Q., Kaplan, D. R., Kabelitz, D., Feller, S. M. & Janssen, O. (2001) *FEBS Lett.* **509**, 255–262.
10. Rivero-Lezcano, O. M., Marcilla, A., Sameshima, J. H. & Robbins, K. C. (1995) *Mol. Cell. Biol.* **15**, 5725–5731.
11. Anton, I. M., Lu, W., Mayer, B. J., Ramesh, N. & Geha, R. S. (1998) *J. Biol. Chem.* **273**, 20992–20995.
12. Gil, D., Schamel, W. W., Montoya, M., Sanchez-Madrid, F. & Alarcon, B. (2002) *Cell* **109**, 901–912.
13. Barda-Saad, M., Braiman, A., Titerence, R., Bunnell, S. C., Barr, V. A. & Samelson, L. E. (2004) *Nat. Immunol.* **6**, 80–89.
14. Qian, J., Lettau, M., Podda, G. & Janssen, O. (2005) *Signal Transduct.* **5**, 195–201.
15. Linkermann, A., Qian, J., Lettau, M., Kabelitz, D. & Janssen, O. (2005) *Expert Opin. Ther. Targets* **9**, 119–134.
16. Lettau, M., Qian, J., Kabelitz, D. & Janssen, O. (2004) *Signal Transduct.* **4**, 206–211.
17. Clark, R. & Griffiths, G. M. (2003) *Curr. Opin. Immunol.* **15**, 516–521.
18. Letourneur, F. & Klausner, R. D. (1992) *Cell* **69**, 1143–1157.
19. Kebache, S., Zuo, D., Chevet, E. & Larose, L. (2002) *Proc. Natl. Acad. Sci. USA* **99**, 5406–5411.
20. Lussier, G. & Larose, L. (1997) *J. Biol. Chem.* **272**, 2688–2694.
21. Zeng, R., Cannon, J. L., Abraham, R. T., Way, M., Billadeau, D. D., Bubeck-Wardenberg, J. & Burkhardt, J. K. (2003) *J. Immunol.* **171**, 1360–1368.

Available online at www.sciencedirect.com
ScienceDirect
Biochemical and Biophysical Research Communications 349 (2006) 310–316
BBRC
www.elsevier.com/locate/ybbrc

Rat nephrin modulates cell morphology via the adaptor protein Nck

Hongping Li [a], Jianxin Zhu [a], Lamine Aoudjit [a], Mathieu Latreille [a], Hiroshi Kawachi [b], Louise Larose [a], Tomoko Takano [a,*]

[a] *Department of Medicine, McGill University, Montreal, Que., Canada*
[b] *Department of Cell Biology, Institute of Nephrology, Niigata University Graduate School of Medical and Dental Sciences, Niigata, Japan*

Received 9 August 2006
Available online 17 August 2006

Abstract

Nephrin is a transmembrane molecule essential for morphology and function of kidney podocytes. We and others reported previously that the cytoplasmic domain of human and mouse nephrin interacts with the adaptor protein, Nck, in a tyrosine phosphorylation-dependent manner. In the current study, we characterized the interaction of rat nephrin with Nck and further addressed its impact on cell morphology. Rat nephrin expressed in Cos-1 cells co-immunoprecipitated with Nck in a manner dependent on the phosphorylation of Y1204 and Y1228. Nephrin from normal rat glomeruli was also tyrosine phosphorylated and associated with Nck. Overexpression of rat nephrin in HEK293T cells induced morphological changes resembling process formation, which became more distinct when the extracellular domain of nephrin was cross-linked by antibodies. The morphological changes were attenuated by expression of dominant negative constructs of Nck. In the rat model of podocyte injury and proteinuria, nephrin tyrosine phosphorylation and nephrin–Nck interaction were both reduced significantly. Taken together, we propose that Nck couples nephrin to the actin cytoskeleton in glomerular podocytes and contributes to the maintenance of normal morphology and function of podocytes.

Keywords: Podocytes; Nephrin; Nck; Tyrosine phosphorylation; Cell morphology; Proteinuria; Puromycin aminonucleoside nephrosis

Visceral glomerular epithelial cells, also known as podocytes, are highly differentiated cells, which surround glomerular capillaries of the kidney and have an important role in the maintenance of glomerular permselectivity. Podocytes project primary processes from the cell body, which further branch into numerous finger like processes called "foot processes". Interdigitating adjacent foot processes of podocytes are connected by the structure called the slit diaphragm [1]. The slit diaphragm is believed to play a central role in regulating the actin cytoskeleton in foot processes, thereby contributing to the maintenance of their intricate morphologies [2]. Nephrin is a transmembrane protein of 180 kDa, which belongs to the Ig superfamily. In addition to its role as a structural protein in the slit diaphragm, nephrin serves as a scaffold of a number of proteins including podocin and CD2AP, and transmits signals from the slit diaphragm into the cells [2]. The cytoplasmic domain of nephrin contains a series of conserved tyrosine-based motifs, which upon phosphorylation can bind to cytoplasmic targets such as phosphoinositide 3-kinase [3], the Src-family kinase, Fyn [4], and the adaptor protein, Nck [5,6].

Nck1/α and Nck2/β comprise a family of adaptor proteins (hereafter called Nck) with three SH3 domains followed by a carboxy-terminal SH2 domain [7]. Nck binds to a variety of molecules at phosphotyrosine-containing motifs via the SH2 domain and recruits other molecules via the SH3 domains. The Nck SH2 domain prefers to bind to the phosphotyrosine–aspartate–glutamate–proline/aspartate/valine (pYDEP/D/V) consensus motif, although some redundancies are known [8]. Tyrosine phosphoproteins known to associate directly with the SH2 domain of Nck include receptor tyrosine kinases, as well as adaptor molecules such as Dok1 and Dok2 [7]. SH3 domains are

* Corresponding author. Fax: +1 514 843 2815.
E-mail address: tomoko.takano@mcgill.ca (T. Takano).

0006-291X/$ - see front matter © 2006 Elsevier Inc. All rights reserved.
doi:10.1016/j.bbrc.2006.08.053

known to bind to proline-rich motifs. The list of molecules that bind to the SH3 domains of Nck is long, including focal adhesion kinase (FAK), p21-activated kinase (PAK), WASP (Wiskott–Aldrich syndrome protein), and more ubiquitous neural (N)-WASP. Notably, most proteins that interact with Nck via its SH3 domains are involved in actin cytoskeletal regulation [7]. Nck1$^{-/-}$and Nck2$^{-/-}$ mice do not show obvious abnormalities, while double null mutation is embryonic lethal, indicating that the function of the two isoforms could be redundant [9].

We [5] and others [6] reported recently that the cytoplasmic domain of human and mouse nephrin interacts with Nck in a tyrosine-dependent manner. Nephrin–Nck interaction led to localized actin polymerization (forming "actin tails") [5,6], while podocyte-specific gene deletion of *Nck1* and *Nck2* led to abnormal foot process development and congenital proteinuria [5], suggesting that nephrin–Nck interaction is critical for the normal development of podocyte foot processes. The current study confirmed tyrosine phosphorylation-dependent nephrin–Nck interaction with rat nephrin and further demonstrated morphological changes of cells as a consequence of actin reorganization induced by nephrin–Nck interaction. In addition, we showed that tyrosine phosphorylation of nephrin, as well as nephrin–Nck interaction, was diminished in a rat model of podocyte injury and proteinuria, suggesting their important role in the maintenance of glomerular permselectivity in the adult kidney.

Materials and methods

Materials. Tissue culture media and lipofectamine 2000 were from Invitrogen-Life Technologies (Burlington, ON). Reagents for molecular biology were from New England BioLabs (Mississauga, ON). Protease inhibitor cocktail was from Roche Diagnostics (Laval, QC). Mouse monoclonal anti-Nck antibody and anti-phosphotyrosine antibody, PY69, were from BD Biosciences (Mississauga, ON). FITC-labeled anti-Myc and anti-HA antibodies were from Santa Cruz Biotechnology (Santa Cruz, CA). Rhodamine–phalloidin was from Molecular Probes (Eugene, OR). FITC-goat anti-mouse IgG and anti-Src [pY^{418}] phospho-specific antibodies were from Biosource International (Camarillo, CA). Src phosphorylated at Y^{418} is known to be active. Since the region surrounding Y418 is highly conserved in all of the related Src-family kinases, the phospho-specific Src antibody cross-reacts with the other members of the family, such as Fyn and Yes. Rabbit anti-Nck (which recognizes both Nck1 and 2) and anti-nephrin antibodies were described previously [10,11]. Fibronectin, puromycin aminonucleoside, and other standard biochemicals were from Sigma–Aldrich (St. Louis, MO).

Plasmids. Construction of rat nephrin and its tyrosine mutants was reported previously [10]. The plasmids for Nck1, GST–Nck, GST–Nck-SH2, GST–Nck-SH3s, HA–Nck-SH3-M3, and Fyn were described previously [10,12,13]. For construction of Myc–Nck-SH2, human Nck1 cDNA corresponding to amino acids 282-377 was amplified by PCR and cloned into pcDNA3.1-Myc (Invitrogen) using *Bam*HI and *Eco*RI sites. Sequence was confirmed by automated sequencing.

Transient transfection, immunoprecipitation, immunoblotting, pull-down assay. Transient transfection was performed in Cos-1 cells or HEK293T cells as described previously using lipofectamine 2000 [10]. Cells or glomeruli were lysed in buffer containing 1% Triton X-100 and immunoprecipitation and immunoblotting were performed as described previously [10]. For immunoprecipitation and immunoblotting of Nck, rabbit anti-Nck antibody and mouse monoclonal anti-Nck antibody were used, respectively. Pull-down assays were performed using Nck1 or its subdomains conjugated with GST as described previously [12].

Cross-linking of nephrin. HEK293T cells were stably transfected with rat nephrin (HEK293T-nephrin or HEK-nephrin in short) and plated on glass coverslips coated with fibronectin (0.05 mg/ml). Cells were incubated with mouse monoclonal mAb5-1-6 antibody (5 μg/ml), which recognizes the extracellular domain of rat nephrin [14], for 60 min at 4 °C in buffer containing 145 mM NaCl, 5 mM KCl, 0.5 mM $MgSO_4$, 0.5 mM $CaCl_2$, 1 mM $NaHPO_4$, 5 mM glucose, and 20 mM Hepes, pH 7.4 (measurement buffer). Cells were washed and incubated with goat anti-mouse IgG (10 μg/ml, with or without FITC) for 60 min (for morphological studies) or 10 min (for tyrosine phosphorylation) at 37 °C in measurement buffer. For morphological studies, cells were fixed with 3% formaldehyde, permeabilized with 0.5% Triton X-100, blocked with 3% BSA, and stained with rhodamine–phalloidin (0.04 μg/ml) plus/minus appropriate secondary antibodies. Cells were examined with a confocal microscope (Olympus, Fluoview FV1000).

Induction of puromycin aminonucleoside nephrosis (PAN) nephrosis and isolation of rat glomeruli. PAN was induced with a single intravenous injection of puromycin aminonucleoside (50 mg/kg body weight) in male Sprague–Dawley rats (150–175 g, Charles River, St. Constant, QC), as described previously [15]. Rats were sacrificed on day 7, when significant proteinuria was observed. Isolation of rat glomeruli was performed by differential sieving and lysates were prepared in buffer containing 1% TritonX-100, as described previously [10]. Studies were approved by the Animal Care Committee at McGill University.

Results

The cytoplasmic domain of rat nephrin associates with Nck in a tyrosine phosphorylation-dependent manner

The cytoplasmic domain of nephrin consists of ~150 amino acids and has a series of tyrosine-containing motifs. Using rat nephrin cDNA, we demonstrated previously that some of the tyrosine residues are phosphorylated by the Src-family kinase Fyn, leading to augmented interaction between nephrin and podocin [10]. We hypothesized that SH2 containing protein(s) may interact with phosphotyrosine containing motifs in the cytoplasmic domain of nephrin. In search of such molecules, we analyzed the protein sequence of the cytoplasmic domain of nephrin by Motif scan analysis (http://scansite.mit.edu). This program identifies potential interacting proteins for various protein motifs in a given molecule. SH2 containing proteins such as Src-family kinases (Src, Fyn, Fgr), as well as the p85 subunit of PI3K, were predicted to bind to nephrin, consistent with the previous reports [3,4]. In addition, it was predicted that the adaptor molecule Nck would bind to nephrin (Fig. 1A). There were three potential Nck binding sites in rat nephrin and five in mouse and human by a low stringency analysis and indeed, we and others reported recently that human [5] and mouse [6] nephrin interact with Nck in a tyrosine phosphorylation-dependent manner. In the current paper, we first characterized the interaction of Nck with rat nephrin.

When rat nephrin was transfected in Cos-1 cells with Fyn, nephrin was strongly tyrosine phosphorylated, while in the absence of Fyn, there was negligible phosphorylation, consistent with our previous report [10] (Fig. 1B). In the presence of Fyn, nephrin co-immunoprecipitated with Nck (Fig. 1B). In the absence of Fyn, there was only a

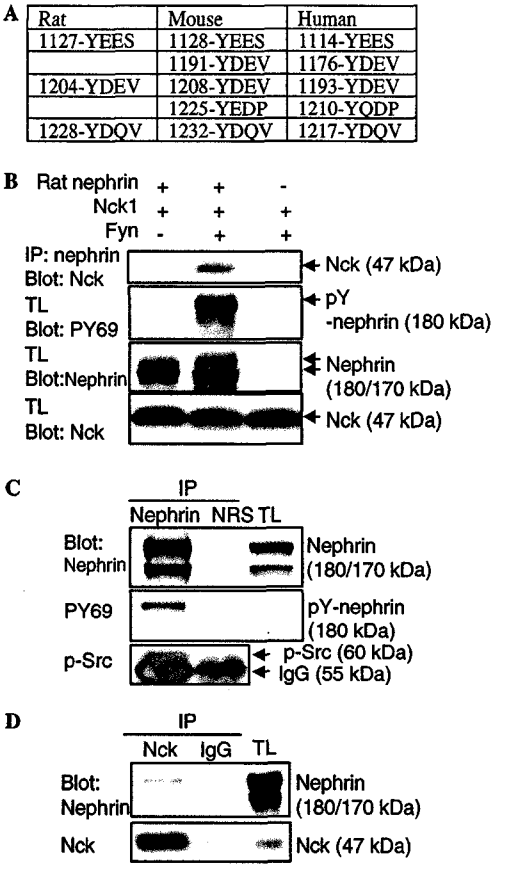

Fig. 1. Nephrin and Nck interact in a tyrosine phosphorylation-dependent manner. (A) Predicted binding sites for Nck1 in the cytoplasmic domain of rat, mouse, and human nephrin by Motif scan analysis. (B) Cos-1 cells were transiently transfected with the indicated plasmids. Cell lysates were immunoprecipitated with anti-nephrin antibody and blotted for Nck. Total lysates (TL) were blotted for phosphotyrosine (Py69), nephrin, and Nck. (C,D) Normal rat glomerular lysates were immunoprecipitated with anti-nephrin antibody and blotted for phosphotyrosine (Py69) and phospho-Src (Y418) (C), or immunoprecipitated with anti-Nck antibody and blotted for nephrin (D). NRS, normal rabbit serum (control antibody).

minor co-immunoprecipitation, indicating that nephrin–Nck interaction is mainly dependent on tyrosine phosphorylation. When normal rat glomerular lysates were immunoprecipitated for nephrin, nephrin was clearly tyrosine phosphorylated, consistent with our previous report [10] (Fig. 1C). In addition, nephrin co-immunoprecipitated with phospho-Src (Y418, this antibody recognized the active form of Src-family kinases), suggesting that Src-family kinases likely interact with and contribute to tyrosine phosphorylation of nephrin in vivo (Fig. 1C). On SDS–PAGE, rat nephrin runs as a doublet, presumably because of differential glycosylations, and phosphorylated nephrin consistently corresponded to the upper band (~180 kDa. Fig. 1B and C). In normal rat glomerular lysates, Nck co-immunoprecipitated with the upper band of nephrin, suggesting that tyrosine phosphorylated nephrin interacts with Nck in vivo (Fig. 1D).

Identification of the nephrin-interacting domain(s) of Nck

We next studied which domain(s) of Nck interact with nephrin, using pull-down assays with GST-fusion proteins of Nck1 or its subdomains. When Cos-1 cells were transfected with rat nephrin and cell lysates were subjected to pull-down assay, nephrin was clearly pulled down by GST–Nck (containing full-length Nck1) and GST–Nck-SH2 (containing the SH2 domain of Nck1) in a Fyn-dependent manner (Fig. 2A, top panel). Only after a longer exposure, we also observed that GST–Nck-SH3s (containing three SH3 domains of Nck1) pulled down nephrin (Fig. 2A, second panel), however, this weak interaction was not affected by Fyn. GST–Nck and GST–Nck-SH2 also pulled down nephrin from normal rat glomerular lysates (Fig. 2D). Taken together, these results indicate that nephrin–Nck interaction occurs predominantly between the SH2 domain of Nck and phosphotyrosine containing motif(s) of the cytoplasmic domain of nephrin in vitro and in vivo. In addition, there appears to be a minor interaction via the SH3 domains of Nck, which is independent of tyrosine phosphorylation.

Identification of the tyrosine residues of rat nephrin responsible for molecular interaction with Nck

By Motif scan, three predicted binding sites for Nck1-SH2 in rat nephrin were, in the order of likelihood, Y1204, Y1228, and Y1127. Our previous study with mutagenesis indicated that Y1127 is not a preferred substrate for Src-family kinases [10], thus we focused on Y1204 and Y1228. We first used pull-down assay to map the binding sites for Nck. When Y1204 and Y1228 were mutated to phenylalanine individually, there was no obvious change in the interaction of nephrin to GST–Nck or GST–Nck-SH2 (Fig. 2B). However, when two tyrosine residues were mutated simultaneously, interaction to GST–Nck and GST–Nck-SH2 was virtually abolished (Fig. 2B). We next expressed rat nephrin and its mutants transiently in HEK293T cells and immunoprecipitated endogenous Nck with rabbit anti-Nck antibody. Wild-type nephrin co-immunoprecipitated with Nck in the presence of Fyn, which was abolished with the Y1204/1228F double mutant (Fig. 2C), similar to the results of pull-down assays. However, unlike the pull-down assay, single mutants of Y1204 or Y1208 also showed markedly reduced interaction with Nck, suggesting that each tyrosine residue contributes significantly to the interaction with Nck at the physiological expression level of Nck. In particular, Nck interaction of Y1228F was not distinguishable from the double mutant, implying that Y1228F may be a preferred Nck binding site in vivo. In human and mouse nephrin, in addition to the two tyrosine residues corresponding to rat Y1204 and Y1228 (Y1193/1217 in human and Y1208/Y1232 in mouse), third residue (Y1176 in human and Y1191 in mouse) also contributed to Nck binding ([5,6] and data not shown).

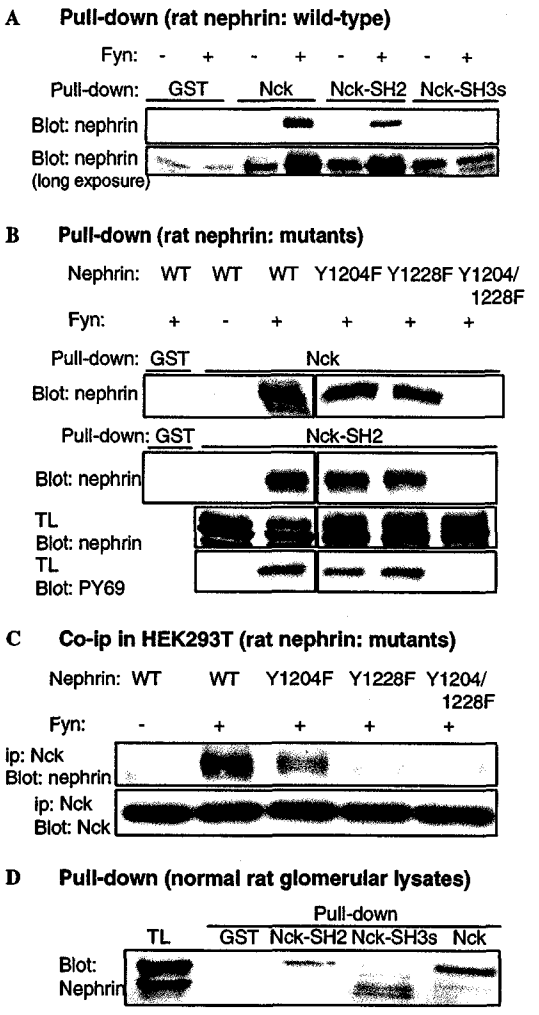

Fig. 2. Mapping of the sites responsible for nephrin–Nck interaction. (A) Cos-1 cells were transiently transfected with wild-type rat nephrin with or without Fyn. Cell lysates were subjected to pull-down assay using GST alone, GST–Nck (containing full-length Nck1), GST–Nck-SH2 (containing the SH2 domain of Nck1 alone), and GST–Nck-SH3s (containing three SH3 domains of Nck1). Precipitates were blotted for nephrin. Short (top panel) and long (bottom panel) exposure are shown. (B) Wild-type rat nephrin and its mutants were expressed in Cos-1 cells and pull-down assay was performed using GST–Nck and GST–Nck-SH2 as in (A). (C) Wild-type rat nephrin and its mutants were expressed in HEK293T cells. Endogenous Nck was immunoprecipitated with anti-Nck antibody and precipitates were blotted for nephrin and Nck. (D) Normal rat glomerular lysates were subjected to pull-down assay as in (A). Identities of the multiple bands seen with GST–Nck-SH3s pull-down are not known, however some of them may represent tyrosine phosphorylation-independent interaction of Nck with nephrin.

Cross-linking of the extracellular domain of nephrin causes actin reorganization and cell morphological changes in a Nck-dependent manner

Nck is a known regulator of actin re-organization [7] and it was shown previously that aggregation of Nck at the plasma membrane leads to localized actin polymerization (formation of "actin tails") [5,6,16]. To further address the functional consequence of nephrin–Nck interaction on the actin cytoskeleton and cell morphology, we stably expressed rat nephrin in HEK293T cells. HEK293T cells express many of the slit diaphragm proteins including podocin, FAT, and P-cadherin, and were successfully used to study homophilic interaction of nephrin previously [17]. Untransfected HEK293T cells showed relatively round morphology with distinct corti-

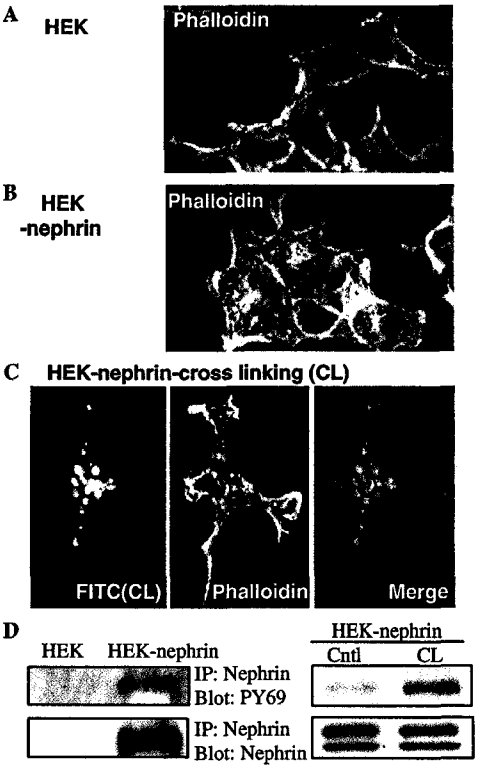

Fig. 3. Nephrin expression and its cross-linking induce morphological changes in HEK293T cells. Untransfected HEK293T cells showed relatively round morphology with distinct cortical F-actin and few cell protrusions (A, HEK). When HEK293T cells were stably transfected with rat nephrin, many cells demonstrated more cell protrusions and appeared more "spikey", as compared with untransfected cells (B, HEK-nephrin). When nephrin was cross-linked with antibodies in HEK-nephrin (Materials and methods), cells showed punctuated cytosolic F-actin, co-localizing at the site of nephrin cross-linking. Morphological changes were further augmented and many cells showed elongated cell shape with prominent cell protrusions (C, HEK-nephrin-cross-linking). Site of nephrin cross-linking is labeled with FITC (green) and phalloidin is labeled with rhodamine (red)). Transfection of HEK293T cells with vector alone, with or without cross-linking treatment, did not induce discernible morphological changes (not shown). (D) Cell lysates of HEK293T or HEK-nephrin cells with or without antibody-mediated cross-linking were immunoprecipitated with anti-nephrin antibody and blotted for phosphotyrosine or nephrin. Nephrin is tyrosine phosphorylated in unstimulated HEK-nephrin cells, which is further augmented by cross-linking. (For interpretation of the references to color in this figure legend, the reader is referred to the web version of this paper.)

cal F-actin and few protrusions (Fig. 3A). When HEK293T cells were stably transfected with rat nephrin (HEK293T-nephrin or HEK-nephrin in short), nephrin was weakly but clearly tyrosine phosphorylated, likely induced by a high expression level of nephrin and homotypic binding of nephrin molecules from adjacent cells (Fig. 3D). Many HEK-nephrin cells demonstrated more cell protrusions and appeared more "spikey", as compared with untransfected cells (Fig. 3B). When nephrin was cross-linked with antibodies in HEK-nephrin (see Materials and methods), tyrosine phosphorylation of nephrin was augmented further (Fig. 3D), consistent with the previous report [18]. Cells showed punctuated cytosolic F-actin, co-localizing at the site of nephrin cross-linking and cell protrusions became more prominent, as compared with non-cross-linked HEK-nephrin. Many cells showed elongated cell shapes with prominent protrusions, resembling process formation, as shown in Fig. 3C. Transfection of HEK293T cells with vector alone or cross-linking treatment of vector transfected cells did not cause any discernible morphological changes, as compared with untransfected cells (not shown).

To study if the changes induced by nephrin expression and cross-linking are mediated by Nck, we first attempted a gene knock-down of Nck1 (Nck2 expression in HEK293T cells is negligible) using a commercially available siRNA. However, the knock-down efficiency was not satisfactory, thus we next utilized two Nck mutants. Myc–Nck-SH2 contains only the SH2 domain of Nck and HA-Nck-SH3-M3 has all three SH3 domains mutated. Both mutants would bind to and occupy the phosphotyrosine containing motifs in nephrin but are not able to recruit the downstream effector molecules via the SH3 domains, thereby blocking the signaling cascade induced by nephrin–Nck interaction. When HEK-nephrin was transfected with GFP alone and nephrin was cross-linked (GFP control), cells showed elongated morphology and prominent protrusions, consistent with the previous results (Fig. 4, top). When HEK-nephrin cells were transfected with Nck-SH2 and nephrin was cross-linked, Nck-SH2 localized mainly at the plasma membrane and transfected cells showed smoother cell contour, more distinct cortical F-actin, and fewer protrusions, as compared with GFP control (Fig. 4, middle). When Nck-SH3-M3 was transfected, it localized both at the plasma membrane and in the cytoplasm. Nck-SH3-M3 transfected cells were also generally less elongated and had fewer protrusions, as compared with GFP control (Fig. 4, bottom). The expression level of Nck-SH2 was much lower than Nck-SH3-M3, however, its dominant negative effect appeared to be more potent than Nck-SH3-M3. We have observed similar differences of the two dominant-negative constructs in other experimental systems (not shown). Although the reason is unclear, Nck-SH3-M3 may still interact with the other intracellular molecules, thereby activating some of the signaling cascades. Taken together, these results suggest that nephrin tyrosine phosphorylation-mediated morphological changes are, at least in part, mediated by Nck.

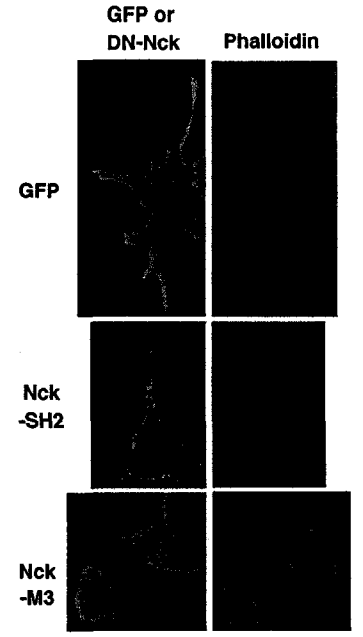

Fig. 4. Morphological changes induced by nephrin cross-linking are attenuated by dominant-negative Ncks. HEK293T-nephrin cells were transiently transfected with GFP alone, Myc–Nck-SH2, or HA–Nck-SH3-M3 (for the construct information, see Results) and nephrin was cross-linked with antibodies for all experiments. Although cross-linking is not visualized, preliminary experiments confirmed >90% efficiency of cross-linking. Expression of transfected plasmids was detected by GFP or FITC-labeled anti-Myc/anti-HA antibodies. F-actin was visualized with rhodamine–phalloidin. GFP did not affect prominent cell protrusions, while Nck-SH2 and, to a lesser extent, Nck-SH3-M3 attenuated them.

Nephrin–Nck interaction is diminished in the rat model of PAN

To study the potential role of nephrin–Nck interaction in the maintenance of glomerular permselectivity in vivo, we next utilized PAN, a well-established rat model of podocyte injury and proteinuria [19]. Seven days after a single intravenous injection of puromycin aminonucleoside, heavy proteinuria was observed (control, 5 ± 1 mg/day; PAN, 162 ± 26 mg/day; $p < 0.01$, $N = 4$ rats each). Nephrin tyrosine phosphorylation, as well as nephrin–Nck co-immunoprecipitation, was decreased by ~57% and ~46%, respectively, in rats with PAN, as compared with control rats (Fig. 5). Expression of Nck and nephrin in total glomerular lysates in rats with PAN was not significantly different, as compared with control rats (nephrin, control: 100 ± 4, PAN: 164 ± 46; Nck, control: 100 ± 3, PAN: 118 ± 13; arbitrary units, $N = 8$ rats per group). Therefore, the decrease in nephrin–Nck co-immunoprecipitation likely represents diminished interaction between these two molecules, rather than decreased glomerular expression of nephrin or Nck in PAN.

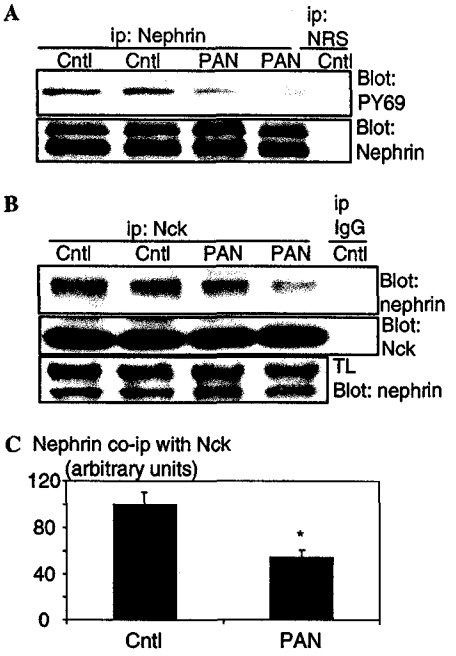

Fig. 5. Nephrin–Nck interaction is decreased in PAN. PAN was induced as in Materials and methods. Glomerular lysates from rats with PAN (day 7) and control rats were immunoprecipitated for nephrin (A) or Nck (B) and precipitates were blotted for phosphotyrosine (A) or nephrin (B). (C) Densitometric analysis of nephrin co-immunoprecipiated with Nck is shown. Error bars are SEM. $^*p < 0.05$ vs. Cntl (by Student's t-test), $N = 6$ rats for each group. Note that expression of nephrin and Nck is not different between PAN and control (see Results).

Discussion

There are three major novel findings in the current study; (1) in addition to human and mouse nephrin, we confirmed that rat nephrin also interacts with Nck predominantly in a tyrosine phosphorylation-dependent manner. Two tyrosine residues in rat nephrin critical for the Nck interaction were conserved among the three species, supporting that this important machinery is conserved through evolutions. (2) We demonstrated for the first time that nephrin expression and tyrosine phosphorylation lead to cell morphological changes, which resemble process formation, an important feature of differentiated podocytes in vivo. (3) We have shown that nephrin–Nck interaction is disturbed in the animal model of podocyte injury in the adult kidney.

Recent advances in podocyte biology highlight the pivotal role of the actin cytoskeleton in the maintenance of normal podocyte morphology and function [1]. It is of great interest that a number of proteins, which interact with the intracellular domain of nephrin, are known for their role in the regulation of the actin cytoskeleton; CD2AP has an actin-binding site and is known to regulate actin reorganization [20]; PI3K has versatile intracellular actions, including regulation of actin polymerization via ADP-ribosylating factor 6 (ARF6) or Rac [21]; IQGAP1 is an effector protein of small GTPases Rac1 and Cdc42 [22]. Another slit diaphragm protein, FAT1 was also shown to regulate actin dynamics via Ena/VASP proteins and FAT1 knockout mice showed deficiency in podocyte foot process development [23,24]. Taken together with the current results, it is not unreasonable to hypothesize that transmembrane proteins at the slit diaphragm, such as nephrin and FAT1, serve as the signaling scaffold, which coordinates actin dynamics in podocyte foot processes. Current results are of particular interest because tyrosine phosphorylation of nephrin and its subsequent interaction with Nck appeared to facilitate process formation of the cells, which is important for the function of podocytes in vivo. These morphological changes were not noted in the previous reports, most likely because of different cell types used (mouse embryonic fibroblasts in [5] and NIH3T3 in [6]). Whether similar morphological changes could be induced in various podocyte cell lines is currently under investigations. As well, downstream effector(s) responsible for process formation are yet to be determined.

We reported previously that podocyte specific gene deletion of Nck1 and Nck2 leads to abnormal podocyte foot process development and heavy proteinuria [5]. However, these results did not allow us to determine whether Nck is critical only for the development of normal podocytes or it is also important in the maintenance of normal podocyte function/glomerular permselectivity in the adult kidney. In the current study, we have shown that podocyte injury in rats induced by puromycin aminonucleoside led to decreased tyrosine phosphorylation of nephrin and nephrin–Nck interaction (Fig. 5). These results strongly suggest that tyrosine phosphorylation-dependent nephrin–Nck interaction has an important role not only in podocyte development but also in the maintenance of podocyte morphology/function in the adult kidney. Its disruption may contribute to impaired glomerular permselectivity in kidney diseases in adults.

Acknowledgments

The authors thank Serge Lemay for the assistance with confocal microscopy. This work was supported by research grants from the Kidney Foundation of Canada and the Canadian Institute of Health Research (to T.T.), from the Ministry of Education, Science, Culture and Sports of Japan (18590886 to H.K.), and from the Natural Sciences and Engineering Research Council of Canada (to L.L.). T.T. and L.L. hold scholarships from the Fonds de la Recherche en Santé du Québec.

References

[1] P. Mundel, S.J. Shankland, Podocyte biology and response to injury, J. Am. Soc. Nephrol. 13 (2002) 3005–3015.
[2] T. Benzing, Signaling at the slit diaphragm, J. Am. Soc. Nephrol. 15 (2004) 1382–1391.
[3] T.B. Huber, B. Hartleben, J. Kim, M. Schmidts, B. Schermer, A. Keil, L. Egger, R.L. Lecha, C. Borner, H. Pavenstadt, A.S. Shaw, G. Walz,

T. Benzing, Nephrin and CD2AP associate with phosphoinositide 3-OH kinase and stimulate AKT-dependent signaling, Mol. Cell. Biol. 23 (2003) 4917–4928.
[4] R. Verma, B. Wharram, I. Kovari, R. Kunkel, D. Nihalani, K.K. Wary, R.C. Wiggins, P. Killen, L.B. Holzman, Fyn binds to and phosphorylates the kidney slit diaphragm component Nephrin, J. Biol. Chem. 278 (2003) 20716–20723.
[5] N. Jones, I.M. Blasutig, V. Eremina, J.M. Ruston, F. Bladt, H. Li, H. Huang, L. Larose, S.S. Li, T. Takano, S.E. Quaggin, T. Pawson, Nck adaptor proteins link nephrin to the actin cytoskeleton of kidney podocytes, Nature 440 (2006) 818–823.
[6] R. Verma, I. Kovari, A. Soofi, D. Nihalani, K. Patrie, L.B. Holzman, Nephrin ectodomain engagement results in Src kinase activation, nephrin phosphorylation, Nck recruitment, and actin polymerization, J. Clin. Invest. 116 (2006) 1346–1359.
[7] L. Buday, L. Wunderlich, P. Tamas, The Nck family of adapter proteins: regulators of actin cytoskeleton, Cell Signal. 14 (2002) 723–731.
[8] J.H. McCarty, The Nck SH2/SH3 adaptor protein: a regulator of multiple intracellular signal transduction events, Bioessays 20 (1998) 913–921.
[9] F. Bladt, E. Aippersbach, S. Gelkop, G.A. Strasser, P. Nash, A. Tafuri, F.B. Gertler, T. Pawson, The murine Nck SH2/SH3 adaptors are important for the development of mesoderm-derived embryonic structures and for regulating the cellular actin network, Mol. Cell. Biol. 23 (2003) 4586–4597.
[10] H. Li, S. Lemay, L. Aoudjit, H. Kawachi, T. Takano, SRC-family kinase Fyn phosphorylates the cytoplasmic domain of nephrin and modulates its interaction with podocin, J. Am. Soc. Nephrol. 15 (2004) 3006–3015.
[11] G. Lussier, L. Larose, A casein kinase I activity is constitutively associated with Nck, J. Biol. Chem. 272 (1997) 2688–2694.
[12] X. Li, M. Meriane, I. Triki, M. Shekarabi, T.E. Kennedy, L. Larose, N. Lamarche-Vane, The adaptor protein Nck-1 couples the netrin-1 receptor DCC (deleted in colorectal cancer) to the activation of the small GTPase Rac1 through an atypical mechanism, J. Biol. Chem. 277 (2002) 37788–37797.
[13] S. Kebache, D. Zuo, E. Chevet, L. Larose, Modulation of protein translation by Nck-1, Proc. Natl. Acad. Sci. USA 99 (2002) 5406–5411.
[14] P.S. Topham, S.A. Haydar, R. Kuphal, J.D. Lightfoot, D.J. Salant, Complement-mediated injury reversibly disrupts glomerular epithelial cell actin microfilaments and focal adhesions, Kidney Int. 55 (1999) 1763–1775.
[15] L. Aoudjit, A. Potapov, T. Takano, Prostaglandin E_2 promotes cell survival of glomerular epithelial cells via the EP4 receptor, Am. J. Physiol. Renal Physiol. 290 (2006) F1534–F1542.
[16] G.M. Rivera, C.A. Briceno, F. Takeshima, S.B. Snapper, B.J. Mayer, Inducible clustering of membrane-targeted SH3 domains of the adaptor protein Nck triggers localized actin polymerization, Curr. Biol. 14 (2004) 11–22.
[17] J. Khoshnoodi, K. Sigmundsson, L.G. Ofverstedt, U. Skoglund, B. Obrink, J. Wartiovaara, K. Tryggvason, Nephrin promotes cell–cell adhesion through homophilic interactions, Am. J. Pathol. 163 (2003) 2337–2346.
[18] J. Lahdenpera, P. Kilpelainen, X.L. Liu, T. Pikkarainen, P. Reponen, V. Ruotsalainen, K. Tryggvason, Clustering-induced tyrosine phosphorylation of nephrin by Src family kinases, Kidney Int. 64 (2003) 404–413.
[19] Y.H. Kim, M. Goyal, D. Kurnit, B. Wharram, J. Wiggins, L. Holzman, D. Kershaw, R. Wiggins, Podocyte depletion and glomerulosclerosis have a direct relationship in the PAN-treated rat, Kidney Int. 60 (2001) 957–968.
[20] N.Y. Shih, J. Li, V. Karpitskii, A. Nguyen, M.L. Dustin, O. Kanagawa, J.H. Miner, A.S. Shaw, Congenital nephrotic syndrome in mice lacking CD2-associated protein, Science 286 (1999) 312–315.
[21] L.C. Cantley, The phosphoinositide 3-kinase pathway, Science 296 (2002) 1655–1657.
[22] X.L. Liu, P. Kilpelainen, U. Hellman, Y. Sun, J. Wartiovaara, E. Morgunova, T. Pikkarainen, K. Yan, A.P. Jonsson, K. Tryggvason, Characterization of the interactions of the nephrin intracellular domain, FEBS J. 272 (2005) 228–243.
[23] L. Ciani, A. Patel, N.D. Allen, C. Ffrench-Constant, Mice lacking the giant protocadherin mFAT1 exhibit renal slit junction abnormalities and a partially penetrant cyclopia and anophthalmia phenotype, Mol. Cell. Biol. 23 (2003) 3575–3582.
[24] M.J. Moeller, A. Soofi, G.S. Braun, X. Li, C. Watzl, W. Kriz, L.B. Holzman, Protocadherin FAT1 binds Ena/VASP proteins and is necessary for actin dynamics and cell polarization, EMBO J. 23 (2004) 3769–3779.

APPENDIX 2

Regulation of Nck Protein Levels by GSK3β and the 26S Proteasome

Figure appendix 2. Regulation of Nck proteins stability by GSK3β and the 26S proteasome (A) Turnover of Nck proteins. HeLa cells were treated with the protein synthesis inhibitor cycloheximide (50 μg/ml) for indicated time. Cell lysates were prepared and analyzed by immunoblotting assay with Nck1 and Nck2 specific-antibodies. Also shown are the levels of p27 and eIF2β that serves as positive and negative controls, respectively. Quantitative analysis (normalized over β-actin levels) is graphed and expressed as percentage of untreated cells (t=0). Inset: immunoblot images of one representative experiment out of 3. (s.e.m.) **(B) Serum starvation triggers downregulation of Nck protein levels**. HeLa cells were treated with 0.1% fetal bovine serum (FBS) for indicated time and cell lysates prepared and analyzed by immunoblotting with indicated antibodies. Level of proteins was quantified and normalized over β-actin levels in each condition (depicted under Nck1 and Nck2 images). Note that Nck1, Nck2 and p27 are markedly downregulated by 8h of serum starvation. **(C) Downregulation of Nck adaptors by starvation is mediated through GSK3β protein kinase**. HeLa cells were transiently transfected with HA-tagged Nck1. The next day, cells were treated with the GSK3β inhibitor $LiCl_2$ at a concentration of 20 mM for 20 hr. Cells were extensively washed with 0.1% FBS and incubated in 0.1% FBS/$LiCl_2$ for indicated time. Note that inhibition of GSK3β rescues HA-Nck1 protein downregulation. **(D) Presence of a highly conserved GSK3β consensus phosphorylation site (S/TXXpS/pT) in both Nck1 and Nck2 proteins.** h: human; m: mouse; x: frog. **(E) Serum starvation-induced Nck protein downregulation is mediated by the 26S proteasome.** HeLa cells were transiently transfected with HA-tagged Nck1. The next day, cells were treated with the proteasome inhibitor MG132 (50 μM) for 18 hr. Cells were extensively washed with 0.1% FBS and incubated in 0.1% FBS/MG132 for indicated time. Cells were harvested and lysates were analyzed by immunoblotting assay with indicated antibodies. Note that inhibition of the proteasome rescues HA-Nck1 serum starvation-induced protein downregulation.

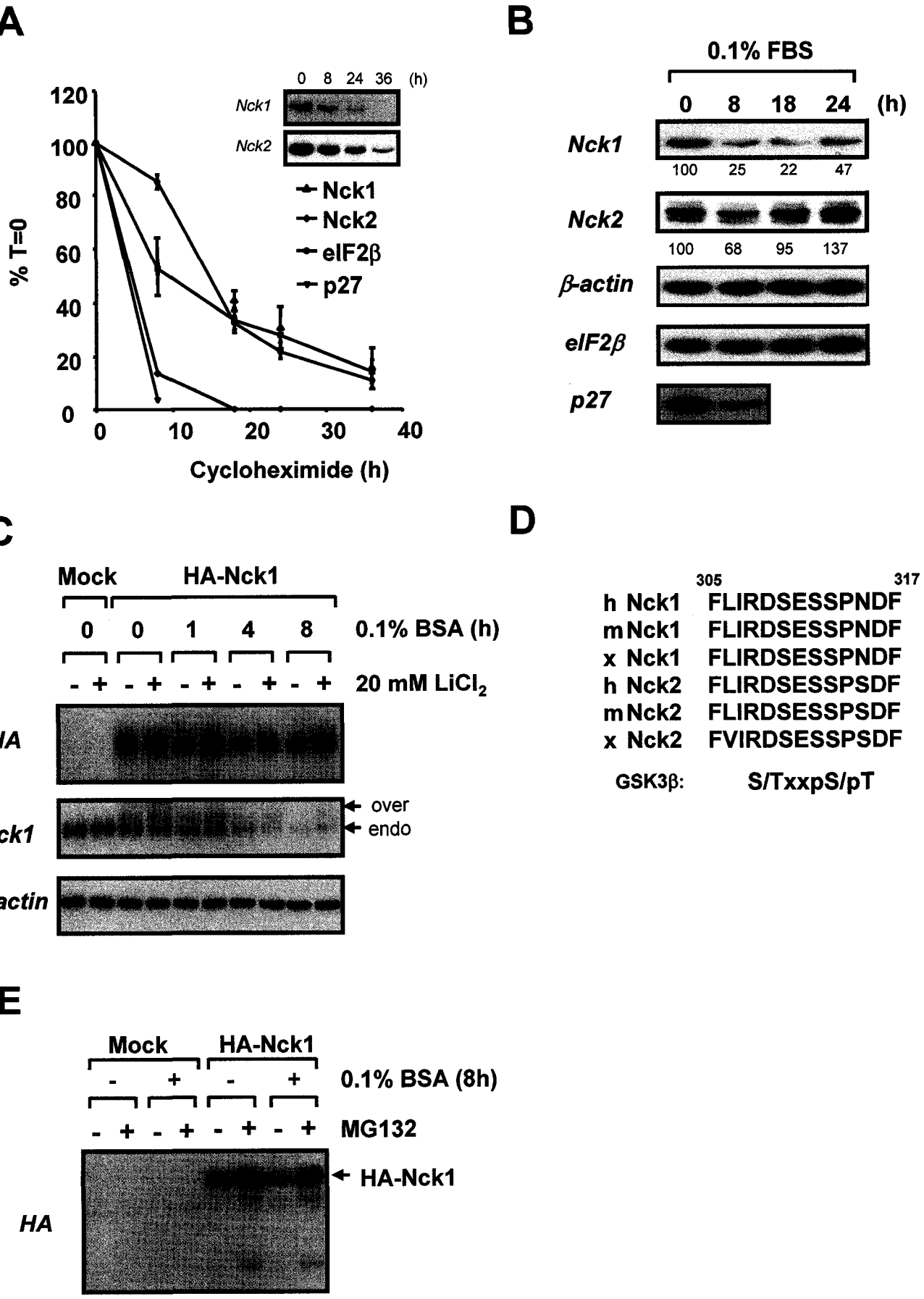
A
0 8 24 36 (h)
Nck1
Nck2
120
100
80
60
40
20
0
% T=0
0 10 20 30 40
Cycloheximide (h)
Nck1
Nck2
eIF2β
p27
B
0.1% FBS
0 8 18 24 (h)
Nck1
100 25 22 47
Nck2
100 68 95 137
β-actin
eIF2β
p27
C
Mock
HA-Nck1
0 0 1 4 8 0.1% BSA (h)
- + - + - + - + - + 20 mM LiCl2
HA
Nck1
over
endo
β-actin
D
305 317
h Nck1 FLIRDSESSPNDF
mNck1 FLIRDSESSPNDF
x Nck1 FLIRDSESSPNDF
h Nck2 FLIRDSESSPSDF
mNck2 FLIRDSESSPSDF
x Nck2 FVIRDSESSPSDF
GSK3β: S/TxxpS/pT
E
Mock
HA-Nck1
- + - + 0.1% BSA (8h)
- + - + - + - + MG132
HA-Nck1
HA

APPENDIX 3

CK1γ2 Inhibits RhoA Signaling and Actin Stress Fibers Formation through CDK5-Dependent $p27^{KIP}$ stabilization

Figure appendix 3. (A) CKIγ2-expressing Rat2 stable cell lines display reduced RhoA levels Immunoblot analysis of total cell lysates from control (C-) and CKIγ2 stable cell lines using indicated antibodies **(B) CKIγ2-expressining Rat2 fibroblasts show reduced RhoA-GTP**. Control (C-) and CKIγ2-expressing Rat2 cells show reduced amounts of GTP-loaded RhoA compared to control. RhoA activation was measured by pull-down using the GST-ROK CRIB domain fusion. Control (C-) and CKIγ2 stable cell lines were transiently transfected with myc-tagged RhoA. **(C) Schematic drawing showing that inhibition of CDK5 rescues morphology and stress fiber formation through $p27^{Kip1}$ destabilization.** $p27^{kip1}$ was found to inhibit RhoA signaling through its stabilization upon phosphorylation of Ser10 by CDK5. This CDK5-dependent pathway was originally characterized in cortical neurons. We present evidences that this pathway exists in Rat2 cells and is activated in CKIγ2-overexpressing clones (See D and E). **(D) Stabilization of $p27^{Kip}$ by Ser10 phosphorylation in CKIγ2 overexpressing clones.** Immunoblot assay of phospho-$p27^{Kip}$ and CDK5 in CKIγ2 Rat2-overexpressing cells. **(E) Destabilization of $p27^{Kip}$ by Roscovitine in Rat2 fibroblasts**. Treatment with the CDK5 inhibitor Roscovitine at either 50 or 100 μM causes destabilization of $p27^{Kip}$ in control and CKIγ2 Rat2 fibroblasts. This result shows that the CDK5-dependent pathway linking $p27^{Kip1}$ to RhoA also take place in fibroblast **(F) Roscovitine rescues morphology and stress fiber formation in CKIγ2-expressing fibroblasts.** Phase contrast microscopy of Phallodin-Rhodhamine stained control and CKIγ2 Wt stable Rat2 clones. Note the reappearance of stress fiber in CKIγ2-expressing cells treated with the CDK5 inhibitor Roscovitine.

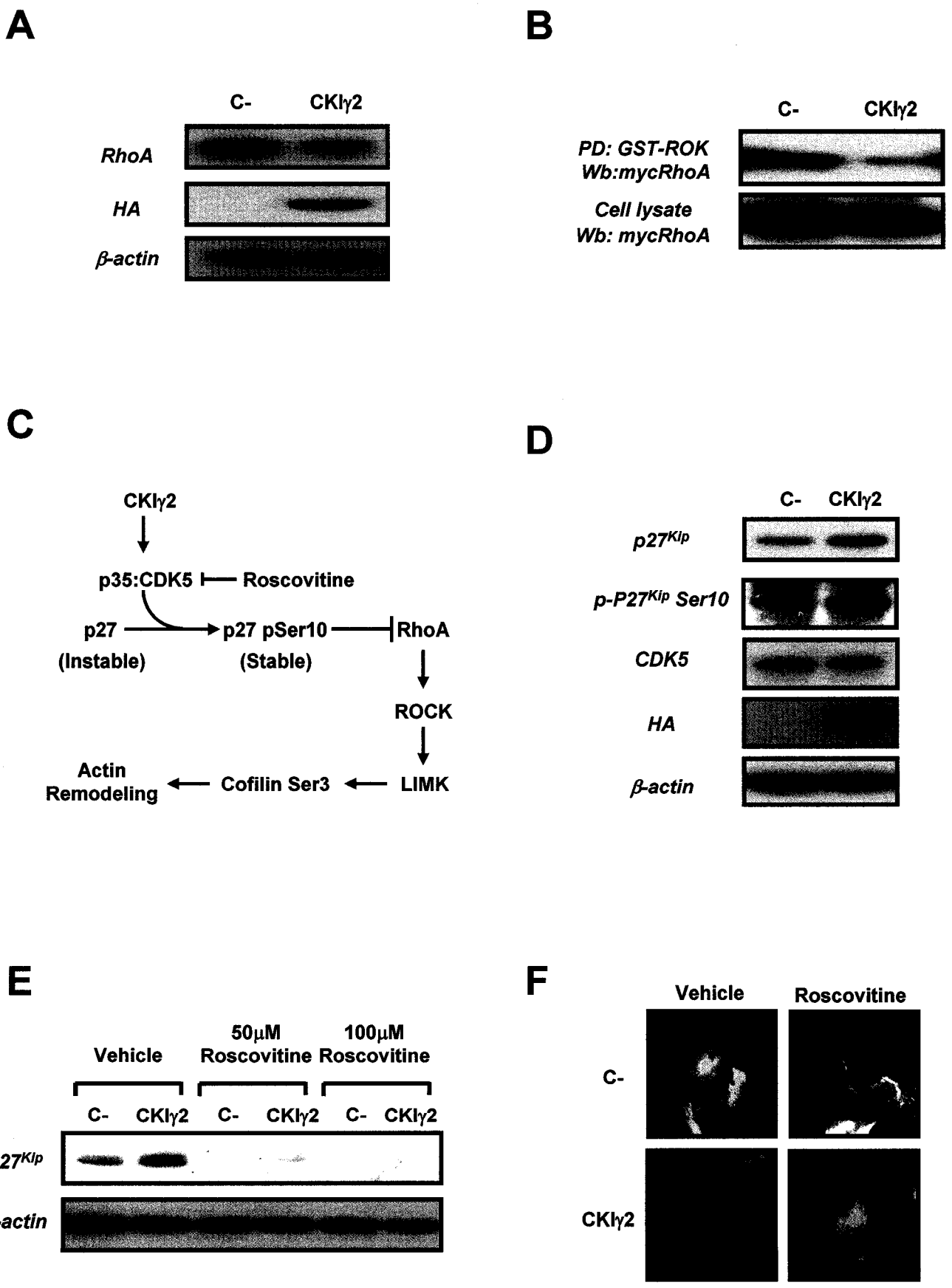
A
C-
CKIγ2
RhoA
HA
β-actin
B
C-
CKIγ2
PD: GST-ROK
Wb:mycRhoA
Cell lysate
Wb: mycRhoA
C
CKIγ2
p35:CDK5
Roscovitine
p27
(Instable)
p27 pSer10
(Stable)
RhoA
ROCK
LIMK
Cofilin Ser3
Actin
Remodeling
D
C-
CKIγ2
p27Kip
p-P27Kip Ser10
CDK5
HA
β-actin
E
Vehicle
50μM
Roscovitine
100μM
Roscovitine
C-
CKIγ2
C-
CKIγ2
C-
CKIγ2
p27Kip
β-actin
F
Vehicle
Roscovitine
C-
CKIγ2

APPENDIX 4

Certificates